

# Enhancing the Properties of Polymer Nanocomposites by Inducing a Stable Dispersion of Carbon Nanotubes through Polymer Wrapping

by

**Muthuraman Namasivayam**

*Thesis  
Submitted to Flinders University  
for the degree of*

**Doctor of Philosophy**  
College of Science and Engineering  
June 2020

---

<b>TABLE OF CONTENTS</b>	<b>i</b>
<b>DECLARATION</b>	<b>vi</b>
<b>ACKNOWLEDGEMENTS</b>	<b>vii</b>
<b>ABSTRACT</b>	<b>viii</b>
<b>LIST OF FIGURES</b>	<b>x</b>
<b>LIST OF TABLES</b>	<b>xv</b>
<b>LIST OF PUBLICATIONS</b>	<b>xvi</b>
<b>CHAPTER 1</b>	<b>01</b>
<b>INTRODUCTION</b>	<b>01</b>
1.1 Carbon Nanotubes	02
1.2 Properties of Polymers	05
1.3 Polymer Nanocomposites	08
1.4 Functionalization	10
1.4.1 <i>Chemical Method</i>	12
1.4.2 <i>Physical Method</i>	13
<i>Adsorption</i>	13
<i>Wrapping</i>	16
1.5 Limitation in Polymer Nanocomposite	19
1.5.1 <i>Volume Fraction</i>	19
1.5.2 <i>Alignment</i>	22
1.6 Polyvinylidene fluoride	24
1.7 Polyvinylpyrrolidone	25
1.8 Poly(4-vinylpyridine)	26
1.9 Polyethylenimine	27
1.10 Aims and Objectives	29
1.11 Thesis Outline	29
1.12 References	31
<b>CHAPTER 2</b>	<b>37</b>
<b>MATERIALS AND METHODS</b>	<b>37</b>
2.1 Materials	38
2.2 Sample Preparation	38

2.3 Raman Spectroscopy	39
2.4 Electrical Conductivity	41
2.5 Thermal Conductivity	42
2.6 Dynamic Mechanical Analyser	43
2.7 Differential Scanning Calorimetry	45
2.8 Scanning Electron Microscopy	48
2.9 References	49
<b>CHAPTER 3</b>	<b>51</b>
<b>PVP FUNCTIONALIZED AS PREPARED SINGLE-WALLED NANOTUBES (AP-SWNT) IN PVDF COMPOSITES</b>	<b>51</b>
3.1 Chapter Introduction	52
3.2 Sample Details	52
3.3 Results & Discussions	52
3.3.1 Thermal Conductivity	52
3.3.2 Crystallization behaviour of PVP@AP-SWNT/PVDF composite	55
3.3.3 Electrical Conductivity	56
3.3.4 Mechanical Characterization	57
3.3.5 Microscopy Results	62
3.3.6 Raman Results	64
3.4 Conclusion	66
3.5 References	66
<b>CHAPTER 4</b>	<b>68</b>
<b>PVP FUNCTIONALIZED P3 SINGLE-WALLED NANOTUBES IN PVDF COMPOSITES</b>	<b>68</b>
4.1 Chapter Introduction	69
4.2 Sample Details	69
4.3 Results and Discussions	69

4.3.1 Thermal Conductivity	69
4.3.2 Crystallization behavior of PVP@P3-SWNT/PVDF composite	76
4.3.3 Electrical Conductivity	77
4.3.4 Mechanical Characterization	78
4.3.5 Microscopy Results	83
4.3.6 Raman Results	85
4.4 Conclusion	86
4.5 References	87
<b>CHAPTER 5</b>	<b>89</b>
<b>PVP FUNCTIONALIZED MULTI-WALLED NANOTUBES IN PVDF COMPOSITES</b>	<b>89</b>
5.1 Chapter Introduction	90
5.2 Sample Details	90
5.3 Results and Discussions	90
5.3.1 Thermal Conductivity	90
5.3.2 Crystallization behaviour of PVP@MWNT/PVDF composite	92
5.3.3 Electrical Conductivity	93
5.3.4 Mechanical Characterization	94
5.3.5 Microscopy Results	99
5.3.6 Raman Results	101
5.4 Conclusion	102
5.5 Collective Conclusion of Chapters 3-5	102
5.6 References	106
<b>CHAPTER 6</b>	<b>107</b>
<b>PVP VERSUS P4VP FUNCTIONALIZED CARBON NANOTUBES IN PVDF COMPOSITE</b>	<b>107</b>
6.1 Chapter Introduction	108
6.2 Sample Details	108
6.3 Results and Discussions	108
<i>AP Single-walled nanotubes</i>	108



6.3.1 Thermal Conductivity	108
6.3.2 Crystallization behavior of PVP/P4VP@AP-SWNT/PVDF composite	109
6.3.3 Electrical Conductivity	110
6.3.4 Mechanical characterization	112
<i>P3</i> Single-walled nanotubes	113
6.3.5 Thermal Conductivity	113
6.3.6 Crystallization behavior of PVP/P4VP@P3-SWNT/PVDF composite	114
6.3.7 Electrical Conductivity	116
6.3.8 Mechanical characterization	117
<i>Multi-walled</i> nanotubes	118
6.3.9 Thermal Conductivity	118
6.3.10 Crystallization behavior of PVP/P4VP@MWNT/PVDF composite	119
6.3.11 Electrical Conductivity	121
6.3.12 Mechanical characterization	122
6.4 Conclusion	123
6.5 References	124
<b>CHAPTER 7</b>	126
<b>PEI FUNCTIONALIZED CARBON NANOTUBES IN PVDF COMPOSITES</b>	126
7.1 Chapter Introduction	127
7.2 Sample Details	127
7.3 Results and Discussions	127
<i>AP</i> Single-walled nanotubes	127
7.3.1 Thermal Conductivity	127
7.3.2 Electrical Conductivity	128
7.3.3 Mechanical characterization	129
<i>P3</i> Single-walled nanotubes	131

7.3.4 Thermal Conductivity	131
7.3.5 Electrical Conductivity	132
7.3.6 Mechanical characterization	133
<i>Multi-walled nanotubes</i>	134
7.3.7 Thermal Conductivity	134
7.3.8 Electrical Conductivity	136
7.3.9 Mechanical characterization	137
7.4 Conclusion	138
7.5 References	140
<b>CHAPTER 8</b>	141
CONCLUSION	141
<b>CHAPTER 9</b>	145
<b>FUTURE DIRECTIONS AND RECOMMENDATIONS</b>	145
9.1 Polymer wrapping	146
9.2 Mechanical Characterization	147
9.3 Surface Analysis	147
9.4 References	148

# DECLARATION

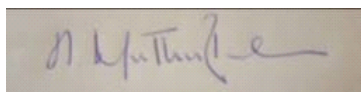
I certify that this work contains no material which has been accepted for the award of any other degree or diploma in my name, in any university or other tertiary institution and to the best of my knowledge and belief, contains no material previously published or written by another person, except where due reference has been made in the text. In addition, I certify that no part of this work will, in the future, be used in a submission in my name, for any other degree or diploma in any university or other tertiary institution without the prior approval of Flinders University and where applicable, any partner institution responsible for the joint-award of this degree.

I give consent to this copy of my thesis when deposited in the University library, being made available for loan and photocopying, subject to the provision of the copy rights act 1968.

The author acknowledges that copyright of published works contained within this thesis resides with the copyright holder(s) of those works,

I also give consent for the digital version of my thesis to be made available on the web, via the University's digital research repository, the library search and also through web search engines, unless permission has been granted by the university to restrict access for a period of time.

 Recoverable Signature

X 

---

Muthuraman Namasivayam

Signed by: 0a0e986e-d799-4678-a195-199e968ea9c5

Date: 03/06/2020

# ACKNOWLEDGEMENT

I could never have finished my doctoral study without the help, support, guidance and efforts of a lot of people. Foremost, I would like to express my deepest gratitude to Professor Joseph G. Shapter for his continuous support of my doctoral study, motivation and immense knowledge, that helped me reach this milestone in my life. I attribute my success in doctoral program to his excellent scientific guidance, encouragement and invaluable experience.

Secondly, I would like to thank my supervisor Professor Mats R. Andersson for his suggestions and guidance throughout this journey that helped me carry out this doctoral study successfully. Special thanks must be given to Dr. Jason Gascooke for his valuable guidance and excellent support in sample analysis. I am truly thankful to Mr. Cheylan Mckinley for his endless help with instrument training. I very much appreciate Mr. Andrew Dunn and Mr. Christopher Price for their technical support, which is a very vital part of this research study.

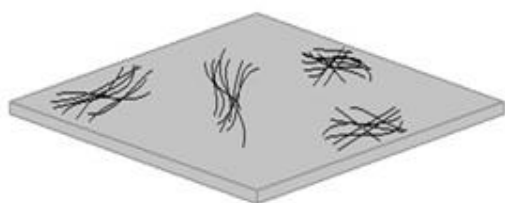
Further, I would like to express my gratitude to all our lab members and colleagues, who have made my Ph.D. study fruitful and enjoyable at Flinders University. I would like to extend my sincerest thanks and appreciation to those patient souls who helped me to learn about and use many state of the art facilities critical to successfully complete high quality research reported in this thesis. These people are Dr. Christopher Gibson, Dr. Cameron Shearer, Dr. Munkhbayar Batmunkh, Alex Sibley, Tom Grace, Xuan Luo, Liam Brownlie, Guler Kocak at Flinders University.

I would like to acknowledge the Research Training Program (RTP) during my Ph.D. study at Flinders. I would also like to acknowledge the expertise, equipment and support provided by the Australian Microscopy and Microanalysis Research Facility (AMMRF) and the Australian National Fabrication Facility (ANFF) at the South Australian nodes of the AMMRF and ANFF under the National Collaborative Research Infrastructure Strategy.

None of this could have been possible without the strong support of my family. Words cannot express the feelings I have for my parents Namasivayam Ramalingam and Ananthi Namasivayam for their unconditional love and endless support. Finally, I thank my lovely wife Ramalakshmi Kalimuthu for her constant support and encouragement throughout these years.

## ABSTRACT

Polymer matrices have some interesting advantages to offer such as being light weight, cost effective and many more. Introducing a conductive filler like carbon nanotubes (CNTs) can enhance the properties of the polymer composite for various industrial applications. Although, carbon nanotubes act as an effective filler, aggregate formation in polymer matrix due to the high van der Waals interactions between the nanotubes is inevitable. Surface functionalization of nanotubes is the best approach to reduce the interaction between nanotubes and can provide stable dispersions in organic solvents. Covalent functionalization has proven effective in terms of stability but the chances of causing damage to the CNTs and altering their intrinsic properties are high. Non-covalent functionalization of nanotubes is an excellent way to overcome aggregate formation and achieve a homogeneous dispersion of nanotubes in the polymer matrix without disrupting the intrinsic characteristics of the nanotubes. In this work, analysis of the physical properties of a non-covalently functionalized carbon nanotube/PVDF composites was undertaken. The amount of CNTs and Polyvinylidene fluoride polymer was essentially kept constant, with only the concentration of the functionalization polymer varied.



Non-functionalized CNT in Polymer Matrix



Functionalized CNT in Polymer Matrix

The first component of this work concentrated on analysis of the effect of the molecular weight of water-soluble polymer (Polyvinylpyrrolidone - PVP) for non-covalent functionalization of carbon nanotubes. A study with four different molecular weights of PVP was conducted. This study discusses the change in polymer wrapping behaviour of different molecular weight with respect to the aspect ratio of nanotubes, amount of nanotubes and structure of nanotubes. The second aspect concentrated on the effect of the structure of the wrapping polymer (Polyvinylpyrrolidone - PVP versus Poly(4-vinylpyridine) – P4VP) on non-covalent functionalization. A comparative study based on polymers of two different structures but of similar molecular weight was conducted. This study discusses the relation between the polymer wrapping pattern of two different polymer structures and the structure of nanotubes. A final

study on non-covalently functionalized cationic polymer (Polyethyleneimine- PEI) in the CNT/PVDF composite was conducted with two different molecular weights of PEI. This is a confirmation study to ascertain the polymer wrapping behaviour of two different molecular weights and its relationship with the structure of nanotube.

## List of Figures:

### Chapter 1

- Fig. 1.1.1: a) Schematic of three different rolling patterns of graphite to form CNT; b) three different structures of nanotubes.
- Fig. 1.1.2: Thermal conductivity as a function of temperature.
- Fig. 1.2.1: Thermal conductivity as a function of the number of chips per gram (number of solid particles per gram) of five different poly (ethylene terephthalate) PET.
- Fig. 1.2.2: Thermal conductivity as a function of molecular weight of five different poly (ethylene terephthalate) PET.
- Fig. 1.2.3: Thermal conductivity as a function of viscosity of five different poly (ethylene terephthalate) PET.
- Fig. 1.2.4: Influence of heat stretching on the thermal conductivity of Ultra High Molecular-Weight Polyethylene (UHMW-PE).
- Fig. 1.3.1: Schematic representation of CNT functionalization.
- Fig. 1.4A: Thermal conductivity of composites with various contents of pristine MWCNTs, acid treated MWCNTs and BTC (benzenetricarboxylic acid) treated MWCNTs.
- Fig. 1.4B: Variation of thermal conductivity of CNT/PVDF composite (PVDFxC) and 1 wt. % PVP functionalized CNT/PVDF composite (PVDFxC1P).
- Fig. 1.4C: Thermal conductivity of the nanocomposites with respect to carbon loading.
- Fig. 1.4.2A: SEM images of films, prepared from  $1 \text{ g L}^{-1}$  MWCNT suspensions, containing  $0.5 \text{ g L}^{-1}$  of (A) Cholic acid sodium salt (CAS) and (B) Taurocholic acid sodium salt (TCAS).
- Fig. 1.4.2B: Schematic representation showing the role of PVP in functionalization and dispersion of CNTs in PVDF matrix. (a) Interaction between CNTs and PVDF, (b) PVP acts as a bridge to intensify the interfacial interaction between PVDF and CNT, (c) dispersion of CNTs in PVDF matrix and (d) PVP promotes the dispersion of CNTs in PVDF matrix.
- Fig. 1.4.2C: The tensile strength and elongation of epoxy/MWNTs and epoxy/P(GMA-co-VCz)/MWNTs at various loading percentage of MWNTs.
- Fig. 1.4.2D: Volume resistivity of epoxy/P(GMA-co-VCz)/MWNTs at various loading percentage of MWNTs.
- Fig. 1.5.1A: Comparison of Thermal conductivity measurement vs weight percent of long and short CNT.
- Fig. 1.5.1B: Thermal conductivity of the nanocomposite as a function of the loading of carbon nanotubes with different aspect ratio.

- Fig. 1.5.1C. Electrical conductivity of the nanocomposite as a function of the loading of carbon nanotubes with different aspect ratio.
- Fig. 1.5.2A. Axial and Transverse aligned thermal conductivity of CNT composites with respect to volume fraction.
- Fig. 1.5.2B. Schematic of the method to align SWNT by hot-press and peel off.
- Fig. 1.6.1: Structure of Polyvinylidene fluoride (PVDF).
- Fig. 1.7.1: Structure of Polyvinylpyrrolidone.
- Fig. 1.7.2: MD simulation of PVP<sub>816</sub>-AgNP (a, b) and PVP<sub>1440</sub>-AgNP (c, d) in aqueous solution: (a) and (c) An initial configuration of single chain PVP<sub>816</sub>/PVP<sub>1440</sub> wrapped around AgNP. (b) and (d) Equilibrium structure of PVP<sub>816</sub>/PVP<sub>1440</sub> coated AgNP taken at the end of 300 ns – exhibiting higher surface coverage with PVP<sub>1440</sub>.
- Fig. 1.8.1: Structure of Poly(4-vinylpyridine).
- Fig. 1.9.1: Structure of Polyethylenimine.
- Fig. 1.9.2: Cell viability study at different temperature

## Chapter 2

- Fig. 2.3.1: Schematic representation of Raman scattering.
- Fig. 2.3.2: Normalized Raman spectra of nanocomposites acquired for different concentrations of PVP<sub>55000</sub> functionalized P3-SWNT/PVDF composite.
- Fig. 2.5.1: Schematic Representation of thermal conductivity measurement rig.
- Fig. 2.5.2: Observed temperature difference in pure brass material.
- Fig. 2.6.1: Storage modulus graph of PVP<sub>55000</sub> functionalized SWNT/PVDF composite.
- Fig. 2.8.1: SEM images of PVP<sub>55000</sub> functionalised SWNT/PVDF composite a) Anterior view and b) fractured side view.

## Chapter 3

- Fig. 3.3.1: Thermal Conductivity measurements of four different PVP functionalized AP-SWNTs in PVDF composites.
- Fig. 3.3.2: Crystallization vs PVP wt. % of PVP functionalized AP-SWNTs in PVDF composites.
- Fig. 3.3.3: Electrical Conductivity measurements of four different PVP functionalized AP-SWNTs in PVDF composites.
- Fig. 3.3.4A: Glass transition measurement of four different PVP functionalized AP-SWNTs in PVDF composites.
- Fig. 3.3.4B: Storage modulus measurement of PVP<sub>10000</sub> functionalized AP-SWNTs in PVDF composites.
- Fig. 3.3.4C: Storage modulus measurement of PVP<sub>40000</sub> functionalized AP-SWNTs in PVDF composites.



- Fig. 3.3.4D: Storage modulus measurement of PVP<sub>55000</sub> functionalized AP-SWNTs in PVDF composites.
- Fig. 3.3.4E: Storage modulus measurement of PVP<sub>360000</sub> functionalized AP-SWNTs in PVDF composites.
- Fig. 3.3.5A: Scanning electron microscope results of non-functionalized AP-SWNTs in PVDF composite; (A) anterior view and (B) fractured side-view - agglomeration of nanotubes are highlighted in red circles.
- Fig. 3.3.5B: Scanning Electron Microscopy results of PVP functionalized AP-SWNTs in PVDF composite - PVP<sub>10000</sub> (A & B) – alignment like formation highlighted in green circle, PVP<sub>40000</sub> (C & D), PVP<sub>55000</sub> (E & F), and PVP<sub>360000</sub> (G & H); anterior view (left) and fracture side view (right).

Fig. 3.3.6: G-band of a Raman spectra of unmodified AP-SWNTs in PVDF composite, PVP<sub>55000</sub> functionalized AP-SWNTs in PVDF composite prepared at a PVP concentration of 6.98 wt. % and 16.67 wt. %.

#### Chapter 4

- Fig. 4.3.1A: Thermal Conductivity measurements of four different PVP functionalized P3-SWNTs in PVDF composites.
- Fig. 4.3.1B: Thermal Conductivity measurements of two different PVP functionalized P3-SWNTs in PVDF composites measured at higher concentration.
- Fig. 4.3.1C: 3-D surface plot of PVP<sub>10000</sub>@ P3-SWNTs in PVDF composites measured for four different concentrations of P3-SWNT.
- Fig. 4.3.1D: 3-D surface plot of PVP<sub>40000</sub>@ P3-SWNTs in PVDF composites measured for four different concentrations of P3-SWNT.
- Fig. 4.3.2: Crystallization vs PVP wt. % of P3-SWNT/PVDF composites.
- Fig. 4.3.3: Electrical Conductivity measurement of four different PVP functionalized P3-SWNTs in PVDF composites.
- Fig. 4.3.4A: Glass transition measurement of four different PVP functionalized P3-SWNTs in PVDF composites.
- Fig. 4.3.4B: Storage modulus measurement of PVP<sub>55000</sub> functionalized P3-SWNTs in PVDF composites.
- Fig. 4.3.4C: Storage modulus measurement of PVP<sub>360000</sub> functionalized P3-SWNTs in PVDF composites.
- Fig. 4.3.4D: Storage modulus measurement of PVP<sub>40000</sub> functionalized P3-SWNTs in PVDF composites.
- Fig. 4.3.4E: Storage modulus measurement of PVP<sub>40000</sub> functionalized P3-SWNTs in PVDF composites.

- Fig. 4.3.5A : Scanning Electron Microscopy results of non-functionalized P3-SWNTs in PVDF composite; anterior view (A) and fractured side view (B)- agglomeration of nanotubes are highlighted in red circles.
- Fig. 4.3.5B : Scanning Electron Microscopy results of PVP functionalized P3-SWNTs in PVDF composite - PVP<sub>10000</sub> (A & B), PVP<sub>40000</sub> (C & D), PVP<sub>55000</sub> (E & F), and PVP<sub>360000</sub> (G & H) – uniform dispersion highlighted in green circle; anterior view (left) and fracture side view (right).
- Fig. 4.3.6: G-band of a Raman spectra of unmodified P3-SWNTs in PVDF composite, PVP<sub>55000</sub> functionalized P3-SWNT/PVDF composite prepared at a PVP concentration of 2.44 wt. % and 16.67 wt. %.

### Chapter 5

- Fig. 5.3.1: Thermal conductivity measurements of three different PVP functionalized MWNTs in PVDF composites.
- Fig. 5.3.2: Crystallization vs PVP wt. % of PVP functionalized MWNTs in PVDF composites.
- Fig. 5.3.3: Electrical conductivity measurements of three different PVP functionalized MWNTs in PVDF composites.
- Fig. 5.3.4A: Glass transition measurement of three different PVP functionalized MWNTs in PVDF composites.
- Fig. 5.3.4B: Storage modulus measurement of PVP<sub>10000</sub> functionalized MWNTs in PVDF composites.
- Fig. 5.3.4C: Storage modulus measurement of PVP<sub>40000</sub> functionalized MWNTs in PVDF composites.
- Fig. 5.3.4D: Storage modulus measurement of PVP<sub>55000</sub> functionalized MWNTs in PVDF composites.
- Fig. 5.3.5A: Scanning electron microscope results of non-functionalized MWNTs in PVDF composite; (A) anterior view and (B) fractured side-view - agglomeration of nanotubes are highlighted in red circles
- Fig. 5.3.5B: Scanning Electron Microscopy results of PVP functionalized MWNTs in PVDF composite - PVP<sub>10000</sub> (A & B), PVP<sub>40000</sub> (C & D), and PVP<sub>55000</sub> (E & F); anterior view (left) and fracture side view (right).
- Fig. 5.3.6: G-band of a Raman spectra of unmodified MWNTs in PVDF composite, PVP<sub>55000</sub> functionalized MWNT/PVDF composite prepared at a PVP concentration of 2.44 wt. % and 16.67 wt. %.
- Fig. 5.5.1: PVP<sub>55000</sub> functionalized AP-SWNTs deposited on a solid substrate (green circle highlighting PVP functionalization).
- Fig. 5.5.2: PVP<sub>55000</sub> functionalized P3-SWNTs deposited on a solid substrate (green circle highlighting PVP functionalization).

- Fig. 5.5.3: PVP<sub>55000</sub> functionalized MWNTs deposited on a solid substrate (green circle highlighting PVP functionalization).

### *Chapter 6*

- Fig. 6.3.1: Thermal conductivity measurements of PVP or P4VP functionalized AP-SWNTs in PVDF composites.
- Fig. 6.3.2: Crystallization vs PVP or P4VP wt. % of non-covalently functionalized AP-SWNTs in PVDF composites.
- Fig. 6.3.3: Electrical conductivity measurements of PVP/P4VP functionalized AP-SWNTs in PVDF composites.
- Fig. 6.3.4A: Storage modulus measurement of PVP<sub>55000</sub> functionalized AP-SWNTs in PVDF composites.
- Fig. 6.3.4B: Storage modulus measurement of PVP<sub>60000</sub> functionalized AP-SWNTs in PVDF composites.
- Fig. 6.3.5: Thermal conductivity measurements of PVP/P4VP functionalized P3-SWNTs in /PVDF composites.
- Fig. 6.3.6: Crystallization vs PVP/P4VP wt. % of non-covalently functionalized P3-SWNTs in PVDF composites.
- Fig. 6.3.7: Electrical conductivity measurements of PVP/P4VP functionalized P3-SWNTs in PVDF composites.
- Fig. 6.3.8A: Storage modulus measurement of PVP<sub>55000</sub> functionalized P3-SWNTs in PVDF composites.
- Fig. 6.3.8B: Storage modulus measurement of PVP<sub>60000</sub> functionalized P3-SWNTs in PVDF composites.
- Fig. 6.3.9: Thermal conductivity measurements of PVP/P4VP functionalized MWNTs in PVDF composites.
- Fig. 6.3.10: Crystallization vs PVP/P4VP wt. % of non-covalently functionalized MWNTs in PVDF composites.
- Fig. 6.3.11: Electrical conductivity measurements of PVP/P4VP functionalized MWNTs in PVDF composites.
- Fig. 6.3.12A: Storage modulus measurement of PVP<sub>55000</sub> functionalized MWNTs in PVDF composites.
- Fig. 6.3.12B: Storage modulus measurement of PVP<sub>60000</sub> functionalized MWNTs in PVDF composites.

### *Chapter 7*

- Fig. 7.3.1: Thermal conductivity measurements of PEI functionalized AP-SWNTs in PVDF composites.

- Fig. 7.3.2: Electrical conductivity measurements of PEI functionalized AP-SWNTs in PVDF composites.
- Fig. 7.3.3A: Storage modulus measurement of PEI<sub>800</sub> functionalized AP-SWNTs in PVDF composites.
- Fig. 7.3.3B: Storage modulus measurement of PEI<sub>25000</sub> functionalized AP-SWNTs in PVDF composites.
- Fig. 7.3.4: Thermal conductivity measurements of PEI functionalized P3-SWNTs in PVDF composites.
- Fig. 7.3.5: Electrical conductivity measurements of PEI functionalized P3-SWNTs in PVDF composites.
- Fig. 7.3.6A: Storage modulus measurement of PEI<sub>800</sub> functionalized P3-SWNTs in PVDF composites.
- Fig. 7.3.6B: Storage modulus measurement of PEI<sub>25000</sub> functionalized P3-SWNTs in PVDF composites.
- Fig. 7.3.7: Thermal conductivity measurements of PEI functionalized MWNTs in PVDF composites.
- Fig. 7.3.8: Electrical conductivity measurements of PEI functionalized MWNTs in PVDF composites.
- Fig. 7.3.9A: Storage modulus measurement of PEI<sub>800</sub> functionalized MWNTs in PVDF composites.
- Fig. 7.3.9B: Storage modulus measurement of PEI<sub>25000</sub> functionalized MWNTs in PVDF composites.

### *Chapter 9*

- Fig. 9.3A: SEM (i and ii) and TEM (iii and iv) micrograph of MWNT in the composite film and Emeraldine Salt (ES) wrapped MWNT in the composite film.
- Fig. 9.3B: TEM image showing the typical morphology of PVP treated MWNTs.

### List of Tables:

#### *Chapter 1*

- Table 1.2.1: Thermal and mechanical properties of most common polymer
- Table 1.4.2A: Comparison of Pros and Cons of Absorption technique.
- Table 1.4.2B: Comparison of Pros and Cons of Wrapping technique.

List of Publications:

- Namasivayam, M.; Shapter, J., Factors affecting carbon nanotube fillers towards enhancement of thermal conductivity in polymer nanocomposites: A review. *Journal of Composite Materials* **2017**, *51* (26), 3657-3668.
- Namasivayam, M.; Andersson, M.R.; Shapter, J. Role of Molecular Weight in Polymer Wrapping and Dispersion of MWNT in a PVDF Matrix. *Polymers* **2019**, *11*, 162.

# CHAPTER 1

## INTRODUCTION

Part of this chapter was published previously in Namasivayam, M.; Shapter, J., Factors affecting carbon nanotube fillers towards enhancement of thermal conductivity in polymer nanocomposites: A review. *Journal of Composite Materials* **2017**, *51* (26), 3657-3668.

## 1.1 Carbon nanotubes

Carbon based materials are now used in various applications including catalysis, drug delivery, electronics, composite materials, sensors as well as in heat exchangers which are crucial in a number of fields including generation of electricity, chemical processing and petroleum refining. Metal heat exchangers that use materials like copper and aluminium might be successful with their high thermal conductivity, but they are not cost effective and are typically heavy. Moreover, corrosion becomes an unavoidable problem with these traditional heat exchangers and causes both economic losses and severe environmental issues. Metal alloys like Cu-Ni alloy offer good resistance to corrosion but can be expensive. Likewise, the recent advances in manufacturing technology permits the use of titanium, which not only exhibits high resistance to corrosion but also due to its low density and high strength can provide more flexibility in design of heat exchangers. However, these corrosion resistant materials have low thermal conductivity compared to copper and aluminium [1].

Since their discovery, extensive research on carbon nanotubes and their potential application in the field of composites has explored their excellent thermal, electrical and mechanical properties. Carbon nanotubes (CNTs) are constructed as hollow cylindrical tubes formed through hexagonal arrangement of carbon atoms with high aspect ratio (~1000) and  $sp^2$  hybridization. This tube can be several microns in length with each end covered by half fullerene molecule cap. It can also be expressed as a sheet of graphene rolled in the form of a tube [2]. Depending on the number of graphene layers, CNTs can be classified as single walled nanotubes (SWNTs), double walled nanotubes (DWNTs) and multi walled nanotubes (MWNTs). Moreover, there are different ways of rolling a sheet of graphene with each end matching a carbon atom leading to different arrangement and geometry. The formation of carbon bonds around the circumference of the nanotube can yield three different structures namely armchair, zig-zag and chiral. This atomic structure is expressed in terms of chirality, a chiral vector ( $C_h=na_1+ma_2$ ) and chiral angle  $\theta$  can be used to define the chirality of a nanotube [3].

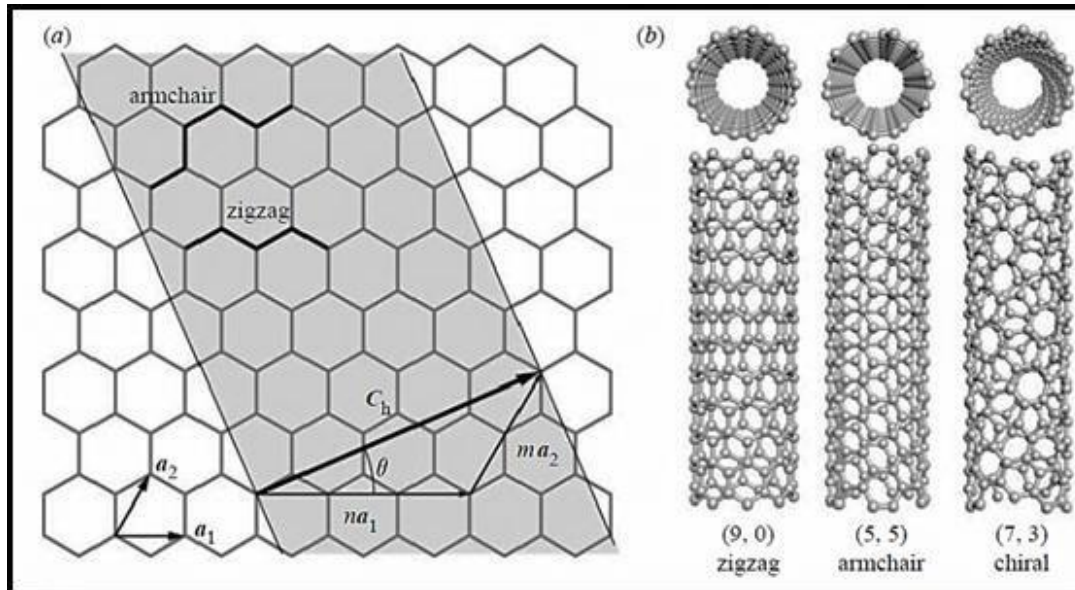


Fig. 1.1.1: a) Schematic of three different rolling patterns of graphene to form CNT; b) three different structures of nanotubes. Reproduced with permission from Ref. [4]

Depending on the chirality, nanotubes can be either metallic or semiconducting in character. In terms of physical and mechanical properties, CNTs possess some tremendous properties including a tensile strength as high as 200GPa and 1.4TPa for SWNTs [5]. They have excellent electrical and thermal properties as well. According to some recent research, the thermal conductivity of SWNT (commercial SWNT samples are mixtures of metallic and semiconducting nanotubes) has been measured to be  $2000 \text{ Wm}^{-1}\text{K}^{-1}$  or above and for MWNT it has been measured to be in the range of  $3000 \text{ Wm}^{-1}\text{K}^{-1}$ [6]. These unique properties elevates carbon nanotubes to be a highly suitable material for a conductive filler in a polymer matrix, forming nanocomposites of improved efficiency.

The thermal conductivity properties of carbon nanotubes are assumed to occur via a phonon conduction mechanism similar to other non-metallic materials. Thermal conductivity measurements in CNTs are mostly based on theoretical simulations and calculations from indirect experiments. Recent thermal conductivity measurements predicts a value between  $200 \text{ W}\cdot\text{m}^{-1}\cdot\text{K}^{-1}$  and  $3000 \text{ W}\cdot\text{m}^{-1}\cdot\text{K}^{-1}$  for MWNTs and above  $2000 \text{ W}\cdot\text{m}^{-1}\cdot\text{K}^{-1}$  for individual SWNT [7] and the thermal conductivity value tends to decrease with temperature [8]. A comparison between thermal properties of SWNTs and MWNTs conducted by Liu et al. reported a lower thermal conductivity in MWNTs than SWNTs. The explanations for the lower conductivity of MWNTs can be attributed to the general assumption that the thermal transport is mainly assisted by the outermost wall and the fact that from theoretical calculations, SWNTs show a high number of phonon vibrational modes and relatively low defect density leading to high



thermal conductivity [9]. There are other parameters in addition to the basic structural morphology that affects the thermal conductivity of carbon nanotubes including chirality, diameter and length of the tube and number of structural defects [10, 11].

Since the mechanism of heat conduction is highly dependent on the band gaps of the material, the thermal conductivity is profoundly dependent on the chirality of the nanotubes which determines the size of their band gaps and electronic properties. In an experiment conducted by Zhang et al., it was reported that the zig-zag and arm chair nanotubes happen to have higher thermal conductivity compared to chiral nanotubes [12]. Atom chains in chiral nanotubes unlike armchair and zig-zag are not parallel to the axis as shown in Fig. 1.1.1. Instead they are in a helix and thus the vibration in atomic chain is likely to have a longer path which causes the low thermal conductivity. Also, comparatively zig-zag nanotubes happen to have higher thermal conductivity than armchair nanotubes, as the sigma bonds along the circumference are strongly strained which in turn lowers the phonon mean free path and thus lowers thermal conductivity. It is also reported that irrespective of the structure, all three types of nanotubes show similar temperature dependence exhibiting a peak in the range from 100 K to 500 K as observed in Fig. 1.1.2 and the thermal conductivity of a single-walled nanotube bulk sample increases with increasing temperature in the range of 0 to 300 K, provided the numbers of the three types of nanotube are equal in a bulk sample.

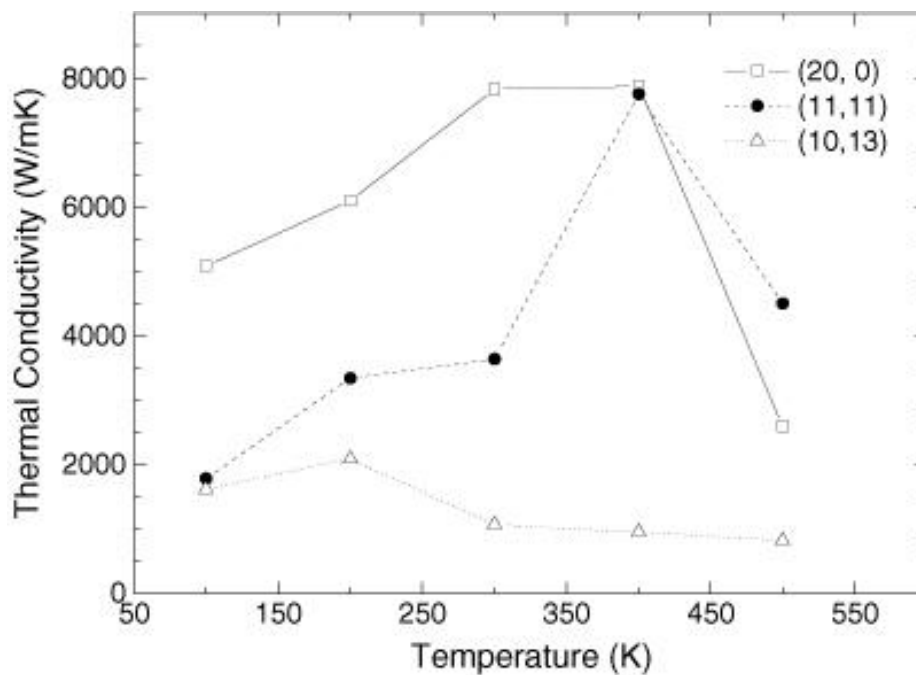


Fig. 1.1.2: Thermal conductivity as a function of temperature conducted with nanotubes of three different structure; zig-zag (20, 0), armchair (11, 11) and chiral (10, 13). Reproduced with permission from Ref. [12]

As described earlier, carbon nanotubes can be defined based on their morphology into single-walled nanotubes (SWNT) or multi-walled nanotubes. Diameter-wise SWNT are smaller than MWNT, which has a significant impact on their thermal conductivity. M. Fujii et al. reported that the interaction of phonons and electrons between the multi-walled layers of a nanotube affects the thermal conductivity[13] meaning, higher number of nanotube layers allows for increased phonon scattering and thus comparatively MWNTs tend to exhibit higher phonon scattering than SWNTs leading to lower thermal conductivity. Likewise, thermal conductivity is also dependent on the tube length and obeys  $L^\beta$  law, where L is the tube length and the value of  $\beta$  being 0.54 ( $100 \text{ nm} < L < 350 \text{ nm}$ ) and 0.77 ( $L < 25 \text{ nm}$ ). The  $\beta$  value depends on the temperature as well as tube radius.  $\beta$  decreases as the temperature increases and at the same temperature  $\beta$  decreases as the tube radius increases. This can be attributed to the fact that at low temperature the vibration of atoms are very small and so the vibration along the transverse axis is much smaller than the ones along the longitudinal axis, whereas at room temperature and at higher temperatures transverse vibration increases and the interaction between transverse mode and longitudinal mode becomes stronger thus leading to a smaller  $\beta$  value [14].

The requirement of present-day heat transfer equipment is that it be compact, lightweight, cheap and possess good manufacturability. Polymers are the most promising material with good anti-corrosion properties and tunable mechanical properties that can be applied for all types of engineered designs. Polymers, though cheap and easy to manufacture, are comparatively poor thermal conductors and the only way of improving this property is through reinforcement with a high thermally conductive fillers in the host matrix. The development of CNT based polymer nanocomposites has evolved significantly over the last two decades owing to their remarkable property enhancement at low filler concentration compared to conventional composites.

## 1.2 Properties of Polymers:

Polymers are large organic molecules comprised of a series of repeating units called monomers connected to each other. They are arranged in long chains typically made out of hydrogen and carbon atoms. In addition to naturally occurring polymers like wood, cotton and rubber, a number of synthetic polymers also exist. These can be categorized a number of different ways but the property of interest to us would be behaviour with respect to thermal conditions and in this regard, a polymer can be distinguished as Thermoplastic; polymers that soften when heated and return to being firm on cooling with a possibility of repeating the process or Thermosets;

plastics that soften when heated and can be molded but permanently harden and when reheated they will decompose[15]. Many of the useful properties of polymers including high strength to weight ratio, toughness, resilience, corrosion resistant, transparency, are in fact unique to polymers and are due to their long chain molecular structure[16].

Properties	Ionomer	LDPE	Nylon-6.6	PC	PEEK	PPS	PPSU	PP	PS	PSU	PTFE	PVDF
Density, g/cc	0.955	0.923	1.12	1.2	1.33	1.43	1.29	0.937	1.05	1.24	2.17	1.78
Water absorption, %	0.01	0.067	2.3	0.17	0.21	0.031	0.37	0.079	0.088	0.41	0.0042	0.032
Moisture absorption at equilibrium, %	0.011	0.01	2	0.27	0.46	0.03	0.85	0.1	0.089	0.32		0.018
Tensile strength, ultimate, MPa	27.1	11	73.1	64	110	86.7	76	36.8	44.9	72	33.6	42.8
Tensile strength, yield, MPa	14.3	10.8	63.6	62	98.8	68.9	72	30.7	43.9	74.9	11.6	44
Elongation at break, %	440	190	82.8	98	36.7	4.1	60	120	6.9	56.8	400	64.6
Tensile modulus, GPa	0.3	0.21	2.1	2.3	4.5	3.6	7.2	1.9	3	2.5	0.61	1.8
Flexural modulus, GPa	0.25	0.27	2.4	2.3	4.8	4.9	2.4	1.4	2.8	2.8	0.52	1.7
Flexural yield strength, MPa			88.4	91.8	170	140	130	36.2	84.2	100		44.2
CTE, linear 20 °C, $\mu\text{m}/\text{m}\cdot^\circ\text{C}$	150	210	100	70.2	44.1	39.2	55.8	120	79.8	60.1	100	140
CTE, linear 100 °C, $\mu\text{m}/\text{m}\cdot^\circ\text{C}$			100	65	39.2	170	55			60	140	145
Thermal conductivity, W/m-K	0.24	0.3	0.26	0.2	0.25	0.3	0.35	0.11	0.14	0.22	0.27	0.19
Melting point, °C	85.1	110	250		340	280		160			330	160
Glass temperature, °C				150	140	88	220		90.4	190		-37.6
Specific heat capacity, J/g·°C	2.4	2.2	2.2	1.2	2			2	2.1	1.2	1.4	1.5

Table 1.2.1: Thermal and mechanical properties of most common polymer. Reproduced with permission from Ref. [15]

But when considering their physical properties, most polymers happen to have a very limited thermal conductivity as shown in Table 1.2.1. This could be due to the fact that, thermal conductivity in most polymer matrices occur through phonon's quantized modes of vibration occurring in rigid lattice. Unlike gases, solids or liquids, phase free movements of electrons are not possible leading to low thermal conductivity but there are strategies to improve electron movements. Thermal conductivity of polymers can be calculated through Debye equation,

$$k = \frac{C_p v \lambda}{3}$$

Where,  $C_p$  is the specific heat capacity per unit volume;  $v$  is the average phonon velocity;  $\lambda$  is the phonon free path [17].

Crystallinity of the polymer also affects the thermal conductivity. Thermal conductivity is highly dependent on the polymer chain orientation and thermal energy transports efficiently along the polymer chain [18]. High thermal conductivity is observed in crystalline polymers as they possess highly ordered polymer chain segments with low defect sites and as a result, they exhibit less phonon scattering. However, amorphous polymers show very low thermal conductivity due to phonon scattering at numerous defects [19]. Besides crystallinity, other factors like molecular weight, molecular density distribution, bond structure, and temperature

also have influence over thermal conductivity of a polymer as shown in Fig. 1.2.1 – 1.2.4. Although polymers have several beneficial properties, improving their thermal conductivity would be the first step in fabricating a useful polymer for a heat exchange application.

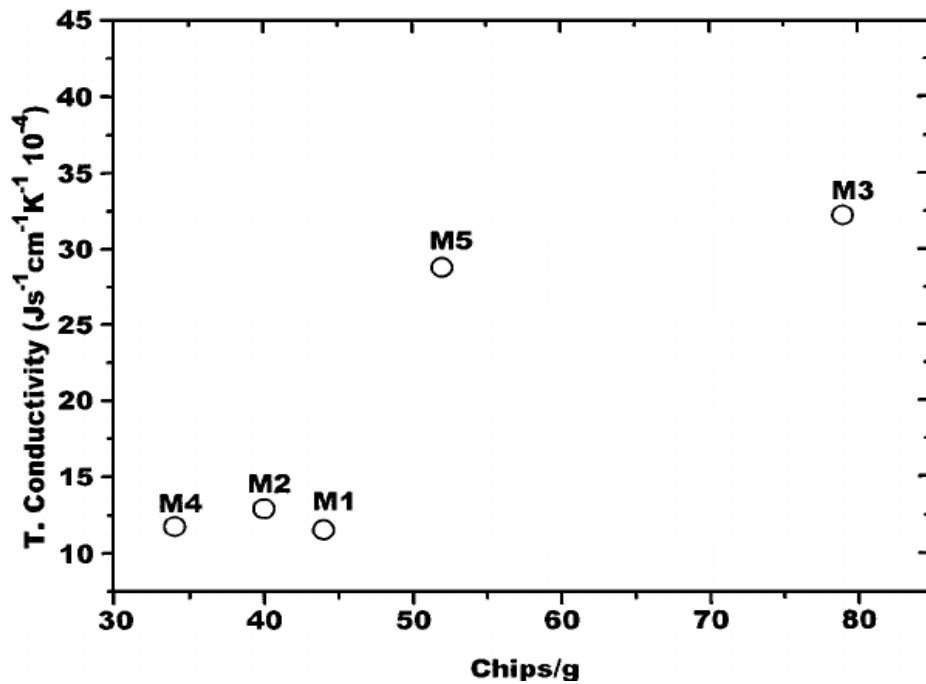


Fig. 1.2.1: Thermal conductivity as a function of the number of chips per gram (number of solid particles per gram) of five different poly (ethylene terephthalate) PET. Reproduced with permission from Ref. [20]

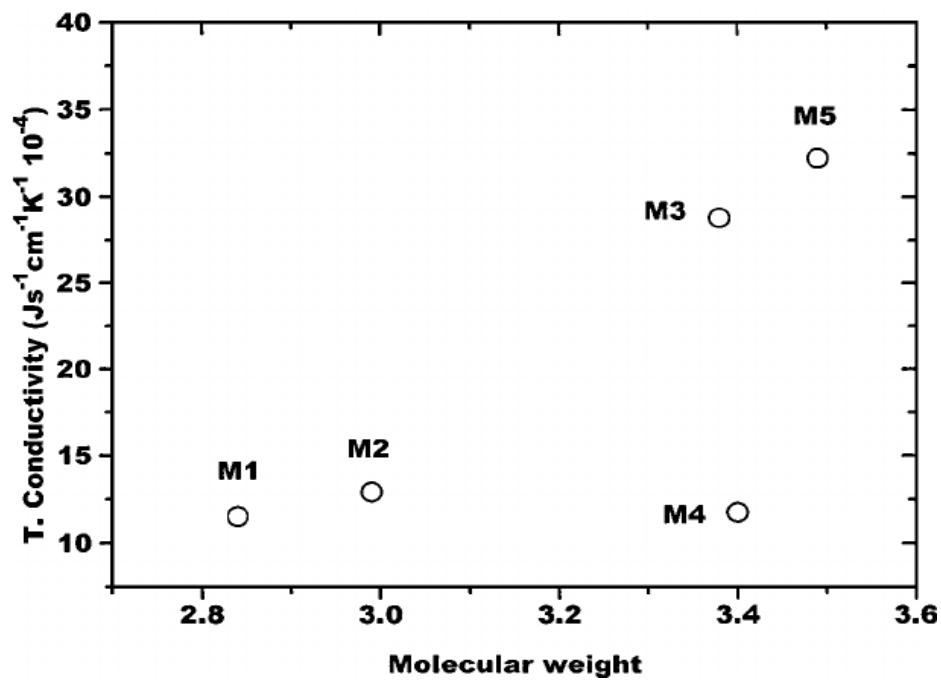


Fig. 1.2.2: Thermal conductivity as a function of molecular weight of five different poly (ethylene terephthalate) PET. Reproduced with permission from Ref. [20]

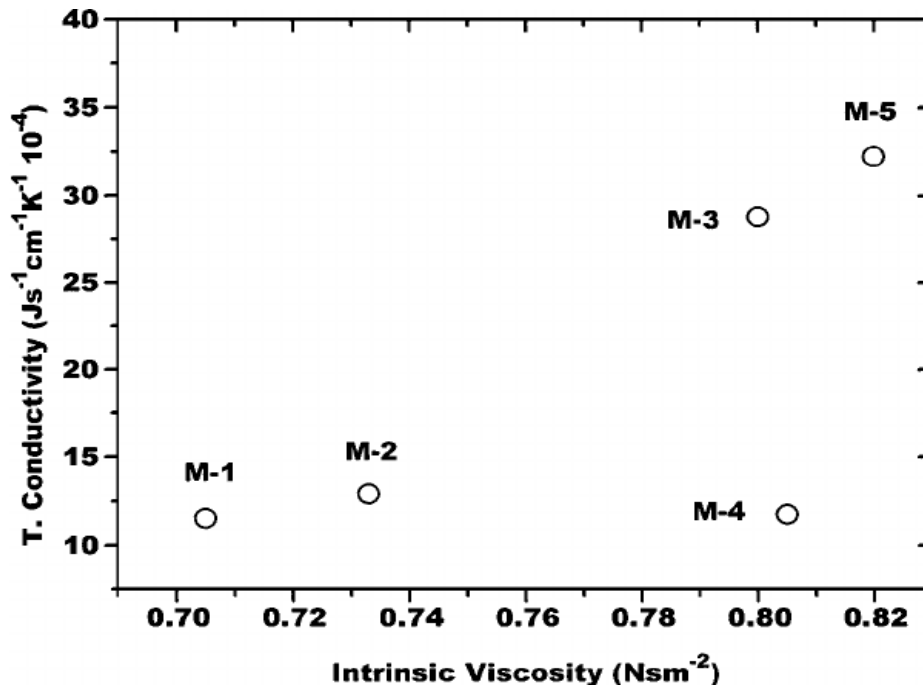


Fig. 1.2.3: Thermal conductivity as a function of viscosity of five different poly (ethylene terephthalate) PET. Reproduced with permission from Ref. [20]

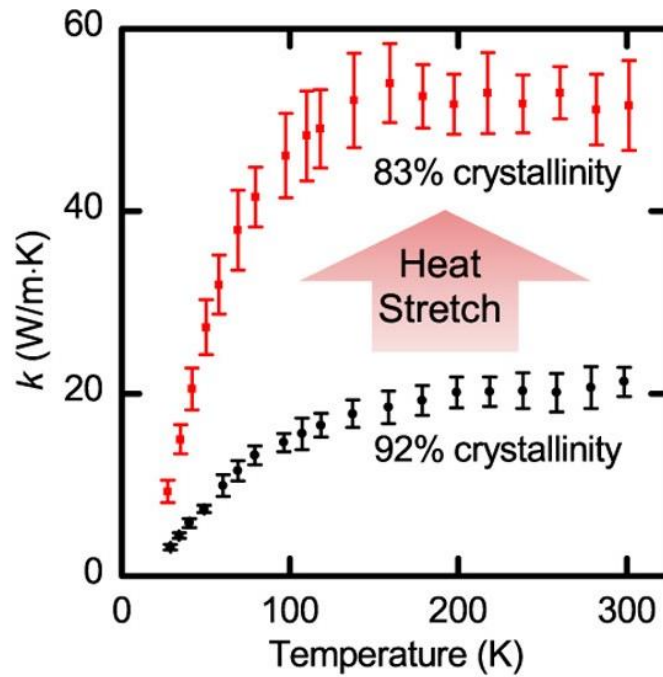


Fig. 1.2.4: Influence of heat stretching on the thermal conductivity of Ultra High Molecular-Weight Polyethylene (UHMW-PE). Reproduced with permission from Ref. [21]

### 1.3 Polymer Nanocomposites

The biggest challenge faced in the development of CNT based polymer nanocomposites would be the intrinsic strength of their agglomerates which prevents good filler distribution in the

matrix. Two fundamental and critical issues must be resolved during the preparation of CNT reinforced polymer composite. Primarily a homogeneous dispersion state of CNTs in polymer matrix must be achieved and secondly the interfacial adhesion between the CNTs and polymer must be improved [22]. CNTs have poor interfacial interaction with polymer matrix owing to the high specific area, van der Waals interaction and  $\pi$ - $\pi$  interaction of nanotubes making them difficult to disperse successfully in polymers, which has a bad effect on the properties of CNTs/polymer composite. When CNTs aggregate, their excellent mechanical and electrical properties are partially lost [23]. One of the best approaches to prevent nanotube aggregation in the polymer matrix is through surface functionalisation. There are various approaches for CNT functionalization including defect functionalization, covalent functionalization, and non-covalent functionalization [24]. Covalent functionalisation on the surface of nanotubes are favoured due to the presence of hydroxyl, epoxy and carboxyl groups [25]. However, non-covalent interaction between CNTs and the polymer matrix is possible with the presence of  $sp^2$  hybridized  $\pi$  network [26].

The covalent modification of CNTs is based on the covalent linkage of functional groups on the outer CNT wall and during an oxidative reaction process, these functional groups react with the carboxylic groups located on CNT defects or other oxygenated groups formed in the process. However, non-covalent functionalisation is realized either by enthalpy-driven interaction such as  $\pi$ - $\pi$ , CH- $\pi$ , NH- $\pi$  between the surface of the CNTs and the dispersants or by entropy-driven interaction such as hydrophobic interaction between the adsorbed molecule (surfactants) and the surface of nanotubes [27].

In terms of stability of functionalization, covalent modification holds a superiority over non-covalent approach especially if the effective reinforcement of the polymer film is possible with covalent modification due to the effective load transfer from the polymer matrix to the CNTs through covalent bonding [28, 29]. Although effective, this method has a high chance of causing damage to CNTs, often cutting them into shorter tubes and the intrinsic properties such as conductivity and mechanical toughness are altered [30]. On the other hand, non-covalent functionalisation preserves the intrinsic properties of CNTs in the polymer matrix and are characterized just by mixing CNTs with molecules under a shear force treatment such as sonication. This kind of interaction does not just enhance solubilisation but also maintains the maximum intrinsic characteristic of an individual nanotube, without altering their original structure and electronic properties.

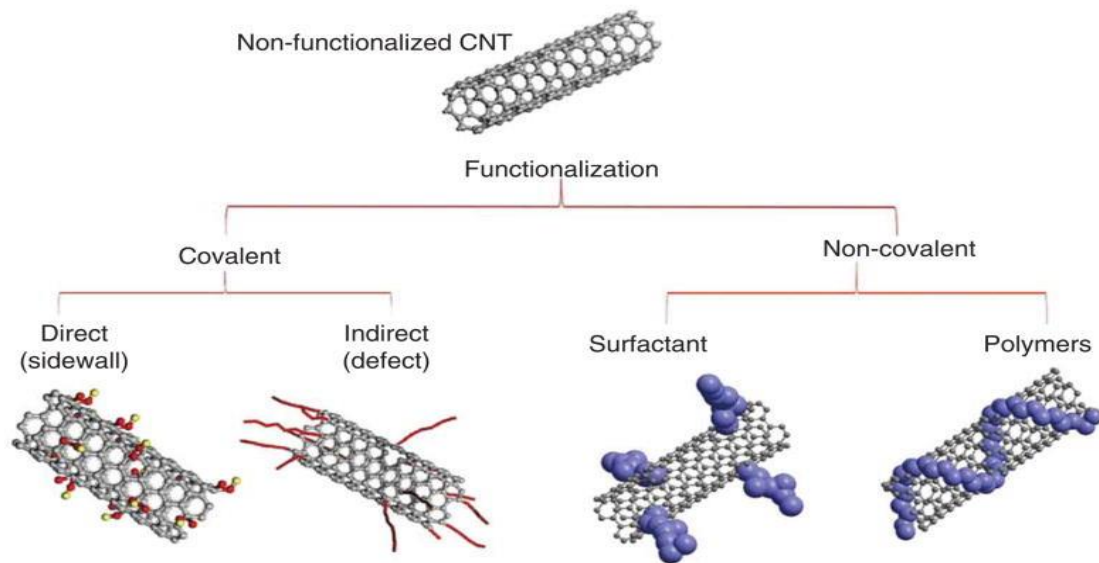


Fig. 1.3.1: Schematic representation of CNT functionalization

#### 1.4 Functionalization

The performance of a CNT/polymer nanocomposite depends mainly on CNT dispersion in the polymer matrix and their inability to disperse effectively in a matrix still poses a tremendous hurdle towards taking advantage of carbon nanotubes in a wide range of applications. The small size and high aspect ratio of carbon nanotubes leads to the formation of bundles and aggregates in a polymer/CNT composite [31]. J. Hong et al. reported that, a large discrepancy existed between experimentally obtained and predicted thermal conductivity value, due to the aggregation of CNTs in the matrix [32]. A thermal conductivity increase of up to 10% was observed with improved CNT dispersion in the matrix. Many methods like high power ultrasonication, surfactant assisted processing and functionalization of nanotubes were proposed to effectively disperse CNTs in a polymer. P. C. Ma et al. reported that, although mechanical dispersion methods like ultra-sonication, ball milling and calendaring process may have proven to be effective, they are prone to possible damage of CNT structure and these tools may not be suitable for dispersion in all type of polymer matrices [33]. However, functionalization of nanotubes proved to be an effective way to improve the thermal performance of the composite by forming a soft interface between the nanotubes and the polymer matrix thus decreasing the thermal resistance at the interface.

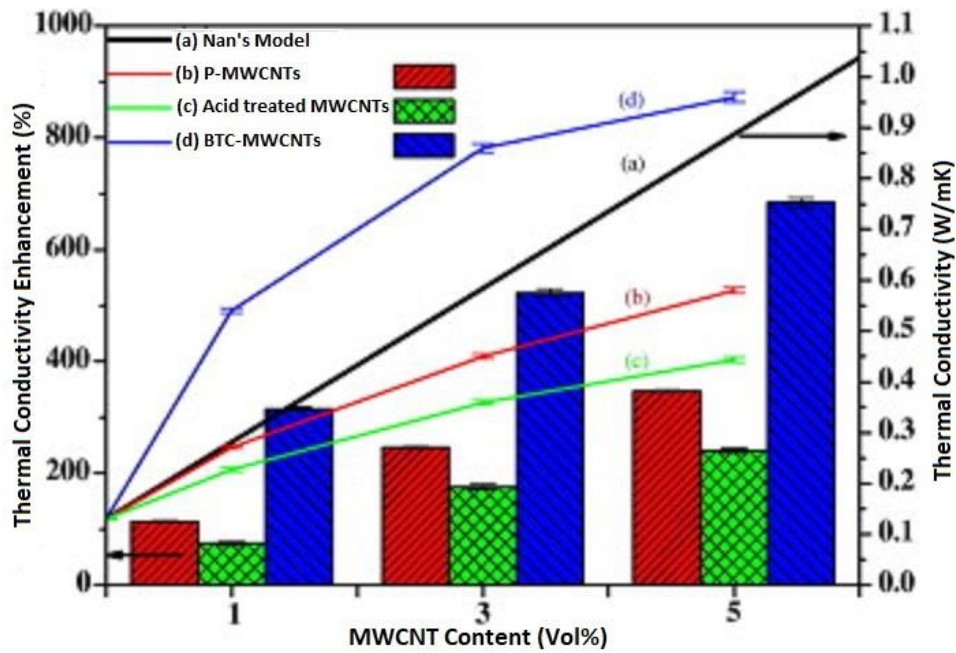


Fig. 1.4A: Thermal conductivity of composites with various contents of pristine MWCNTs, acid treated MWCNTs and BTC (benzenetricarboxylic acid) treated MWCNTs. Reproduced with permission from Ref. [34]

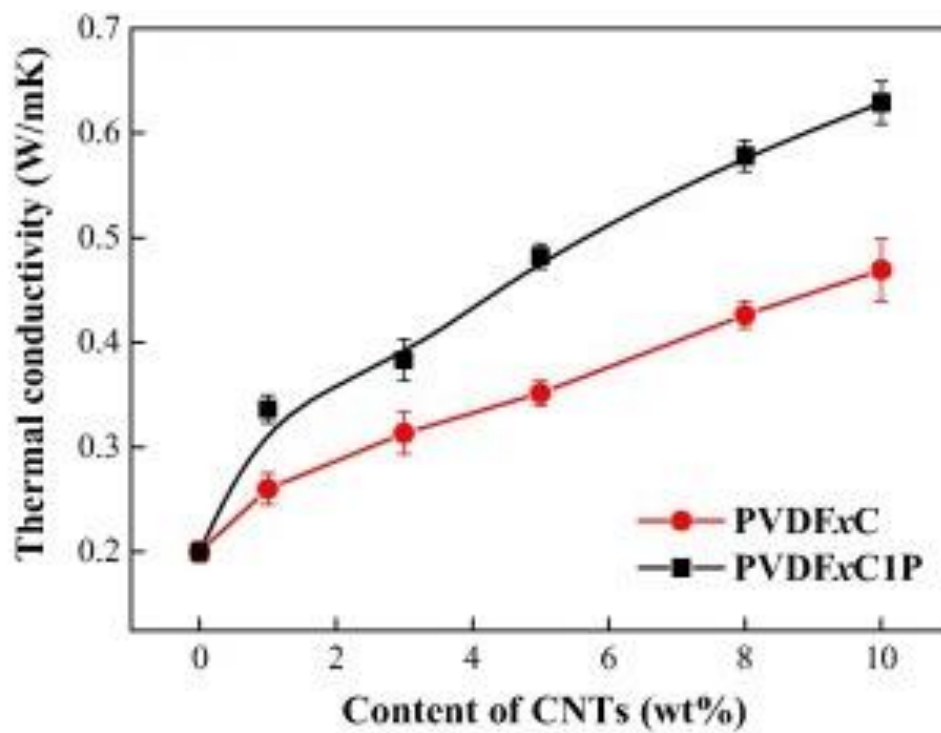


Fig. 1.4B: Variation of thermal conductivity of CNT/PVDF composite (PVDFxC) and 1 wt. % PVP functionalized CNT/PVDF composite (PVDFxCIP). Reproduced with permission from Ref. [35]



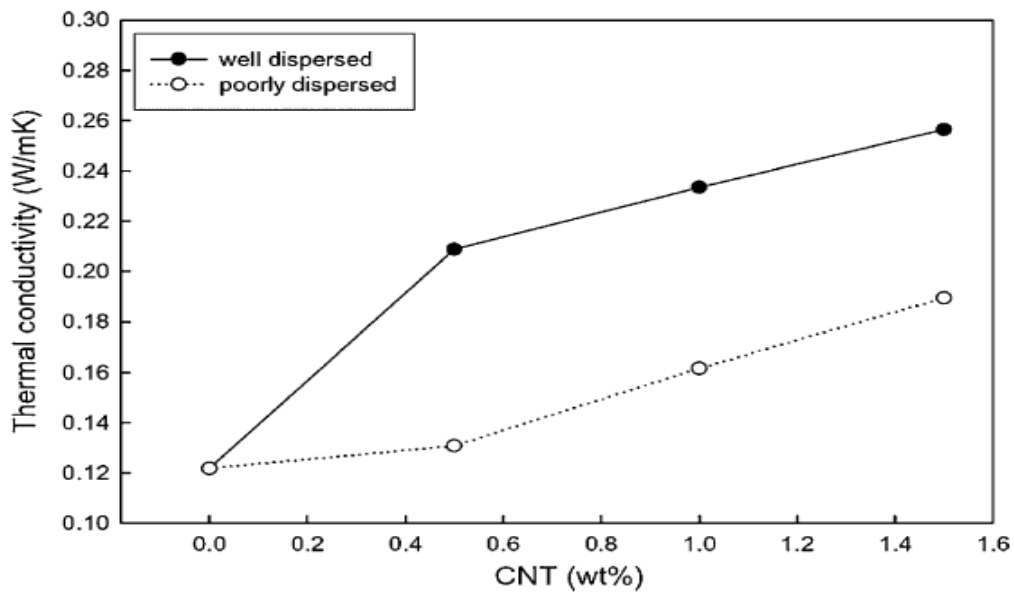


Fig. 1.4C. Thermal conductivity of the CNTs/ epoxy composites with respect to carbon loading. Reproduced with permission from Ref. [36]

#### 1.4.1 Chemical Method

Defect functionalization is a method that takes advantage of the chemical transformation of defect sites on CNTs. Defect sites are created on side walls and at the open ends of CNTs as the result of a strong acid treatment such as concentrated sulphuric acid and/or nitric acid. This leaves the holes functionalized with oxygenated functional groups such as carboxylic acids, ketones etc. CNTs functionalized this way can be used as a precursor for further chemical reactions including covalent functionalization and are effectively partially soluble in organic solvents due to change in their nature from hydrophobic to hydrophilic with the attachment of polar groups. Similarly, an acid-based titration method was used to determine the percentage of acidic sites of purified SWNTs. However, the defect sites created by this method are extremely sparse and they do not promote an effective dispersion of CNT in the polymer matrix [22, 37]. Also, the CNTs are broken into shorter tubes in this oxidizing method, which not only compromises the aspect ratio but also the overall thermal conductivity [22].

Carbon nanotubes have an enhanced tendency to covalently attach themselves to a chemical species because of the  $\pi$  orbitals of  $sp^2$  hybridized carbon atoms. In the case of direct covalent functionalization, the translational symmetry CNT sidewall is disrupted with a change of hybridization from  $sp^2$  to  $sp^3$  carbon atoms and a simultaneous loss of  $\pi$  conjugation system of graphene layer. This process can be accomplished by reaction with some highly reactive

molecules such as fluorine. Amino, alkyl and hydroxyl groups can also be successfully substituted for fluorine atoms and an effective dispersion can be achieved [38]. Shenogin et al. also reported that the chemical bonding significantly reduces the thermal boundary resistance between the nanotubes and the polymer matrix [39]. But, the major negative impact of functionalization by chemical methods is that the CNTs are prone to formation of defect sites along the sidewall and in some extreme cases the CNT structure is highly disrupted. These effects result in a severe degradation of their mechanical properties and the defect sites act as scattering centres for acoustic phonons which are responsible for thermal conduction in CNTs [40]. Secondly, use of concentrated acids is highly unfriendly to the environment. Moreover, the chances of re-agglomeration is also high in these methods [41].

#### *1.4.2 Physical Method*

Non-covalent functionalization is an attractive alternative method to successfully disperse carbon nanotubes in a polymer matrix, without damaging or disrupting the intrinsic properties of carbon nanotubes. In this method, organic mediating molecules such as surfactants, aromatic compounds and polymers were used to non-covalently functionalize nanotubes. CNTs surface characteristics are altered by these mediating molecules either through adsorption or by wrapping of polymer onto the surface [42]. Clever selection of the polymer allows in situ polymerization in the presence of CNTs which can produce high quality composites [43].

#### *Adsorption*

Surfactant molecules that are physically adsorbed onto the surface of the CNTs lower the surface tension thus preventing the CNTs from forming aggregates and effectively overcoming the van der Waals interaction by electrostatic or steric repulsive forces. Whereas surfactants alone are not capable of dispersing nanotubes effectively, vigorous ultra-sonication is required to weaken the van der Waal's forces between the nanotube bundles to exfoliate into individual nanotubes. The hydrophilic region of the surfactant interacts with the polar solvent molecules whereas the hydrophobic region adsorbs on the surface of CNT thus enhancing the dispersibility of the CNT in a non-destructive approach. The process of dispersing CNT into individual nanotubes depends strongly on the length of the hydrophobic region and the types of hydrophilic groups of the surfactant. D. Ponnamma et al. studied the effect of surfactant adsorbed onto the surface of MWCNT and its role in dispersion in natural rubber latex (NRL) medium with the rheological property of nanocomposites [44]. It has been reported that sodium dodecyl sulphate (SDS) adsorbs on the surface and enhances the rate of MWCNT dispersion

through an electrostatic repulsion mechanism [45]. It was also observed that the anionic head of the SDS attaches itself to the latex surface and the cationic part to the CNTs promoting better interaction of NRL and CNTs forming a uniform dispersion and interfacial interaction. Sun et al. studied stable dispersions of SWNT in deionized water with six different surfactants. The quality of dispersion depends on the electrostatic repulsion force between surfactant coated nanotubes and can be significantly improved by coating nanotubes with surfactants that record a zeta potential of 100mV or higher [46]. Likewise, L. Vaisman et al. studied the role of surfactants in the dispersion of CNTs and concluded that the surfactant adsorption not only enhances the dispersion quality but also the behaviour of surfactant in dispersing CNTs is similar to that of dispersing solid particles [47]. So far, most studies have been conducted for surfactant assisted carbon nanotube dispersion in aqueous medium. However, Gong et al. experimented with the surfactant assisted processing of CNT in a polymer matrix and confirmed that using surfactant as a processing aid improves the thermomechanical property of CNT/polymer composite, whereas even with increasing surfactant concentration a complete homogeneous dispersion of nanotube in polymer composite could not be achieved [48]. A complete understanding of the interfacial chemistry and better understanding of the adhesion between carbon nanotubes and the polymer matrix is needed.

Similarly, Ata et al. reviewed a new strategy for the non-covalent functionalization and dispersion of CNTs using small molecules such as commercial salts of bile acids (BAS) and organic dyes [49]. Research interest on BAS and organic dyes have developed recently due to their ability to facilitate CNT dispersion through a bundle ‘unzipping’ mechanism. This mechanism involves formation of gaps or spaces at the CNT bundle ends in the ultrasonicated suspension. The small molecule adsorption and diffusion then propagate the open space along the bundle length facilitating the separation of individual CNTs [50, 51]. Due to high solubility in water, BAS have generated significant interest for CNT dispersion in aqueous suspension. BAS has a rigid amphiphilic structure which is basically different from the typical head tail surfactants, composed of long hydrophobic tails and polar head groups [52, 53]. This rigid amphiphilic structure of BAS allows the formation of stable micelles around SWNT, which facilitates efficient dispersion. Moreover, the structure of BAS also has a short hydrocarbon tail with anionic  $\text{COO}^-$  or  $\text{SO}_3^-$  groups and as a general feature, BAS have convex hydrophobic and concave hydrophilic sides which include methyl and OH groups [53]. The adsorption of BAS on CNTs is largely driven by hydrophobic interaction of hydrophobic convex faces of steroid BAS backbones with CNTs. In a conventional surfactant, the flexible head-tail linear

structures organize themselves perpendicular to the SWNT surface providing a lower coverage level. However, with hydrophobic interaction the steroidal surfactant wraps around SWNT like a ring with hydrophobic faces directed inward and hydrophilic faces pointed outward thus enhancing not just BAS-SWNT interaction but also enhanced BAS coverage on CNT surface [51, 54].

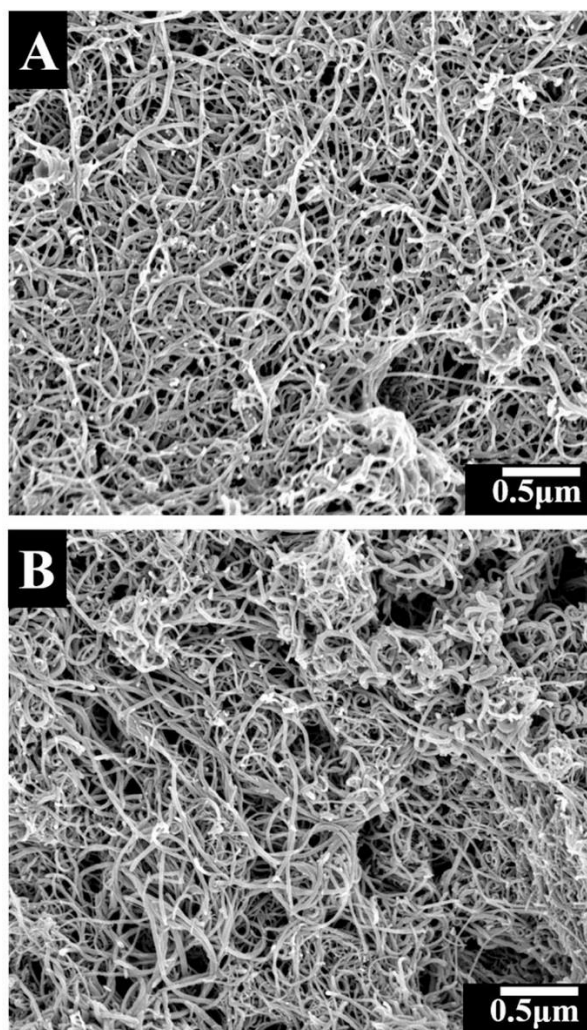


Fig. 1.4.2A: SEM images of films, prepared from  $1 \text{ g L}^{-1}$  MWCNT suspensions, containing  $0.5 \text{ g L}^{-1}$  of (A) Cholic acid sodium salt (CAS) and (B) Taurocholic acid sodium salt (TCAS). Reproduced with permission from Ref. [49]

Likewise, aromatic compounds are known to interact with the graphitic side walls of CNTs via  $\pi$ - $\pi$  interactions and the electronic properties of the CNTs remains unchanged by these interactions [55]. Research on the adsorption of aromatic compound on CNTs revealed the contributions of functional groups aiding in this mechanism in such a way that, adsorption increases with increasing number of aromatic rings and OH substitution group in the aromatic systems. An enhanced  $\pi$ - $\pi$  interaction can be observed in the adsorption behaviour of organic

dyes on CNTs due to their polyaromatic structure and various functional substitution groups of the dyes enhances their adsorption [56]. Dye removal from industrial wastewater using CNT based adsorbents is a subject of intensive investigation [57].

PROS	CONS
<ul style="list-style-type: none"> <li>○ Highly Cost Effective.</li> <li>○ Readiness to commercial disposability.</li> <li>○ Simplicity of use.</li> <li>○ No damage to CNT structure</li> </ul>	<ul style="list-style-type: none"> <li>○ An effective dispersion of CNT is achieved only with an additional external force such as ultra-sonication.</li> <li>○ Re-agglomeration is possible in polymer matrix.</li> </ul>

Table 1.4.2A: Comparison of Pros and Cons of Absorption technique.

### *Wrapping*

Strong  $\pi$ - $\pi$  interaction allows conjugated polymers to adsorb on the CNT surfaces and drives the wrapping of polymer around them forming a supra molecular complex. This weakens the van der Waals interaction between nanotubes and increases dispersibility of CNTs in various polymers. Other forms of polymer wrapping interaction including CH- $\pi$  and Cation- $\pi$ , although comparatively weaker, are capable of forming stable CNT-polymer dispersion. The aqueous solubility of CNTs can be improved through polymer wrapping in water soluble polymers such as polyvinylpyrrolidone (PVP). Phonon transport along the CNT sidewall remains unaffected due to the preservation of  $sp^2$  carbon atoms and thus the CNTs are thermally conductive [58]. CNT functionalized through the polymer wrapping method preserves not just the structure but also their electronic properties which is highly suitable for solar cell applications. G. De Filpo et al. fabricated a dye- sensitised solar cell with non-covalently functionalised SWNTs and recorded a power efficiency of 6.21 % [59]. P. H. Wang et al. studied the effect of polymer coated MWCNT in a polypropylene nanocomposite and observed an overall property enhancement with the presence of polymer wrapping on MWCNTs due to the fact that it proved to be a better nucleating agent for polymer crystallization. A better solvent resistance and homogeneous dispersion is observed in the polymer coated MWCNT/polypropylene nanocomposite than non-coated MWCNT/polymer composite [60]. Similarly Liu et al. studied a non-covalent functionalization of MWCNT using poly (vinylcarbazole) based compatibilizer in epoxy composite and confirmed that the mechanical and electrical properties of the epoxy composites were largely improved with the presence of the compatibilizer as shown in Fig. 1.4.2A and 1.4.2B. It was also mentioned that  $\pi$ - $\pi$  interaction between MWCNTs and the

backbone of P(GMA-*co*-VCz) and the covalent bonding between the epoxide group of P(GMA-*co*-VCz) and the epoxy matrix functions as an effective bridge between MWCNTs and epoxy matrix and thus not only improves the dispersion state of MWCNTs but also greatly enhances their interfacial interactions [61]. J. Huang et al. reported an effective thermal conductivity in polyethyleneimine (PEI) functionalized carbon nanotube in epoxy matrix [62]. Comparatively, PEI functionalized CNTs are better dispersed and exhibit higher thermal conductivity than the non-functionalized ones.

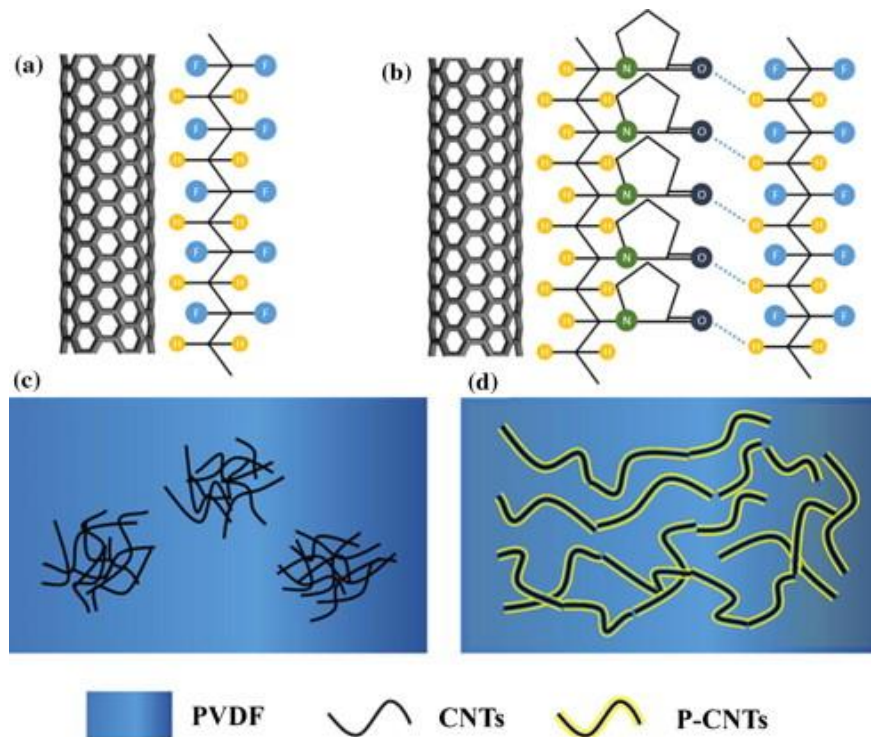


Fig. 1.4.2B: Schematic representation showing the role of PVP in functionalization and dispersion of CNTs in PVDF matrix. (a) Interaction between CNTs and PVDF, (b) PVP acts as a bridge to intensify the interfacial interaction between PVDF and CNT, (c) dispersion of CNTs in PVDF matrix and (d) PVP promotes the dispersion of CNTs in PVDF matrix. Reproduced with permission from Ref. [35]

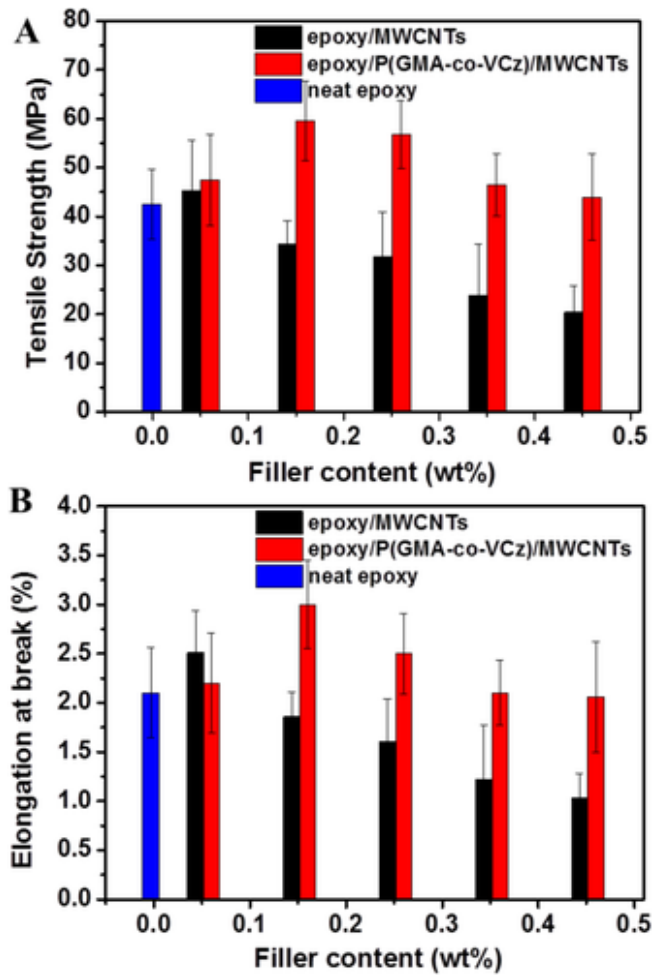


Fig. 1.4.2C. The tensile strength and elongation of epoxy/MWNTs and epoxy/P(GMA-co-VCz)/MWNTs at various loading percentage of MWNTs. Reproduced with permission from Ref. [61]

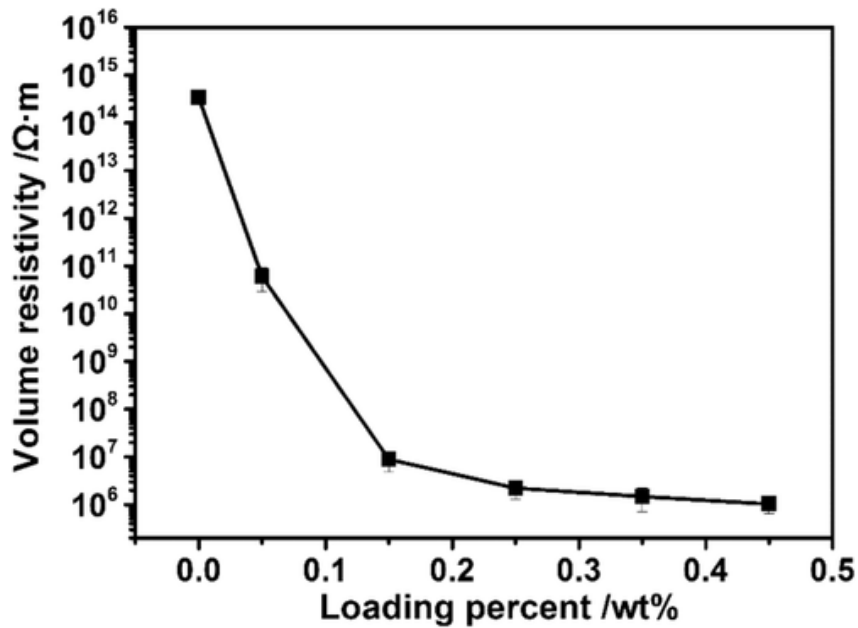


Fig. 1.4.2D. Volume resistivity of epoxy/P(GMA-co-VCz)/MWNTs at various loading percentage of MWNTs. Reproduced with permission from Ref. [61]

Thermal conductivity of the polymer composite depends on both the thermal conductivity of the polymer matrix and the filler [63]. Among the inorganic fillers, carbon nanotubes have been shown to be better at enhancing the thermal conductivity of the polymer matrix, but they fail to match theoretical predictions [43]. This can be attributed to factors like volume fraction, alignment [64] and most importantly dispersion of the nanotubes in the matrix [65]. The interaction of the filler and the matrix plays a key role in designing a composite with high thermal conductivity.

PROS	CONS
<ul style="list-style-type: none"> <li>○ Thermodynamically stable coating on the surface of CNTs.</li> <li>○ Possible to remove unbound polymer without disturbing the polymer wrapping on CNTs.</li> <li>○ No damage to CNT structure.</li> </ul>	<ul style="list-style-type: none"> <li>○ The strength of interaction varies according to the miscibility between matrix and the polymer wrapping on CNT.</li> </ul>

Table 1.4.2B: Comparison of Pros and Cons of Wrapping technique [66].

## 1.5 Limitation in Polymer Nanocomposite

### 1.5.1 Volume Fraction

Percolation theory predicts that with increasing concentration of a high thermal conductivity constituent in a random composite, the thermal conductivity of the matrix increases according to the scaling law i.e.  $\sigma$  which is proportional to  $(\Phi - \Phi_c)^t$ , where  $\Phi$  is the volumetric concentration of the composite,  $\Phi_c$  is the volumetric concentration of the conductor and  $t$  is the conductivity exponent [67]. However, in the case of carbon nanotube/polymer composite either there exists no such thermal percolation concentration or a very low percolation threshold is observed. The lack of thermal percolation in the CNT composite is due to the fact that carbon nanotubes are separated by the formation of a polymer thin film thus preventing a direct phonon transport across nanotubes [68]. Wang et al. showed that incomplete contact at the interface allows large phonon scattering leading to large thermal resistance and thus low thermal conductivity [69]. I. V. Singh et al. reported that the filler interface plays a major role on the effective thermal conductivity of the composite [70]. Increasing the content of CNTs reduces the matrix region between nanotubes in a composite and facilitates their interaction thus contributing to improved thermal conductivity. The effect of the interface on the overall thermal conductivity of composite is smaller for short nanotubes than long nanotubes.



Increasing the volume concentration through changing the length and radius of the nanotube gives a positive outcome towards enhancing the thermal conductivity [71] whereas increasing the amount of the CNTs with constant length has a very minor effect on the effective thermal conductivity of the composite. This can be attributed to the fact that the effective resistance remains almost constant until the length of the nanotube enforced is altered.

Russ et al. also observed only a modest increase in thermal conductivity with increasing the loading percentage of the nanotube filler [72]. However, a sizeable variation in the thermal conductivities between the long and short nanotubes was observed. Higher thermal conductivity is achieved by nanotubes with large aspect ratio than with nanotubes of small aspect ratio at same concentration as shown in Fig.1.5.1A. This can be attributed to the fact that in order to achieve percolation, shorter aspect ratio tubes require exponential increase in the number of contacts resulting in greater phononic scattering and interfacial thermal resistance. Additionally, due to high viscosity of the composite, aggregate formation is inevitable above a certain loading fraction so high aspect ratio nanotubes are a likely candidate for a filler in a polymer composite. Rahul et al. reported enhancement in thermal conductivity with increasing aspect ratio [73]. Likewise, Chen and Yan studied the effect of CNT aspect ratio in epoxy nanocomposite by comparing nanocomposite materials containing CNTs with 800 and 80 aspect ratios and confirmed that the aspect ratio plays an important role in determining the physical property of the nanocomposite, the electrical and thermal conductivity in particular shown in Fig. 1.5.1B & Fig. 1.5.1C. Their findings support the theory that the aspect ratio can affect the nature of percolation network of CNT within a polymer matrix. A high aspect ratio exhibited high thermal and electrical conductivity. The difference observed is explained as the necessity for the sharp increase in the number of contacts required by the nanocomposite material containing low aspect ratio carbon nanotubes to reach the percolation threshold [74]. However, increasing aspect ratio by increasing the length has a greater effect on the thermal conductivity of composite than lowering the diameter. H. S. Kim et al. reported MWCNTs with a high aspect ratio exhibit favourable intertube interaction according to the direction of process orientation and MWCNTs are easily oriented in the in-plane direction [75]. Thus, it is more favourable to enhance in plane thermal conductivity. It has also been observed that the level of defects act as a less important factor compared to the length of nanotube in enhancing thermal conductivity. Despite having high defect level on the MWCNTs and high phonon scattering as a result, the long MWCNTs based composite achieved higher thermal conductivity.

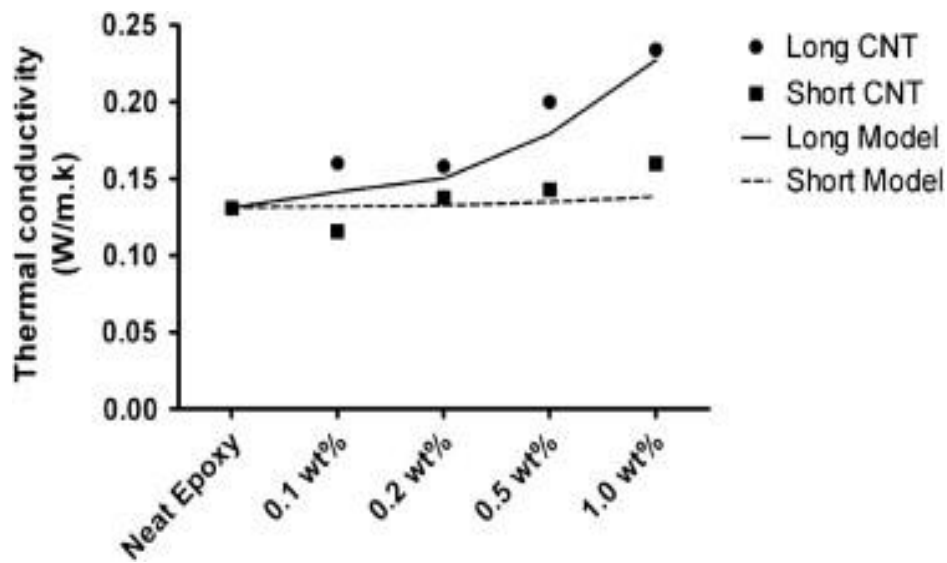


Fig. 1.5.1A. Comparison of Thermal conductivity measurement vs weight percent of long and short CNT. Reproduced with permission from Ref. [72]

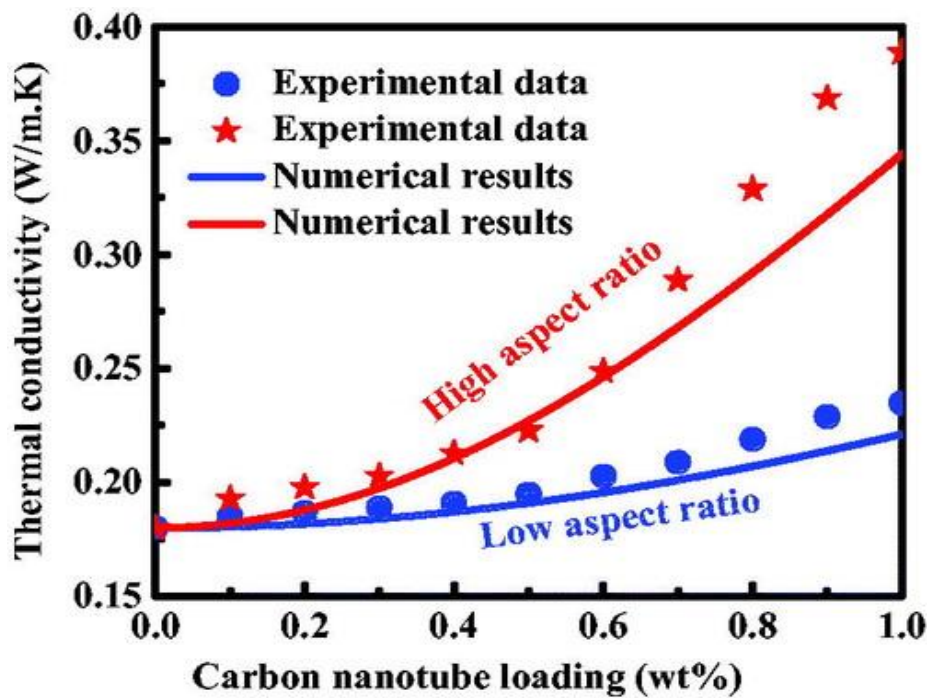


Fig. 1.5.1B. Thermal conductivity of the nanocomposite as a function of the loading of carbon nanotubes with different aspect ratio. Reproduced with permission from Ref. [74]

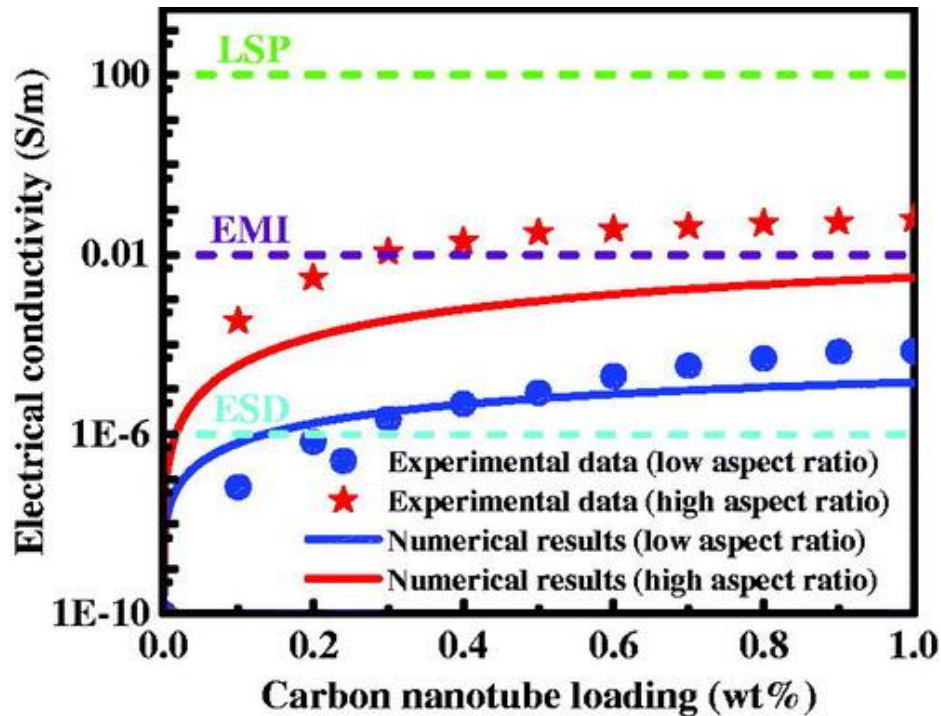


Fig. 1.5.1C. Electrical conductivity of the nanocomposite as a function of the loading of carbon nanotubes with different aspect ratio. Dashed lines represents the lower limit of electrical conductivity required for the specified applications such as lightning strike protection (LSP), electromagnetic interference shielding (EMI), and electrostatic dissipation (ESD) . Reproduced with permission from Ref. [74]

### 1.5.2 Alignment

Enhancing the thermal conductivity of a composite through higher loading of carbon nanotube results in a thermal conductivity value that is far below its theoretical prediction. This is due to the large interface scattering and contact resistance. This can be reduced through alignment of CNTs in the composite thus increasing thermal conductivity. Choi et al. observed enhancement of electrical and thermal conductivity of CNT-epoxy composites with magnetic field processing [76]. It is also reported that cooperative alignment of nanotubes is the main cause for enhancement of electrical and thermal conductivity in the polymer nanocomposite [77]. Although, for alignment achieved through magnetic field processing, high field strength is usually required for preparing bulk composites and due to the relatively low magnetic susceptibility, carbon nanomaterials may need functionalization by introducing magnetic particles so that they can be aligned under a low-strength magnetic field [78]. According to P. Gonnet et al. to fabricate nanocomposites, it is extremely difficult to effectively disperse nanotubes in a polymer matrix beyond 10 wt. % due to the CNT nanoscale dimension and extra-large surface area [79]. Q. Jiang et al. reported that by adding aligned MWNTs in a polymer matrix the thermal conductivity increases by nearly 681 times which is higher than

unidirectional carbon fibre composite and carbon nanotube composite with high volume fraction [80]. This confirms the transfer of phonons along the length direction of nanotubes.

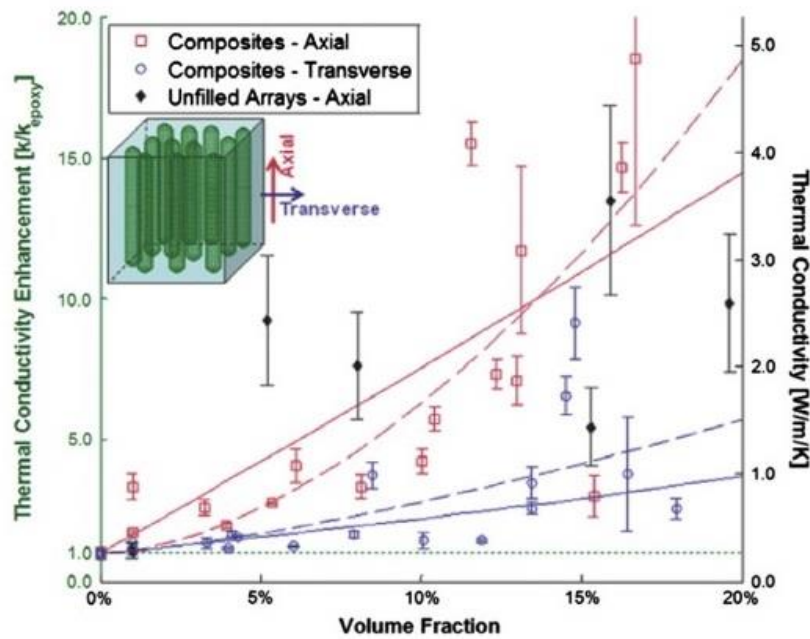


Fig. 1.5.2A. Axial and Transverse aligned thermal conductivity of CNT composites with respect to volume fraction. Reproduced with permission from Ref. [81]

The problem with most alignment processes arises when combining the carbon nanotubes with polymer matrix to form a composite material. Any alignment formation achieved prior to mixing into a composite are unable to be maintained post mixing in a polymer matrix and is dispersed into random orientation. However, there are methods to align carbon nanotubes in a polymer matrix. P. Gonnet et al. achieved in plane SWCNT alignment under a high magnetic field [79]. Flexible and scratch resistant composite films with high CNT content, uniform dispersion of CNTs, and controlled patterned CNT structures can be easily fabricated through in situ imidization. Using this approach, Ning et al. constructed a super aligned carbon nanotube/polyimide composite that exhibits improved in mechanical strength, Young's modulus, electrical conductivity and shows good thermal stability [82]. Likewise, Q. Jiang et al. successfully fabricated a unidirectional MWCNT reinforced polyimide composite through spray winding method [80]. It was also reported that through this method a high level of alignment is preserved and can effectively make high volume fraction carbon nanotube composites. H. Zhao et al. introduced a novel and facile hot-press combined with peel-off (HPPO) method to vertically align nanotubes over a polymeric substrate [83]. Single walled carbon nanotube spray deposited on a nylon membrane can conglutinate with a PSF membrane

upon hot pressing like a sandwich at a nominal 100 °C. These membranes upon separation through peel off, aligns the CNTs vertically as shown a Fig. 1.5.2B. Shear force and mechanical stress are proposed to be the main force behind effective perpendicular alignment to the substrate surface.

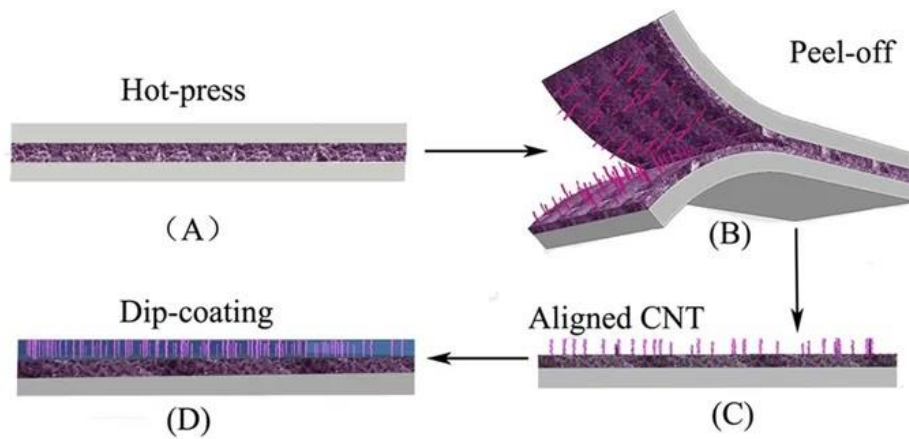


Fig. 1.5.2B. Schematic of the method to align SWNT by hot-press and peel off. Reproduced with permission from Ref. [83]

C. Ma et al. studied the effects of carbon nanotube loading and magnetic field aligned carbon nanotubes on fracture toughness of the polymer composite [84]. It is observed that higher CNT loading significantly reduces the degree of carbon nanotube alignment which has some significant effects on their fracture resistance. It is also reported that an improvement in fracture toughness is observed with aligned CNTs. Carbon nanotubes aligned perpendicular to the crack plane were observed to exhibit much higher fracture toughness than parallel aligned nanotubes or randomly oriented nanotubes composite.

1.6 Polyvinylidene fluoride (PVDF) is an outstanding thermoplastic polymer that has received great attention as a membrane material in recent times due to its excellent chemical stability, processing stability, high hydrophobicity and mechanical properties, thus making it a potential material in various industrial applications. Although its high thermal stability makes it a viable membrane material in heat exchangers, its low thermal conductivity which was determined to be in the range of  $0.2 \text{ Wm}^{-1}\text{K}^{-1}$  is a very big hurdle to overcome. To date, remarkable progress are being made with the fabrication of PVDF membranes by introducing conductive fillers to improve the thermal conductivity but there are still significant challenges to be overcome.

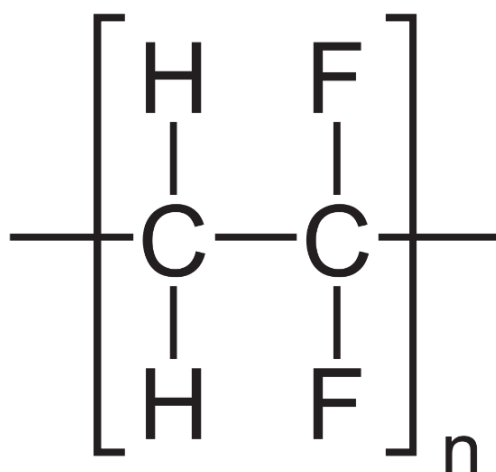


Fig. 1.6.1: Structure of Polyvinylidene fluoride (PVDF)

1.7 Polyvinylpyrrolidone (PVP) is a non-ionic, non-toxic polymer with C=O, C-N, & CH<sub>2</sub> functional groups, that contains strong hydrophilic component (pyrrolidone moiety) and a considerable hydrophobic group (the alkyl group). The highly polar amide group within the pyrrolidone ring and apolar methylene and methane groups in the ring and along its backbone makes PVP dissolvable in both aqueous and many non-aqueous solutions [85]. The repulsive forces that arise from its hydrophobic carbon chain extend into solvents and interact with each other (steric hindrance effect) preventing aggregation to form nanoparticles and nanotubes. Thus, PVP acts as a great stabilizer [86]. A recent report on Ag nanoparticles capped with PVP oligomers, revealed that the length of the chain played an important role in stabilizing the nanoparticles. A longer chain is expected provide enhanced stability [87]. Moreover, MD (molecular dynamics) simulation of AgNP coated PVP<sub>816</sub>/PVP<sub>1440</sub> oligomers revealed that the increase in the length of the PVP chain primarily leads to the formation of an additional external layer around the nanoparticle leading to a higher surface coverage.

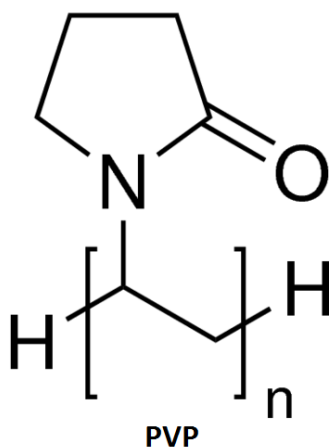


Fig. 1.7.1: Structure of Polyvinylpyrrolidone [88].



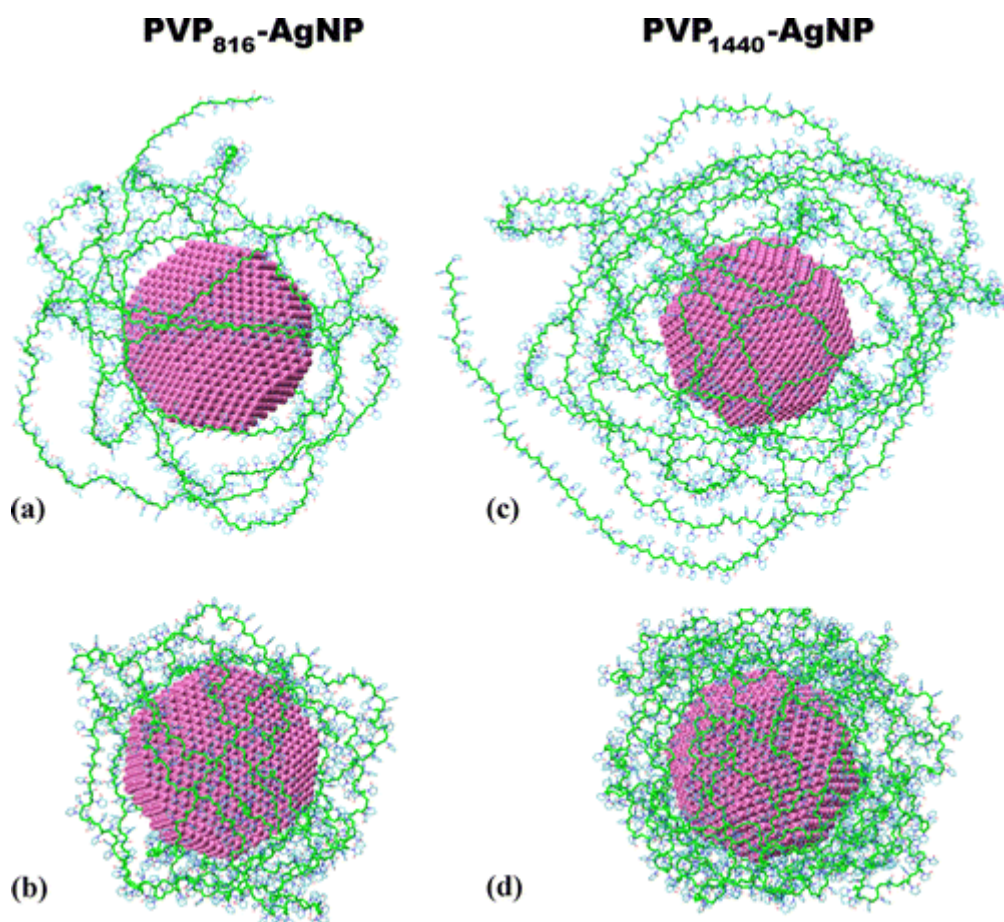


Fig. 1.7.2: MD simulation of PVP<sub>816</sub>-AgNP (a, b) and PVP<sub>1440</sub>-AgNP (c, d) in aqueous solution: (a) and (c) An initial configuration of single chain PVP<sub>816</sub>/PVP<sub>1440</sub> wrapped around AgNP. (b) and (d) Equilibrium structure of PVP<sub>816</sub>/PVP<sub>1440</sub> coated AgNP taken at the end of 300 ns – exhibiting higher surface coverage with PVP<sub>1440</sub>.

Reproduced with permission from Ref. [87]

1.8 Poly(4-vinylpyridine) (P4VP) is derived from the polymerization of 4-vinyl pyridine, which is a derivative of pyridine ring with a vinyl group in the 4 position. P4VP is a hydrophobic polymer that is insoluble in water until approximately 35 % of the pyridine groups are charged by protonation [89]. On the other hand, pyridine molecules can form hydrogen bonds with water molecules and due to its pyridine group exhibiting coordinative reactivity with transition metals. For this reason, their application in catalysis or as antimicrobial materials has been widely studied. It is also reported that P4VP stabilized SWNTs have shown good dispersion in both organic solvents and aqueous solution (pH=2) [90]. A study on formation of carbon nanotube/sol-gel composite confirmed that P4VP aid in the formation of nanocomposites not only by allowing uniform dispersion of SWNTs in the silica as small bundles, but also appears to foster adhesion between the silica and the nanotubes [91].

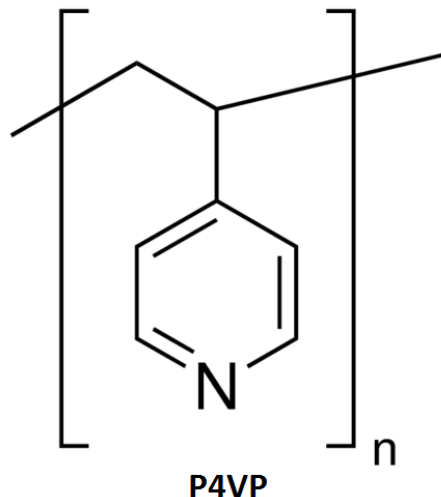


Fig. 1.8.1: Structure of Poly(4-vinylpyridine) [88].

*Fig. 1.8.2 has been removed due to copyright restriction.*

1.9 Polyethylenimine (PEI) is a cationic water-soluble polymer that contains repeating units composed of amine group and two carbon aliphatic  $\text{CH}_2\text{CH}_2$  spacer. PEI has the highest cationic density, as every third atoms of this polymer is a protonable amino nitrogen [92] and depending on the linkage of the ethylenimine units, it occurs as branched or linear morphological isomers [93]. Linear PEI contains secondary amines in its backbone except the terminal primary group. Conversely, branched PEI contains primary, secondary and tertiary amino groups at an estimated ratio of 1:2:1. The molecular weight and degree of branching of PEI polymer influences the average  $\text{pK}_a$  value, which is estimated to be between 8.5 and 9 [94]. CNTs modified with PEI have already been used in drug and gene delivery systems shown in Fig. 1.9.2 [95]. A study using PEI functionalised SWNT and PEI functionalised MWNT to deliver small interfering RNA (SiRNA) into human cervical cancer cells were conducted where PEI functionalisation were observed to increase the positive charge on the surface of SWNTs and MWNTs which allowed the carbon nanotubes to electrostatically interact with negatively charged molecules (SiRNA). Moreover, the solubility of the SWNTs and MWNTs in aqueous solution were greatly improved with PEI functionalisation and with centrifugation, large aggregates are further removed producing a more stable suspension of reduced particle size, improved homogeneity, and dispersity [62].



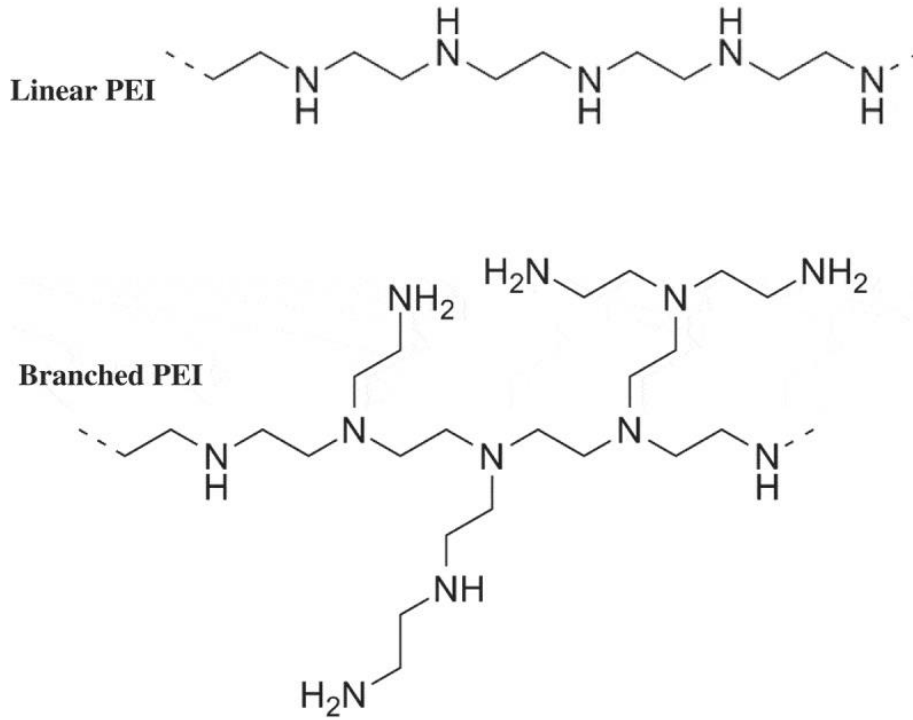


Fig. 1.9.1: Structure of Polyethylenimine [96]

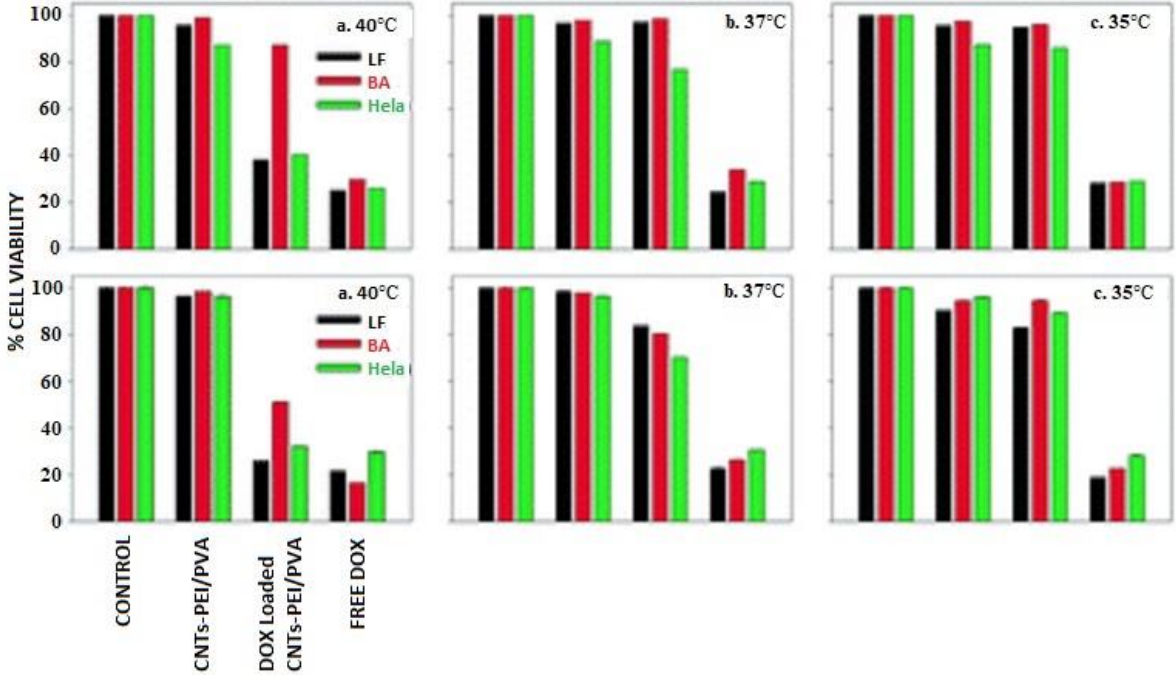


Fig. 1.9.2: Cell viability study at different temperature. Lung fibroblast (LF) - Black colour, Breast Adenocarcinoma (BA) - Red colour and HeLa - Green colour (a) 40 °C (b) 37 °C (c) 35 °C using the Alamar blue method; LF, BA and HeLa at (d) 40 °C (e) 37 °C (f) 35 °C using the LDH method indicating that CNTs-PEI/PVA work more efficiently in delivering drug to tumours at temperatures higher than 37°C. Reproduced with permission from Ref. [95]

## 1.10 Aims and Objectives

The aim of this PhD thesis is to perform a detailed comparative analysis of the behaviour of non-covalently functionalised CNTs of different morphology and different carboxyl content in a PVDF polymer matrix and characterize the composites obtained in terms of their thermal, electrical and mechanical properties. Also, non-covalent functionalisation is performed with polymers of different molecular weight and different structure to study the extent of their impact towards the improvement of properties in the nanocomposite. The novelty of this work lies in the application of various CNTs, different molecular weight polymers for functionalization and polymers of different molecular structures which will elucidate the critical factors in the meticulous selection of molecular weight and specific concentration range of a polymer to non-covalently functionalize carbon nanotubes of specific weight percent and specific morphology to achieve a PVDF nanocomposite with improved thermal, electrical and mechanical properties.

## 1.11 Thesis Outline

Chapter 1: This chapter discusses the role of carbon-based materials in polymer composites and extensively reviews the factors affecting carbon nanotubes fillers towards enhancement of physical properties in polymer nanocomposites.

Chapter 2: A detailed description on the preparation of polymer nanocomposites, sample characterization and instrument information are provided.

Chapter 3: This chapter concentrates on the effect of nanotube aspect ratio on the polymer wrapping behaviour. A study on physical properties of the composites prepared with non-covalently functionalized As Prepared Single-walled nanotubes (AP-SWNT) by four different molecular weights of Polyvinylpyrrolidone (PVP) polymer are compared. A higher degree of dispersion and an enhancement in physical properties is only observed in composites prepared with nanotubes functionalized by PVP of low molecular weights at low concentration, which is attributed to the aspect ratio of AP-SWNTs leading to a strong assumption that nanotubes of different aspect ratio might achieve a similar result with PVP of different molecular weights.

Chapter 4: This chapter explores the relation between the amount of nanotubes and the polymer chain length defining the wrapping behaviour. A study on physical properties of the composites prepared with non-covalently functionalized P3 Single-walled nanotubes (P3-SWNT) using

four different molecular weights of Polyvinylpyrrolidone (PVP). Contrary to AP-SWNT composites from Chapter 3, the results from PVP functionalized P3-SWNTs exhibit an enhanced physical property with highest molecular weight at low concentration followed by lower molecular weights at a comparatively higher concentration of PVP, which could be attributed to the fact that the wrapping behaviour is highly influenced by the lower aspect ratio. There may also be effects due to the mild presence of carboxyl content and defect sites due to chemical processing of AP-SWNTs in order to produce P3-SWNTs with a purification level of more than 98 %. Additionally, the amount of nanotubes plays a key role in achieving a uniform dispersion of nanotubes with a specific molecular weight of PVP.

Chapter 5: This chapter discusses the change in polymer wrapping behaviour with respect to the structure of nanotubes. Although, the multi-walled nanotubes (MWNT) have undergone a similar chemical processing as the P3-SWNTs achieving a similar level of purity and carboxyl content, the large diameter of the MWNTs leads to a different aspect ratio compared to P3-SWNTs. A comparative study was conducted on polymer composites prepared with various molecular weights of Polyvinylpyrrolidone (PVP) used to functionalize MWNTs. The composite exhibits a completely different result compared to AP-SWNTs and P3-SWNTs, such that a higher degree of nanotube dispersion compared to unmodified nanotube composites is achieved in MWNTs functionalized by PVP of low molecular weights at low concentration and with higher molecular weights at a comparatively higher concentration.

Chapter 6: The effect of polymer structure on polymer wrapping are discussed through a comparative study on the physical properties of PVP or Poly(4-vinylpyridine) (P4VP) functionalized CNT polymer composite, with PVP and P4VP exhibiting different molecular structure but similar molecular weight. The study is conducted with AP-SWNTs, P3-SWNTs and MWNTs and compared. The result exhibits an effective formation of a conductive path of nanotube network only among MWNTs and not among SWNTs, which could be attributed to the possibility of a different wrapping pattern for P4VP compared to PVP.

Chapter 7: A comparative study of the physical properties of polymer composites prepared through non-covalent functionalization of CNTs by cationic polymer Polyethylenimine (PEI) are compared in terms of two different molecular weight weights of PEI. These results are compared to PVP results from earlier chapters indicating the fact PEI wrapping behaviour is different from PVP wrapping behaviour for SWNTs but exhibits a similar behaviour for MWNTs.

Chapter 8: Conclusions discussing the factors influencing the selection of polymers of certain chain lengths for certain types of carbon nanotubes of specific concentrations in order to achieve an enhancement in physical properties of the composites are provided. An overview of potential future work is also discussed in detail.

## 1.12 REFERENCES

1. Chen, X., et al., *Recent research developments in polymer heat exchangers – A review*. Renewable and Sustainable Energy Reviews, 2016. **60**: p. 1367-1386.
2. Georgakilas, V., et al., *Broad Family of Carbon Nanoallotropes: Classification, Chemistry, and Applications of Fullerenes, Carbon Dots, Nanotubes, Graphene, Nanodiamonds, and Combined Superstructures*. Chemical Reviews, 2015. **115**(11): p. 4744-4822.
3. Thostenson, E.T., Z. Ren, and T.-W. Chou, *Advances in the science and technology of carbon nanotubes and their composites: a review*. Composites Science and Technology, 2001. **61**(13): p. 1899-1912.
4. Rashad, A., et al., *Synthesis of carbon nanotube -a review*. 2016.
5. Ruoff, R.S., D. Qian, and W.K. Liu, *Dossier: Carbon nanotubes: state of the art and applications* Mechanical properties of carbon nanotubes: theoretical predictions and experimental measurements. Comptes Rendus Physique, 2003. **4**(9): p. 993-1008.
6. Han, Z. and A. Fina, *Thermal conductivity of carbon nanotubes and their polymer nanocomposites: A review*. Progress in Polymer Science, 2011. **36**(7): p. 914-944.
7. Biercuk, M.J., et al., *Carbon nanotube composites for thermal management*. Applied Physics Letters, 2002. **80**(15): p. 2767-2769.
8. Mohamed, A.O. and S. Deepak, *Temperature dependence of the thermal conductivity of single-wall carbon nanotubes*. Nanotechnology, 2001. **12**(1): p. 21.
9. Qingwei, L., et al., *Measuring the thermal conductivity of individual carbon nanotubes by the Raman shift method*. Nanotechnology, 2009. **20**(14): p. 145702.
10. Kim, S.Y., Y.J. Noh, and J. Yu, *Thermal conductivity of graphene nanoplatelets filled composites fabricated by solvent-free processing for the excellent filler dispersion and a theoretical approach for the composites containing the geometrized fillers*. Composites Part A: Applied Science and Manufacturing, 2015. **69**: p. 219-225.
11. Noh, Y.J., et al., *Thermal Conductivity of Polymer Composites With Geometric Characteristics of Carbon Allotropes* Advanced Engineering Materials, 2016. **18**(7): p. 1127-1132.
12. Wei, Z., et al., *Chirality dependence of the thermal conductivity of carbon nanotubes*. Nanotechnology, 2004. **15**(8): p. 936.
13. Fujii, M., et al., *Measuring the Thermal Conductivity of a Single Carbon Nanotube*. Physical Review Letters, 2005. **95**(6): p. 065502.
14. Zhang, G. and B. Li, *Thermal conductivity of nanotubes revisited: Effects of chirality, isotope impurity, tube length, and temperature*. The Journal of Chemical Physics, 2005. **123**(11): p. 114714.
15. T'Joen, C., et al., *A review on polymer heat exchangers for HVAC&R applications*. International Journal of Refrigeration, 2009. **32**(5): p. 763-779.

16. *Characteristics, Applications and Properties of Polymers, in Polymer Engineering Science and Viscoelasticity: An Introduction*, H.F. Brinson and L.C. Brinson, Editors. 2008, Springer US: Boston, MA. p. 55-97.
17. Agari, Y., et al., *Thermal diffusivity and conductivity of PMMA/PC blends*. *Polymer*, 1997. **38**(4): p. 801-807.
18. Xu, Y., R. Gunawidjaja, and B. Abdel-Magid, *Thermal behavior of single-walled carbon nanotube polymer–matrix composites*. *Composites Part A: Applied Science and Manufacturing*, 2006. **37**: p. 114-121.
19. Boudenne, A., L. Ibos, and Y. Candau, *Thermophysical Properties of Multiphase Polymer Systems*, in *Handbook of Multiphase Polymer Systems*. p. 387-423.
20. Valcárcel M, J.P., J.A. Palacios, and J.J. Alvarado-Gil, *Determination of the thermophysical properties of polymers (PET) using photoacoustic spectroscopy*. *Journal of Materials Science*, 1999. **34**(9): p. 2113-2119.
21. Huang, C., X. Qian, and R. Yang, *Thermal conductivity of polymers and polymer nanocomposites*. *Materials Science and Engineering: R: Reports*, 2018. **132**: p. 1-22.
22. Sahoo, N.G., et al., *Polymer nanocomposites based on functionalized carbon nanotubes*. *Progress in Polymer Science*, 2010. **35**(7): p. 837-867.
23. Díaz Costanzo, G., et al., *Stable Solutions of Multiwalled Carbon Nanotubes Using an Azobenzene Dye*. *The Journal of Physical Chemistry C*, 2010. **114**(34): p. 14347-14352.
24. Moniruzzaman, M. and K.I. Winey, *Polymer Nanocomposites Containing Carbon Nanotubes*. *Macromolecules*, 2006. **39**(16): p. 5194-5205.
25. Peng, H., et al., *Sidewall Carboxylic Acid Functionalization of Single-Walled Carbon Nanotubes*. *Journal of the American Chemical Society*, 2003. **125**(49): p. 15174-15182.
26. Punetha, V.D., et al., *Functionalization of carbon nanomaterials for advanced polymer nanocomposites: A comparison study between CNT and graphene*. *Progress in Polymer Science*, 2017. **67**: p. 1-47.
27. Strano, M.S., et al., *The Role of Surfactant Adsorption during Ultrasonication in the Dispersion of Single-Walled Carbon Nanotubes*. *Journal of Nanoscience and Nanotechnology*, 2003. **3**(1-2): p. 81-86.
28. Tasis, D., et al., *Chemistry of Carbon Nanotubes*. *Chemical Reviews*, 2006. **106**(3): p. 1105-1136.
29. Coleman, J.N., et al., *Small but strong: A review of the mechanical properties of carbon nanotube–polymer composites*. *Carbon*, 2006. **44**(9): p. 1624-1652.
30. Skákalová, V., et al., *Effect of Chemical Treatment on Electrical Conductivity, Infrared Absorption, and Raman Spectra of Single-Walled Carbon Nanotubes*. *The Journal of Physical Chemistry B*, 2005. **109**(15): p. 7174-7181.
31. Marshall, M.W., S. Popa-Nita, and J.G. Shapter, *Measurement of functionalised carbon nanotube carboxylic acid groups using a simple chemical process*. *Carbon*, 2006. **44**(7): p. 1137-1141.
32. Jinho Hong, D.W.P.a.S.E.S., *A Review on Thermal Conductivity of Polymer Composites Using Carbon-Based Fillers : Carbon Nanotubes and Carbon Fibers*. *Carbon Letters*, 2010. **11**(4): p. 347-356.
33. Ma, P.-C., et al., *Dispersion and functionalization of carbon nanotubes for polymer-based nanocomposites: A review*. *Composites Part A: Applied Science and Manufacturing*, 2010. **41**(10): p. 1345-1367.

34. Yang, S.-Y., et al., *Effect of functionalized carbon nanotubes on the thermal conductivity of epoxy composites*. Carbon, 2010. **48**(3): p. 592-603.
35. Zhang, W.-b., et al., *High thermal conductivity of poly(vinylidene fluoride)/carbon nanotubes nanocomposites achieved by adding polyvinylpyrrolidone*. Composites Science and Technology, 2015. **106**: p. 1-8.
36. Song, Y.S. and J.R. Youn, *Influence of dispersion states of carbon nanotubes on physical properties of epoxy nanocomposites*. Carbon, 2005. **43**(7): p. 1378-1385.
37. Hu, H., et al., *Determination of the acidic sites of purified single-walled carbon nanotubes by acid–base titration*. Chemical Physics Letters, 2001. **345**(1): p. 25-28.
38. In-Yup Jeon, D.W.C., Nanjundan Ashok Kumar and Jong-Beom Baek *Functionalization of Carbon Nanotubes*, in *Carbon Nanotubes - Polymer Nanocomposites*, S. Yellampalli, Editor. 2011, InTech. p. 91-110.
39. Shenogin, S., *Role of thermal boundary resistance on the heat flow in carbon-nanotube composites*. Journal of Applied Physics, 2004. **95**(12): p. 8136.
40. Gulotty, R., et al., *Effects of Functionalization on Thermal Properties of Single-Wall and Multi-Wall Carbon Nanotube–Polymer Nanocomposites*. ACS Nano, 2013. **7**(6): p. 5114-5121.
41. Julkapli, N.M., S. Bagheri, and S.M. Sapuan, *Multifunctionalized Carbon Nanotubes Polymer Composites: Properties and Applications*, in *Eco-friendly Polymer Nanocomposites: Processing and Properties*, V.K. Thakur and M.K. Thakur, Editors. 2015, Springer India: New Delhi. p. 155-214.
42. Backes, C., *Noncovalent Functionalization of Carbon Nanotubes*. 2012, Germany: Springer. 203.
43. Kim, S.Y., Y.J. Noh, and J. Yu, *Improved thermal conductivity of polymeric composites fabricated by solvent-free processing for the enhanced dispersion of nanofillers and a theoretical approach for composites containing multiple heterogeneities and geometrized nanofillers*. 2014. **101**: p. 79-85.
44. Ponnamma, D., et al., *Influence of non-covalent functionalization of carbon nanotubes on the rheological behavior of natural rubber latex nanocomposites*. European Polymer Journal, 2014. **53**: p. 147-159.
45. Oleszczuk, P. and B. Xing, *Influence of anionic, cationic and nonionic surfactants on adsorption and desorption of oxytetracycline by ultrasonically treated and non-treated multiwalled carbon nanotubes*. Chemosphere, 2011. **85**(8): p. 1312-1317.
46. Sun, Z., et al., *Quantitative Evaluation of Surfactant-stabilized Single-walled Carbon Nanotubes: Dispersion Quality and Its Correlation with Zeta Potential*. The Journal of Physical Chemistry C, 2008. **112**(29): p. 10692-10699.
47. Vaisman, L., H.D. Wagner, and G. Marom, *The role of surfactants in dispersion of carbon nanotubes*. Advances in Colloid and Interface Science, 2006. **128–130**: p. 37-46.
48. Gong, X., et al., *Surfactant-Assisted Processing of Carbon Nanotube/Polymer Composites*. Chemistry of Materials, 2000. **12**(4): p. 1049-1052.
49. Ata, M.S., et al., *New developments in non-covalent surface modification, dispersion and electrophoretic deposition of carbon nanotubes*. Carbon, 2018. **130**: p. 584-598.
50. S Strano, M., et al., *The Role of Surfactant Adsorption During Ultrasonication in the Dispersion of Single-Walled Carbon Nanotubes*. Journal of nanoscience and nanotechnology, 2003. **3**: p. 81-6.

51. Gubitosi, M., et al., *Characterization of carbon nanotube dispersions in solutions of bile salts and derivatives containing aromatic substituents*. Journal of Physical Chemistry B, 2014. **118**(4): p. 1012-1021.
52. Mukhopadhyay, S. and U. Maitra, *Chemistry and biology of bile acids*. Current Science, 2004. **87**(12): p. 1666-1683.
53. Wenseleers, W., et al., *Efficient Isolation and Solubilization of Pristine Single-Walled Nanotubes in Bile Salt Micelles*. Advanced Functional Materials, 2004. **14**(11): p. 1105-1112.
54. Wang, Z., et al., *Adsorption and desorption of phenanthrene on carbon nanotubes in simulated gastrointestinal fluids*. Environmental Science and Technology, 2011. **45**(14): p. 6018-6024.
55. Tournus, F., et al.,  *$\pi$ -stacking interaction between carbon nanotubes and organic molecules*. Physical Review B, 2005. **72**(7): p. 075431.
56. Ferreira, G.M.D., et al., *Adsorption of red azo dyes on multi-walled carbon nanotubes and activated carbon: A thermodynamic study*. Colloids and Surfaces A: Physicochemical and Engineering Aspects, 2017. **529**: p. 531-540.
57. Gong, J.-L., et al., *Removal of cationic dyes from aqueous solution using magnetic multi-wall carbon nanotube nanocomposite as adsorbent*. Journal of Hazardous Materials, 2009. **164**(2): p. 1517-1522.
58. Kim, S.W., et al., *Surface modifications for the effective dispersion of carbon nanotubes in solvents and polymers*. Carbon, 2012. **50**(1): p. 3-33.
59. Giovanni De Filpo, F.P.N., Luca Ciliberti, Patrizia Formoso, Giuseppe Chidichimo, *Non-covalent functionalisation of single wall carbon nanotubes for efficient dye-sensitised solar cells* Journal of Power Sources, 2015. **274**: p. 274-279.
60. Wang, P.-H., et al., *Polypropylene nanocomposites with polymer coated multiwall carbon nanotubes*. Polymer, In Press.
61. Liu, R., et al., *Noncovalent functionalization of carbon nanotube using poly(vinylcarbazole)-based compatibilizer for reinforcement and conductivity improvement in epoxy composite*. Journal of Applied Polymer Science, 2017. **134**(26).
62. Huang, Y.-P., et al., *Delivery of small interfering RNAs in human cervical cancer cells by polyethylenimine-functionalized carbon nanotubes*. Nanoscale research letters, 2013. **8**(1): p. 267-267.
63. Kim, H.S., et al., *Thermal conductivity of polymer composites with the geometrical characteristics of graphene nanoplatelets*. Scientific Reports, 2016. **6**: p. 26825.
64. Ghose, S., et al., *Thermal conductivity of ethylene vinyl acetate copolymer/nanofiller blends*. Composites Science and Technology, 2008. **68**(7): p. 1843-1853.
65. Hong, J., et al., *Effect of dispersion state of carbon nanotube on the thermal conductivity of poly(dimethyl siloxane) composites*. Current Applied Physics, 2010. **10**(1): p. 359-363.
66. Ma, P.-C., et al., *Dispersion and functionalization of carbon nanotubes for polymer-based nanocomposites: A review*. Composites Part A: Applied Science and Manufacturing, 2010. **41**(10): p. 1345-1367.
67. Tian, W. and R. Yang, *Phonon transport and thermal conductivity percolation in random nanoparticle composites*. Tech Science Press CMES, 2008. **24**: p. 123-141.
68. Martin-Gallego, M., et al., *Thermal conductivity of carbon nanotubes and graphene in epoxy nanofluids and nanocomposites*. Nanoscale Research Letters, 2011. **6**(1): p. 1-7.
69. Wang, Z.L., et al., *Thermal boundary resistance and temperature dependent phonon conduction in CNT array multilayer structure*. International Journal of Thermal Sciences, 2013. **74**: p. 53-62.

70. Singh, I.V., M. Tanaka, and M. Endo, *Effect of interface on the thermal conductivity of carbon nanotube composites*. International Journal of Thermal Sciences, 2007. **46**(9): p. 842-847.
71. Nan, C.-W., et al., *Interface effect on thermal conductivity of carbon nanotube composites*. Applied Physics Letters, 2004. **85**(16): p. 3549-3551.
72. Russ, M., et al., *Length-dependent electrical and thermal properties of carbon nanotube-loaded epoxy nanocomposites*. Composites Science and Technology, 2013. **81**: p. 42-47.
73. Kapadia, R.S., B.M. Louie, and P.R. Bandaru, *The Influence of Carbon Nanotube Aspect Ratio on Thermal Conductivity Enhancement in Nanotube–Polymer Composites*. Journal of Heat Transfer, 2013. **136**(1): p. 011303-011303.
74. Chen, J. and L. Yan, *Effect of Carbon Nanotube Aspect Ratio on the Thermal and Electrical Properties of Epoxy Nanocomposites*. Fullerenes, Nanotubes and Carbon Nanostructures, 2018. **26**(11): p. 697-704.
75. Kim, H.S., et al., *Thermal conductivity of polymer composites based on the length of multi-walled carbon nanotubes*. Composites Part B: Engineering, 2015. **79**: p. 505-512.
76. Choi, E.S., et al., *Enhancement of thermal and electrical properties of carbon nanotube polymer composites by magnetic field processing*. Journal of Applied Physics, 2003. **94**(9): p. 6034-6039.
77. Kim, Y.A., et al., *Fabrication of aligned carbon nanotube-filled rubber composite*. Scripta Materialia, 2006. **54**(1): p. 31-35.
78. Wu, S., S. Peng, and C.H. Wang, *Multifunctional Polymer Nanocomposites Reinforced by Aligned Carbon Nanomaterials*. Polymers, 2018. **10**(5): p. 542.
79. Gonnet, P., et al., *Thermal conductivity of magnetically aligned carbon nanotube buckypapers and nanocomposites*. Current Applied Physics, 2006. **6**(1): p. 119-122.
80. Jiang, Q., et al., *Mechanical, electrical and thermal properties of aligned carbon nanotube/polyimide composites*. Composites Part B: Engineering, 2014. **56**: p. 408-412.
81. Marconnet, A.M., et al., *Thermal Conduction in Aligned Carbon Nanotube–Polymer Nanocomposites with High Packing Density*. ACS Nano, 2011. **5**(6): p. 4818-4825.
82. Ning, W., et al., *Multifunctional super-aligned carbon nanotube/polyimide composite film heaters and actuators*. Carbon, 2018. **139**: p. 1136-1143.
83. Zhao, H., et al., *A facile method to align carbon nanotubes on polymeric membrane substrate*. Scientific Reports, 2013. **3**: p. 3480.
84. Ma, C., et al., *Fracture resistance, thermal and electrical properties of epoxy composites containing aligned carbon nanotubes by low magnetic field*. Composites Science and Technology, 2015. **114**: p. 126-135.
85. Graf, C., et al., *A General Method for the Controlled Embedding of Nanoparticles in Silica Colloids*. Langmuir, 2006. **22**(13): p. 5604-5610.
86. Si, R., et al., *Self-Organized Monolayer of Nanosized Ceria Colloids Stabilized by Poly(vinylpyrrolidone)*. The Journal of Physical Chemistry B, 2006. **110**(12): p. 5994-6000.
87. Kyrychenko, A., et al., *Atomistic Simulations of Coating of Silver Nanoparticles with Poly(vinylpyrrolidone) Oligomers: Effect of Oligomer Chain Length*. The Journal of Physical Chemistry C, 2015. **119**(14): p. 7888-7899.
88. O'Connell, M.J., et al., *Reversible water-solubilization of single-walled carbon nanotubes by polymer wrapping*. Chemical Physics Letters, 2001. **342**(3): p. 265-271.
89. Raczowska, J., et al., *Temperature-responsive properties of poly(4-vinylpyridine) coatings: influence of temperature on the wettability, morphology, and protein adsorption*. RSC Advances, 2016. **6**(90): p. 87469-87477.



90. Su, M., *Remarkable crystallization morphologies of poly(4-vinylpyridine) on single-walled carbon nanotubes in CO<sub>2</sub>-expanded liquids*. *Express Polymer Letters*, 2011. **5**: p. 1102-1112.
91. Rouse, J.H., *Polymer-Assisted Dispersion of Single-Walled Carbon Nanotubes in Alcohols and Applicability toward Carbon Nanotube/Sol–Gel Composite Formation*. *Langmuir*, 2005. **21**(3): p. 1055-1061.
92. Yuan, W. and H. Li, *Chapter 14 - Polymer-based nanocarriers for therapeutic nucleic acids delivery*, in *Nanostructures for Drug Delivery*, E. Andronescu and A.M. Grumezescu, Editors. 2017, Elsevier. p. 445-460.
93. Nimesh, S., *10 - Polyethylenimine nanoparticles*, in *Gene Therapy*, S. Nimesh, Editor. 2013, Woodhead Publishing. p. 197-223.
94. Farvadi, F., et al., *Polyionic complex of single-walled carbon nanotubes and PEG-grafted-hyperbranched polyethyleneimine (PEG-PEI-SWNT) for an improved doxorubicin loading and delivery: development and in vitro characterization*. *Artificial Cells, Nanomedicine, and Biotechnology*, 2017. **45**(5): p. 855-863.
95. Mashat, A., et al., *Zippered release from polymer-gated carbon nanotubes*. *Journal of Materials Chemistry*, 2012. **22**(23): p. 11503-11508.
96. Zakeri, A., et al., *Polyethylenimine-based nanocarriers in co-delivery of drug and gene: a developing horizon*. *Nano reviews & experiments*, 2018. **9**(1): p. 1488497-1488497.

# CHAPTER 2

## MATERIALS and METHODS

Part of this chapter was published previously in Namasivayam, M.; Andersson, M.R.; Shapter, J. Role of Molecular Weight in Polymer Wrapping and Dispersion of MWNT in a PVDF Matrix. *Polymers* **2019**, *11*, 162.

## 2.1 Materials:

Multi-walled carbon nanotubes used in this research were purchased from Sigma-Aldrich (Product No.: 755133, St. Louis, MO, USA) with an average diameter of 9.5 nm, a length of 1.5  $\mu\text{m}$  and an impurity of less than 5% metal oxide. AP-SWNTs (As prepared) and P3-SWNTs were purchased from Carbon Solutions (Riverside, CA 92507, USA) with an individual tube length ranging from 0.5 – 3  $\mu\text{m}$  and an average diameter of 1.4 nm. AP-SWNTs used in this research are about 60 - 70 % pure with a metal content of less than 30 %, a bundle length of 1 to 5  $\mu\text{m}$  and a bundle diameter range of 2 to 10 nm. P3-SWNT used were more than 90 % pure with the presence of 5 - 7 % metal content and a bundle length of 500 nm to 1.5  $\mu\text{m}$  ( $\sim 1 \mu\text{m}$ ) with a diameter range of 4 - 5 nm. Commercial P3-SWNTs and MWNTs were purified through acid treatment with nitric acid.

PVDF with a melt flow rate (MFR) of 20-35 g per 10 min (230  $^{\circ}\text{C}$ , 3.8  $\text{Kg}^{-1}$ ), density of 1.78  $\text{g}\cdot\text{ml}^{-1}$  at 25  $^{\circ}\text{C}$  and an average molecular weight of 180000  $\text{g}\cdot\text{mol}^{-1}$  (Sigma Aldrich) was used as the polymer matrix. Polyvinylpyrrolidone with molecular weights of 10000  $\text{g}\cdot\text{mol}^{-1}$ , 40000  $\text{g}\cdot\text{mol}^{-1}$ , 55000  $\text{g}\cdot\text{mol}^{-1}$  and 360000  $\text{g}\cdot\text{mol}^{-1}$  (Sigma Aldrich), poly (4-vinylpyridine) with molecular weight of 60000  $\text{g}\cdot\text{mol}^{-1}$  (Sigma Aldrich) and polyethyleneimine with molecular weights 800  $\text{g}\cdot\text{mol}^{-1}$  and 25000  $\text{g}\cdot\text{mol}^{-1}$  (Sigma Aldrich) were used for non-covalent functionalization of nanotubes.

## 2.2 Sample Preparation:

Prior to use, all the nanotubes have undergone a dilute nitric acid (3M  $\text{HNO}_3$ ) reflux for 16 hours to achieve a high level of purity. The resultant carbon nanotubes are filtered and dried overnight in an oven with a temperature ranging from 80  $^{\circ}\text{C}$  to 90  $^{\circ}\text{C}$ .

The nanocomposites were prepared through solution mixing method, which includes two steps.

The first step was to obtain the “solution” containing polymer wrapped CNTs and the second step was to mix the “solution” and the PVDF polymer in the same solvent, followed by a controlled evaporation process through deposition over a glass or silicon substrate resulting in a film thickness of approximately 40 $\mu\text{m}$ . An Elmasonic S30H 280W power bath sonicator was used for the sample preparation.

First step: 1 mg of unmodified CNTs was suspended in 250  $\mu\text{L}$  of DMF and sonicated for 10 minutes to produce a uniform dispersion [1]. Then, a defined amount of functionalization polymer (PVP or P4VP or PEI) was dispersed in the CNT solution. The mixture was sonicated

for a period of 45 minutes and then left undisturbed overnight in order to confirm that the prepared solution can sustain a dispersion without re-aggregation for a period of 12-15 hours [2, 3].

Second step: The mixture is combined with 20 mg of PVDF polymer in 200  $\mu\text{L}$  of DMF and sonicated for a period of 4 hours [4]. The resulting non-covalently functionalized CNT/PVDF mixture is then deposited on a clean silicon/glass wafer of about 2 cm in length and 2 cm in breadth, and dried in an oven at a temperature at 100  $^{\circ}\text{C}$  for 24 hours.

In this work, the amount of CNT and PVDF remained essentially constant with only the concentration of functionalization polymer varied at a weight percent of 1.48 % to 41.18 % (0.025 mg to 0.7 mg) with respect to the amount of CNT used to make the composite. A comparative result is produced.

### 2.3 Raman Spectroscopy:

This is a spectroscopic technique based on inelastic scattering of monochromatic light, usually a laser source. When a molecule is irradiated with a light source, the photons of the laser light are absorbed by the sample and scattered. Most of the light scattering, called elastic Rayleigh scattering, happens at the same frequency,  $\nu_0$ , as the incident light but as a result of interaction between oscillation of light and molecular vibration, a very small fraction of light gets scattered at a different frequency  $\nu_m$  and exhibits inelastic scattering. This phenomenon is called Raman scattering and by analysing the spectrum of Raman scattered light, it is possible to analyse the composition of materials as the frequency modulation would be specific to molecular vibrations and/or phonons in crystal. The frequency of the Raman scattering could be either higher (Anti-stokes scattering) or lower (Stokes scattering) than the frequency of the incident photon.

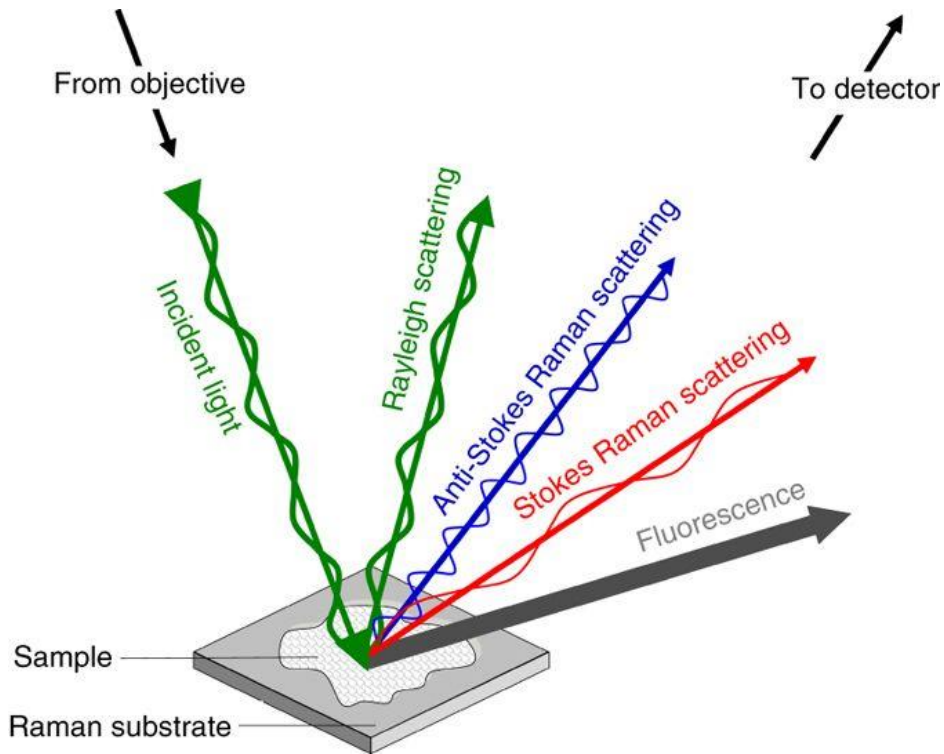


Fig. 2.3.1: Schematic representation of Raman scattering. Reproduced with permission from Ref. [5]

About 99.999% of all incident photons undergo elastic Rayleigh scattering and only about 0.001% of photon produces in-elastic Raman scattering with frequencies  $\nu_0 \pm \nu_m$  useful enough for molecular characterisation. Special measures to distinguish Raman scattering from Rayleigh scattering should be taken. Instruments such as notch filters, tuneable filters, laser stop apertures, double and triple spectrometric system are used to reduce Rayleigh scattering and obtain high quality Raman spectra.

Raman spectra of functionalized and non-functionalized nanocomposites were analysed using XplorRA Horiba Scientific Confocal Raman Microscope with a 532 nm laser operating at 1 % laser power (0.079 mW). The laser power was kept at minimum in order to avoid causing damage to the PVDF polymer matrix and thus affecting the nanotube dispersion in the composite. MWNTs have been characterised using 1800T grating at a slit width of 100  $\mu\text{m}$  and a hole size of 500  $\mu\text{m}$ . Both AP-SWNTs and P3-SWNTs have been characterised using 2400T grating at a slit width of 100  $\mu\text{m}$  and a hole size of 100  $\mu\text{m}$ .

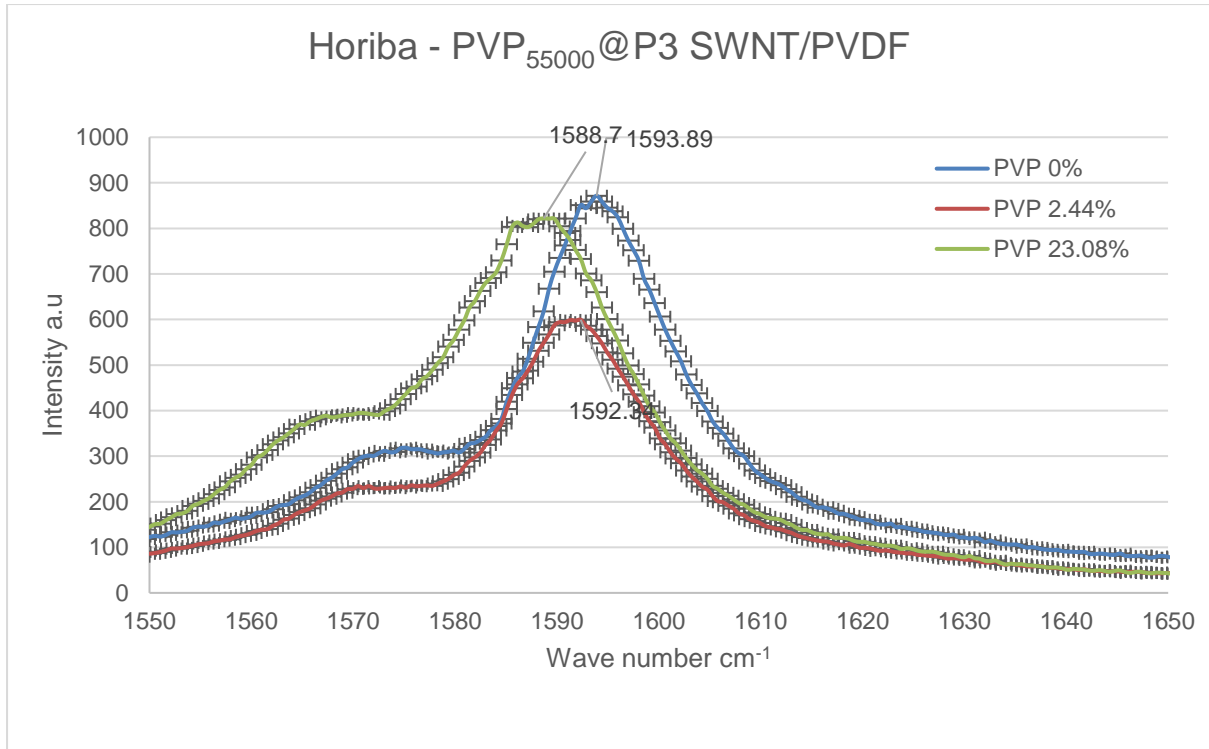


Fig. 2.3.2: Normalized Raman spectra of nanocomposites acquired for different concentrations of PVP<sub>55000</sub> functionalized P3-SWNT/PVDF composite.

As mentioned earlier, Raman spectroscopy is a form of vibrational spectroscopy. It provides molecular analysis by giving information on the composite material structure by evaluation of relevant vibrational features. When the functionalization of nanotubes affects the degree of nanotube dispersion in the polymer composite, a change in the C-C bond vibration leading to a change in vibrational frequencies of the normal mode is pertinent. This can be observed as a position shift in the Raman band [6].

#### 2.4 Electrical Conductivity

Nanocomposites were deposited on a clean glass substrate and electrical conductivity was measured at room temperature using a four-point probe method.

Sheet resistivity is measured using the voltage and current reading from the probe:

$$\rho \left( \frac{\Omega}{\square} \right) = \frac{\pi}{\ln(2)} \cdot \frac{V}{I}$$

Where:

$$\frac{\pi}{\ln(2)} = 4.532$$

In typical usage, the current is set to 4.53 mA so that the resistivity is simply the voltage reading in mV.

Electrical conductivity of the composite is measured to be

$$S/m = \frac{1}{(R * t)}$$

R is in ohms/sq. and t is film thickness in m.

## 2.5 Thermal Conductivity

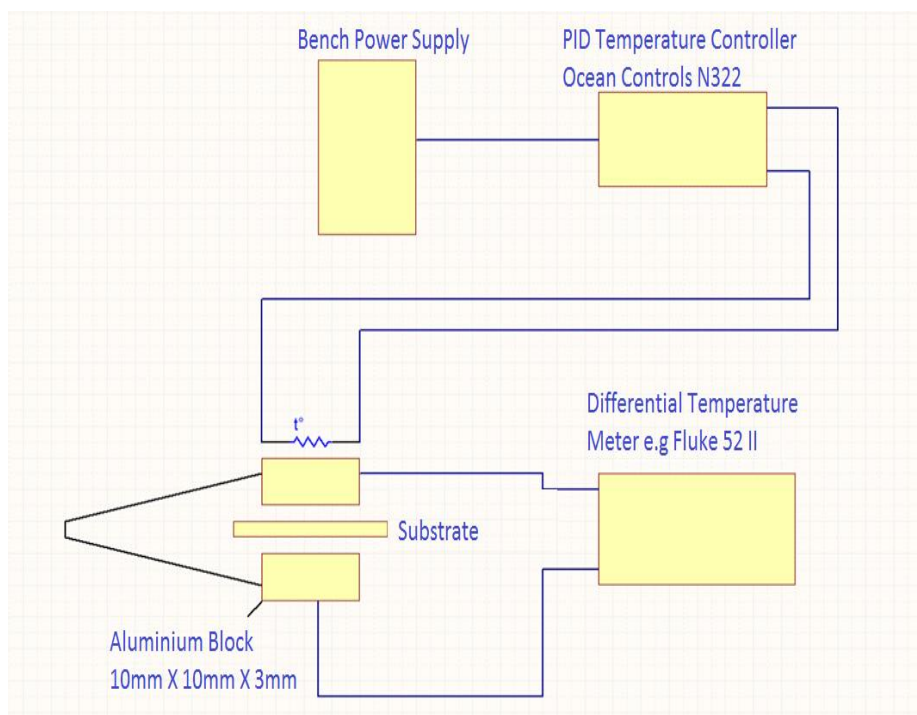


Fig. 2.5.1: Schematic Representation of thermal conductivity measurement rig.

Thermal conductivity was measured using a steady state technique in a well-insulated chamber, where the sample is placed between a heat source and a heat sink with a known amount of heat supplied through a steady state power input using a PID Temperature controller (Ocean Controls N322). The temperature difference across a given length of the sample was measured using a differential temperature meter (Fluke 52 II) after a steady-state temperature distribution is acquired. Thermal conductivity of the sample was calculated using Fourier's Law of Heat Conduction.

$$k = \frac{qL}{A\Delta T} \quad (\text{W}\cdot\text{m}^{-1}\cdot\text{K}^{-1})$$

Where, q is the amount of heat supplied through the sample, A is the cross-sectional area of the sample. L being the distance through which heat flows and ΔT is the temperature difference observed.

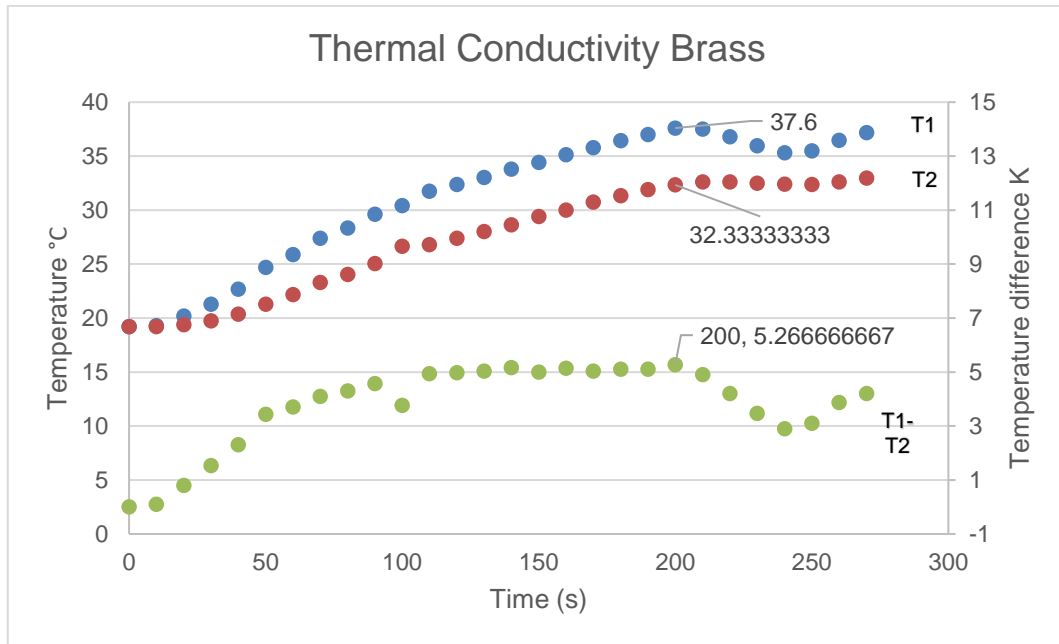


Fig. 2.5.2: Observed temperature difference in pure brass material. T1 is the incoming temperature to the substrate. T2 is the outgoing temperature through the substrate. ΔT is the temperature difference.

$$\begin{aligned} k &= \frac{qL}{A\Delta T} = \frac{59.616 \text{ W} \cdot 0.311 \text{ cm}}{3.24 \text{ cm}^2 \cdot 5.27 \text{ K}} \\ &= 1.086 \text{ W}\cdot\text{m}^{-1}\cdot\text{K}^{-1} \\ &= 108.6 \text{ W}\cdot\text{m}^{-1}\cdot\text{K}^{-1} \text{ (Measured Value)} \end{aligned}$$

Thermal Conductivity for Brass:  $109 \text{ W}\cdot\text{m}^{-1}\cdot\text{K}^{-1}$  (Theoretical value)[7]

## 2.6 Dynamic Mechanical Analyser (DMA):

DMA is a material characterization technique, where an oscillatory strain is applied to the material at a frequency and temperature of interest and the resulting stress developed in the material is analyzed [8]. Storage modulus ( $G'$ ), loss modulus ( $G''$ ), and damping co-efficient ( $\text{Tan}\delta$ ), properties that changes significantly when crystalline structure changes to amorphous



phase, are measured as a function of temperature, time or frequency. The modulus is defined as the measure of a material's resistance to deformation or in simple terms, a higher modulus value is an indication of more rigidity of the material. The operating principle is that, during these phase transition a proportionally larger change occurs in the mechanical property of the sample than in its specific heat and that is why even though there are several techniques available to determine glass transition temperature, DMA is considered highly sensitive[9].

In DMA, the stiffness and loss of the sample are being measured and the choice of geometry will be dependent on the sample under investigation. A sample can be characterized through tension, compression, bending or torsion depending on their thickness and the sample material. For example, films of less than 1mm thickness can only be measured accurately under tension but anything thicker would be too stiff and the bending mode would be a preferred choice. Likewise, torsion is a good geometry, but the sample size must be reasonably large. For low modulus samples like rubber, gels and paste a simple shear would be an excellent approach. Although compression mode would exhibit high geometrical errors, is often the only way of measuring irregular shaped samples [10].

The polymer nanocomposite samples prepared in this research have a thickness of about 40 microns and a TA Instruments Q800 DMA (New Castle, DE, USA) was used to analyse the mechanical characterisation of the sample. The mode of oscillation used was Tensile Strain and the procedure performed was temperature ramp with a frequency sweep. The experiments were performed in a temperature range of -90 °C to 200 °C at a temperature ramp of 3 °C·min<sup>-1</sup> with a soak time of 1 min, meaning the sample is maintained at -90 °C for 1 minute to make sure the sample actually reached the temperature before the experiment begins. An amplitude of 20µm and a static force of 0.05 Newton were applied and maintained throughout the experiment. Storage modulus and Tan delta of the composite were characterised as a function of temperature and compared.

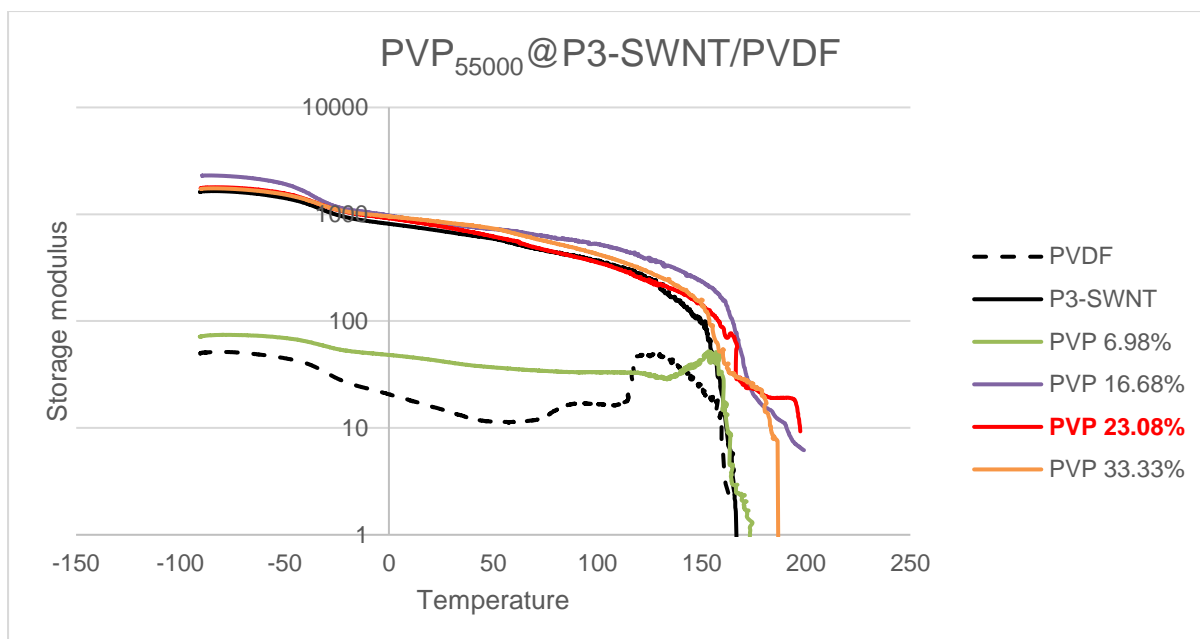


Fig. 2.6.1: Storage modulus graph of PVP<sub>55000</sub> functionalized SWNT/PVDF composite.

The storage modulus graphs for five different samples of PVP<sub>55000</sub> functionalized SWNT/PVDF composite are displayed in Fig. 2.5.1. All the samples contained a constant amount of carbon nanotube and PVDF polymer but with varying content of PVP functionalization from 0 % to 33.33 %. Almost all the samples exhibited similar storage modulus, which is expected as the presence of carbon nanotubes would increase the tensile strength of the composite but only a composite that has well dispersed nanotubes is expected to have formed a nanotube network that exhibits a higher mechanical strength to hold the sample together even when the host polymer (PVDF) begins to melt and hence can sustain the stress at a comparatively higher temperature. This was observed at a temperature range above 165 °C, which happens to be the melting temperature of the PVDF polymer. In the case of PVP<sub>55000</sub> functionalized SWNT/PVDF composite, a PVP content of 23.08 wt. % is required to produce a sample with highest mechanical strength. This result is expected to change for different molecular weight of PVP and for different polymers.

## 2.7 Differential Scanning Calorimetry:

DSC is a thermal analytical technique that measures the heat flow occurring in a sample when heated, cooled or held isothermally stable at constant temperature. The DSC setup is composed of a measurement chamber operatable by a computer. Two pans, a sample pan with the material being investigated and a reference pan typically empty are heated in the measurement chamber. The computer is used to monitor the temperature and regulate the rate at which the temperature of the pans changes, with the typical heat rate around 10 °C per min [11].

With the heat flows, the composition of the material in the sample pan may undergo physical changes such as phase change causing a differentiation from the reference pan in the rate of temperature change for a given amount of heat. In order to maintain a constant temperature between the two pans, the system varies the amount of heat provided to one of the pans. The output is a plot of the difference in heat ( $q$ ) recorded versus time ( $t$ ), also known as the heat flow ( $q/T$ ). Whereas, the heating rate is the time rate change of temperature ( $\Delta T/t$ ),  $\Delta T$  being the change in temperature. The heat capacity  $C_p$  (Joules/ $^{\circ}\text{C}$ ) can be derived from the heat flow and the heating rate.

$$C_p = \frac{q/t}{\Delta T/t} = \frac{q}{\Delta T} \text{ Joules}/^{\circ}\text{C}$$

If the heat capacity of a material (polymer) is constant over some temperature range then the plot of heat flow against temperature would exhibit a line with zero slope. A polymer in its molten state will at some point reach its glass transition temperature ( $T_g$ ) when cooled. At this point, due to changes in chain mobility, the mechanical properties of the polymer change from those of an elastic material to those of a brittle one. The heat capacity of a polymer is different prior to and after its glass transition temperature and it is usually higher above  $T_g$ . The transition happens over a range of temperatures instead of at one unique temperature point forming an inclined portion in the plot of heat flow against temperature and the middle point of this inclined region is considered as  $T_g$ .

The polymer chains have high mobility above the glass transition temperature and at some point above  $T_g$  the chains have enough energy to form ordered arrangements and undergo crystallization. Being an exothermic process, heat is released to the surroundings during crystallization. Therefore, providing less heat is sufficient to keep the temperature of both the sample pan and reference pan constant resulting in a decrease in the recorded heat flow. This is witnessed as a dip in the plot of heat flow versus temperature, also known as crystallization peak and the temperature at which the lowest point of the dip observed is known as crystallization temperature ( $T_c$ ).

Unlike during crystallization, the polymer chains are able to move around freely at the melting temperature ( $T_m$ ) and thus do not have ordered arrangement. Melting is an endothermic process requiring the absorption of heat and despite continued heating there is not much change in temperature during melting process. This is due to the fact that the energy added during this time is only used to melt the crystalline region and does not increase the average kinetic energy

of the chains that are already in the melt. After melting, the temperature again increases with heating. This appears in the plot as a jump discontinuity at the melting point known as melting peak and melting temperature ( $T_m$ ) is defined as the temperature at the peak apex.

Not all polymers tend to go through all three transitions. Only polymers capable of forming crystals would exhibit crystallization and melting peaks and since crystalline polymers possess amorphous domains, they exhibit glass transition as well while amorphous polymers will only undergo a glass transition. The exact temperature at which these transitions occur is solely dependent on the structure of the polymer. Even a subtle change in structure would create a huge change in  $T_g$ .

*Fig. 2.7.1 has been removed due to copyright restriction.*

A TA Instruments 2930 DSC (New Castle, DE, USA) was used to investigate the crystallisation and melting behaviour of the sample. A sample of about 9 mg was first heated from a temperature of 20 °C to 200 °C and then maintained at 200°C for one minute before cooling down from 200 °C to 20 °C at a rate of 10 °C min<sup>-1</sup>. The steps were repeated to acquire a second heating scan. The degree of crystallinity is obtained from the enthalpy of melting  $\Delta H_f$ , enthalpy of crystallization  $\Delta H_c$  and enthalpy of melting for a fully crystalline polymer  $\Delta H_{f,100\%}$ .

$$\text{Degree of crystallinity} = \frac{\Delta H_f - \Delta H_c}{\Delta H_{f,100\%}} * 100$$

## 2.8 Scanning Electron Microscopy (SEM):

SEM is a powerful tool for material characterization. A focused electron beam is scanned over the surface of a sample in order to produce a signal that can be used to obtain information about surface topography and composition. Image formation is dependent on the acquisition of signal produced from the electron beam and specimen interaction. Accelerated electrons possess a significant amount of energy which can be dissipated as a variety of signals such as secondary electrons, backscattered electrons, diffracted backscattered electrons, photons, visible light and heat produced due to electron-sample interactions. Among these, scattered electrons are most valuable in characterizing the morphology and topography of the sample and back scattered electrons are most valuable for illustrating contrasts in composition in multiphase samples [12].

Non-electrically conductive samples can be challenging to image as the negatively charged electrons make the sample negatively charged which can cause image distortion. However, the samples prepared for this research are composites of PVDF polymer and carbon nanotubes which are naturally conductive and hence the necessity for a conductive coating has been avoided. The dispersion of the nanotubes in the polymer matrix has a very significant impact on the topography of the composite. An Inspect F50 SEM (FEI) had been used to characterize the composites at an accelerating voltage of 10 kV. Samples with and without functionalisation have been characterized from both the anterior and fractured side view.

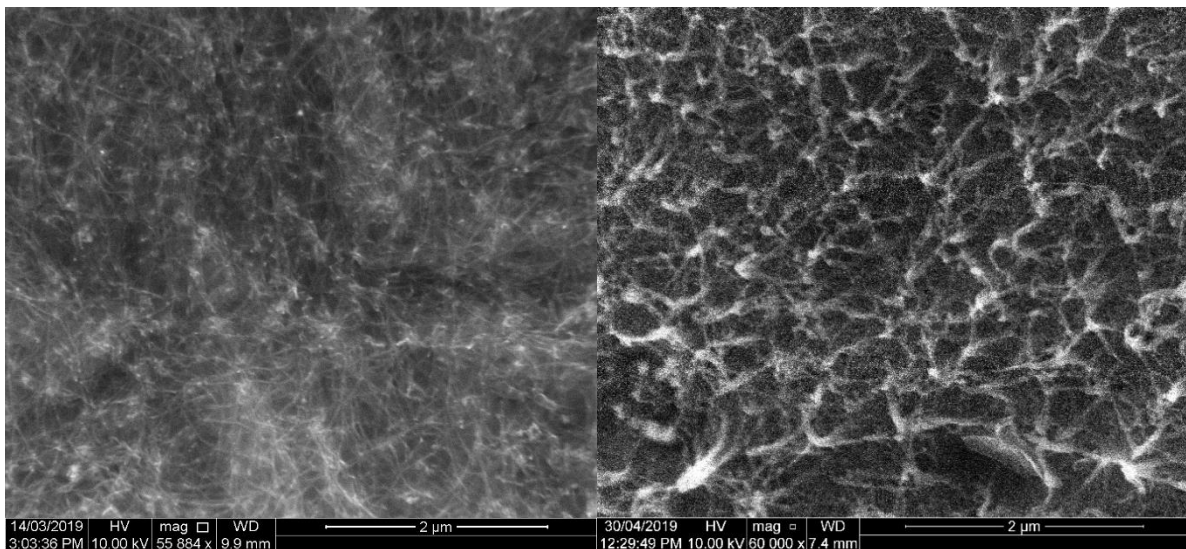


Fig. 2.8.1: SEM images of PVP55000 functionalised SWNT/PVDF composite a) Anterior view and b) fractured side view.

## 2.9 REFERENCES

1. Liu, C.-X. and J.-W. Choi, *Improved Dispersion of Carbon Nanotubes in Polymers at High Concentrations*. Vol. 2. 2012. 329-347.
2. El Achaby, M., et al., *Nanocomposite films of poly(vinylidene fluoride) filled with polyvinylpyrrolidone-coated multiwalled carbon nanotubes: Enhancement of  $\beta$ -polymorph formation and tensile properties*. *Polymer Engineering & Science*, 2013. **53**(1): p. 34-43.
3. Steinert, B. and D. Dean, *Electroconductive PET/SWNT films by solution casting*. 2008.
4. Wong, I., et al. *Effects of Ultra-low Concentrations of Carbon Nanotubes on the Electromechanical Properties of Cement Paste*. in *Nanotechnology in Construction*. 2015. Cham: Springer International Publishing.
5. Butler, H.J., et al., *Using Raman spectroscopy to characterize biological materials*. *Nature Protocols*, 2016. **11**: p. 664.

6. Batakliiev, T., et al., *Effects of Graphene Nanoplatelets and Multiwall Carbon Nanotubes on the Structure and Mechanical Properties of Poly(lactic acid) Composites: A Comparative Study*. Applied Sciences, 2019. **9**: p. 469.
7. Young, H.D. and F.W. Sears, *University physics*. 1992, Reading, Mass.: Addison-Wesley Pub. Co.
8. *9 - Modification and Engineering of HSREP to Achieve Unique Properties*, in *Elastomeric Polymers with High Rate Sensitivity*, R.G. Barsoum, Editor. 2015, William Andrew Publishing: Oxford. p. 319-345.
9. Ebnesajjad, S., *Chapter 4 - Surface and Material Characterization Techniques*, in *Surface Treatment of Materials for Adhesive Bonding (Second Edition)*, S. Ebnesajjad, Editor. 2014, William Andrew Publishing: Oxford. p. 39-75.
10. Ebnesajjad, S. and P.R. Khaladkar, *10 - Failure Analysis*, in *Fluoropolymers Applications in the Chemical Processing Industries*, S. Ebnesajjad and P.R. Khaladkar, Editors. 2005, William Andrew Publishing: Norwich, NY. p. 315-357.
11. Koshy, O., L. Subramanian, and S. Thomas, *Chapter 5 - Differential Scanning Calorimetry in Nanoscience and Nanotechnology*, in *Thermal and Rheological Measurement Techniques for Nanomaterials Characterization*, S. Thomas, et al., Editors. 2017, Elsevier. p. 109-122.
12. Zhou, W., et al., *Fundamentals of Scanning Electron Microscopy (SEM)*, in *Scanning Microscopy for Nanotechnology: Techniques and Applications*, W. Zhou and Z.L. Wang, Editors. 2007, Springer New York: New York, NY. p. 1-40.

Chapters 3-5 discuss the degree of nanotube dispersion and enhancement of physical properties of PVP functionalized CNTs in PVDF composites prepared with PVP of four different molecular weights for As Prepared single-walled nanotubes (Chapter 3) and P3 single-walled nanotubes (Chapter 4) and three different polymer molecular weights for multi-walled nanotubes (Chapter 5). The nanotubes are differentiated in terms of aspect ratio, carboxyl content, and structure. AP-SWNT and P3-SWNT share a similar diameter but different length leading to a difference in their aspect ratio. Unlike AP-SWNTs, P3-SWNTs are chemically processed to achieve high purification leading to a mild presence of carboxyl content and defect sites according to the supplier (Carbon Solutions-Riverside, CA 92507, USA), which would affect the thermal conductivity of pristine nanotubes. Similarly, MWNTs are also chemically processed to achieve high purification (Sigma-Aldrich, USA) like P3-SWNTs but possess a larger diameter compared to both AP-SWNT and P3-SWNT. The change in the degree of dispersion and the formation of nanotube networks for all three types of nanotubes with respect to the length of polymer chain are discussed in terms of the physical properties of the composites as a collective conclusion in chapter 5.

## CHAPTER 3

# PVP FUNCTIONALIZED AS PREPARED SINGLE WALLED NANOTUBES (AP- SWNT) IN PVDF COMPOSITES



### 3.1 CHAPTER INTRODUCTION

As prepared single-walled nanotubes (AP-SWNTs) used in this research were obtained from Carbon Solutions Ltd., at a carbonaceous purity level of 60-70 % with a metal content of less than 30 wt. %. AP-SWNTs are close ended with a bundle length of 1-5  $\mu\text{m}$ , average diameter of 1.4 nm, bundle diameter of 2-10 nm and a density of about 1.2-1.5  $\text{g}/\text{cm}^3$ . They are prepared using an electric-arc discharge method and due to the absence of chemical processing, the carboxyl content and numbers of defect sites is very low in AP-SWNTs. In this chapter the non-covalent functionalization of AP-SWNTs by PVP polymer with different molecular weights is compared and the physical properties of the composites formed with the addition of the PVP functionalized AP-SWNTs to PVDF are analysed extensively.

### 3.2 SAMPLE DETAILS

The composites used in the study were prepared with 1mg of unmodified AP-SWNTs functionalized with polyvinylpyrrolidone (PVP) of various concentration from 0 to 33.33 weight percent, dispersed in 20 mg of PVDF polymer. Four sets of composites were prepared with PVP with four different molecular weights. The amount of AP-SWNTs and PVDF polymer were maintained constant throughout the study. A minimum of three composites for every concentration range were prepared and an average result is analysed.

### 3.3 RESULTS & DISCUSSION

#### *3.3.1 Thermal Conductivity*

Comparative thermal conductivity results for composites prepared using four different molecular weights of PVP are shown in Fig. 3.3.1.

The introduction of pristine AP-SWNTs in a PVDF composite has improved the thermal conductivity from  $0.2 \text{ W}\cdot\text{m}^{-1}\cdot\text{K}^{-1}$  for the pure PVDF polymer to a thermal conductivity value of  $4.37 \text{ W}\cdot\text{m}^{-1}\cdot\text{K}^{-1}$  for the composite containing unfunctionalized nanotubes. This is observed at 0 wt. % and is denoted with a solid black circle in Fig. 3.3.1. This increase can be attributed to the high aspect ratio of the AP-SWNTs. The thermal and mechanical properties of a nanocomposite are highly influenced by the filler dimensions meaning nanocomposites prepared with nanotubes of higher aspect ratio presented better conductivity and enhanced mechanical properties [1]. Moreover, strong interfacial bonding between the polymer matrix and CNT is highly influenced by the aspect ratio of CNTs. Even though a very high thermal conductivity is observed, due to high van der Waals interaction nanotubes tend to form

aggregates in the polymer matrix leading to poor interfacial interaction between the nanotubes and the polymer and this has a negative impact on the physical properties of the composite including thermal conductivity. A polymer composite containing a homogeneous dispersion of nanotubes would enhance the overall thermal conductivity even further and this can be achieved only through surface functionalization of nanotubes. Polymers like polyvinylpyrrolidone (PVP) functionalize nanotubes in a non-covalent manner that not only improves the interfacial interaction between the functionalized nanotubes and polymer matrix but also preserves the intrinsic property of the nanotubes. O’Connell et al. reported that PVP wraps helically around a SWNT [2], and helical wrapping geometries maximise the number of polymer units interacting with the nanotube surface with increasing polymer chain length at the expense of some torsional energy.

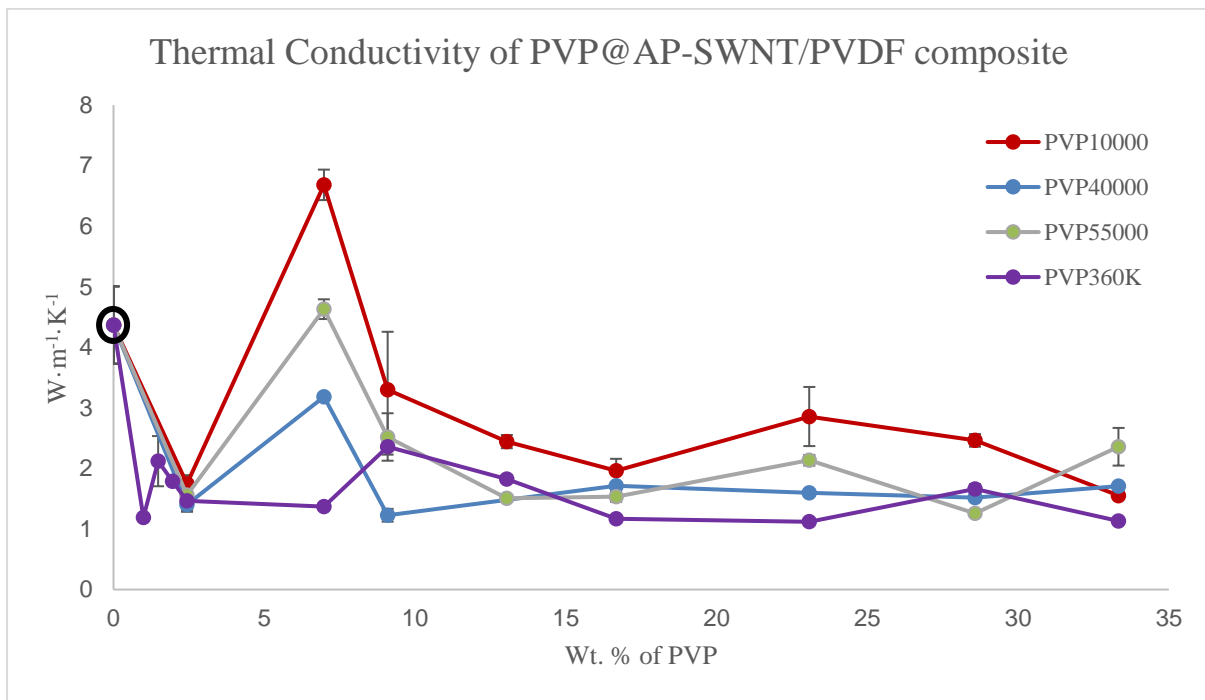


Fig.3.3.1: Thermal Conductivity measurements of four different PVP functionalized AP-SWNTs in PVDF composites.

Four different molecular weights of PVP was used in this study 10000, 40000, 55000, 360000  $\text{g}\cdot\text{mol}^{-1}$ . Among these a decent thermal conductivity improvement is observed in composite prepared with PVP<sub>10000</sub> functionalized nanotubes. A thermal conductivity of  $6.683 \text{ W}\cdot\text{m}^{-1}\cdot\text{K}^{-1}$  is observed at a PVP concentration of 6.98 wt. % which is a 52.86 percent increase and in the similar concentration range, composites prepared with PVP<sub>55000</sub> functionalized nanotubes exhibit a thermal conductivity of  $4.63 \text{ W}\cdot\text{m}^{-1}\cdot\text{K}^{-1}$  which is a 5.95 percent increase compared to composites with unmodified nanotubes. Although, composites prepared with PVP<sub>40000</sub>

functionalized nanotubes exhibit an increase in thermal conductivity compared to other composites prepared with PVP<sub>40000</sub> at similar concentration range, they are comparatively lower than composites with unmodified nanotubes. A similar result is observed in composites prepared with PVP<sub>360000</sub> functionalized nanotubes, but the observed thermal conductivities are even lower than those for PVP<sub>40000</sub> and in all cases lower than the composite prepared with unfunctionalized nanotubes. The results observed could be attributed to the length and diameter of the nanotubes used in this study. Considering the absence of chemical processing and defect sites, the only other parameter that could influence the polymer wrapping in AP-SWNTs would be their aspect ratio. However, the high aspect ratio coupled with strong intrinsic van der Waals attraction between nanotubes leads to formation of ropes, meaning collection of aligned SWNTs that are uniform in diameter. The difference in wrapping behaviour exhibited for the same polymer of different molecular weights would be due to the fact that different lengths of the polymer chain lead to different amount of surface area coverage of the nanotubes.

The most important factor to form an effective polymer nanocomposite with high thermal conductivity is to achieve a homogeneous dispersion of nanotubes in the polymer matrix with more structured CNT network, which provides a denser conductive path for the propagation of phonon vibration [3]. This is observed as a form of nanotube alignment in the SEM image of composites prepared with lowest molecular weight polymer PVP<sub>10000</sub> functionalized nanotubes (see Figure 3.3.10), but not with higher molecular weights of PVP functionalized nanotube composites. This could be attributed to the abrupt changes in surface coverage of CNTs of certain diameter with polymer chain of certain length [4]. It is possible that the polymer wrapping achieved with PVP<sub>360000</sub> polymer could have led to higher surface coverage of nanotubes isolating them from the neighbouring nanotubes thus compromising the nanotube network and an effective phonon conduction. Likewise, the thermal conductivity observed for PVP<sub>40000</sub> and PVP<sub>55000</sub> functionalized nanotube composite could be the result of a network formation, but just not an effective conductive path as observed in PVP<sub>10000</sub> leading to an enhancement in thermal conductivity yet lower compared to the thermal conductivity of unmodified AP-SWNT/PVDF composite. The results clearly show that the length of the polymer chain plays a very important role in the polymer wrapping and eventually in the formation of a nanotube network. There is a high possibility that with nanotubes of different aspect ratios, longer polymer chains might prove effective. Some similar observations has been reported by Salazar-Rios et al. in a study involving the selection mechanism of the polymer wrapping technique of three different polymers towards semiconducting SWNTs with two

different diameters [5]. Among the three polymers, PF12 tends to be a good dispersant of large diameter nanotubes but not with small diameter nanotubes even though the difference in diameter is only approximately 0.5 nm. While both P12CPDTBT and P3DDT tend to be a good dispersant of both small and large diameter nanotubes, P12CPDTBT was comparatively more effective. However, P3DDT exhibits the best outcome regarding the selectivity towards semiconducting species, with a dispersion yield of 15 % for smaller diameter nanotubes and 21 % for larger diameter nanotubes. Similarly, Samanta et al. studied the debundling and dispersion of SWNT by flexible conjugated polymers such as PF<sub>x</sub> and P<sub>3</sub>AT [6]. The SWNTs are functionalized through the  $\pi$ - $\pi$  interaction that occurs between the conjugated backbone of the polymer and the electron surface of the nanotube and solubilizing alkyl side chains of optimal length supports debundling and dispersion of organic solvent. Their result confirms that polyfluorenes with alkyl chain length of eight carbons is effective in dispersing SWNTs of diameter 0.8-1.2 nm and longer alkyl chain with 12-15 carbons are favoured for the dispersion of nanotubes of increased diameter up to 1.5 nm. So, it is plausible to consider that PVP polymer also exhibits a similar mechanism, such that only a polymer chain of certain length is capable of achieving a homogeneous dispersion of nanotubes in the PVDF matrix without compromising the network formation leading to the different thermal conductivity result observed for different molecular weight.

### *3.3.2 Crystallization behaviour of PVP@AP-SWNT/PVDF composite*

Interaction between nanotubes and polymer is vital in order to initiate a nucleation effect in the polymer matrix and this is expected to be higher with high aspect ratio carbon nanotubes. The possibility for an increase in the growth and development of crystals in a polymer matrix is high with high aspect ratio nanotubes owing to their greater nucleating efficiency due to strong interfacial interaction[7]. The crystallization behaviour observed in Fig. 3.3.2, for AP-SWNT composites functionalized with four different molecular weights of PVP show some resemblance with their respective thermal conductivity result observed in Fig. 3.3.1. Composites prepared with PVP<sub>10000</sub> functionalized nanotubes exhibit a high degree of crystallization of about 37.83 %, which is small 3.16 % (relative) increase from the degree of crystallization observed for unmodified AP-SWNT/PVDF composite of 36.67 %. This is followed by PVP<sub>40000</sub> and PVP<sub>55000</sub> functionalized nanotube composites, exhibiting the next best crystallization behaviour of about 37.54 % and 37.53 % showing a 2.37 % (relative) and 2.35 % (relative) increase. Composites with PVP<sub>360000</sub> functionalized nanotubes also exhibits an improvement in crystallization behaviour of about 37 % in a similar concentration range.

This enhancement in the degree of crystallization confirms the improvement in nucleation observed with better dispersion of nanotubes. The decrease in crystallization at higher concentration of PVP is attributed to the fact that a higher amount of PVP polymer leads to higher surface coverage of the nanotubes thus reducing the interfacial interaction between the nanotubes and PVDF polymer.

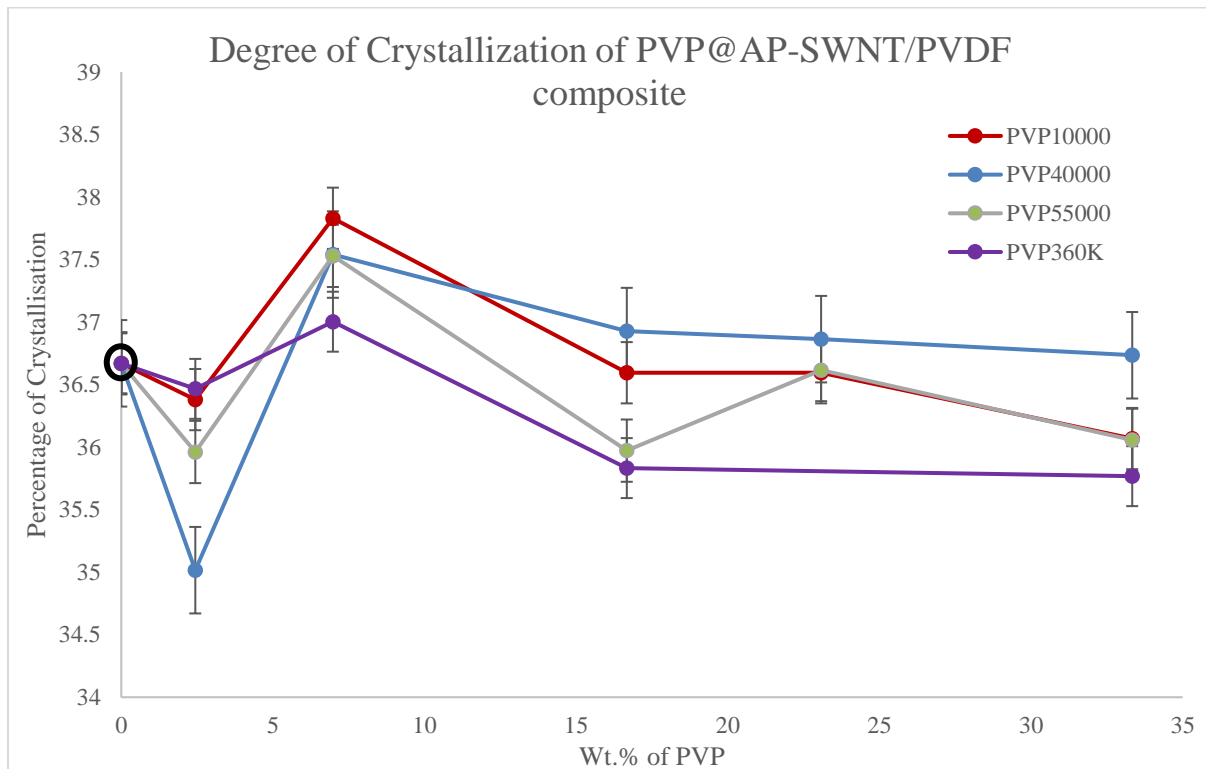


Fig. 3.3.2: Crystallization vs PVP wt. % of PVP functionalized AP-SWNTs in PVDF composites.

### 3.3.3 Electrical Conductivity

The electrical conductivity results obtained for PVP functionalized AP-SWNTs in PVDF composites of four different molecular weights are shown in Fig. 3.3.3. A conductivity of  $25.1 \text{ S}\cdot\text{cm}^{-1}$  is observed for composites prepared with unmodified AP-SWNTs. Similar to the thermal conductivity and crystallization results, composites prepared with PVP<sub>10000</sub> functionalized nanotubes exhibit an increase in conductivity to  $27.6 \text{ S}\cdot\text{cm}^{-1}$  at a PVP concentration of 9.09 wt. % which is a 9.96 % increase compared to composites prepared with unmodified nanotube. This confirms that in this concentration range PVP<sub>10000</sub> functionalized nanotube composites achieved a stable dispersion of nanotubes and also allows the formation of an effective nanotube network. Whereas, a threshold point is reached at higher concentrations of PVP due to higher surface coverage of nanotubes that compromises the contacts between the nanotubes, thus disrupting the effective nanotube network leading to a

decrease in conductivity as observed in Fig. 3.3.3. Although, PVP<sub>40000</sub> functionalized nanotube composites exhibit a good electrical conductivity of about 23.2 S·cm<sup>-1</sup> at a PVP concentration of 9.09 wt. %, the electrical conductivities are comparatively lower than the unmodified nanotube composites and the threshold point is reached with increasing PVP concentration leading to a decrease in conductivity. This confirms that even though a stable dispersion of nanotubes and a good formation of nanotube network can be achieved with PVP<sub>40000</sub> functionalization, they are still not as effective as the PVP<sub>10000</sub> functionalized nanotube composite. However, composites prepared PVP<sub>55000</sub> and PVP<sub>360000</sub> functionalized nanotubes exhibit a very low electrical conductivity of about 0.156 S·cm<sup>-1</sup> and 0.154 S·cm<sup>-1</sup> at a PVP concentration of 2.44 wt. % and reaches a threshold point leading to further lower conductivity with increasing PVP concentrations thus confirming the occurrence of higher surface coverage of nanotubes with longer polymer chains leads to formation of a poor nanotube network compared to PVP<sub>10000</sub> and PVP<sub>40000</sub> functionalized nanotube composites.

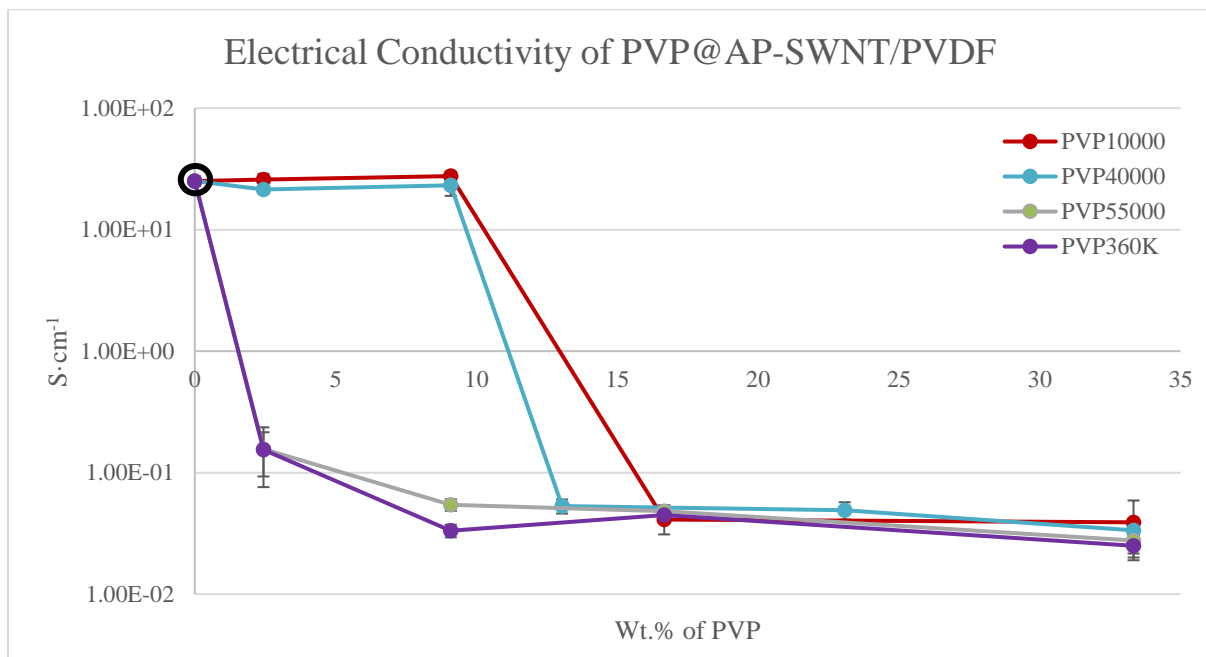


Fig. 3.3.3: Electrical Conductivity measurements of four different PVP functionalized AP-SWNTs in PVDF composites.

### 3.3.4 Mechanical Characterization

Glass transition temperatures measured for PVP functionalized AP-SWNTs in PVDF composites at various PVP concentration are plotted in Fig. 3.3.4A. The glass transition temperature of unmodified AP-SWNT/PVDF composite were plotted at 0 along the x-axis and is observed to be -35.12 °C.

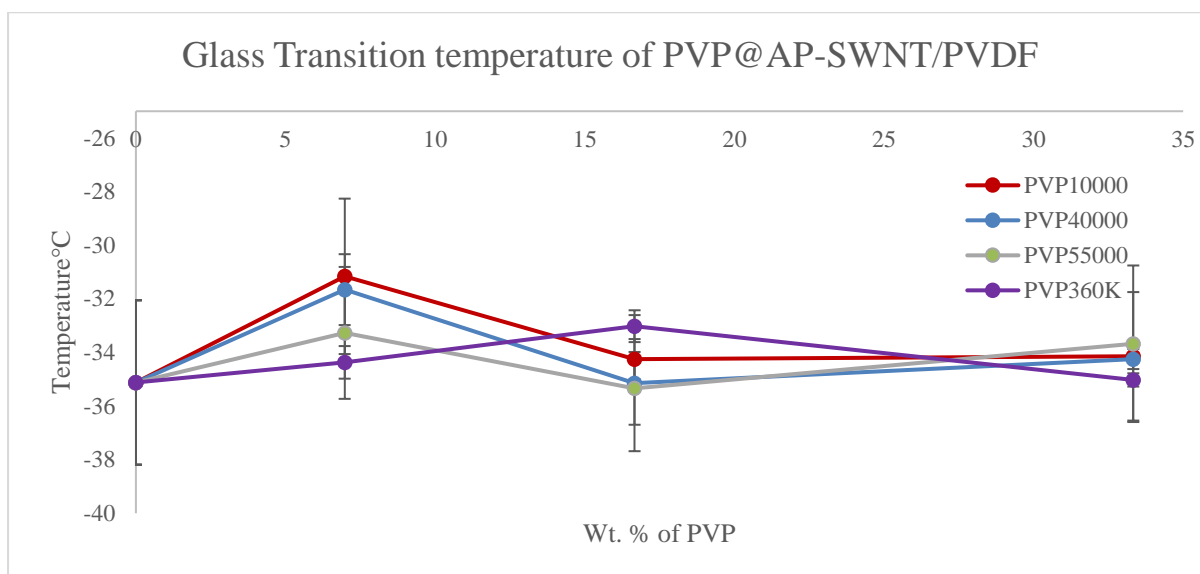


Fig. 3.3.4A: Glass transition measurement of four different PVP functionalized AP-SWNTs in PVDF composites.

Functionalization of nanotubes with PVP<sub>10000</sub> showed the largest increase in the glass transition temperature to about -31.16 °C at a PVP concentration of 6.98 wt. % confirming that the polymer molecular structure has become more ordered due to increased interaction between the nanotubes and the PVDF polymer. Likewise, PVP<sub>40000</sub> and PVP<sub>55000</sub> functionalized nanotube composites also exhibit an increase in glass transition temperature of about -31.66 °C and -33.27 °C at a similar concentration range but comparatively lower than PVP<sub>10000</sub> functionalized nanotube composites. Whereas, PVP<sub>360000</sub> functionalized nanotube composite exhibits an increase in glass transition temperature of about -33.02 °C at a slightly higher concentration range of about 16.67 wt. %. This result confirms the fact that a better dispersion of nanotubes leads to increased interaction between the nanotube and the polymer, thus forming a more ordered polymer molecular structure. Moreover, increasing PVP concentration leads to higher surface coverage of nanotubes that tends to disrupt an effective nanotube network and the polymer molecular structure, this leads to a decrease in the glass transition temperature as witnessed in Fig. 3.3.4A.

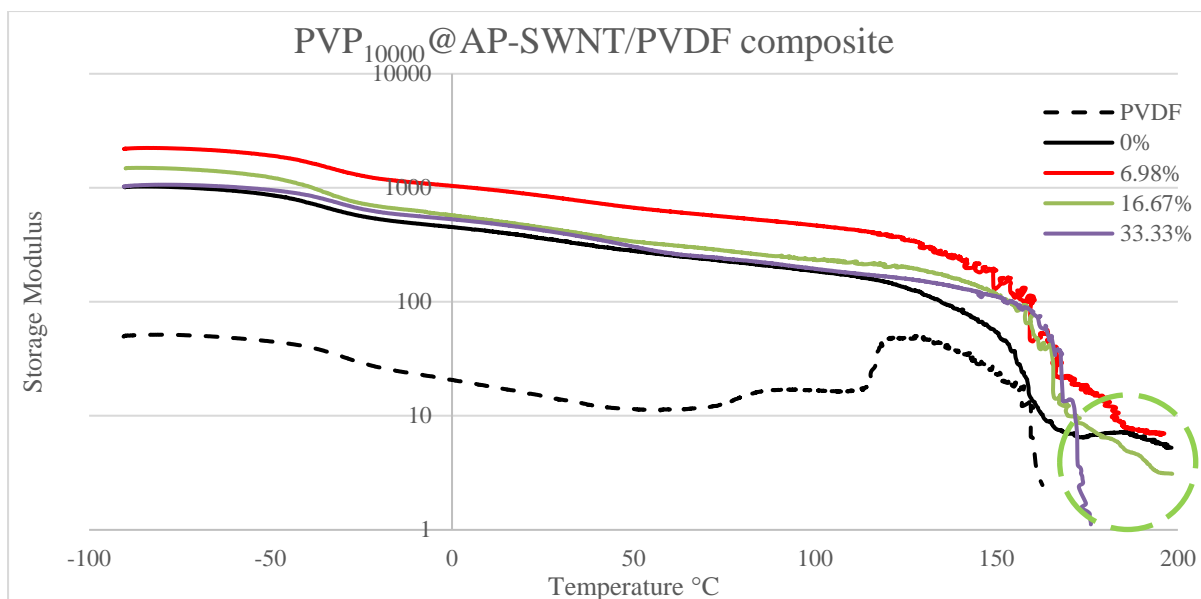


Fig. 3.3.4B: Storage modulus measurement of PVP<sub>10000</sub> functionalized AP-SWNTs in PVDF composites.

The storage modulus of the pure PVDF polymer (dotted black line) showed a major improvement with the addition of unmodified AP-SWNT filler (solid black line) as shown in Fig. 3.3.4B - 3.3.4E. However, a stable dispersion of nanotubes would enhance the interaction between the nanotubes and PVDF polymer compared to unmodified nanotube composites which would increase the storage modulus even further. PVP<sub>10000</sub> functionalized nanotube composites exhibits a higher storage modulus for composites functionalized with a range of PVP concentrations as shown in Fig. 3.3.4B, and the highest storage modulus is observed for composites functionalized with 6.98 wt. % of PVP<sub>10000</sub> which correlates with the highest thermal conductivity result observed for PVP<sub>10000</sub> functionalized composites in Fig. 3.3.1. This could be because the interaction between the nanotubes and PVDF polymer tends to be higher in this concentration range. Although higher concentrations of PVP<sub>10000</sub> functionalized composites tend to exhibit a similar storage modulus as an unmodified nanotube composites, they tend to decrease at higher temperatures leading to a lower storage modulus above 172 °C compared to unmodified nanotube composites.

The melting temperature of a pure PVDF polymer composite is observed to be at 162.69 °C (dotted black line) and the composites prepared with unmodified AP-SWNT composites exhibit a good mechanical strength at temperatures beyond the melting temperature of PVDF polymer. This could be due to the fact that the high aspect ratio of the AP-SWNTs allows the composites to have some network like formation which helps the composite maintain a mechanical strength at temperatures as high as 198.26 °C (an error rate of 0.3% was observed),



highlighted in the green dashed circles in Fig. 3.3.4B – 3.3.4E. Among the PVP<sub>10000</sub> functionalized nanotube composites, the composite prepared at a PVP concentration of 6.98 wt. % is the only composite that tends to exhibit a higher storage modulus compared to unmodified nanotube composite beyond the melting temperature of PVDF and can withstand temperatures as high as 196.18 °C. Although composites prepared at a PVP concentration of 16.67 wt. % can withstand a temperature as high as 198.45 °C, a decrease in storage modulus compared to unmodified nanotube composites is observed beyond a temperature of about 178.55 °C which could be due to a weaker interaction between the nanotubes and the polymer at high temperatures. The composites prepared at a PVP concentration of 33.33 wt. % exhibits a comparatively low mechanical strength and are unable to withstand a temperature beyond 176.01 °C. This observation confirms the presence of a more ordered polymer molecular structure at a PVP concentration of 6.98 wt. % compared to unmodified nanotube composite and it could be due to the formation of a nanotube network achieved through a stable dispersion of nanotubes in the PVDF matrix.

The composites prepared with PVP<sub>40000</sub> and PVP<sub>55000</sub> functionalized nanotubes composites at different concentrations of PVP either exhibit a low mechanical strength at high temperature range or are unable to withstand higher temperatures compared to unmodified nanotube composite as shown in Fig. 3.3.4C and Fig. 3.3.4D, highlighted in the green dashed circles. This confirms that a PVP<sub>40000</sub> and PVP<sub>55000</sub> functionalized nanotubes could not exhibit a stable network like formation of nanotubes beyond the melting temperature of PVDF polymer as effective as an unmodified AP-SWNT/PVDF composite.

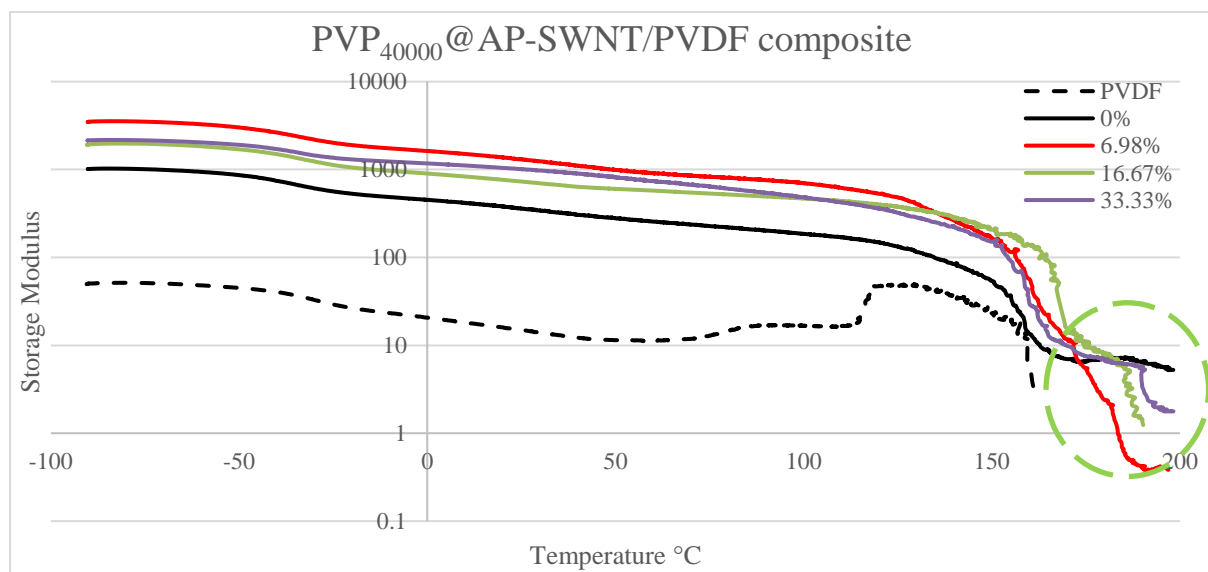


Fig. 3.3.4C: Storage modulus measurement of PVP<sub>40000</sub> functionalized AP-SWNTs in PVDF composites.

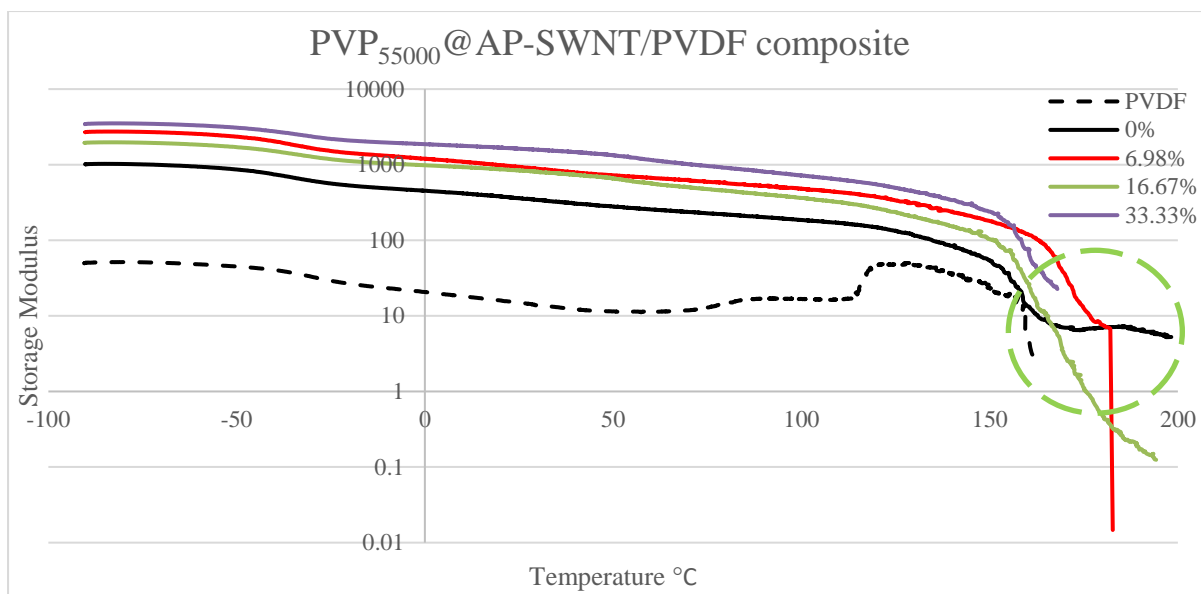


Fig. 3.3.4D: Storage modulus measurement of PVP<sub>55000</sub> functionalized AP-SWNTs in PVDF composites.

PVP<sub>360000</sub> functionalized nanotube composites exhibit a similar result in Fig. 3.3.4E to those observed for PVP<sub>40000</sub> and PVP<sub>55000</sub>. The composites with different concentrations of PVP<sub>360000</sub> either exhibit a comparatively low mechanical strength at high temperatures or reach a yielding point at a comparatively lower temperature of about 191.17 °C as observed in composites prepared at a PVP<sub>360000</sub> concentration of 16.67 wt. %. Although a similar result is observed in composites with a PVP concentration of 33.33 wt. %, they exhibit a fairly similar storage modulus and also yields at a slightly lower temperature of about 197.25 °C compared to unmodified AP-SWNT/PVDF composite.

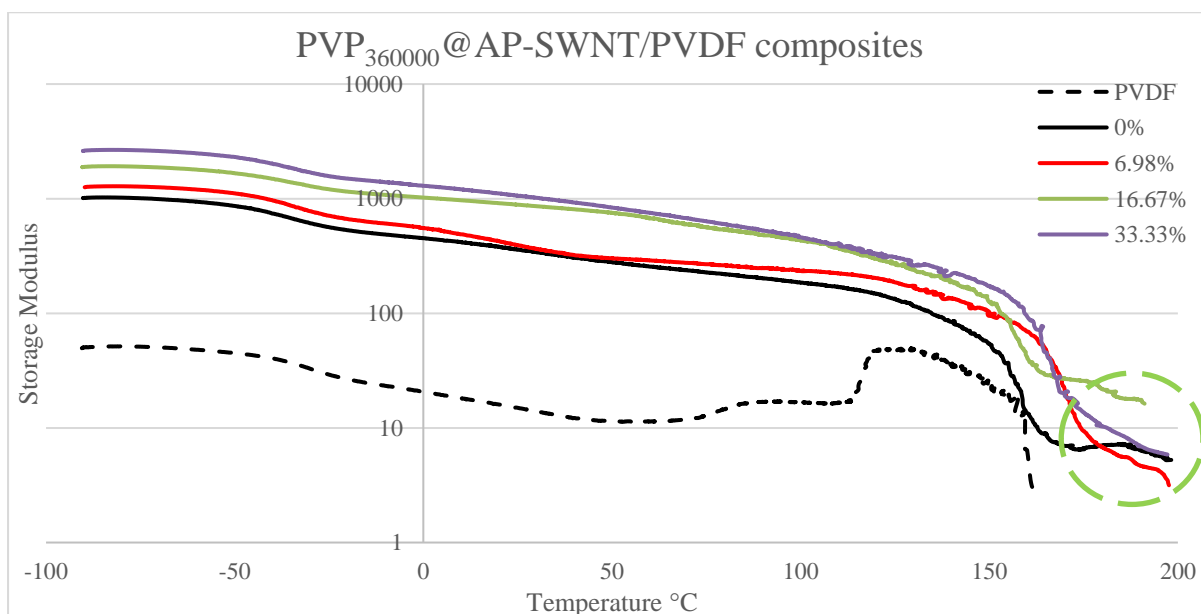


Fig. 3.3.4E: Storage modulus measurement of PVP<sub>360000</sub> functionalized AP-SWNTs in PVDF composites.

The results from the mechanical characterization of PVP functionalized AP-SWNTs in PVDF composite show some resemblance to the thermal conductivity measurement observed in Fig. 3.3.1, such that an effective network of nanotubes exhibiting both a higher mechanical strength and increased glass transition temperature compared to unmodified nanotube composite is observed only with PVP<sub>10000</sub> functionalized nanotube composite at a concentration range of 6.98 wt. %.

### 3.3.5 Microscopy Results

An SEM image of the anterior view of a non-functionalized AP-SWNTs in PVDF composite is shown in Fig.3.3.5A (A) and the fractured side-view image shown on Fig.3.3.5A (B) which is achieved by fracturing the composite after exposing to liquid nitrogen and analyzing along its thickness. High van der Waals interaction among the nanotubes tend to form clusters in the polymer matrix leading to poor dispersion. Although, the high aspect ratio of AP-SWNTs made it difficult to observe the aggregate formation in the SEM image of an unmodified nanotube composites, some clusters formations can still be seen in Fig. 3.3.5A as highlighted by the red circles.

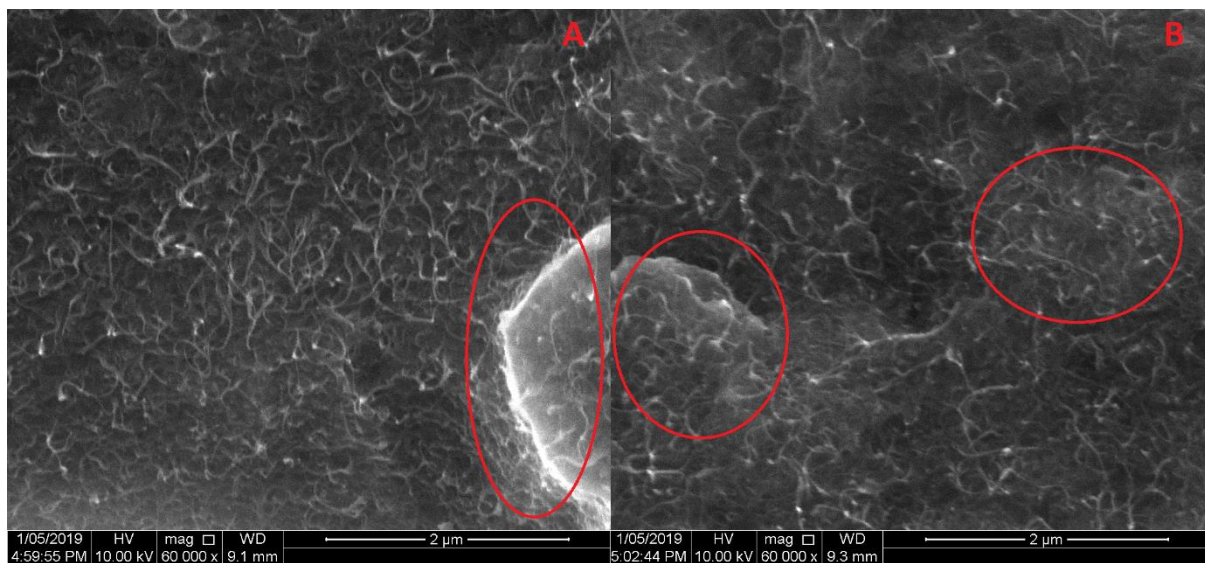
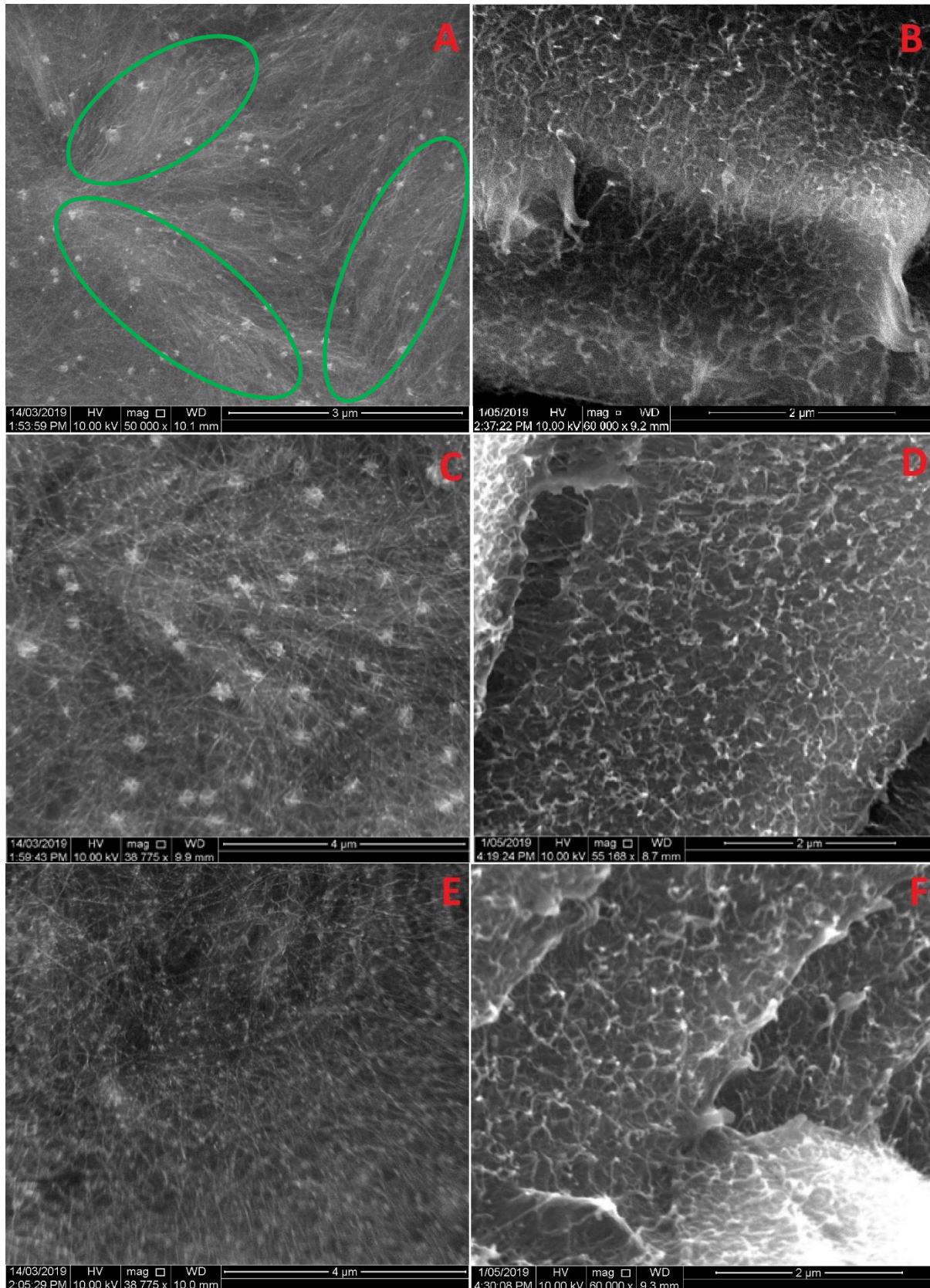


Fig. 3.3.5A: Scanning electron microscope results of non-functionalized AP-SWNTs in PVDF composite; (A) anterior view and (B) fractured side-view - agglomeration of nanotubes are highlighted in red circles

SEM analysis of composites prepared at the concentration that exhibited the highest thermal conductivity (as shown in Fig. 3.3.1) for four different molecular weights of PVP are shown in Fig. 3.3.5B. PVP functionalization has reduced the van der Waals interaction and enhances the dispersion of nanotubes in the polymer matrix leading to the absence of aggregate formation.



The presence of PVP polymer in the composite appears as white spots on the surface and is clearly visible in the anterior view of the SEM image.



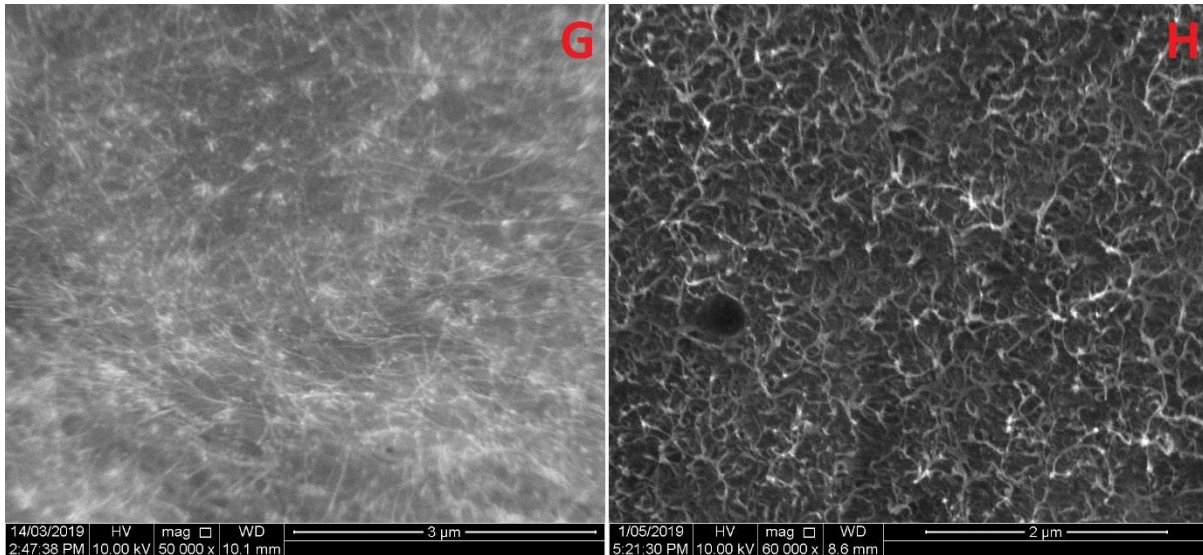


Fig. 3.3.5B: Scanning Electron Microscopy results of PVP functionalized AP-SWNTs in PVDF composite - PVP<sub>10000</sub> (A & B) – alignment like formation highlighted in green circle, PVP<sub>40000</sub> (C & D), PVP<sub>55000</sub> (E & F), and PVP<sub>360000</sub> (G & H); anterior view (left) and fracture side view (right).

Although a stable dispersion of nanotubes is achieved through PVP functionalization in all the four molecular weights of PVP as shown in Fig. 3.3.5B, only PVP<sub>10000</sub> functionalized nanotube exhibited a more pronounced conductive path for an effective thermal conduction as observed in Fig. 3.3.1. This is clearly observed among the dispersed nanotubes in the SEM image of PVP<sub>10000</sub> functionalized nanotube composites, shown in Fig. 3.3.5B (A) as highlighted by green circles. Whereas, such an alignment like formation are not observed with the nanocomposites functionalized with higher molecular weights of PVP. This type of formation could have allowed for an increased interaction between the polymer and the nanotubes, thus achieving a comparatively high thermal and electrical conductivity and higher degree of crystallization.

### 3.3.6 Raman Results

Raman Spectroscopy acts as a useful tool for analysing the interaction between the polymer and the carbon nanotubes. The three main features of a Raman spectrum would be (i) low energy modes or so called radial breathing modes at low frequencies ( $<400\text{ cm}^{-1}$ ), (ii) the defect induced double resonant D band at  $\sim 1350\text{ cm}^{-1}$  and (iii) the tangential modes that are the most intensive high energy mode forming the G-band resulting from in-plane vibrations of  $sp^2$  carbon-carbon bonds[8, 9]. The shift in the tangential mode is an effect often observed upon chemical modification of nanotubes. In addition, it was found that the Raman peak position shifts significantly under compression. The interatomic distance of a material changes when a

strain is applied and thus the vibrational frequencies of some of the normal modes change causing a Raman peak position shift [10]. A stable dispersion of nanotubes in polymer matrix favours mechanical compression. Jang et al. studied the influence of carbon nanotube clustering on the performance properties of cement paste. Their result confirmed the reduction in compressive strength of CNT/cement composites due to poor dispersion and an increase in compressive strength is observed with increasing nanotube dispersion[11].

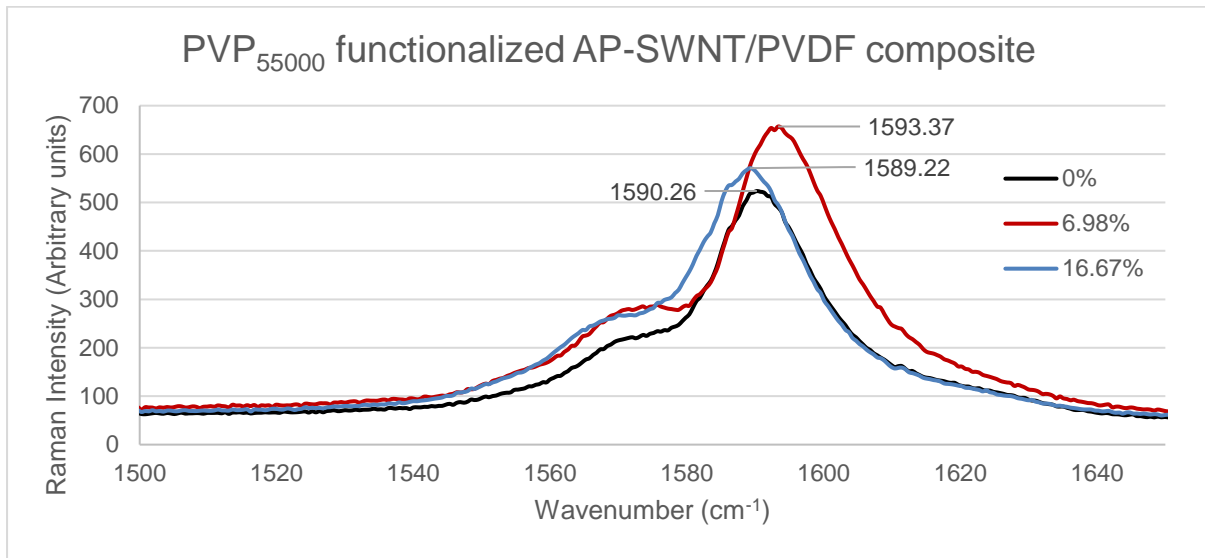


Fig. 3.3.6: G-band of a Raman spectra of unmodified AP-SWNT/PVDF composite, PVP<sub>55000</sub> functionalized AP-SWNT/PVDF composite prepared at a PVP concentration of 6.98 wt. % and 16.67 wt. %.

The G-band of a PVP<sub>55000</sub> functionalized nanotube composite prepared at two different concentrations are compared with G-band of unmodified nanotube composite to analyse the surface functionalization of AP-SWNTs as shown in Fig. 3.3.6. A shift in the peak position of the G-band is observed with PVP functionalization. The G-band for an unmodified nanotube composite is observed at 1590.26 cm<sup>-1</sup> and the G-band for the composite prepared at a PVP concentration of 16.67 wt. % is observed at 1589.22 cm<sup>-1</sup> exhibiting a difference of ~1 wavenumber. Whereas, the G-band observed at 1593.37 cm<sup>-1</sup> for the composite prepared at a concentration of 6.98 wt. % exhibits a difference of more than 3 wavenumbers. The peak shift could be due to the difference in interaction level between the nanotubes and the polymer confirming different level of nanotube dispersion observed with different concentrations of PVP and it is clear from the result that the composite prepared at a concentration of 6.98 wt. % tend to exhibit a different degree of nanotube dispersion compared to unmodified nanotube composite, thus exhibiting a shift of more than 3 wavenumbers.

### 3.4 CONCLUSION

High aspect ratio nanotubes without surface functionalization are effective in the formation of a nanotube network in the polymer matrix thus exhibiting improved thermal, electrical and mechanical properties yet aggregate formation is inevitable due to high van der Waals interaction among the nanotubes. An analysis of the PVDF composite prepared with non-covalently functionalized AP-SWNTs with four different molecular weights of PVP were conducted. Although a stable dispersion of nanotubes is achieved with all the four molecular weights of PVP, a homogeneous dispersion of nanotubes is achieved only with PVP<sub>10000</sub> functionalized nanotube composite at a concentration of 6.98 wt. %. This could be due to the formation of conductive nanotube network that allows for higher thermal and electrical conductivity, higher degree of crystallization, improved mechanical strength. Whereas, PVP with higher molecular weights tend to exhibit a lower degree of network formation compared to PVP<sub>10000</sub> functionalized nanotube composite and unmodified nanotube composite. The diameter of the nanotube and amount of surface coverage of nanotubes plays the key role. A change in aspect ratio would increase the probability for PVP of higher molecular weights to exhibit an effective conductive network.

### 3.5 REFERENCES

1. Ayatollahi, M.R., et al., *Effect of multi-walled carbon nanotube aspect ratio on mechanical and electrical properties of epoxy-based nanocomposites*. Polymer Testing, 2011. **30**(5): p. 548-556.
2. O'Connell, M.J., et al., *Reversible water-solubilization of single-walled carbon nanotubes by polymer wrapping*. Chemical Physics Letters, 2001. **342**(3): p. 265-271.
3. Zhang, W.-b., et al., *High thermal conductivity of poly(vinylidene fluoride)/carbon nanotubes nanocomposites achieved by adding polyvinylpyrrolidone*. Composites Science and Technology, 2015. **106**: p. 1-8.
4. Yang, H., et al., *Diameter-Selective Dispersion of Carbon Nanotubes via Polymers: A Competition between Adsorption and Bundling*. ACS Nano, 2015. **9**(9): p. 9012-9019.
5. Salazar-Rios, J.M., et al., *Understanding the Selection Mechanism of the Polymer Wrapping Technique toward Semiconducting Carbon Nanotubes*. Small Methods, 2018. **2**(4): p. 1700335.
6. Samanta, S.K., et al., *Conjugated Polymer-Assisted Dispersion of Single-Wall Carbon Nanotubes: The Power of Polymer Wrapping*. Accounts of Chemical Research, 2014. **47**(8): p. 2446-2456.
7. Ding, C., et al., *Effects of diameter and aspect ratio of carbon nanotubes on crystalline and electrical properties of poly(ethylene terephthalate) nanocomposites*. Polymer Engineering & Science, 2016. **56**(4): p. 408-417.

8. Graupner, R., *Raman spectroscopy of covalently functionalized single-wall carbon nanotubes*. Journal of Raman Spectroscopy, 2007. **38**(6): p. 673-683.
9. Mu, M., et al., *An in situ Raman spectroscopy study of stress transfer between carbon nanotubes and polymer*. Nanotechnology, 2009. **20**(33): p. 335703.
10. Schadler, L.S., S.C. Giannaris, and P.M. Ajayan, *Load transfer in carbon nanotube epoxy composites*. Applied Physics Letters, 1998. **73**(26): p. 3842-3844.
11. Jang, S.-H., S. Kawashima, and H. Yin, *Influence of Carbon Nanotube Clustering on Mechanical and Electrical Properties of Cement Pastes*. Materials (Basel, Switzerland), 2016. **9**(4): p. 220.



## CHAPTER 4

# PVP FUNCTIONALIZED P3 SINGLE WALLED NANOTUBES IN PVDF COMPOSITES

## 4.1 CHAPTER INTRODUCTION

P3 Single-walled nanotubes used in this study are obtained from Carbon Solutions Ltd. at a purity level of above 90 % achieved through purification of AP-SWNT with nitric acid and obtained in a highly functionalized form with a metal content of about 5-7wt.%. As a result, the carboxyl content of P3-SWNT would be higher than AP-SWNT. In this chapter, the presence of carboxyl content and its impact towards the non-covalent functionalization of P3-SWNT by polyvinylpyrrolidone (PVP) and subsequently the dispersion of the PVP/SWCNT complex in a PVDF matrix is studied. This study also extends towards understanding the relation between the amount of nanotubes and concentration of polymer and their effect in achieving a more homogeneous dispersion.

## 4.2 SAMPLE DETAILS

The composites used in the study were prepared with 1mg of unmodified P3-SWNTs functionalized with polyvinylpyrrolidone (PVP) of various concentration from 0 to 66.67 weight percent, dispersed in 20mg of PVDF polymer. The amount of P3-SWNTs and PVDF polymer were maintained constant throughout the study.

An additional study was performed with composites prepared with 0.25 mg, 0.5 mg, 0.75 mg and 1 mg of unmodified P3-SWNTs functionalized with various amount of polyvinylpyrrolidone ranging from 0.025 mg to 0.5 mg. The amount of PVDF polymer used remains unchanged at 20 mg.

## 4.3 RESULTS & DISCUSSION

### 4.3.1 Thermal Conductivity

Four different molecular weights of PVP were used to non-covalently functionalize P3-SWNTs in the preparation of P3-SWNT/PVDF composites. The concentration of PVP was varied from a weight percent of 0 %, which is a composite prepared with pristine non-functionalized P3-SWNTs, up to a weight percent of 33.33 %. A minimum of three composites for every concentration range were prepared to avoid experimental errors and the thermal conductivity of these composites were measured and an average result is shown in Fig. 4.3.1A.

The theoretical thermal conductivity of pure PVDF polymer was observed to be about  $0.2 \text{ W}\cdot\text{m}^{-1}\cdot\text{K}^{-1}$  [1] and the presence of pristine non-functionalized P3-SWNT has increased the thermal conductivity of the composites to  $2.93 \text{ W}\cdot\text{m}^{-1}\cdot\text{K}^{-1}$ . This can be attributed to the fact that introducing P3-SWNT fillers has increased the thermal conduction of the composite but it

is also safe to consider that due to high van der Waals interaction between the nanotubes, a homogeneous dispersion of nanotubes would not have been achieved and that the nanotubes would have formed aggregates in the polymer matrix. Non-covalent functionalization of nanotubes with polymers such as polyvinylpyrrolidone are observed to have a positive impact towards the enhancement of thermal conductivity of the overall composite [2].

The molecular weights of PVP polymers used in this study were 10000, 40000, 55000, and 360000  $\text{g}\cdot\text{mol}^{-1}$ . Among these a decent thermal conductivity improvement can be seen for the two highest molecular weight polymers 55000  $\text{g}\cdot\text{mol}^{-1}$  and 360000  $\text{g}\cdot\text{mol}^{-1}$ . Composites prepared with PVP<sub>55000</sub> records the highest value of  $4.27 \text{ W}\cdot\text{m}^{-1}\cdot\text{K}^{-1}$  at a concentration of 23.08 wt. %, which is a 46.23 % increase over the composite made with nanotubes only. The composite prepared with PVP<sub>360000</sub>  $\text{g}\cdot\text{mol}^{-1}$  records a highest value of  $3.67 \text{ W}\cdot\text{m}^{-1}\cdot\text{K}^{-1}$  at a concentration of 1.48 wt. %, which is a 25.68 % increase over the non-functionalized nanotube composite.

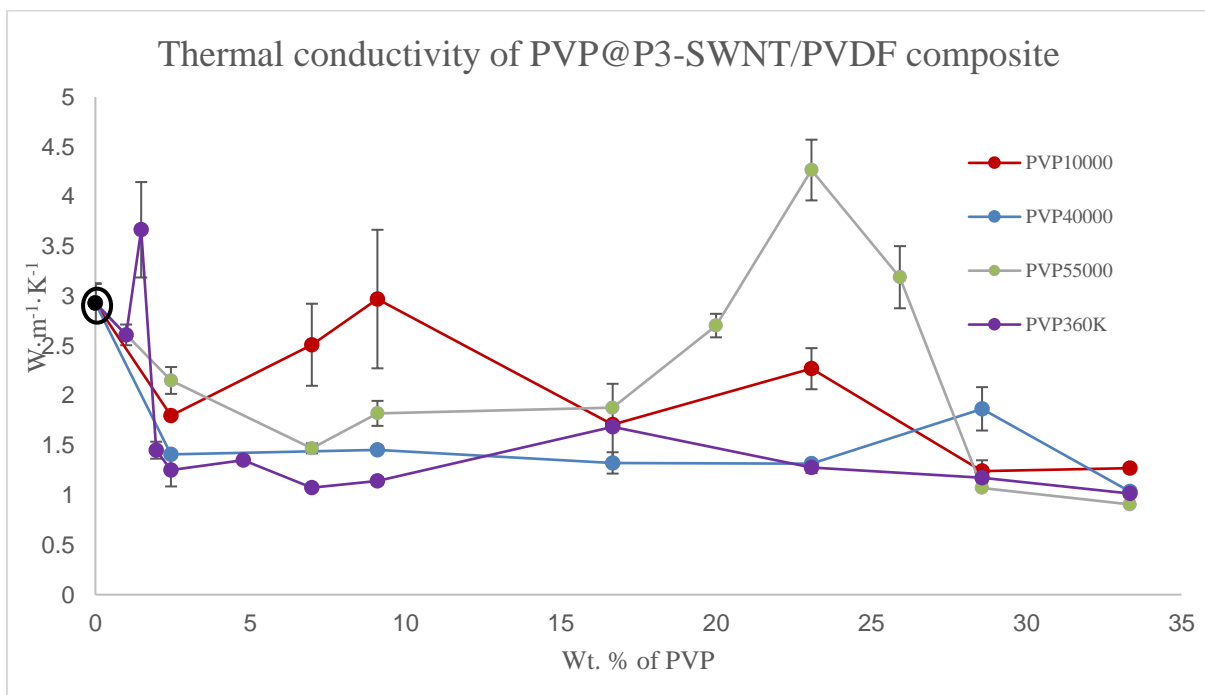


Fig. 4.3.1A: Thermal Conductivity measurements of four different PVP functionalized P3-SWNTs in PVDF composites.

However, composite prepared with PVP<sub>10000</sub> & PVP<sub>40000</sub>  $\text{g}\cdot\text{mol}^{-1}$  has shown an increase in thermal conductivity only at higher concentrations as shown in Fig. 4.3.1B.

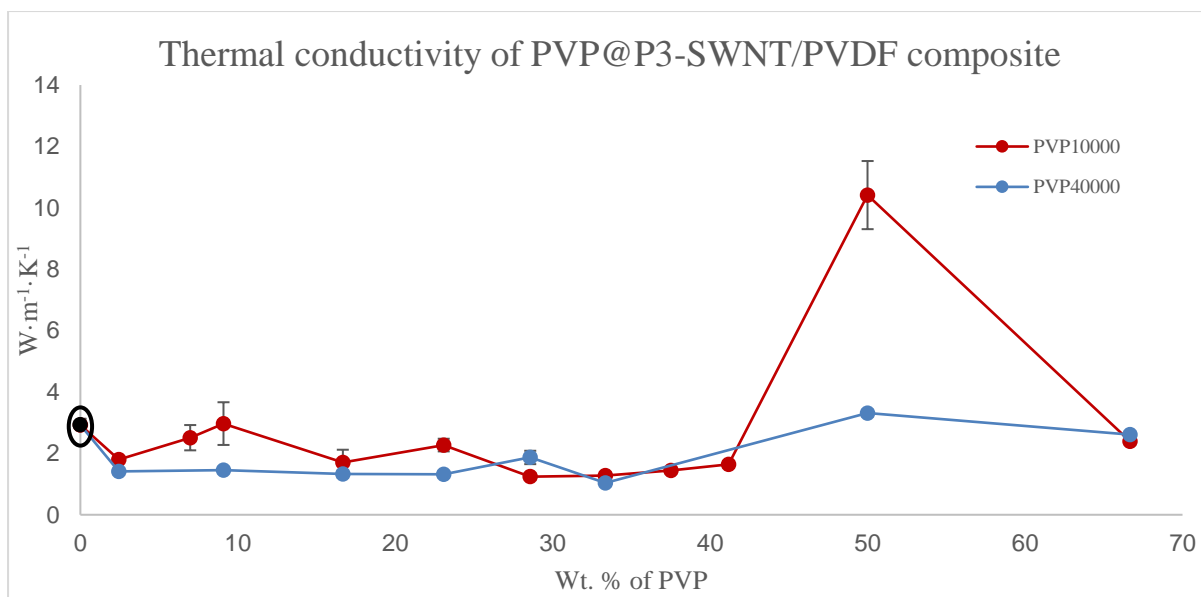


Fig. 4.3.1B: Thermal Conductivity measurements of two different PVP functionalized P3-SWNTs in PVDF composites measured at higher concentration.

The highest thermal conductivity observed in the composite prepared with PVP<sub>10000</sub> is 10.41 W·m<sup>-1</sup>·K<sup>-1</sup> at a concentration range of 50 wt. %, which is a 256.51 % increase compared to composite with non-functionalized nanotubes. Likewise, the composites prepared with PVP<sub>40000</sub> have shown a 13.5 % increase in thermal conductivity with a recorded value of 3.314 W·m<sup>-1</sup>·K<sup>-1</sup> at a concentration of 50 wt. %. It can be assumed from the thermal conductivity results observed for other molecular weights of PVP that the chance of a higher degree of nanotube dispersion for composites prepared with PVP<sub>40000</sub> functionalized P3-SWNTs are high at concentration range higher than the peak position of PVP<sub>55000</sub> composites and lower than the peak position of PVP<sub>10000</sub> composites owing to the length of polymer chain and its influence in polymer wrapping in order to achieve a uniform dispersion of nanotubes. This could lead to a further increase in thermal conductivity observed for PVP<sub>40000</sub> functionalized P3-SWNTs in PVDF composite somewhere along the concentration range between 33.33 wt. % and 50 wt. %. This difference in thermal conductivity measured for different molecular weights could be attributed to the relation between the length of the polymer chain and the amount of single strand of P3-SWNT present in the composite.

The length of the polymer chain defines the molecular weight of the polymer meaning a short polymer chain would yield a polymer with a low molecular weight. In the case of polymer functionalization of nanotubes, the polymer wraps around the surface of the nanotube forming a supra molecular complex thus enhancing the dispersibility of nanotubes in organic solvents. The result observed here could be attributed to the fact that, the surface area of the nanotubes

could not be covered by PVP<sub>10000</sub> at low concentrations as will be the case with PVP<sub>360000</sub> at similar concentrations. The amount of nanotubes wrapped by PVP<sub>360000</sub> at a low concentration is substantial enough to create a positive impact towards the overall thermal conductivity of the composite. However, PVP<sub>55000</sub> could create a similar impact only a comparatively higher concentrations which are then followed by PVP<sub>40000</sub> and PVP<sub>10000</sub>. The requirement for achieving a better thermal conduction in the polymer nanocomposite is to achieve well dispersed nanotubes that still have some sort of connection with the neighbouring nanotubes in the composite just like a network but not be entirely isolated from one another. Excess polymer in the composite might wrap the nanotubes in their entirety, isolating them from the neighbouring nanotubes thus compromising the transport of phonon among the nanotubes leading to decrease in thermal conductivity, as observed at concentration higher than the thermal conductivity peak in Fig. 4.3.1A with PVP<sub>360000</sub> and PVP<sub>55000</sub> functionalization.

Although, a homogeneous dispersion is achieved at a far higher concentration range, a small increase in thermal conductivity values were witnessed both in PVP<sub>10000</sub> at 9.09 wt. % and 23.08 wt. % and in PVP<sub>40000</sub> at 28.57 wt. %. This could be attributed to the fact that at this low concentration range a small group of nanotubes in the composites were randomly functionalized and dispersed leading to a minor improvement in thermal conductivity but a much higher concentration is required to cover the surface area of all the nanotubes thus achieving homogeneous dispersion. A similar experiment by Liang et al. on polyfluorene based SWNT dispersion selectivity, confirmed that the selectivity of PF12 polymer for specific type of carbon nanotube type is dependent on both the nanotube ratio present in the initial sample and the polymer concentration used. Their findings confirmed that PF12 polymer of specific concentration predominantly wraps and disperses semiconducting SWNTs from the mixture over metallic SWNTs, provided the percentage of metallic SWNTs is less than 67 % in the mixture. If this percentage increases to above 67 % then PF12 begins to disperse metallic SWNTs in addition to semiconducting SWNTs. They also reported that if the concentration of the polymer increases, the threshold at which metallic SWNTs begin to disperse shifts to lower values, and beyond a certain increase in concentration, it becomes hard to keep track of this threshold. This confirms a relation between the amount of nanotubes and the concentration of the polymer[3]. Similarly, Z. Li et al. evaluated the network formation of poly (9,9-didodecylfluorene) PFDD wrapped semiconducting SWNT. SEM characterization of the composite prepared with SWNT concentration of 9 mg·mL<sup>-1</sup> and 4/1 weight ratio of PFDD/SWNT revealed a uniform and dense network while a composite prepared with the same

SWNT concentration but a higher polymer ratio of 20/1 leads to poor adhesion. Likewise, increasing the concentration of SWNT from  $9 \text{ mg}\cdot\text{mL}^{-1}$  to  $27 \text{ mg}\cdot\text{mL}^{-1}$  by maintaining the polymer ratio of 20/1 also leads to non-uniform network. It has been confirmed that as the nanotube concentration increases at a fixed polymer/tube ratio or polymer/tube ratio increases at a fixed nanotube concentration, a larger portion of the polymer interacts with the nanotubes likely due to more inter-molecular interactions leading to more effective energy transfer from the polymer to nanotubes[4]. This relation between the nanotubes and polymer are more likely the reason for achieving high thermal conductivity at different concentration in the PVP wrapped P3SWNT/PVDF composite of different molecular weights as observed in Fig. 4.3.1A & 4.3.1B. The wrapping behaviour of a polymer over a single walled nanotube happens similarly but the surface coverage that a polymer chain can achieve would be different with different molecular weights.

To understand more about the relation between the amount of nanotubes and concentration of the polymer, composites with different concentration of nanotubes were prepared at a range of polymer concentrations and their thermal conductivities are plotted in a 3-D graph in Fig. 4.3.1C and Fig. 4.3.1D.

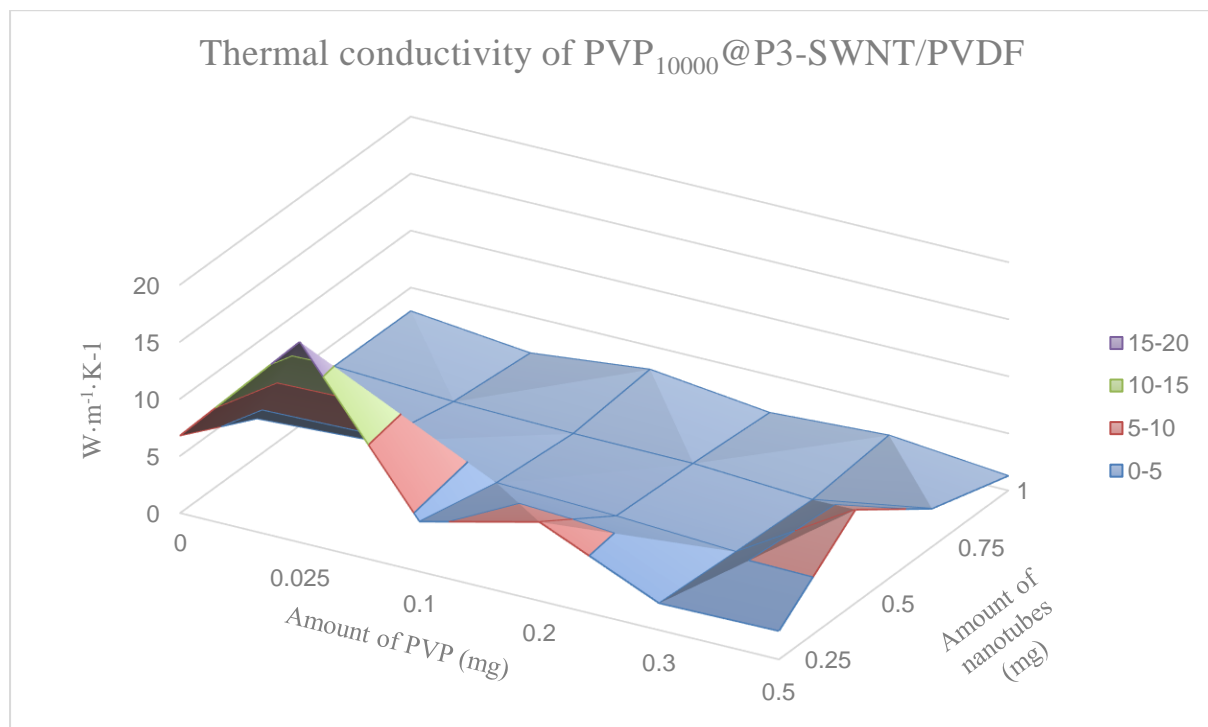


Fig. 4.3.1C: 3-D surface plot of PVP<sub>10000</sub>@P3-SWNT/PVDF composites measured for four different concentrations of P3-SWNT.

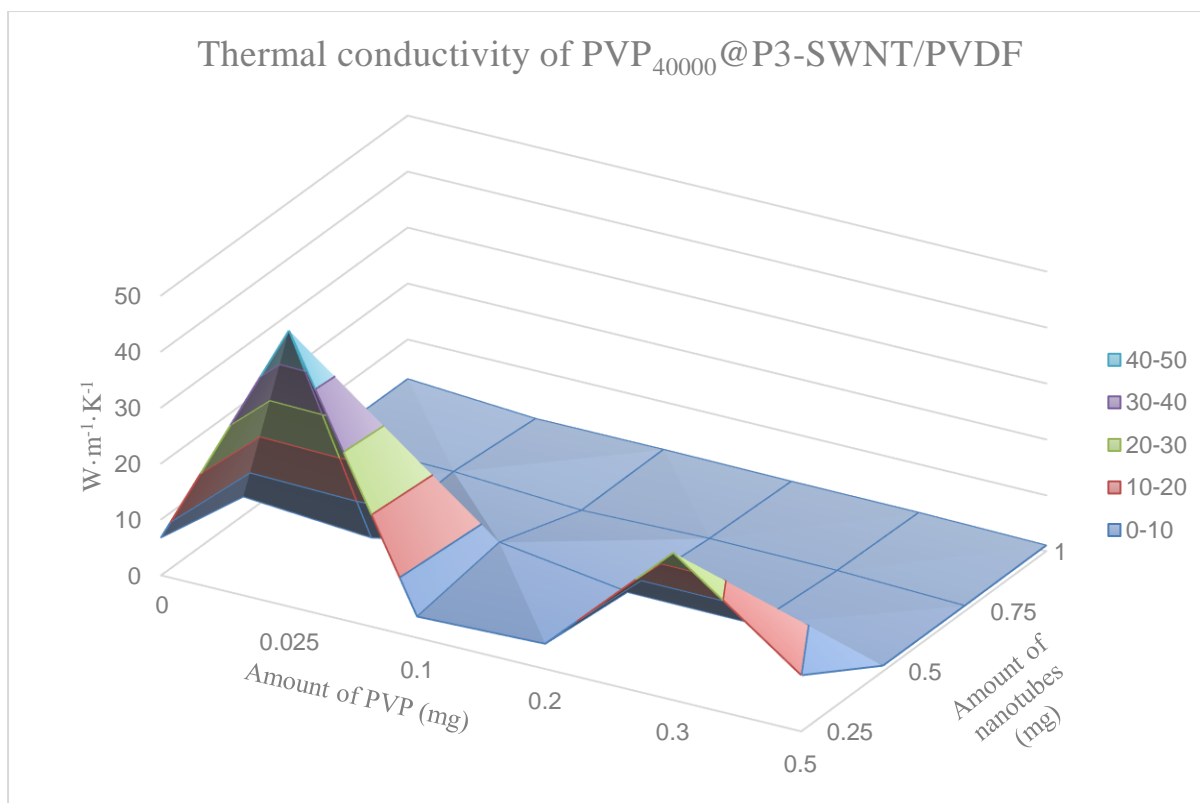


Fig. 4.3.1D: 3-D surface plot of PVP<sub>40000</sub>@P3-SWNTs in PVDF composites measured for four different concentrations of P3-SWNT.

Thermal conductivity of pristine non functionalized P3-SWNTs in PVDF composite with four different amount of nanotubes such as 0.25 mg, 0.5 mg, 0.75 mg and 1 mg with a PVDF amount of 20 mg were measured to be  $6.79 \text{ W}\cdot\text{m}^{-1}\cdot\text{K}^{-1}$ ,  $3.35 \text{ W}\cdot\text{m}^{-1}\cdot\text{K}^{-1}$ ,  $2.99 \text{ W}\cdot\text{m}^{-1}\cdot\text{K}^{-1}$  and  $2.93 \text{ W}\cdot\text{m}^{-1}\cdot\text{K}^{-1}$ . The decrease in the thermal conductivity with the increasing amount of nanotubes can be attributed to the increase in phonon scattering because the higher numbers of nanotubes leads to increased van der Waals interactions between nanotubes but poor interfacial interaction between nanotubes and the base polymer. This leads to poor dispersions and poor formation of CNT networks in the composites. However, lower concentration of nanotubes exhibits comparatively high thermal conductivity due to better interaction with the base polymer leading to better networks of CNTs.

In particular, composites prepared with 0.25 mg of P3-SWNTs exhibit a comparatively high thermal conductivity for both functionalized and non-functionalized SWCNTs. PVP<sub>10000</sub> functionalization of 0.25 mg P3-SWNT composite records a high thermal conductivity value of  $17.56 \text{ W}\cdot\text{m}^{-1}\cdot\text{K}^{-1}$  at very low concentrations of PVP of 9.09 wt. % (0.025 mg) which is a 258.6 % increase compared to composites prepared with unfunctionalized nanotubes. Also, PVP<sub>40000</sub> functionalized 0.25 mg P3-SWNT composite records a high thermal conductivity of

49.35  $\text{W}\cdot\text{m}^{-1}\cdot\text{K}^{-1}$  at the same concentration range which is 726.8 % increase compared to the unfunctionalized nanotubes composites. This can be explained as a homogeneous dispersion and formation of a uniform network, allowing unrestricted phonon transport. However, higher amounts of nanotubes leads to formation of more aggregates or bundles and would require higher concentrations of polymer to achieve a homogeneous dispersion. This is clear in composites containing more than 0.25 mg of P3-SWNTs.

A 50.66 % decrease in thermal conductivity is observed in composites containing non-functionalized 0.5 mg P3-SWNTs compared to non-functionalized 0.25 mg P3-SWNT composite. Though, a minor improvement in thermal conductivity of about 17 % compared to the system without SWCNT functionalization is observed with PVP<sub>10000</sub> functionalization at low concentration of 0.025 mg (9.09 wt. %), a homogeneous dispersion is only achieved at a concentration range of about 0.5 mg (50 wt. %) leading to a high thermal conductivity value of 8.17  $\text{W}\cdot\text{m}^{-1}\cdot\text{K}^{-1}$  which is a 143.88 % increase compared to unmodified 0.25 mg P3-SWNT composites. This confirms that the relation between amount of nanotubes and the polymer concentration plays a vital role in achieving a homogeneous dispersion.

It is not just the concentration of the polymer but also the length of the polymer chain that is important. In the composite containing 0.5 mg P3-SWNT functionalized with PVP<sub>40000</sub> a homogeneous dispersion is achieved at a comparatively lower concentration of 0.1 mg (16.67 wt. %) with a thermal conductivity increase compared to the unfunctionalized system of 88.36 % exhibiting a value of 6.31  $\text{W}\cdot\text{m}^{-1}\cdot\text{K}^{-1}$ . This observation in PVP<sub>40000</sub> can be attributed to the fact that, the longer polymer chains are capable of covering a larger surface area of the nanotubes than a short polymer chain does at the same concentration range.

However, such a dispersion is not observed in composites containing 0.75 mg and 1 mg of P3-SWNTs for the polymer concentration range of 0.025 mg to 0.5 mg. Although an increase in thermal conductivity of about 11.04 % is observed with PVP<sub>10000</sub> functionalized 0.75 mg P3-SWNT composite at 0.5 mg (40 wt. % PVP) concentration range, it is safe to consider this a minor enhancement and a homogeneous dispersion occurs at a much higher concentration range. This is confirmed from Fig. 4.3.1B where a homogeneous dispersion in the 1mg composites are only achieved at a concentration range higher than 33.33 wt. % in both PVP<sub>10000</sub> and PVP<sub>40000</sub> functionalized composites.



### 4.3.2 Crystallization behaviour of PVP@P3-SWNT/PVDF composite

Various studies confirming the fact that carbon nanotubes are an excellent nucleating agent and observations of the crystallization of a polymer matrix by introducing unmodified pristine nanotubes in the composite have been reported[5]. However, some recent research has focussed on understanding the effect of an interfacial interaction between nanotubes and the polymer and its impact on the crystallinity of the polymer matrix.

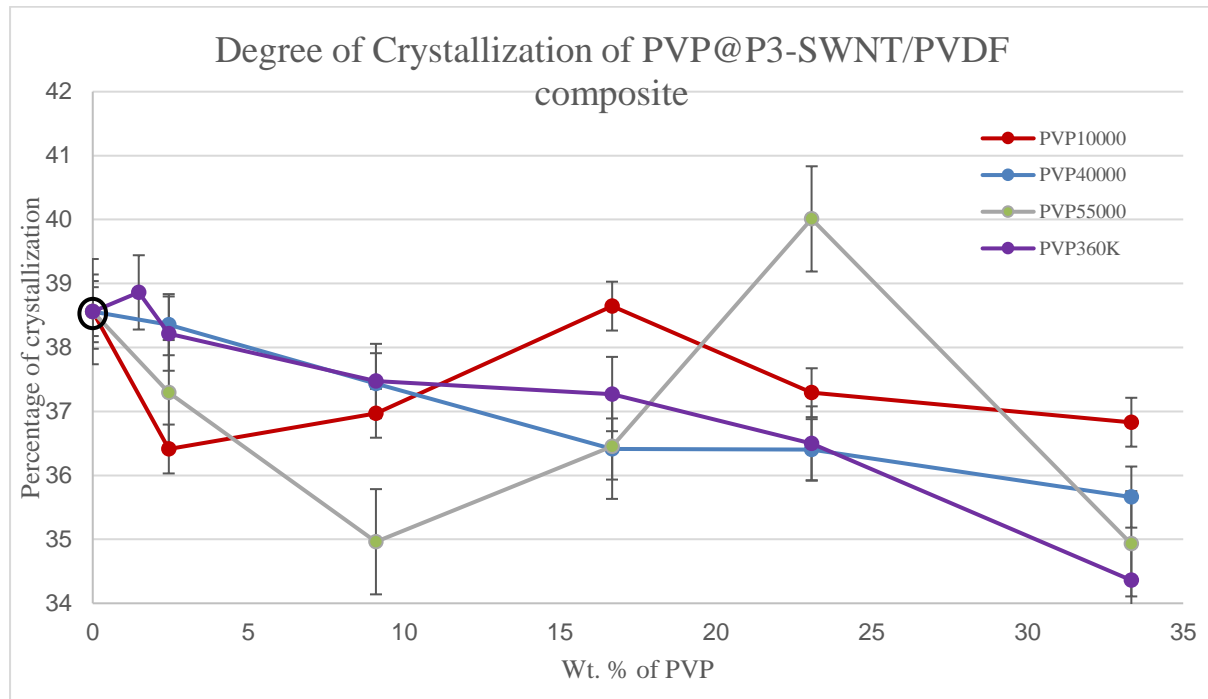


Fig. 4.3.2: Crystallization vs PVP wt. % of P3-SWNT/PVDF composites.

The degree of crystallinity observed for composites prepared with P3-SWNTs fillers functionalized by PVP of four different molecular weights are shown in Figure 4.3.2. The result observed shows some resemblance to their respective thermal conductivity curves. A minor improvement in the degree of crystallization is observed in PVP<sub>360000</sub> at a concentration range of 1.48 wt. % and in PVP<sub>55000</sub> at a concentration range of 23.08 wt. %. However, both PVP<sub>10000</sub> and PVP<sub>40000</sub> do not exhibit any improvement in the concentration lower than 33.33 wt. %. This observation can be attributed to the fact that at these concentration the composites prepared with nanotubes functionalized with PVP<sub>10000</sub> and PVP<sub>40000</sub> might not exhibit a homogeneous dispersion to trigger a nucleation effect for the entire polymer matrix. Although, there could be an improvement in crystallization in these composites at higher concentrations but unfortunately time did not permit to go further high on the concentration.

### 4.3.3 Electrical Conductivity

The electrical conductivity of P3-SWNT/PVDF composites made using nanotubes wrapped with PVP of four different molecular weights were analysed as shown in Fig 4.3.6. Similar to the thermal conductivity results, the composite functionalized with PVP of highest molecular weight tend to exhibit an improvement in electrical conductivity at the lowest range.

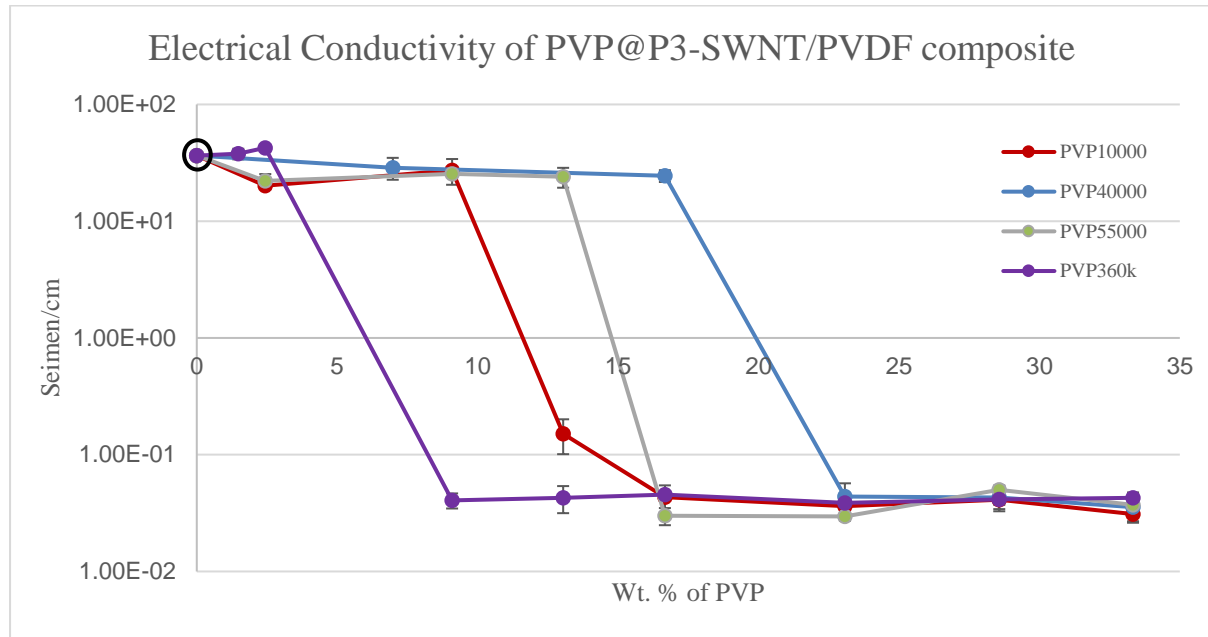


Fig. 4.3.3: Electrical Conductivity measurement of four different PVP functionalized P3-SWNTs in PVDF composites.

PVP<sub>360000</sub> records an increased value of  $42.5 \text{ S}\cdot\text{cm}^{-1}$  in a low concentration range near 2.43 wt. % compared to composites prepared with unmodified nanotubes which have an electrical conductivity of  $36.5 \text{ S}\cdot\text{cm}^{-1}$  and a threshold point is reached at higher concentrations contributing to the fact that, any further introduction of polymer after achieving a homogeneous dispersion compromises the contacts between the nanotubes leading to poor formation of the network and less conductivity. PVP<sub>55000</sub> and PVP<sub>40000</sub> also exhibit good electrical conductivity at low concentrations but reach a threshold point at a comparatively higher concentration than PVP<sub>360000</sub> as observed in the Fig. 4.3.3. This is due to the difference in the length of molecular chain that leads to polymer wrapping and the concentration at which a homogeneous dispersion is achieved. Similarly, percolation threshold is achieved in PVP<sub>360000</sub> in a lower concentration range followed by PVP<sub>55000</sub> and then by PVP<sub>40000</sub>. This could be attributed to their polymer chain length and surface coverage of nanotubes, meaning higher polymer chain length allows for higher surface coverage of nanotubes leading to isolation of nanotube from their neighbours. Although a fairly good electrical conductivity is achieved in PVP<sub>55000</sub> and

PVP<sub>40000</sub>, it is lower compared to composites prepared with unmodified nanotubes and PVP<sub>360000</sub> functionalized nanotubes. This is due to the fact that higher amounts of polymer present in the composite restricts the movement of electrons from a nanotube to neighbouring nanotubes and lowers the conductivity of the composite but polymer wrapping of nanotubes is imperative to achieve a homogeneous dispersion. The key to achieve this without compromising the formation of a network is through functionalization of nanotubes with polymer of high molecular weight. This would lead to a dispersion at a very low concentration, leading to lower wrapping polymer presence and high connectivity between nanotubes. Even though, PVP<sub>10000</sub> exhibits some electrical conductivity in the low concentration range, the conductivity is lower than unmodified nanotube composites and also PVP<sub>10000</sub> with its short polymer chain exhibits a homogeneous dispersion only at higher concentration range as observed with the thermal conductivity results in Fig. 4.3.1B. The electrical conductivity at such high concentrations is expected to be very low. So there is a chance the presence of PVP<sub>10000</sub> might not have created an impact in the electrical conductivity of the composite at this low concentration range and the electrical conductivity observed could be entirely due to the presence of unmodified nanotubes in the composite.

#### *4.3.4 Mechanical Characterization*

The interfacial interaction between the nanotubes and polymer has a direct correlation with the glass transition temperature. Gissinger et al. studied the nanoscale structure – property relationships of polyacrylonitrile/CNT composite and confirmed that the glass-transition temperature of the composite increases in correlation with the amount of CNT/polymer interfacial area per unit volume but inversely with the CNT diameter as the interfacial area per unit volume tends to decrease for larger diameter of CNTs[6].

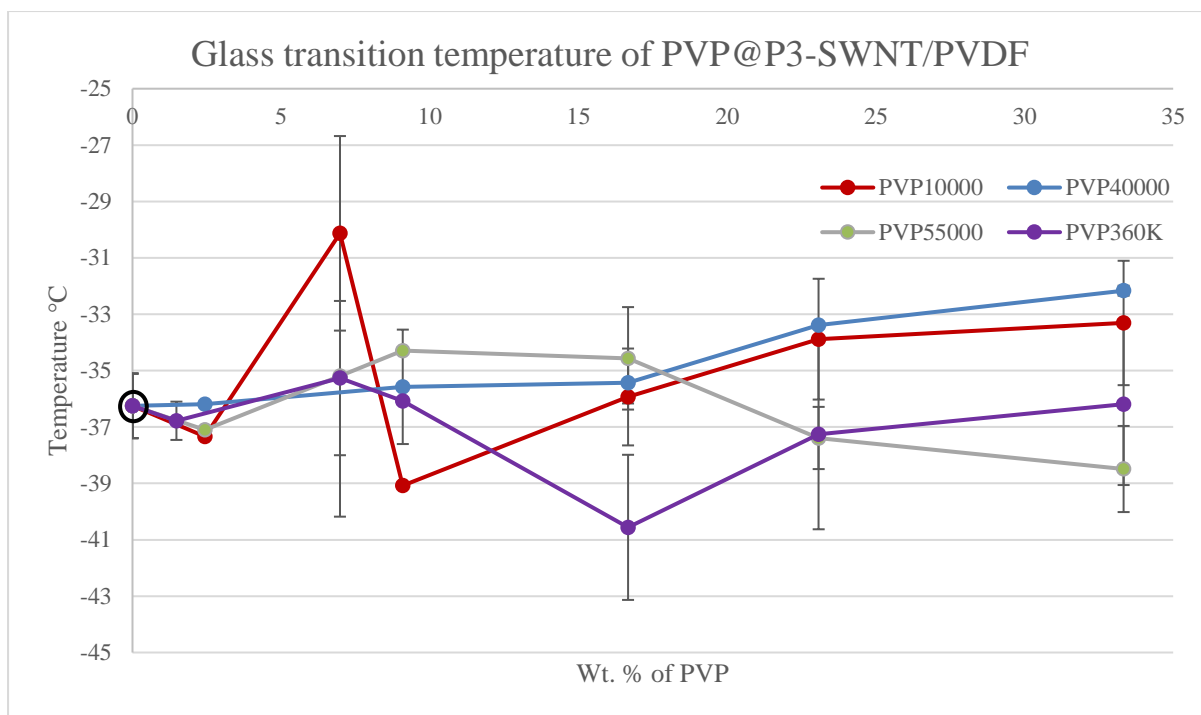


Fig. 4.3.4A: Glass transition measurement of four different PVP functionalized P3-SWNTs in PVDF composites.

Glass transition temperatures of P3-SWNT/PVDF composite functionalized with four different molecular weights of PVP were measured and are plotted in Fig. 4.3.4A, with respect to the concentration of PVP polymer. The composite prepared with non-functionalized P3-SWNTs were plotted at 0 along the x-axis and exhibits a glass transition temperature of  $-36.25\text{ }^{\circ}\text{C}$ . Functionalization of nanotubes with PVP has clearly shown an increase among the two highest molecular weight polymers PVP<sub>360000</sub> and PVP<sub>55000</sub> at lower concentrations and PVP<sub>55000</sub> in particular exhibits an increase in the concentration range between 6.98 wt. % and 23.08 wt. %. This result also correlates with the thermal conductivity result observed for PVP<sub>360000</sub> and PVP<sub>55000</sub> in Fig. 4.3.1A, confirming an increased interaction with the PVDF polymer and PVP functionalized P3-SWNT in this concentration range. On the contrary, a homogeneous dispersion is expected to be achieved in PVP<sub>10000</sub> and PVP<sub>40000</sub> only at far higher concentrations. This leads to the observation in Fig. 4.3.4A, exhibiting a gradual increase in glass transition temperature with increasing concentration of PVP polymer.

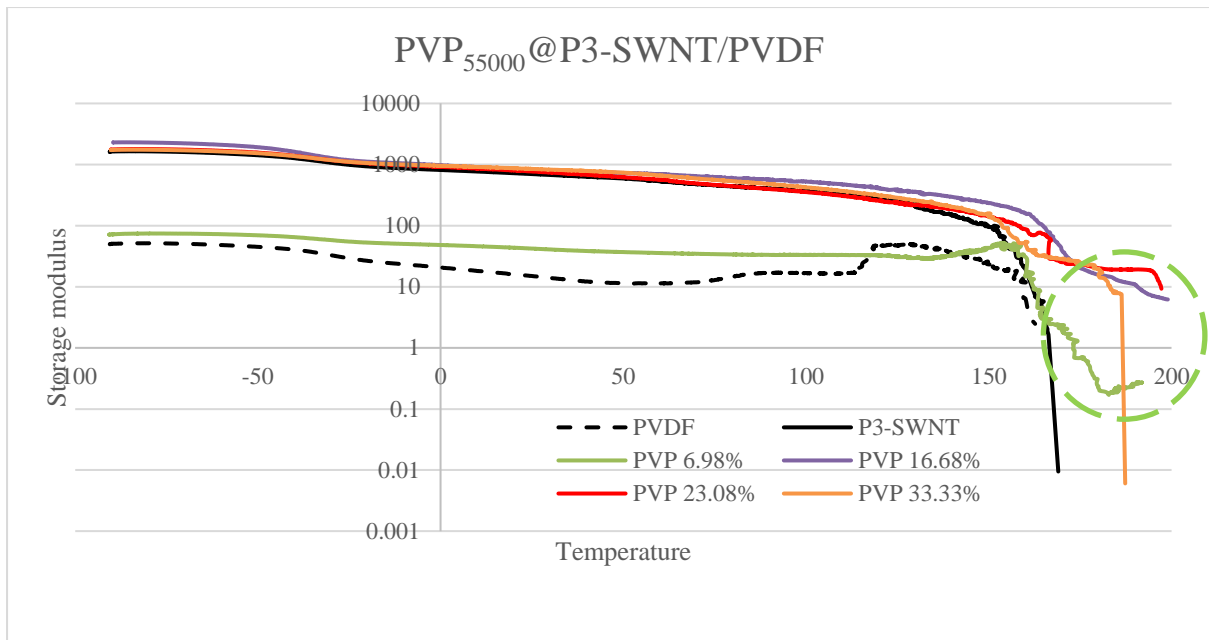


Fig. 4.3.4B: Storage modulus measurement of PVP<sub>55000</sub> functionalized P3-SWNTs in PVDF composites.

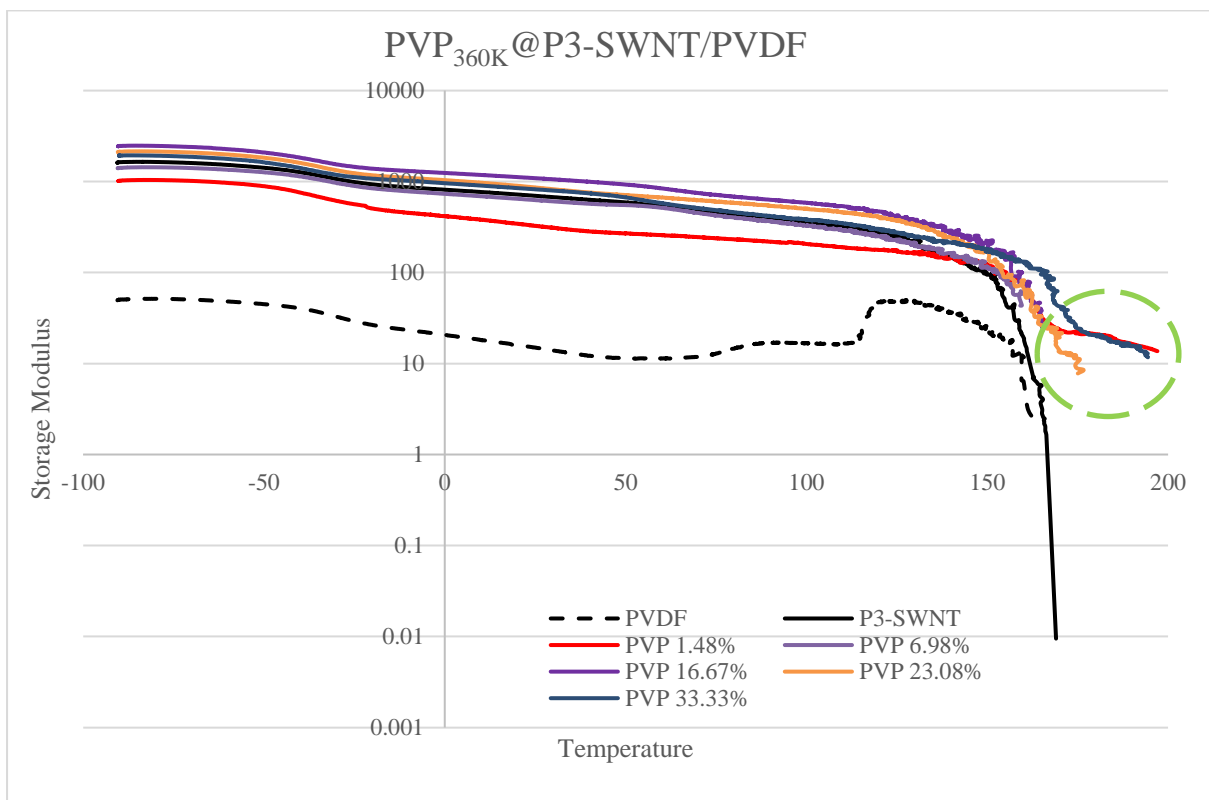


Fig. 4.3.4C: Storage modulus measurement of PVP<sub>360000</sub> functionalized P3-SWNTs in PVDF composites.

The dotted plot in the graph Fig. 4.3.4B and Fig. 4.3.4C, represents the result of a pure PVDF polymer film and introducing non-functionalized P3 single walled nanotubes in the mixture has shown a major increase in storage modulus of the composite (solid black line). Both, PVP<sub>55000</sub> and PVP<sub>360000</sub> functionalized P3-SWNT composites have shown a similar storage

modulus as the unmodified nanotube composites but they tend to exhibit a different mechanical strength at higher concentration range. The melting temperature of a PVDF polymer is observed to be 162.69 °C and the composites prepared with unmodified P3-SWNT nanotubes does not exhibit a good dispersion and tend to form bundles or agglomerates due to van der Waals interaction. This results in the composite not being able to maintain a mechanical strength when the base PVDF polymer begins to melt and cannot withstand a temperature beyond their yielding point at 169.02 °C as observed in Fig. 4.3.4C. On the contrary, the composites that exhibit a homogeneous dispersion forms some kind of a nanotube network and is observed to exhibit a mechanical strength even at temperatures higher than the yielding point of unmodified P3-SWNT/PVDF composites and this correlates with their respective thermal conductivity result. PVP<sub>360000</sub> functionalized nanotubes exhibits high thermal conductivity in composites prepared at a PVP concentration of 1.48 wt. %. This composite is also observed to exhibit some mechanical strength at temperatures as high as 197.04 °C, confirming the presence of some sort of nanotube network that holds the composite together. A similar observation is experienced in composites with PVP<sub>55000</sub> functionalized nanotubes. A minimal mechanical strength is even observed at temperatures as high as 197.24 °C in composites at the same concentration of PVP that exhibits high thermal conductivity.

A homogeneous dispersion in composites with PVP<sub>40000</sub> functionalized nanotubes is expected to be achieved at a far higher concentration. This will be reflected in the mechanical strength of the composite and is clearly observed in Fig. 4.3.4D. The composites in the concentration range lower than 33.33 wt. % exhibits no effective mechanical strength above the yielding point of unmodified nanotube composite with the exception of 2.44 wt. %. Even though, the composites can maintain a certain amount of mechanical strength at temperature of about 178.64 °C which is higher than the yielding point of an unmodified nanotube composite. They are still not capable of reaching a higher temperature as observed in composites prepared with PVP<sub>55000</sub> or PVP<sub>360000</sub> functionalized nanotube composite shown in Fig. 4.3.4B & Fig. 4.3.4C. It is quite certain from the observation that the polymer-nanotube interaction observed in PVP<sub>40000</sub> functionalized nanotube composites of 2.44 wt. % are not as effective as a PVP<sub>55000</sub> or PVP<sub>360000</sub> functionalized nanotube composite. This confirms that concentration of PVP<sub>40000</sub> is not enough to disperse all the nanotubes well in the composite in order to create a network with the neighbouring nanotubes thus holding the composite together.

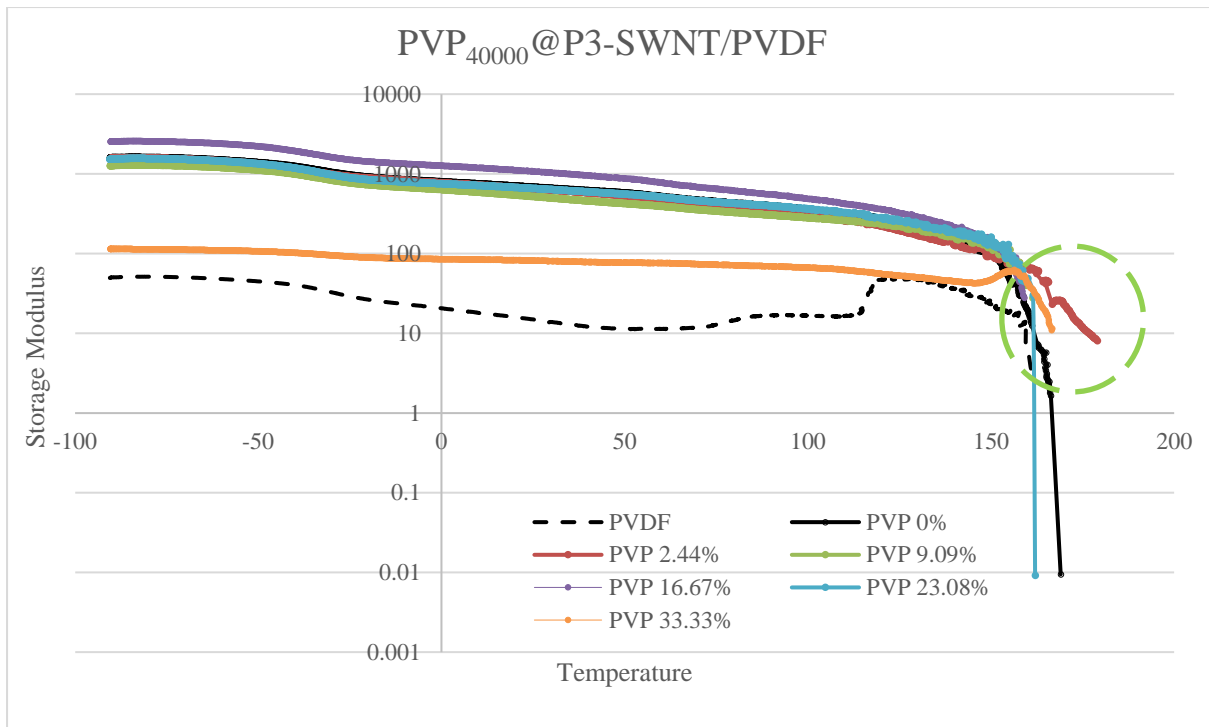


Fig. 4.3.4D: Storage modulus measurement of PVP<sub>40000</sub> functionalized P3-SWNTs in PVDF composites.

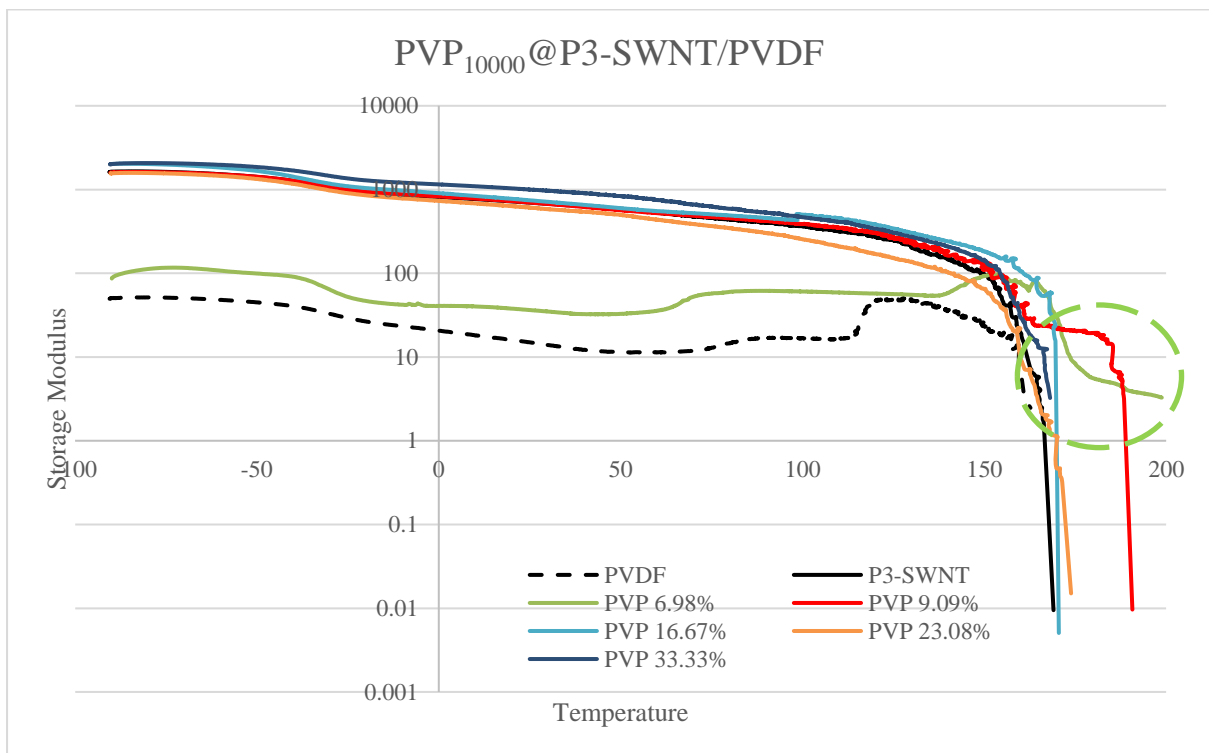


Fig. 4.3.4E: Storage modulus measurement of PVP<sub>10000</sub> functionalized P3-SWNTs in PVDF composites.

Just like other composites, PVP<sub>10000</sub> also correlates with their respective thermal conductivity results. A thermal conductivity increase is observed in Fig. 4.3.1A, between 6.98 wt. % and 9.09 wt. % and these composites also exhibit some mechanical strength above the yielding

temperature of unmodified nanotube composite at a temperature as high as 198.8 °C and 190.7 °C. The composites that exhibited improved mechanical strength also exhibits higher glass transition temperature as shown in Fig. 4.3.4A, thus confirming the hypothesis that the short polymer chain of PVP<sub>10000</sub> disperse nanotubes in smaller groups until enough concentration of PVP is present to cover the surface area of all nanotubes leading to a homogeneous dispersion.

#### 4.3.5 Microscopy Results

SEM images of non-functionalized P3-SWNTs in PVDF nanocomposite are shown in Fig. 4.3.5A. The left side image is the anterior view of the sample and the right side image is achieved by exposing the composite to liquid nitrogen and fracturing the sample so the composite formation can be analysed along the thickness of the sample through SEM. It can be seen that the nanotubes in the composite exhibits poor dispersion due to high van der Waals interaction, thus forming aggregates that are highlighted by red circles. SEM analysis of the composites prepared at concentrations that exhibit an increased thermal conductivity (as shown in Fig. 4.3.1A) for four different molecular weights of PVP are shown in the Fig. 4.3.5B. SWCNT aggregates are not observed in composites that are prepared with PVP functionalization of nanotubes. The presence of PVP is observed as white spots on the surface and is clearly visible in the anterior view of the sample.

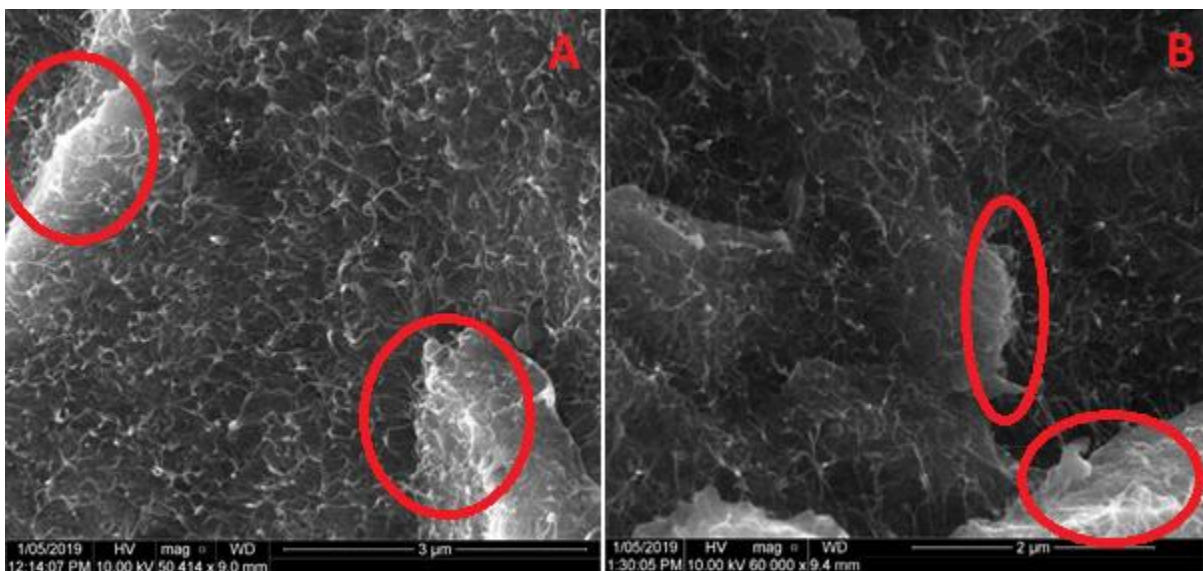
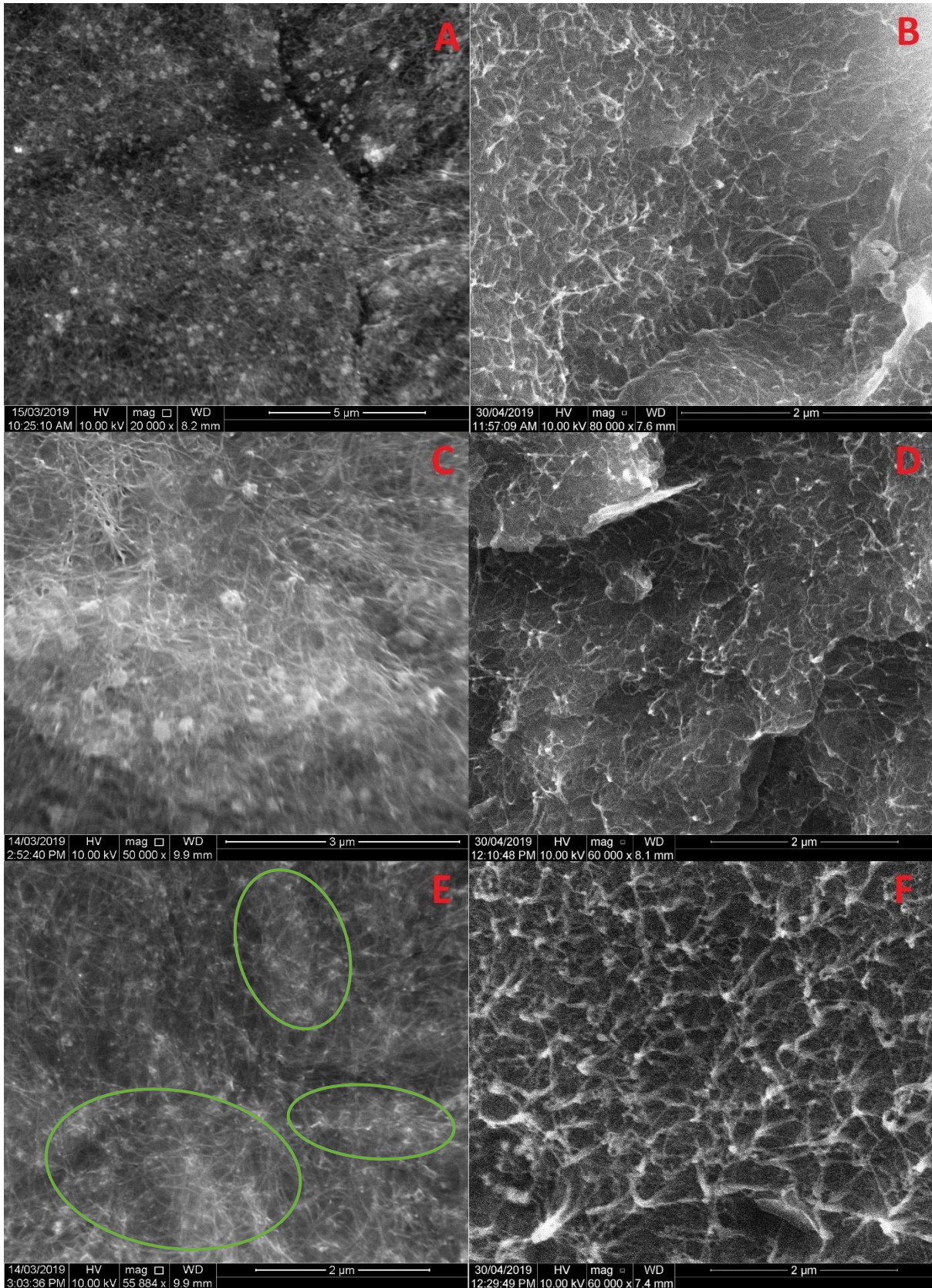


Fig. 4.3.5A : Scanning Electron Microscopy results of non-functionalized P3-SWNTs in PVDF composite; anterior view (A) and fractured side view (B). Agglomeration of nanotubes are highlighted in red circles.





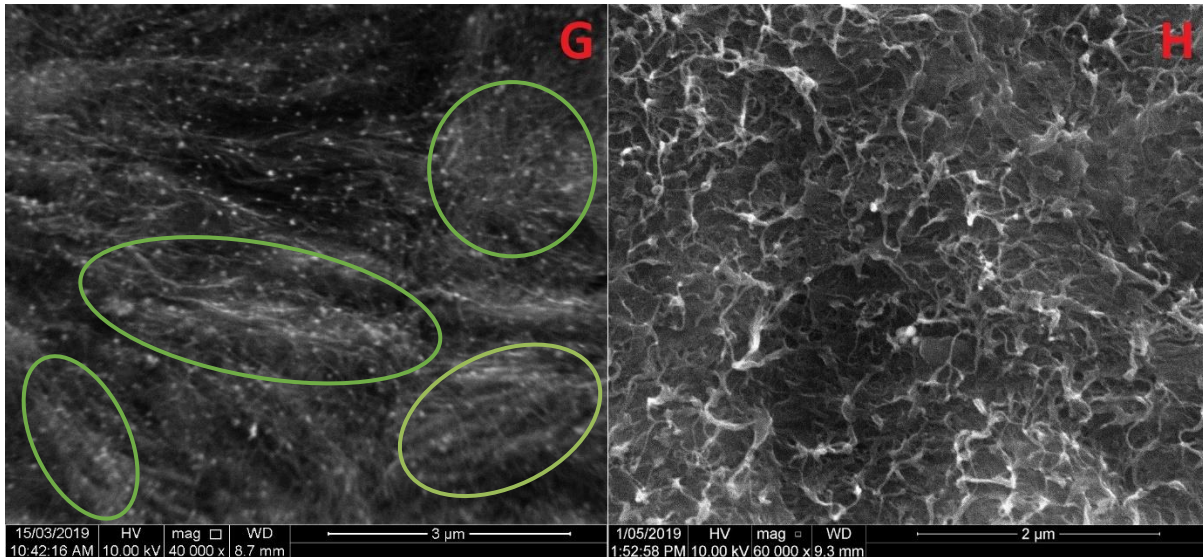


Fig. 4.3.5B : Scanning Electron Microscopy results of PVP functionalized P3-SWNTs in PVDF composite - PVP<sub>10000</sub> (A & B), PVP<sub>40000</sub> (C & D), PVP<sub>55000</sub> (E & F), and PVP<sub>360000</sub> (G & H) – uniform dispersion highlighted in green circle; anterior view (left) and fracture side view (right).

Among the four different molecular weights, PVP<sub>55000</sub> and PVP<sub>360000</sub> achieve homogeneous dispersion at low concentration and thus exhibit high thermal conductivity. This can be observed in the image (E & G) of Fig. 4.3.5B highlighted in the green circles where a large proportion of the nanotubes exhibit a uniform dispersion. Likewise, the fractured side view image (F & H) also exhibits a uniform surface without any presence of aggregate formation. Nonetheless, PVP<sub>40000</sub> and PVP<sub>10000</sub> functionalized nanotube composites exhibit a certain degree of nanotube dispersion as observed in the SEM image (A & C) of Fig. 4.3.5B but they still exhibit lower thermal and electrical conductivity compared to unmodified nanotube composite due to poor formation of nanotube network along the concentration range lower than 33.33 wt. %.

#### 4.3.6 Raman Results

Raman spectroscopy plays an important role to study and investigate the dispersion of single walled carbon nanotube in polymer matrix [7, 8]. Microscopic load transfer from the matrix to the nanotubes can be studied from the shift of the Raman band under applied stress or strain [9]. A shift in Raman peak is observed if the stress applied to the composite material is transferred to CNT. This shift varies linearly with applied strain in the elastic range and they highly depends on the orientation of nanotubes and the properties of the polymer matrix [10, 11]. Raman peaks of SWNTs down shift to lower wavenumber when axial strain is applied on the tubes [12]. Zhang et al. studied the Raman shift in PVA composite film prepared with PVP



wrapped SWNT and confirmed a downshift of Raman G band observed with increasing strain% [13].

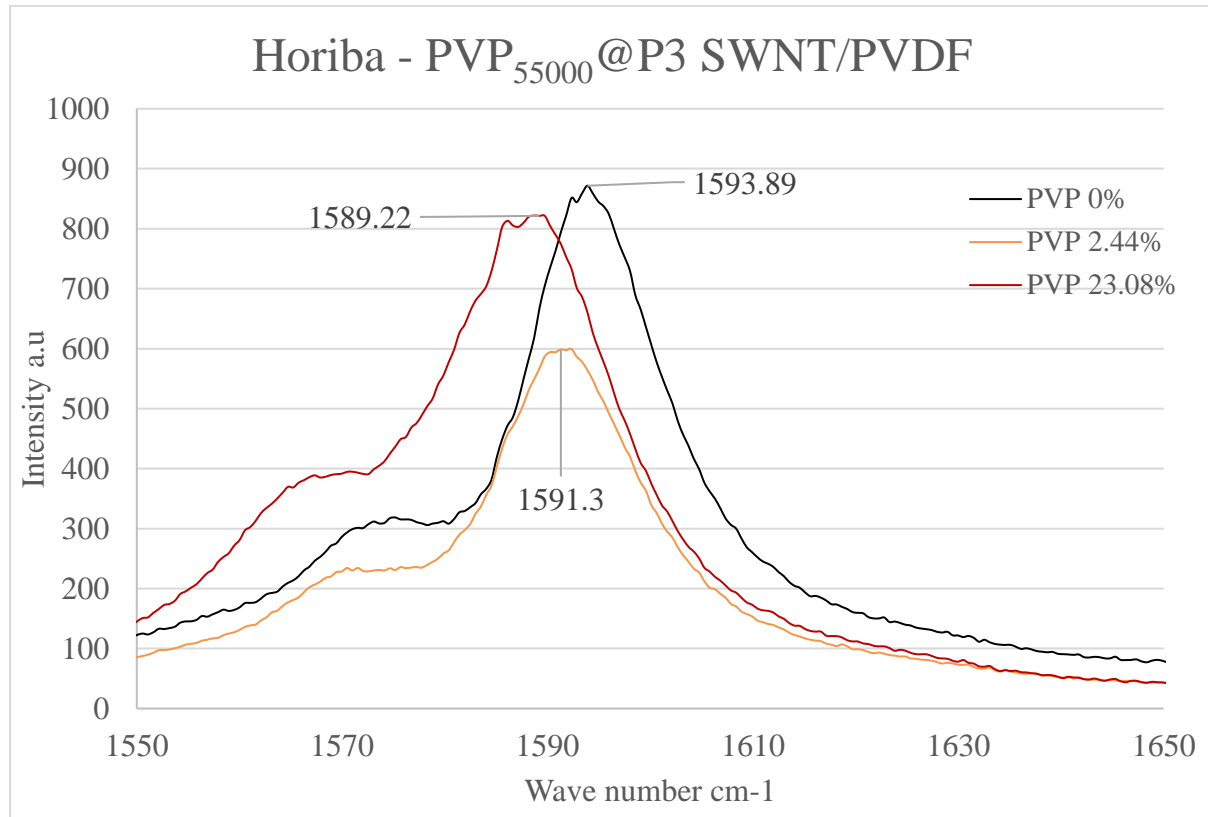


Fig. 4.3.6: G-band of a Raman spectra of unmodified P3-SWNT/PVDF composite, PVP<sub>55000</sub> functionalized P3-SWNTs in PVDF composite prepared at a PVP concentration of 2.44 wt. % and 16.67 wt. %

A shift in the peak position of an unmodified nanotube composite is observed with PVP<sub>55000</sub> functionalization of nanotubes. The G band of an unmodified nanotube composite is observed at 1593.89 cm<sup>-1</sup> and the G band for composite prepared at a PVP<sub>55000</sub> concentration of 2.44 wt. % is observed at 1591.3 cm<sup>-1</sup> exhibiting a shift of about 2.5 wavenumbers. Similarly, a peak shift of about 4.6 wavenumbers is observed with the G band position at 1589.22 cm<sup>-1</sup> for the composite prepared at a PVP<sub>55000</sub> concentration of 23.08 wt. %. The peak shift could be attributed to the difference in amount of strain applied on the nanotubes as a result of a homogeneous dispersion of nanotubes in the polymer matrix leading to an increased level of interaction between the polymer and nanotube.

#### 4.4 CONCLUSION

Knowledge regarding the relation between the amount of nanotubes and the molecular weight of the wrapping polymer is crucial in achieving non-covalent functionalization and an effective homogeneous dispersion of nanotubes in a polymer matrix. A comparison of pristine P3-

SWNT/PVDF composite and non-covalently functionalized P3-SWNTs in PVDF composite with PVP of four different molecular weights has been analysed.

Homogeneous dispersions are achieved in composites with PVP of high molecular weights at low concentration and with lower molecular weights at comparatively higher concentrations. However, a better formation of conductive nanotube network is achieved in composites prepared with PVP<sub>360000</sub> and PVP<sub>55000</sub> functionalized nanotubes compared to other two molecular weights, which are observed in their respective thermal conductivity and electrical conductivity measurements. Further results obtained from mechanical characterization confirms a network kind of connection between the nanotubes in composites that are functionalized with PVP<sub>360000</sub> and PVP<sub>55000</sub>, that allows the composite to sustain a mechanical strength even at temperature beyond the melting point of base polymer. The results obtained depends on the amount of nanotubes used in this research meaning a decreased amount of nanotubes would require PVP of shorter polymer chain or lower molecular weight to obtain a similar results. This work confirms that an enhanced physical property in a composite prepared with a certain amount of single walled nanotubes can be achieved by tailoring the composite with a polymer of specific molecular weight at a specific concentration range.

#### 4.5 REFERENCES

1. dos Santos, W.N., C.Y. Iguchi, and R. Gregorio, *Thermal properties of poly(vinylidene fluoride) in the temperature range from 25 to 210°C*. Polymer Testing, 2008. **27**(2): p. 204-208.
2. Zhang, W.-b., et al., *High thermal conductivity of poly(vinylidene fluoride)/carbon nanotubes nanocomposites achieved by adding polyvinylpyrrolidone*. Composites Science and Technology, 2015. **106**: p. 1-8.
3. Liang, S., et al., *Effect of Single-walled Carbon Nanotube (SWCNT) Composition on Polyfluorene-Based SWCNT Dispersion Selectivity*. Chemistry – A European Journal, 2018. **24**(39): p. 9799-9806.
4. Li, Z., et al., *Surface effects on network formation of conjugated polymer wrapped semiconducting single walled carbon nanotubes and thin film transistor performance*. Organic Electronics, 2015. **26**: p. 15-19.
5. Hegde, M., et al., *SWCNT Induced Crystallization in an Amorphous All-Aromatic Poly(ether imide)*. Macromolecules, 2013. **46**(4): p. 1492-1503.
6. Gissing, J.R., et al., *Nanoscale Structure–Property Relationships of Polyacrylonitrile/CNT Composites as a Function of Polymer Crystallinity and CNT Diameter*. ACS Applied Materials & Interfaces, 2018. **10**(1): p. 1017-1027.
7. Chang, T.E., et al., *Conductivity and mechanical properties of well-dispersed single-wall carbon nanotube/polystyrene composite*. Polymer, 2006. **47**(22): p. 7740-7746.

8. Bibi, S., et al., *Chitosan/CNTs green nanocomposite membrane: Synthesis, swelling and polyaromatic hydrocarbons removal*. *Materials Science and Engineering: C*, 2015. **46**: p. 359-365.
9. Wood, J., et al., *Carbon nanotubes: From molecular to macroscopic sensors*. *Phys. Rev. B*, 2000. **62**.
10. Wood, J., Q. Zhao, and D. Wagner, *Orientation of carbon nanotubes in polymers and its detection by Raman spectroscopy*. *Composites Part A: Applied Science and Manufacturing*, 2001. **32**: p. 391-399.
11. Wood, J.R., et al., *Mechanical Response of Carbon Nanotubes under Molecular and Macroscopic Pressures*. *The Journal of Physical Chemistry B*, 1999. **103**(47): p. 10388-10392.
12. Ma, W., et al., *High-Strength Composite Fibers: Realizing True Potential of Carbon Nanotubes in Polymer Matrix through Continuous Reticulate Architecture and Molecular Level Couplings*. *Nano Letters*, 2009. **9**(8): p. 2855-2861.
13. Zhang, X., et al., *Poly(vinyl alcohol)/SWNT Composite Film*. *Nano Letters*, 2003. **3**(9): p. 1285-1288.

## CHAPTER 5

# PVP FUNCTIONALIZED MULTI WALLED NANOTUBES IN PVDF COMPOSITES

Part of this chapter was published previously in Namasivayam, M.; Andersson, M.R.; Shapter, J. Role of Molecular Weight in Polymer Wrapping and Dispersion of MWNT in a PVDF Matrix. *Polymers* **2019**, *11*, 162.

## 5.1 CHAPTER INTRODUCTION

Multi-walled nanotubes used in this research were obtained from Sigma-Aldrich prepared by chemical vapor deposition with less than 5 % metal oxide content. The average diameter of the MWNT is 9.5 nm, length being 1.5  $\mu\text{m}$ , density of  $\sim 2.1 \text{ g}\cdot\text{mL}^{-1}$  at 25 °C and a melting point of 3652 – 3697 °C. In this chapter the non-covalent functionalization of MWNTs by PVP polymer with different molecular weights is compared and the physical properties of the composites prepared with the addition of the PVP functionalized MWNTs to PVDF polymer are analysed extensively.

## 5.2 SAMPLE DETAILS

The composites used in the study were prepared with 1mg of unmodified MWNTs functionalized with polyvinylpyrrolidone (PVP) of various concentration from 0 to 33.33 weight percent, dispersed in 20 mg of PVDF polymer. Three sets of composites were prepared with PVP with three different molecular weights. The amount of MWNTs and PVDF polymer were maintained constant throughout the study. A minimum of three composites for every concentration range were prepared and an average result is analysed.

## 5.3 RESULTS & DISCUSSION

### 5.3.1 *Thermal Conductivity*

Three different molecular weight PVPs were used to non-covalently functionalize the surface of MWNT to prepare PVP@MWNT/PVDF nanocomposites at a range of concentrations and the thermal conductivity of each sample was measured. Fig. 5.3.1 shows the thermal conductivity of polyvinylpyrrolidone (PVP) wrapped MWNTs in PVDF composites. The measurement observed at 0 concentration is the thermal conductivity of the MWNT/PVDF composite without the presence of any PVP. This is the thermal conductivity of unwrapped pristine MWNT in the PVDF matrix.

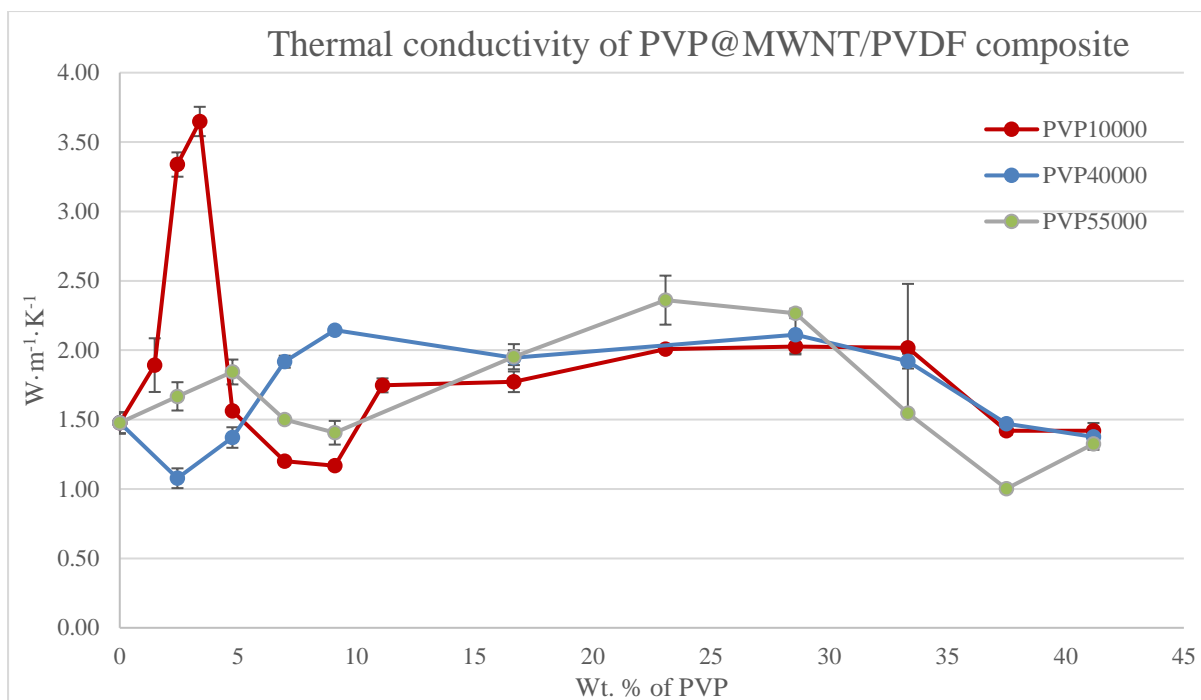


Fig. 5.3.1: Thermal conductivity measurements of three different PVP functionalized MWNT in PVDF composites. Reproduced with permission.

A thermal conductivity of  $1.48 \text{ W}\cdot\text{m}^{-1}\cdot\text{K}^{-1}$  is observed for the MWNT sample prepared with no PVP wrapping, which is greater than the thermal conductivity value of a pure PVDF polymer of  $0.2 \text{ W}\cdot\text{m}^{-1}\cdot\text{K}^{-1}$ . This increase in thermal conductivity can be attributed to the presence of CNT in the polymer matrix. Due to high van der Waals interactions, CNTs have a tendency to form aggregates and weak interactions between the polymer and MWNTs are expected. However, these interactions between MWNTs can be overcome through the proper functionalization of CNTs with an appropriate polymer, such as PVP, and thus, the overall thermal conductivity of the polymer nanocomposite can be increased.

The molecular weights of PVP used in this study were 10,000, 40,000 and 55,000  $\text{g}\cdot\text{mol}^{-1}$ . From the thermal conductivity graph in Fig. 5.3.1, it can be observed that the presence of PVP yielded an increase in the thermal conductivity. The higher polarity of PVP compared to PVDF could induce strong  $\pi$ - $\pi$  interactions with MWNT and as a result, could produce a more homogeneous composite due to the better dispersion of nanotubes. However, the difference in the molecular weight of these polymers plays a key role in the overall dispersion. One can observe from the result that PVP with a lower molecular weight of 10,000  $\text{g}\cdot\text{mol}^{-1}$  records a value of  $3.64 \text{ W}\cdot\text{m}^{-1}\cdot\text{K}^{-1}$  at 3.38 wt. %, which is a 146 % increase in the thermal conductivity from the non-functionalized MWNT in PVDF composite.



PVP<sub>40000</sub> and PVP<sub>55000</sub> display their highest thermal conductivity values of  $2.14 \text{ W}\cdot\text{m}^{-1}\cdot\text{K}^{-1}$  and  $2.40 \text{ W}\cdot\text{m}^{-1}\cdot\text{K}^{-1}$  at 9.09 wt. % and 23.08 wt. %, respectively. Although they exhibit an increase in thermal conductivity of about 44.6 % and 62.1 % compared to pure PVDF, they are comparatively lower than the highest thermal conductivity observed for PVP<sub>10000</sub>. The difference observed with changes in molecular weight, could be attributed to factors like wrapping behaviour, polymer structure and the geometric parameters of the constituents in the nanocomposites. PVP has amide bonds and pyrrolidone rings and tends to possess a flexible backbone structure which leads to the polymer forming an interchain coil rather than a helical conformation [1, 2]. Mu et al. reported that a substantially increased tensile modulus can be observed when the radius of gyration of the polymer is greater than the diameter of the high aspect ratio filler [3, 4]. However, Davijani and Kumar reported that the wrapping behaviour observed in few walled nanotubes (FWNT) and MWNT is different from SWNT due to the difference in their diameter, and as a result, helically ordered wrapping is only observed in SWNT [5].

Our thermal conductivity results illustrate that the presence of a functionalization polymer with a low molecular weight produces high thermal conductivity in the composite at low concentrations. This could be attributed to the fact that PVP with high molecular weight possess longer polymer chains that wrap the nanotubes almost entirely. A thicker layer of polymer around the CNTs due to higher surface coverage on the nanotube will still allow phonon transport from a nanotube through the layer of PVP to other nanotubes in the network, but this transport will be hindered, thus reducing the overall thermal conduction when compared to PVP with a low molecular weight. On the contrary, PVP with lower molecular weight and shorter polymer chains wrap the nanotubes with a comparatively thin layer of polymer to induce a proper dispersion without disrupting the phonon transport in the nanotubes, resulting in higher thermal conductivity.

### *5.3.2 Crystallization behaviour of PVP@MWNT/PVDF composite*

The degree of crystallinity exhibits an apparent influence over the thermal conductivity of polymer-based nanocomposites [6, 7]. Furthermore, it is a known fact that CNTs exhibit an excellent nucleation effect for the crystallisation of semicrystalline polymers [8]. W.-b Zhang et al. found that the crystal form of PVDF does not change in a MWNT–PVDF or PVP functionalized MWNT–PVDF nanocomposite, confirming that the enhancement of thermal

conductivity and variation of crystallinity are not induced by the change in crystal form of PVDF, but are dependent on the contents of CNTs in the polymer matrix [9].

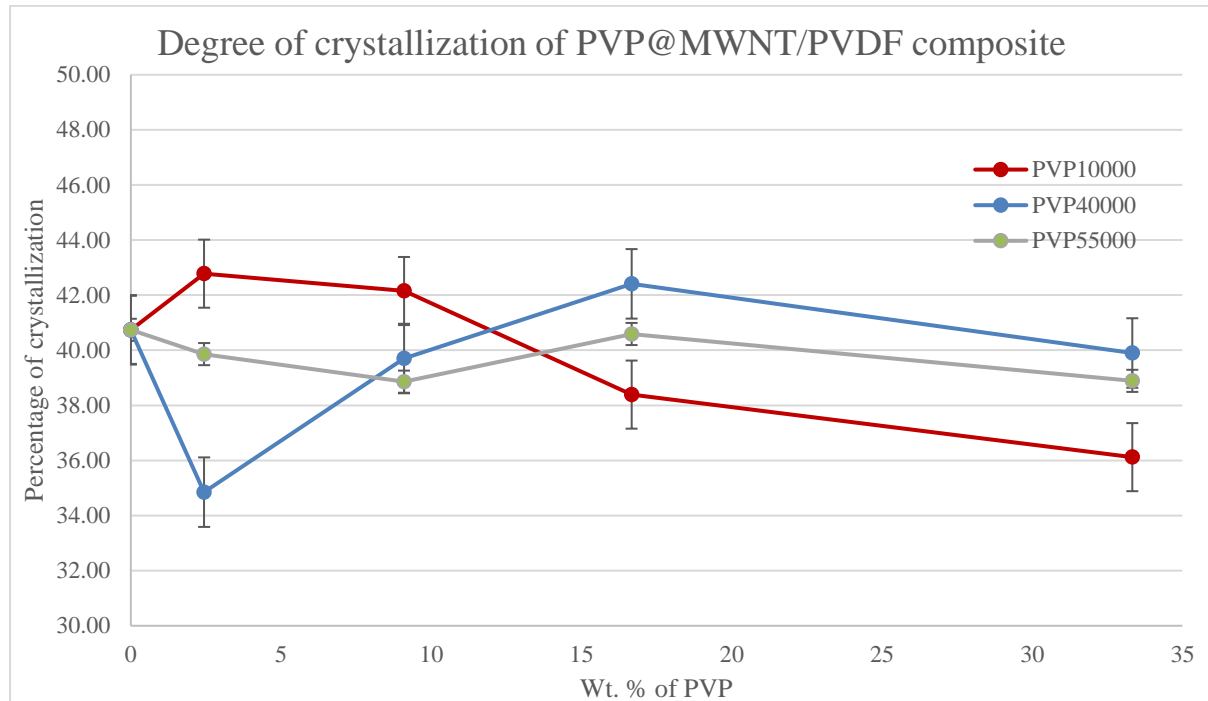


Fig. 5.3.2: Crystallization vs PVP wt. % of PVP functionalized MWNT in PVDF composites. Reproduced with permission.

Fig. 5.3.2 provides the degree of crystallinity observed for each composite as a function of concentration for each molecular weight of the wrapping polymer. The DSC results obtained for the three types of PVP mimic their respective thermal conductivity results. PVP<sub>10000</sub> exhibits a better thermal conductivity at a concentration range of 2.44 wt. % and also displays a high degree of crystallisation of about 42.78 %. Similarly, a high degree of crystallisation is observed in PVP<sub>40000</sub> and PVP<sub>55000</sub> at a concentration range of 16.67 wt. % but a comparatively lower thermal conductivity is displayed. This is due to the fact that in these concentration ranges of PVP, the MWNT, in addition to being well dispersed, also exhibits a conductive network in the PVDF matrix, thus allowing a high thermal conductivity and an increased amount of crystallisation.

### 5.3.3 Electrical Conductivity

The electrical conductivities of the PVP@MWNT/PVDF composites are illustrated in Fig. 5.3.3, with three different molecular weights measured separately. The results exhibit electrical conductivities of 26 and 28.9 S·cm<sup>-1</sup> for PVP<sub>10000</sub> and PVP<sub>40000</sub>, respectively, at the concentrations that yield high thermal conductivity, confirming the presence of an electrically

conducting network in the composite at these concentrations. However, in the case of PVP<sub>55000</sub>, a weak conductive network has been observed owing to the fact that the long polymer chain could have wrapped more than a single MWNT together or a single nanotube wrapped entirely, leading to higher surface coverage, thus compromising the formation of a conductive network. This could have hindered the transport of electrons in the overall composite, yielding a comparatively low electrical conductivity of 1.09 S·cm<sup>-1</sup> which continues to decrease with an increasing concentration of PVP until a threshold point is reached. Percolation threshold is reached at a PVP concentration of 16.67 wt. % with PVP<sub>40000</sub> and PVP<sub>55000</sub>, beyond which no relative change in electrical conductivity is observed. The threshold point in PVP<sub>10000</sub> is reached at a comparatively higher concentration of 23.08 wt. %. This could be attributed to the fact that higher surface coverage of nanotubes for the higher molecular weight polymers leads to an isolation from neighbouring nanotubes compromising effective electron transport in the composite. This is achieved with polymers of higher molecular weights at a lower concentration due to their longer polymer chains compared to polymers of lower molecular weight and their short chain length.

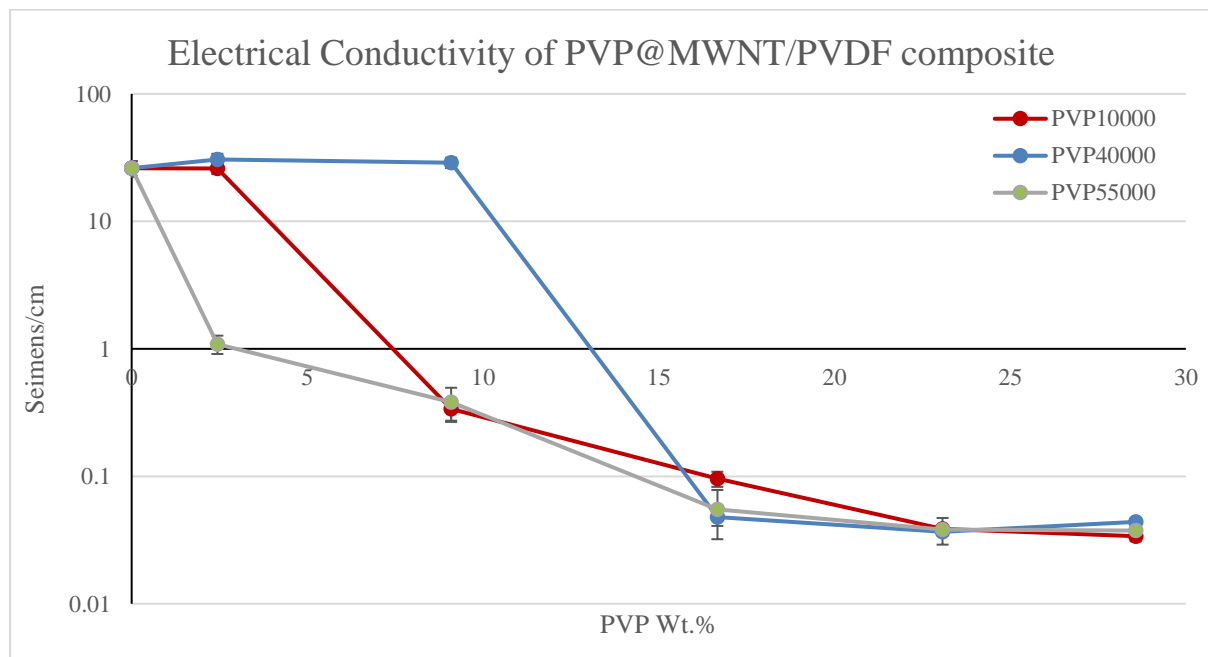


Fig. 5.3.3: Electrical conductivity measurements of three different PVP functionalized MWNT in PVDF composites. Reproduced with permission.

#### 5.3.4 Mechanical Characterization

Ajayan et al. reported that surface (filler) – polymer interaction greatly influences the glass transition temperature. An increase in glass transition temperature is due to the increase in

density and decrease in the mobility of the polymer chains [10]. The increase in glass transition temperature is indicative of a strong interaction presented between the nanotubes and the polymer matrix. A study on the glass transition temperature of a carbon nanotube based epoxy composite performed by Smrutishika Bal confirmed that an increase in glass transition temperature is observed with better dispersion of nanotubes [11]. Similarly, Verma et al. reported that factors like dispersion of MWNT and average length of the nanotubes together with their diameter directly influences the packing fraction of MWNT in the composite which in turn plays a decisive role in the enhancement of glass transition temperature [12].

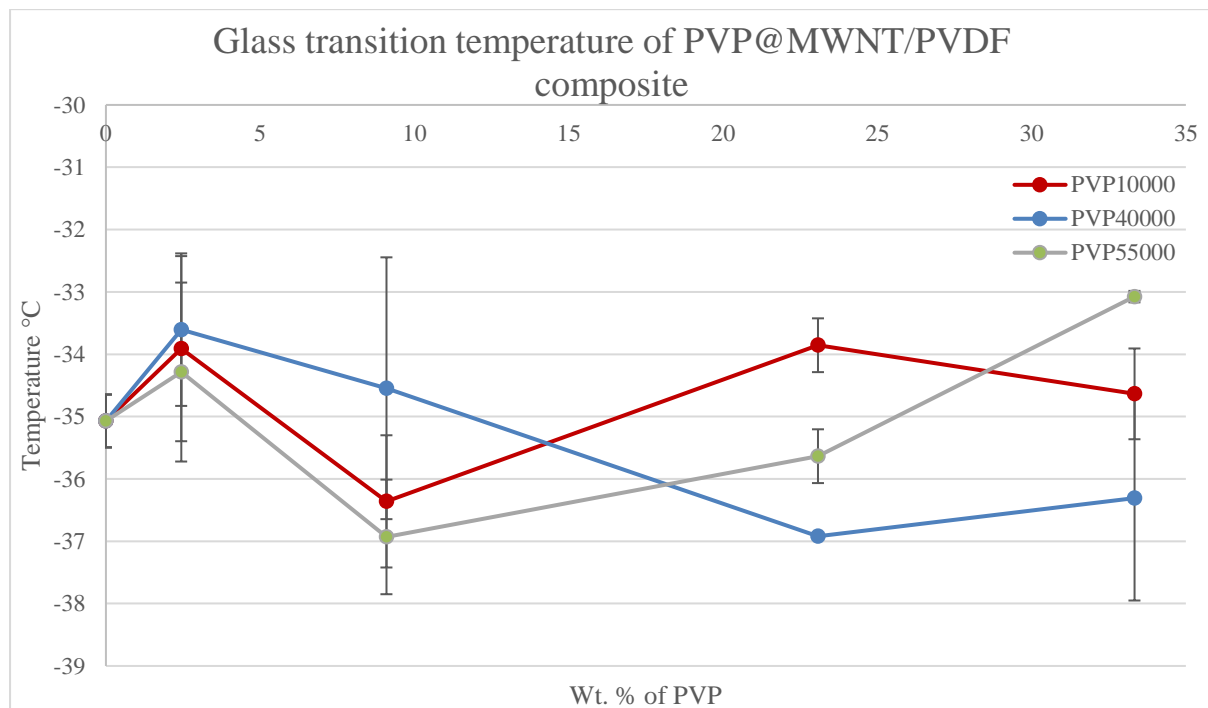


Fig. 5.3.4A: Glass transition measurement of four different PVP functionalized P3-SWNT in PVDF composites.

The glass transition temperature ( $T_g$ ) measured for different molecular weights of PVP functionalized MWNT in PVDF composite at various PVP concentration are plotted in Fig. 5.3.4A. The glass transition temperature for the unmodified MWNT/PVDF composite is observed to be  $-35.07\text{ }^\circ\text{C}$  and plotted at 0 along the x-axis.

An increase in glass transition temperature is observed in all three molecular weights of PVP functionalization. PVP<sub>10000</sub> functionalized nanotube composite exhibit an increase in  $T_g$  at lower concentration of about 2.44 wt. % followed by a drop and then exhibited an increase before reaching higher concentration range of about 33.33 wt. %. PVP<sub>40000</sub> functionalized nanotube composites tend to exhibit a high  $T_g$  at a low concentration range followed by a gradual decrease with increasing concentration and reached a minimum at higher concentration

range. Although, PVP<sub>55000</sub> functionalized nanotube composites exhibited an increase at low concentration range. They tend to exhibit their highest  $T_g$  on higher concentration range. This is attributed to the fact that uniform dispersion of MWNT in PVDF matrix increases some order of crystallinity of PVDF allowing increased polymer-nanotube interaction, which improves the strength and hence storage modulus and glass transition temperature of nanocomposites [12].

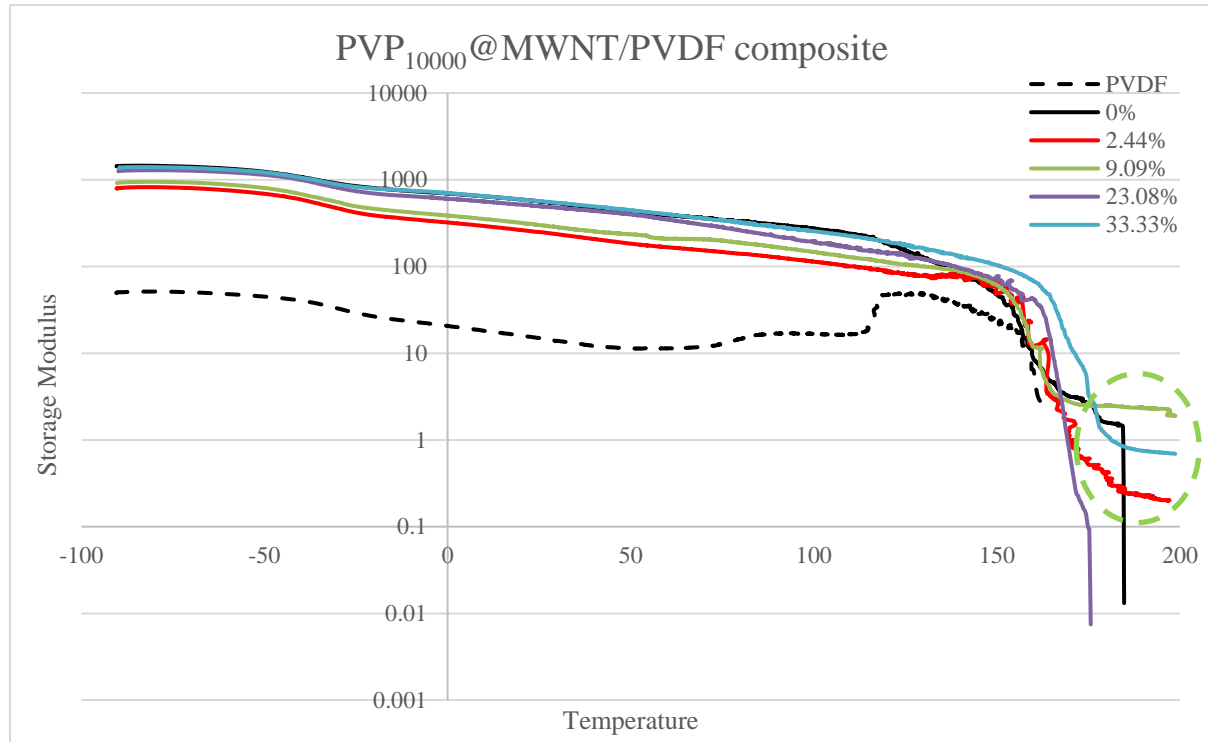


Fig. 5.3.4B: Storage modulus measurement of PVP<sub>10000</sub> functionalized MWNT in PVDF composites.

The storage modulus of the PVDF composite (dotted black line) is significantly increased with the introduction of pristine MWNTs (solid black line) confirming the fact that the presence of MWNT has increased the mechanical strength of the composites. The unmodified MWNT/PVDF composites tend to maintain the mechanical strength up to a temperature of about 184.78 °C above the melting temperature of the PVDF polymer which is 162.69 °C. This increase in mechanical strength is purely influenced by the presence of multi walled nanotubes and a stable dispersion of nanotubes would allow for a further improvement in the mechanical strength. PVP functionalization has improved the dispersion of nanotubes in the PVDF matrix leading to a formation of nanotube network that allows the composites to maintain the mechanical strength at temperatures higher than the yielding point of the unmodified nanotube composite, highlighted in the green dashed circles in Fig. 5.3.4B - 5.3.4D.

Storage modulus of PVP<sub>10000</sub> functionalized MWNTs in PVDF composites of various PVP concentrations are shown in Fig. 5.3.4B. A homogeneous dispersion was achieved at a PVP<sub>10000</sub> concentration of 2.44 wt. % in the PVP<sub>10000</sub> functionalized nanotube composite. This leads to the higher thermal conductivity and crystallization behaviour as shown in Fig. 5.3.1 and 5.3.2. This composite (solid red line) exhibits fairly similar storage modulus as an unmodified nanotube composite but still they tend to maintain the mechanical strength to a temperature as high as 197.18 °C. Likewise, composites prepared at a PVP<sub>10000</sub> concentration of 9.09 wt. % and 33.33 wt. % also tend to exhibit a mechanical strength at temperatures as high as 198.82 °C and 198.73 °C. This is entirely due to PVP functionalization of nanotubes leading to improved dispersion of nanotubes and increased interaction between the nanotubes and polymer matrix.

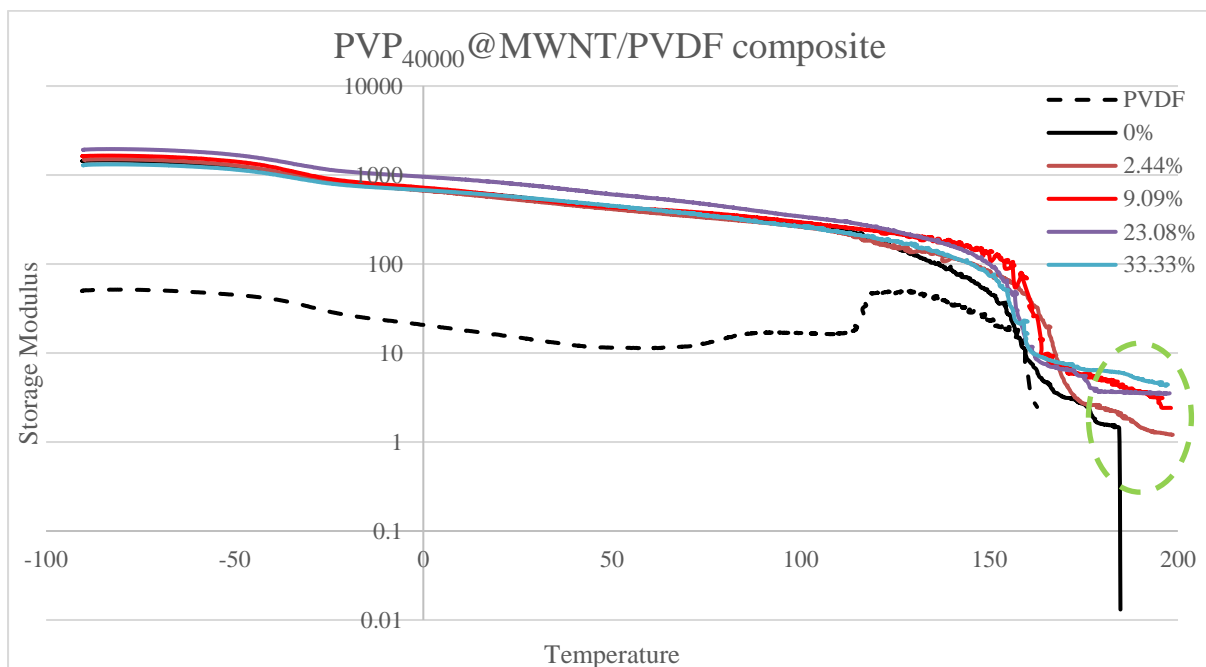


Fig. 5.3.4C: Storage modulus measurement of PVP<sub>40000</sub> functionalized MWNTs in PVDF composites.

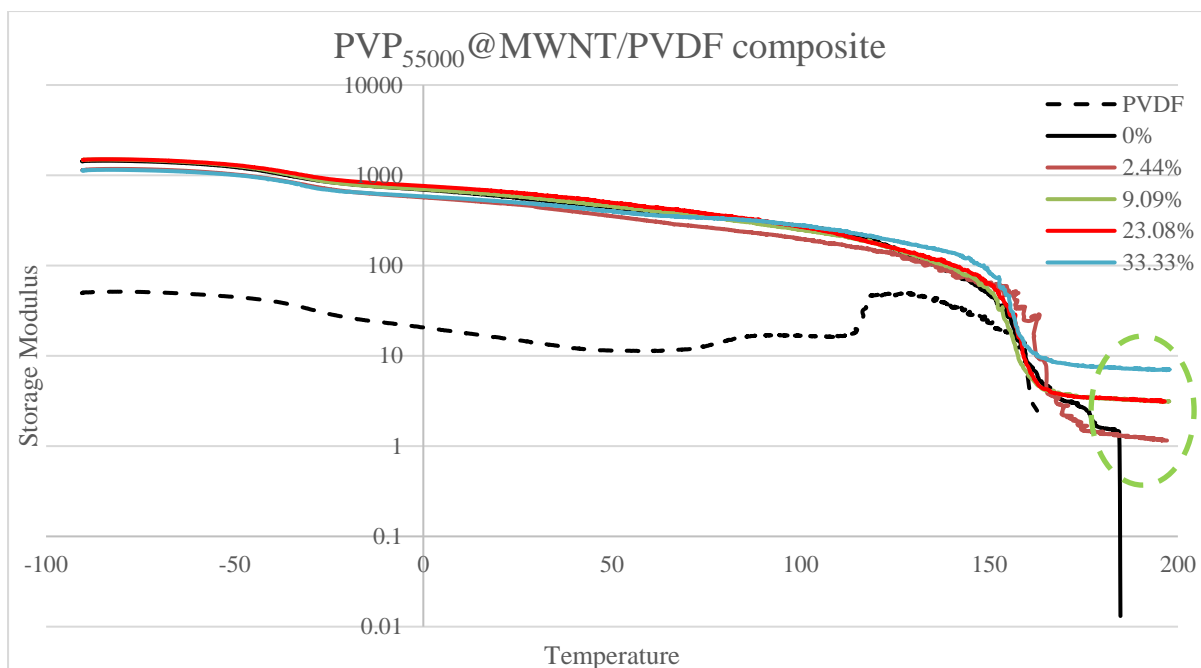


Fig. 5.3.4D: Storage modulus measurement of PVP<sub>55000</sub> functionalized MWNTs in PVDF composites.

A homogeneous dispersion is achieved in PVP<sub>40000</sub> functionalized nanotube composite at a concentration of 9.09 wt. % which exhibits a similar storage modulus as an unmodified nanotube composite shown in Fig. 5.3.4C. However, the composite maintains the mechanical strength up to a temperature of about 198.18 °C beyond the yielding point of unmodified nanotube composite and the composites prepared at higher PVP<sub>40000</sub> concentration of 23.08 wt. % and 33.33 wt. % also exhibit a similar mechanical strength at higher temperatures and reaches an yielding point at 197.83 °C and 197.37 °C, thus confirming an increased interaction between the nanotubes and polymer matrix. Whereas, composites prepared at lower PVP<sub>40000</sub> concentration of 2.44 wt. % exhibit a lower storage modulus compared to unmodified nanotube composite yet the interaction between the nanotubes and polymer is effective to maintain the mechanical strength up-to a temperature of about 198.65 °C.

PVP<sub>55000</sub> functionalized nanotube composites also exhibit a similar result. Composites prepared at a lower concentration of 2.44 wt. % reach a yielding point at a higher temperature of about 197.12 °C compared to the yielding point of unmodified nanotube composite observed at 184.78 °C. However, above a temperature of about 165.2 °C, the storage modulus of 2.44 wt. % composites are lower compared to unmodified nanotube composites. Whereas higher concentrations of PVP<sub>55000</sub> functionalized nanotube composite exhibit a higher storage modulus compared to unmodified nanotube composites and tend to maintain the mechanical strength at a comparatively higher temperature. Higher thermal conductivity and crystallization

behaviour is observed in PVP<sub>55000</sub> functionalized nanotube composite at a concentration of 23.08 wt. % due to homogeneous dispersion of nanotubes and the mechanical strength of this composite is higher compared to unmodified nanotube composite and is maintained until a yielding point is reached at 196.53 °C. Also, composites prepared at a concentration of 9.09 wt. % and 33.33 wt. % exhibit a higher storage modulus and reach a yielding point at a temperature of about 197.72 °C and 197.75 °C. The results observed in Fig. 5.3.4B - 5.3.4D confirm that an interaction between the polymer and the nanotubes was achieved for all molecular weights of PVP thus maintaining a mechanical strength beyond the yielding point of an unmodified nanotube composite. However, composites prepared at low concentrations of PVP of all molecular weights tend to exhibit a lower storage modulus. This could be because the dispersion of nanotubes at low concentrations could have created a network formation that acts a conductive path for phonon and electron transport but yet an improvement in nanotube-polymer interaction is required to exhibit a higher storage modulus and this can be achieved with higher concentrations of PVP.

### 5.3.5 Microscopy Results

Nanocomposites prepared with non-functionalized MWNT in a PVDF matrix exhibit poor dispersion. From the SEM image in Fig. 5.3.5A (A), high cluster of nanotubes can be seen and is highlighted in the image by red circles. Due to high van der Waals interactions, the nanotubes present are clustered together in the form of aggregates.

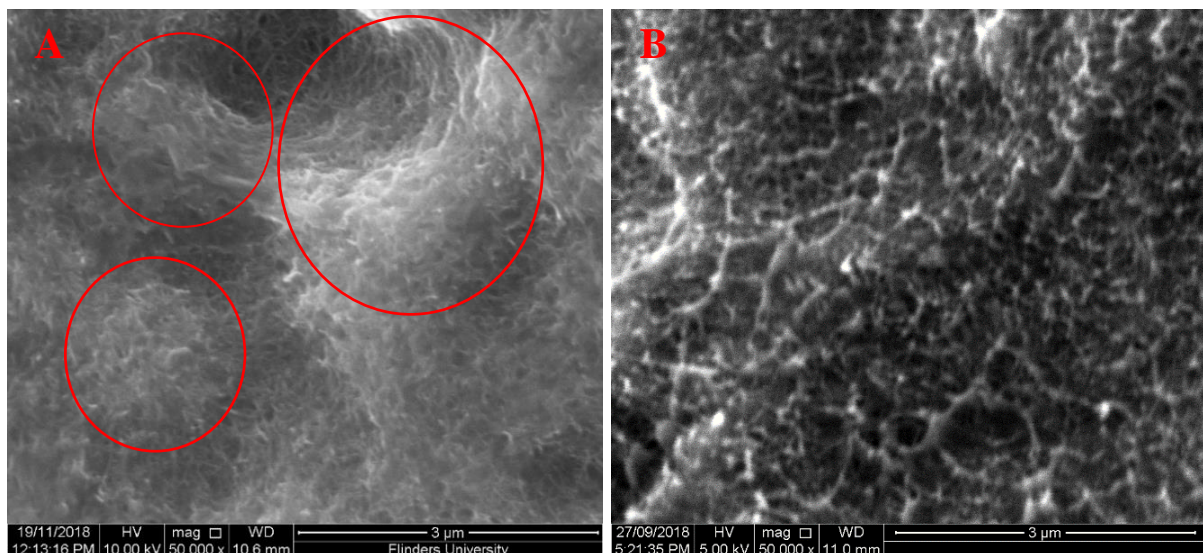
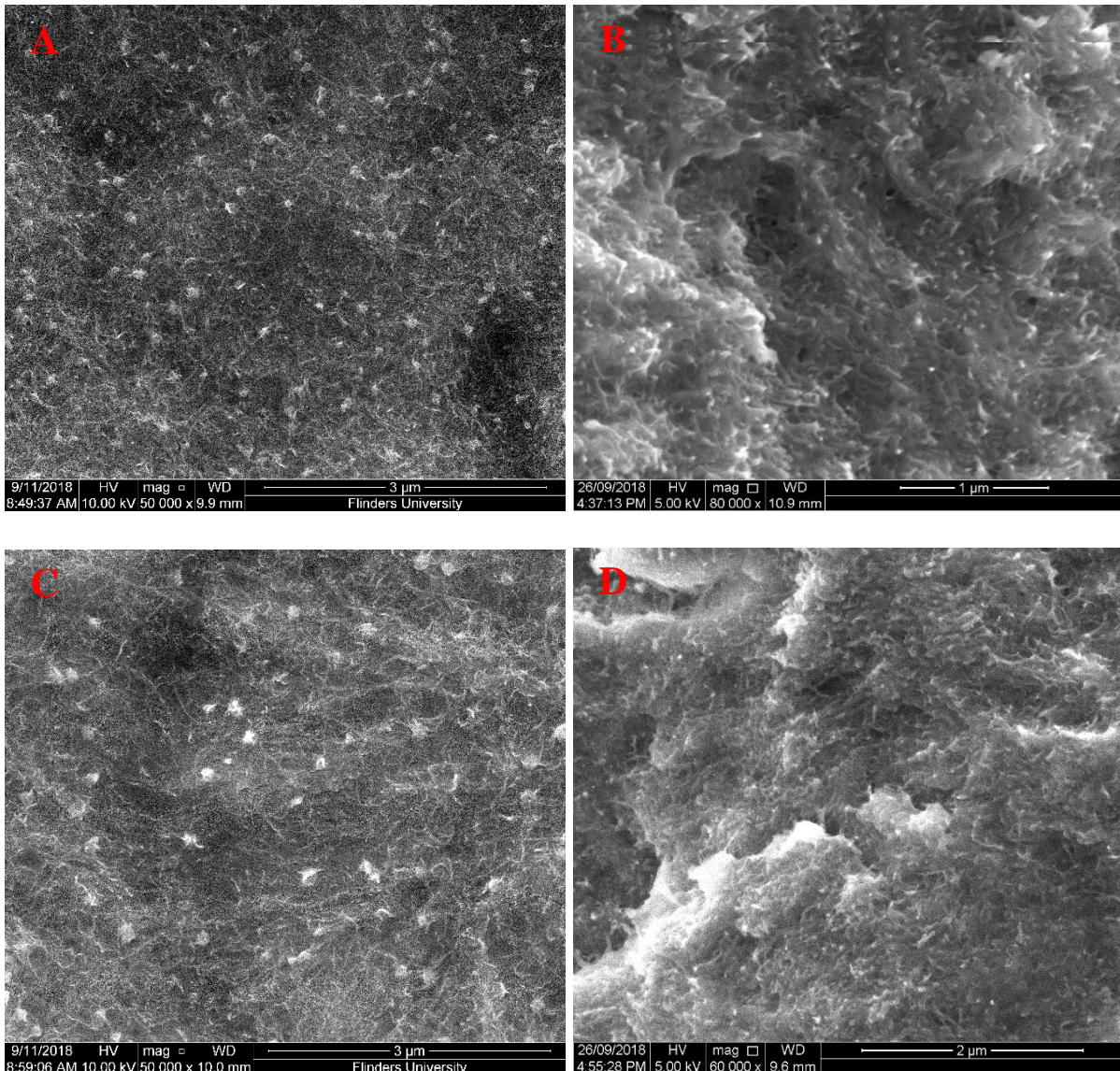


Fig. 5.3.5A: Scanning electron microscope results of non-functionalized MWNTs in PVDF composite; (A) anterior view and (B) fractured side-view - agglomeration of nanotubes are highlighted in red circles.

Reproduced with permission.



However, in the PVP functionalized MWNTs in PVDF samples, unlike non-functionalized samples, an absence of clusters can be observed. This is due to the presence of PVP polymer in the composite, which adsorbs onto the walls of the CNTs, thus decreasing the van der Waals interactions between the nanotubes and increasing the interaction between PVDF polymer and nanotubes. This is also witnessed in the fractured side view of the sample, unmodified nanotubes are observed to be clustered together due to high Vander Waals interaction in Fig. 5.3.5A (B), but PVP functionalized nanotubes are observed to be fused together with the PVDF polymer in Fig. 5.3.5B confirming an increase in nanotube-PVDF interaction. This distribution of MWNT in the PVDF matrix can be witnessed for all three molecular weights of PVP confirming that the dispersion of MWNTs in the PVDF matrix is significantly improved with the wrapping of PVP, irrespective of the length of the polymer chain. A similar observation can be witnessed in the fractured SEM images.



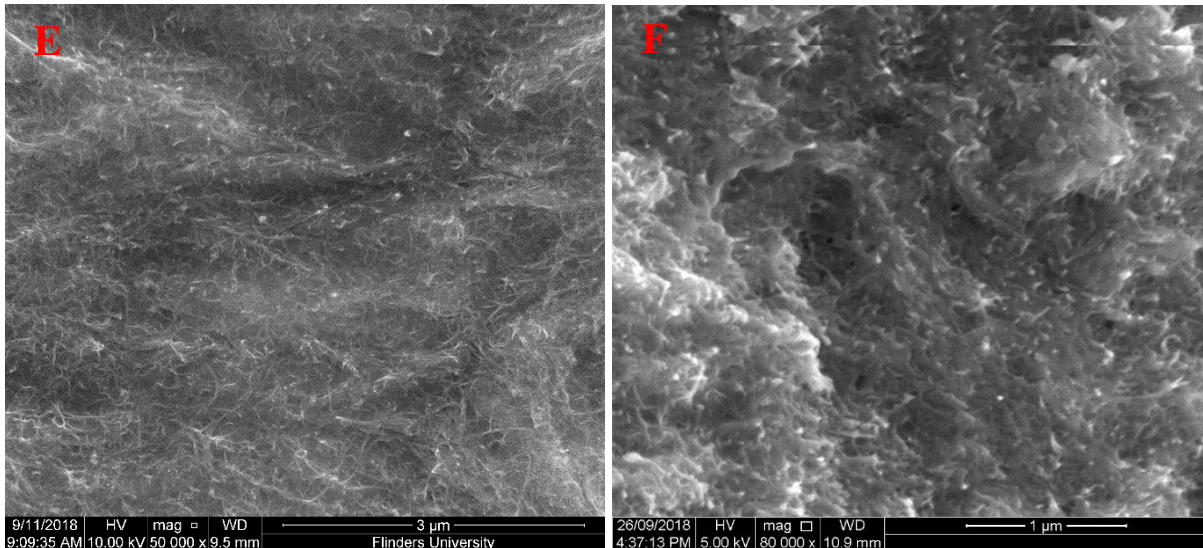


Fig. 5.3.5B: Scanning Electron Microscopy results of PVP functionalized MWNTs in PVDF composite - PVP<sub>10000</sub> (A & B), PVP<sub>40000</sub> (C & D), and PVP<sub>55000</sub> (E & F); anterior view (left) and fracture side view (right).

Reproduced with permission.

### 5.3.6 Raman Spectroscopy

The G-band of a PVP<sub>55000</sub> functionalized MWNTs in PVDF composite prepared at a concentration of 2.44 wt. % and 16.67 wt. % were compared with the G-band of an unmodified MWNT/PVDF composite. PVP functionalization allows for an effective dispersion of nanotubes leading to increased interaction of polymer and nanotubes. This might have applied a strain on the surface of the MWNTs leading to a change in the vibrational frequencies of some of the normal modes and also chemical modification of nanotube has an impact over the shift in tangential mode [13]. As a result, a shift in G-band from 1599.1  $\text{cm}^{-1}$  to 1597.54  $\text{cm}^{-1}$  is observed in composites prepared with PVP functionalized nanotubes at a concentration of 2.44 wt. % and a further shift to a position of 1596.91  $\text{cm}^{-1}$  is observed in composites prepared at a concentration of 16.67 wt. %. Similarly, a peak shift from 1351.79  $\text{cm}^{-1}$  to 1347.27  $\text{cm}^{-1}$  in D-band is observed in composites prepared with PVP functionalized nanotubes. The interaction level between the polymer and nanotube differs with different concentration of polymers and it is the reason for the observed peak shift.



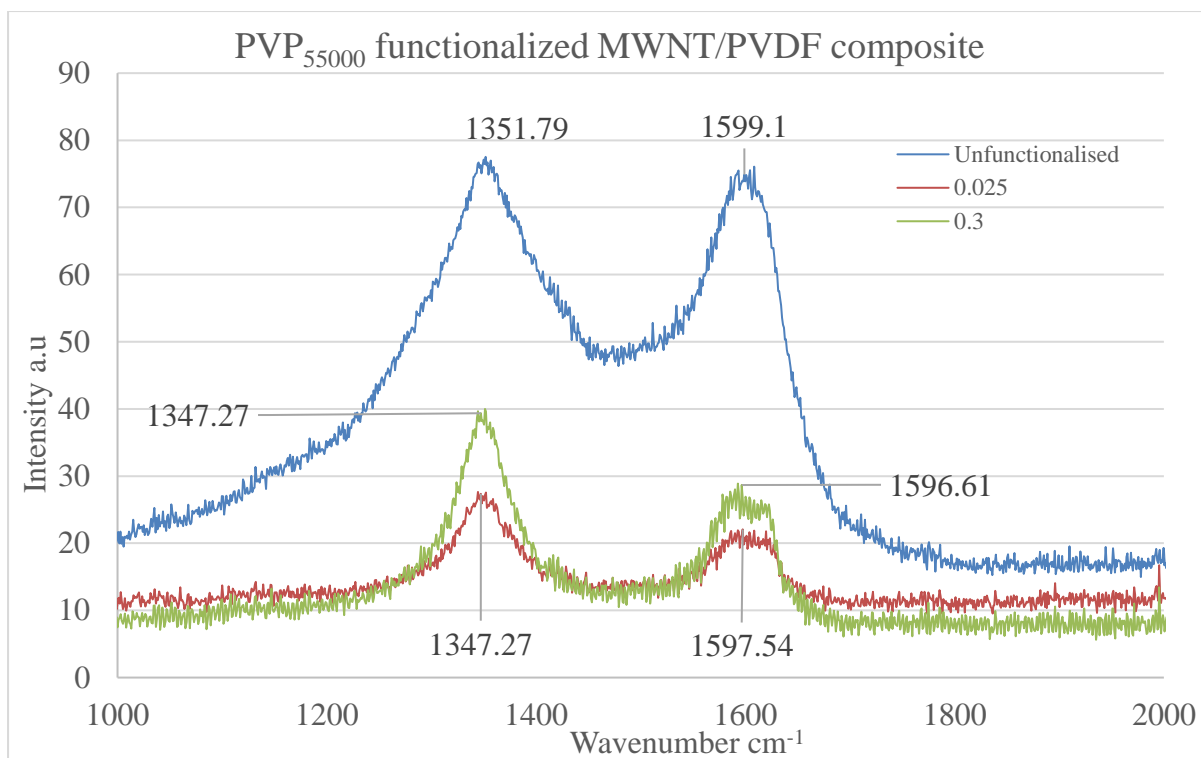


Fig. 5.3.6: G-band of a Raman spectra of unmodified MWNT/PVDF composite, PVP<sub>55000</sub> functionalized MWNTs in PVDF composite prepared at a PVP concentration of 2.44 wt. % and 16.67 wt. %.

#### 5.4 CONCLUSION

In summary, a comparison of pristine MWNTs in PVDF composites and non-covalently functionalized MWNTs in PVDF composites with different molecular weights of PVP as the functionalization polymers for CNTs were analyzed. The thermal conductivity measurements of the nanocomposites show an overall increase. The molecular weight of the polymer used in the functionalization of MWNTs has a significant impact on the thermal conductivity of the composites.

The dispersion of MWNTs in the polymer matrix was improved with all three molecular weights of PVP, but the thermal conductivity and the crystallization behaviour shows a better response with low molecular weights due to the fact that short polymer chains wrap the nanotubes better improving the dispersion without compromising the connectivity of the nanotube network. The mechanical strength of the composite was improved with enhanced nanotube-polymer interaction and is achieved at moderately higher polymer concentrations.

#### 5.5 COLLECTIVE CONCLUSION OF CHAPTERS 3-5

As mentioned earlier in Chapter 2 section 2.2, the amount of CNTs used in the preparation of the polymer nanocomposite is essentially kept constant. However, the results show that the

molecular weight of PVP capable of achieving a higher degree of nanotube dispersion in the composite leading to the formation of a conductive nanotube network compared to unmodified nanotube composite are different for different types of nanotubes. A higher degree of dispersion and formation of a nanotube network is achieved in AP-SWNTs only through PVP functionalization of low molecular weights at low concentration. Although higher molecular weights initiate a stable dispersion of nanotubes in the composite, they fail to achieve an effective network formation as observed in chapter 3 Section 3.3.1., due to the difference in surface coverage of nanotubes achieved through polymer wrapping by polymers of different chain length. Higher surface coverage of nanotubes could disrupt the formation of a structured nanotube network through isolation of nanotubes from their neighbours, thus compromising effective conductive path in the overall composite. However, P3-SWNTs of same amount as AP-SWNTs exhibits a contrast result in the composite where PVP of higher molecular weight exhibits a higher degree of dispersion at low concentrations. This difference in results achieved for nanotubes of similar diameter could be attributed to the fact that the difference in surface coverage required to establish a higher degree of dispersion are different for AP-SWNTs and P3-SWNTs. Although, a similar diameter is observed for AP-SWNTs and P3-SWNTs, the average length of the nanotubes in AP-SWNTs is observed to be more than twice than that of P3-SWNTs. This allows for more than twice the number of single nanotubes in a certain amount (5 wt. % with respect to the amount of PVDF) of P3-SWNTs compared to AP-SWNTs of similar amount, requiring a higher number of nanotubes to be functionalized in order to achieve a stable dispersion in the composite with P3-SWNTs. This could have resulted in the necessity for P3-SWNTs to be functionalized with PVP of longer polymer chain (higher molecular weight) to achieve a higher degree of dispersion, which PVP of smaller polymer chain could achieve in AP-SWNTs. Moreover, smaller polymer chains (lower molecular weight) tend to exhibit a similar result in P3-SWNTs only at comparatively higher concentrations of PVP as observed in Chapter 4 Section 4.3.1 (Fig. 4.3.1B). Smaller polymer chains can exhibit a higher degree of dispersion at low concentration of PVP, when the amount of nanotubes are reduced leading to a decrease in the number of individual nanotubes hence decreasing the surface area of nanotubes requiring functionalization to achieve higher dispersion compared to unmodified nanotube composites as observed in chapter 4 Section 4.3.1 (Fig. 4.3.1C and Fig. 4.3.1D).

MWNTs of same amount exhibits a completely different result as observed in chapter 5 Section 5.3.1. A higher degree of dispersion and an effective network formation is achieved through

PVP functionalization of lower molecular weight at low concentration of PVP and a similar result is achieved in composites prepared through PVP functionalization of higher molecular weights at comparatively high concentration. The structure of the nanotube plays a key role in the results as observed in chapter 5. The larger diameter of the nanotube could have allowed longer polymer chain PVP to have double or triple helical wrapping requiring higher concentration of PVP in order to cover all the individual nanotubes to create a uniform dispersion in the nanotubes which a small polymer chain could achieve at low concentration.

SEM images of PVP<sub>55000</sub> functionalized CNTs (for the various CNTs used) deposited directly on a solid substrate are shown in Fig. 5.5.1 - Fig. 5.5.3. The amount of CNTs used were maintained constant and the samples were prepared at the respective PVP<sub>55000</sub> concentration that exhibited the highest thermal conductivity for all the three types of CNTs as observed in chapter 3-5. Differences in the wrapping pattern and surface coverage of nanotubes are observed for all the three types of nanotubes.

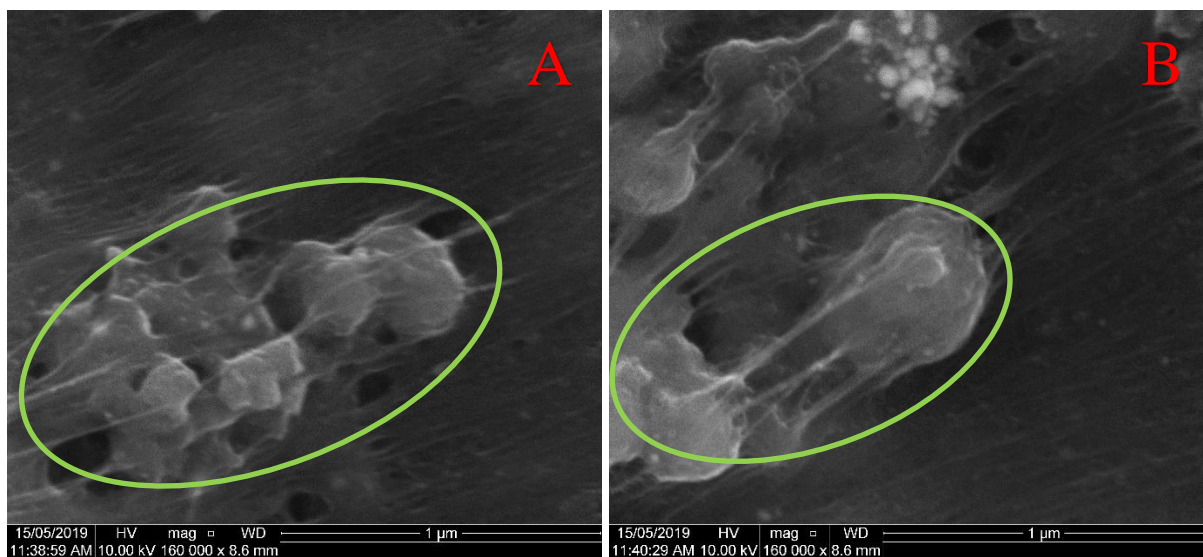


Fig. 5.5.1: PVP<sub>55000</sub> functionalized AP-SWNTs deposited on a solid substrate prepared at PVP concentration of 6.98 wt. % (green circle highlighting PVP functionalization).

AP-SWNTs exhibits some kind of an alignment like formation when deposited on the solid substrate, which could be attributed to the smaller diameter and high aspect ratio of AP-SWNTs as clearly observed as longer nanotubes in Fig. 5.5.1. PVP<sub>55000</sub> tend to adsorb on to AP-SWNTs in portions as highlighted in green circles, thus failing to functionalize higher amounts of nanotubes in order to achieve an effective formation of nanotube network. This is reflected in the poor thermal, electrical and mechanical property of PVDF composite prepared with PVP functionalized AP-SWNTs.

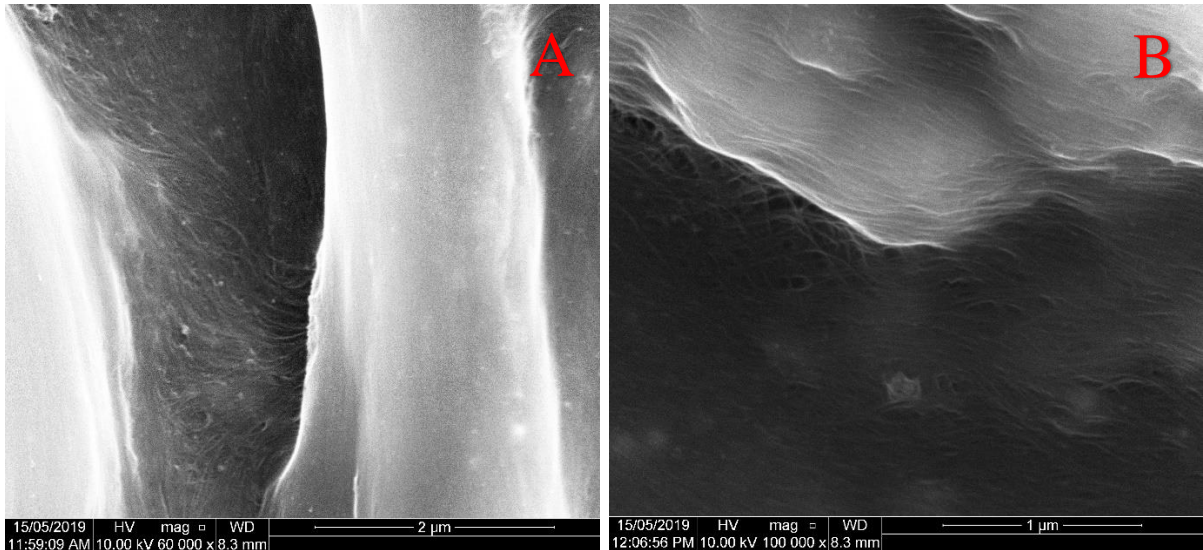


Fig. 5.5.2: PVP<sub>55000</sub> functionalized P3-SWNTs deposited on a solid substrate prepared at PVP concentration of 23.08 wt. %.

Similar to AP-SWNTs, P3-SWNTs also exhibit an alignment like formation owing to their small diameter but PVP<sub>55000</sub> functionalization happens in a bundle like pattern as observed in Fig. 5.5.2. This could be attributed to the short aspect ratio and the amount of nanotubes influencing the polymer wrapping behaviour.

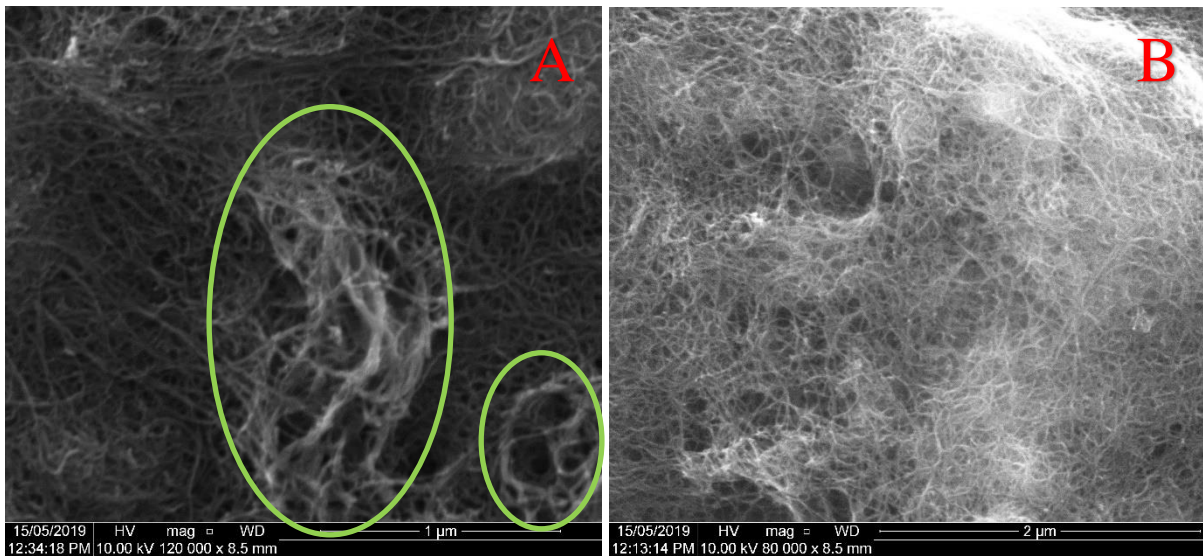


Fig. 5.5.3: PVP<sub>55000</sub> functionalized MWNTs deposited on a solid substrate prepared at PVP concentration of 23.08 wt. % (green circle highlighting PVP functionalization).

MWNTs seem to exhibit more complicated formation when deposited on a solid substrate and they exhibit no alignment like formation which could be attributed to the larger diameter of the nanotubes. Unlike P3-SWNTs, PVP<sub>55000</sub> functionalization of multi walled nanotubes happens on every individual nanotube separately as observed in Fig. 5.5.3 (A) and unlike AP-SWNTs,

a larger portion of nanotubes are functionalized as observed in Fig. 5.5.3 (B) allowing the formation of an effective nanotube network leading to an enhanced thermal and mechanical property. However, it is pertinent to understand that polymer functionalization of CNTs observed on solid substrates could exhibit a different behaviour in polymer matrix.

## 5.6 REFERENCES

1. Ntim, S.A., et al., *Effects of polymer wrapping and covalent functionalization on the stability of MWCNT in aqueous dispersions*. Journal of colloid and interface science, 2011. **355**(2): p. 383-388.
2. Behera, M. and S. Ram, *Interaction between poly(vinyl pyrrolidone) PVP and fullerene C 60 at the interface in PVP-C 60 nanofluids–A spectroscopic study*. IOP Conference Series: Materials Science and Engineering, 2018. **330**(1): p. 012016.
3. Mu, M. and K.I. Winey, *Improved Load Transfer in Nanotube/Polymer Composites with Increased Polymer Molecular Weight*. The Journal of Physical Chemistry C, 2007. **111**(48): p. 17923-17927.
4. Jakubka, F., et al., *Effect of Polymer Molecular Weight and Solution Parameters on Selective Dispersion of Single-Walled Carbon Nanotubes*. ACS Macro Letters, 2012. **1**(7): p. 815-819.
5. Bakhtiary Davijani, A.A. and S. Kumar, *Ordered wrapping of poly(methyl methacrylate) on single wall carbon nanotubes*. Polymer, 2015. **70**: p. 278-281.
6. Haggemueller, R., et al., *Single Wall Carbon Nanotube/Polyethylene Nanocomposites: Thermal and Electrical Conductivity*. Macromolecules, 2007. **40**(7): p. 2417-2421.
7. Yu, J., et al., *Thermal conductivity of highly crystallized polyethylene*. Polymer, 2014. **55**(1): p. 195-200.
8. Cadek, M., et al., *Morphological and mechanical properties of carbon-nanotube-reinforced semicrystalline and amorphous polymer composites*. Applied Physics Letters, 2002. **81**(27): p. 5123-5125.
9. Zhang, W.-b., et al., *High thermal conductivity of poly(vinylidene fluoride)/carbon nanotubes nanocomposites achieved by adding polyvinylpyrrolidone*. Composites Science and Technology, 2015. **106**: p. 1-8.
10. Schadler, L.S., *Polymer-Based and Polymer-Filled Nanocomposites*, in *Nanocomposite Science and Technology*. p. 77-153.
11. Bal, S., *Dispersion and reinforcing mechanism of carbon nanotubes in epoxy nanocomposites*. Bulletin of Materials Science, 2010. **33**(1): p. 27-31.
12. Verma, M., et al., *Storage Modulus and Glass Transition Temperature of MWNT/PMMA Polymer Nanocomposite Films with Different wt% of MWNT*. Journal of NanoScience, NanoEngineering & Applications, 2014. **4**: p. 28-33.
13. Schadler, L.S., S.C. Giannaris, and P.M. Ajayan, *Load transfer in carbon nanotube epoxy composites*. Applied Physics Letters, 1998. **73**(26): p. 3842-3844.

CHAPTER 6

PVP VERSUS P4VP

FUNCTIONALIZED CARBON

NANOTUBES IN PVDF COMPOSITES

Part of this chapter was published previously in Namasivayam, M.; Andersson, M.R.; Shapter, J. Role of Molecular Weight in Polymer Wrapping and Dispersion of MWNT in a PVDF Matrix. *Polymers* **2019**, *11*, 162.



## 6.1 CHAPTER INTRODUCTION

In this chapter, the non-covalent functionalization of various carbon nanotubes by PVP polymer of molecular weight  $55000 \text{ g}\cdot\text{mol}^{-1}$  and P4VP polymer of molecular weight  $60000 \text{ g}\cdot\text{mol}^{-1}$  is compared and the physical properties of the composites prepared with the addition of PVP<sub>55000</sub> or P4VP<sub>60000</sub> functionalized CNTs to PVDF polymer are analysed extensively. Carbon nanotubes of three different structures were used in this study.

## 6.2 SAMPLE DETAILS

The composites used in the study were prepared with 1mg of unmodified CNTs functionalized with polyvinylpyrrolidone (PVP) or poly(4-vinylpyridine) (P4VP) of various concentrations from 0 to 33.33 weight percent, dispersed in 20 mg of PVDF polymer. The amount of CNTs and PVDF polymer were maintained constant throughout the study. A minimum of three composites for every concentration range were prepared and an average result is analysed.

## 6.3 RESULTS & DISCUSSION

### AP Single-walled nanotubes

#### *6.3.1 Thermal Conductivity*

Comparative thermal conductivity results for composites prepared with PVP or P4VP functionalized AP-SWNTs are shown in Fig. 6.3.1.

As shown in Chapter 3 Section 3.3.1, the introduction of AP-SWNTs has improved the thermal conductivity of the PVDF composite from  $0.2 \text{ W}\cdot\text{m}^{-1}\cdot\text{K}^{-1}$  to a thermal conductivity value of  $4.37 \text{ W}\cdot\text{m}^{-1}\cdot\text{K}^{-1}$  which is highlighted with a solid black circle. The high thermal conductivity of a pristine AP-SWNTs in PVDF composite could be attributed to the high aspect ratio of AP-SWNTs. Functionalization of nanotubes with PVP<sub>55000</sub> or P4VP<sub>60000</sub> has improved the nanotube dispersion in the polymer matrix leading to an increase in thermal conductivity observed at a concentration of 6.98 wt. %. Although a stable dispersion of nanotubes is achieved with both PVP<sub>55000</sub> and P4VP<sub>60000</sub> functionalization, an effective formation of a conductive nanotube network is not observed. This leads to either a very low thermal conductivity enhancement of  $4.63 \text{ W}\cdot\text{m}^{-1}\cdot\text{K}^{-1}$  as observed in PVP<sub>55000</sub> functionalized nanotube composite which is a 5.95 % increase or a lower thermal conductivity of  $3.74 \text{ W}\cdot\text{m}^{-1}\cdot\text{K}^{-1}$  as observed in P4VP<sub>60000</sub> functionalized nanotube composite compared to unmodified nanotube composite.

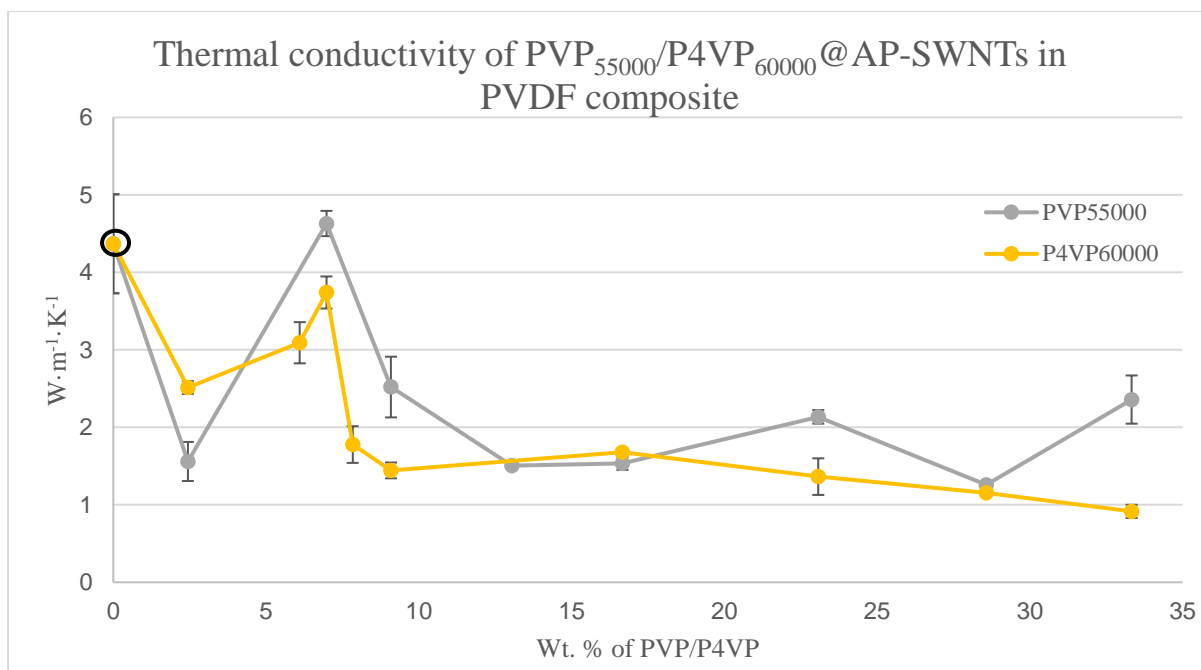


Fig. 6.3.1: Thermal conductivity measurements of PVP or P4VP functionalized AP-SWNTs in PVDF composites (PVP data reproduced from Fig. 3.3.1 in chapter 3).

### 6.3.2 Crystallization behaviour of PVP/P4VP@AP-SWNTs in PVDF composite

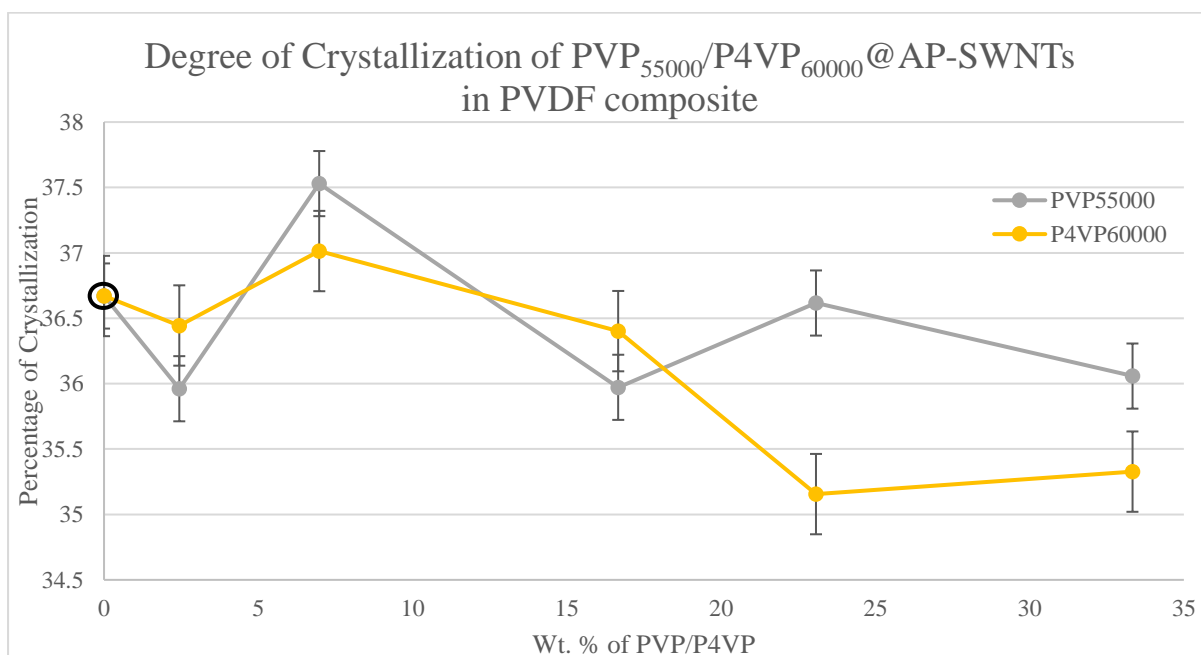


Fig. 6.3.2: Crystallization vs PVP or P4VP wt. % of non-covalently functionalized AP-SWNTs in PVDF composites (PVP data reproduced from Fig. 3.3.2 in chapter 3).

The degree of crystallization shown in Fig. 6.3.2, exhibits some resemblance to the thermal conductivity result observed in Fig. 6.3.1. The high aspect ratio of the nanotubes allows for a 36.67 % of crystallization in unmodified nanotube composite and an increase in crystallization

is observed with PVP or P4VP functionalization. PVP<sub>55000</sub> and P4VP<sub>60000</sub> functionalized nanotube exhibited a crystallization behaviour of 37.53 % and 37.01 % at a concentration of 6.98 wt. %. This enhancement in crystallization is a result of an enhanced nucleation effect observed in the PVDF polymer composite achieved through higher degree of nanotube dispersion.

O'Connell et al. reported that PVP polymer wraps helically around a SWNT [1]. However, the wrapping mechanism of a P4VP is completely different. Su et al. studied the morphologies of poly (4-vinylpyridine) on single walled nanotubes and reported that the diameter of the SWNT plays a crucial role in the morphology control of P4VP crystals on CNTs surface [2]. Investigation on CXL (CO<sub>2</sub>-expanded liquids)-assisted P4VP crystal growth mechanism on SWNT confirmed that the P4VP wrapping pattern undergoes a notable morphological evolution from dot like crystals to bottle-brush like then to nanohybrid shish-kebab (NHSK) like conformation with the polymer chain parallel to SWNT axis. The NHSK conformation of the P4VP/SWNT composite including compact kebabs, less compact kebabs and sparsely dotted kebabs is attributed to 'size-dependent soft epitaxy growth' mechanism. The average diameter of the AP-SWNT used in this study is about 1.4 nm with the bundle diameter ranging between 2-10 nm causing a high possibility for mixed morphology. This difference in conformational behaviour could have been the reason for achieving an improved degree of crystallization but yet low thermal conductivity compared to unmodified nanotube composite.

### 6.3.3 Electrical Conductivity

The electrical conductivity of the P4VP<sub>60000</sub> functionalized nanotube composites shown in Fig. 6.3.3 exhibit a different result compared to PVP<sub>55000</sub> functionalized nanotube composite. Unmodified nanotube composite exhibit an electrical conductivity of 25.1 S·cm<sup>-1</sup> and mild increase in electrical conductivity with increasing concentration of P4VP is observed in P4VP<sub>60000</sub> functionalized nanotube composite until a concentration of 23.08 wt. %, which exhibited an electrical conductivity of 33.9 S·cm<sup>-1</sup>. A decrease in electrical conductivity is observed with increasing concentrations of P4VP until a threshold point is reached at 28.57 wt. % beyond which no significant change is observed. However, PVP<sub>55000</sub> functionalized nanotube composite exhibited a very low electrical conductivity of 0.16 S·cm<sup>-1</sup> at a concentration of 2.44 wt. % and reaches a threshold point at 9.09 wt. %.

The difference in the wrapping behaviour of PVP and P4VP could have led to the observed results. The helical conformation of PVP<sub>55000</sub> polymer could have achieved higher surface

coverage of nanotubes leading to isolation from neighbouring nanotubes. This leads to low thermal conductivity enhancement and even lower electrical conductivity. Whereas, the nano hybrid shish-kebab conformation of P4VP<sub>60000</sub> polymer parallel to the surface of the AP-SWNTs tend to exhibit a lower degree of dispersion meaning nanotubes are more closely packed than PVP<sub>55000</sub> functionalized nanotube composites. This could have been the reason for observing a decent electrical conductivity. The chance of phonon scattering is high with closely packed nanotubes and this could have hindered the phonon vibration along the nanotube surface leading to low thermal conductivity compared to unmodified nanotube composite as observed in Fig. 6.3.1.

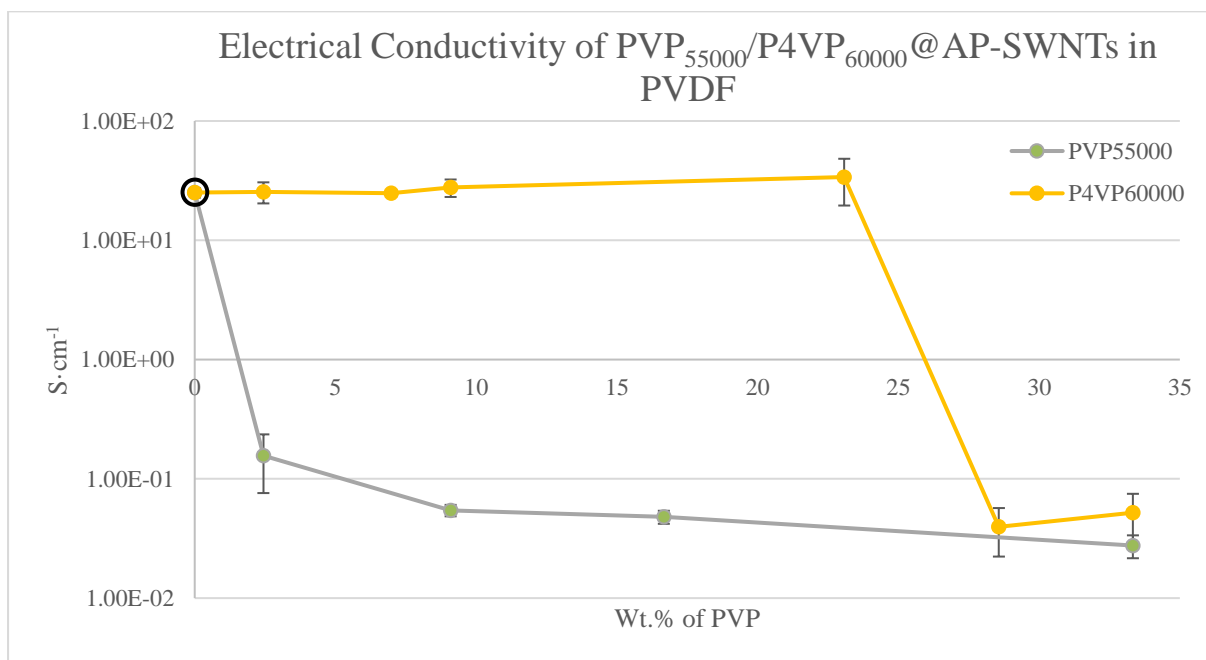


Fig. 6.3.3: Electrical conductivity measurements of PVP/P4VP functionalized AP-SWNTs in PVDF composites (PVP data reproduced from Fig. 3.3.3 in chapter 3).

### 6.3.4 Mechanical Characterization

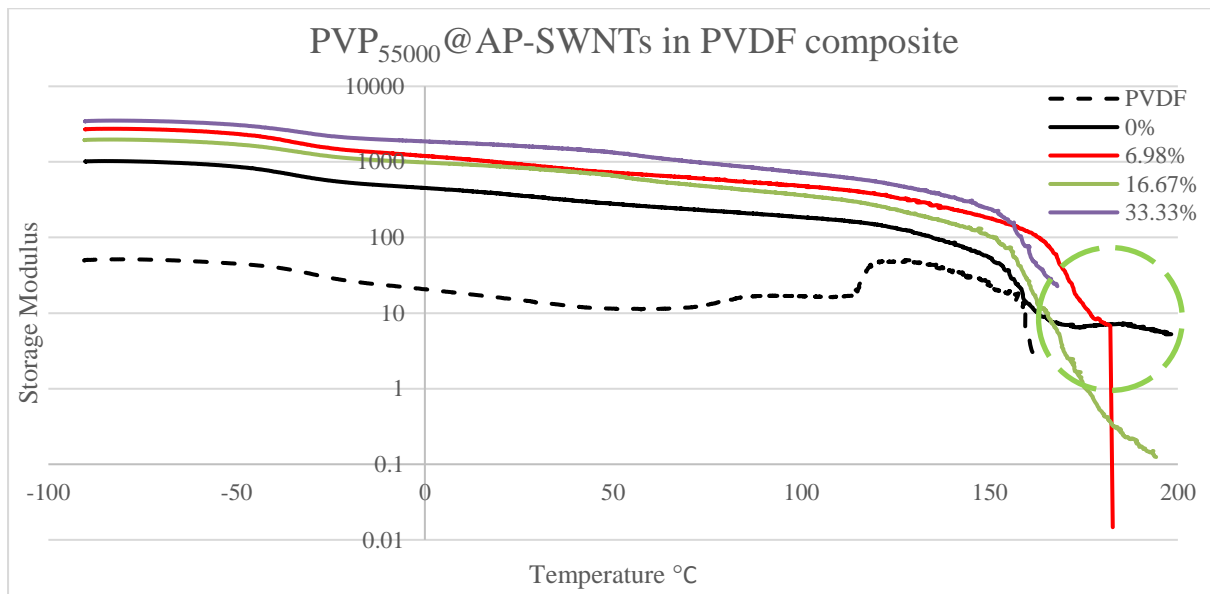


Fig. 6.3.4A: Storage modulus measurement of PVP<sub>55000</sub> functionalized AP-SWNTs in PVDF composites (data reproduced from Fig. 3.3.4D in chapter 3).

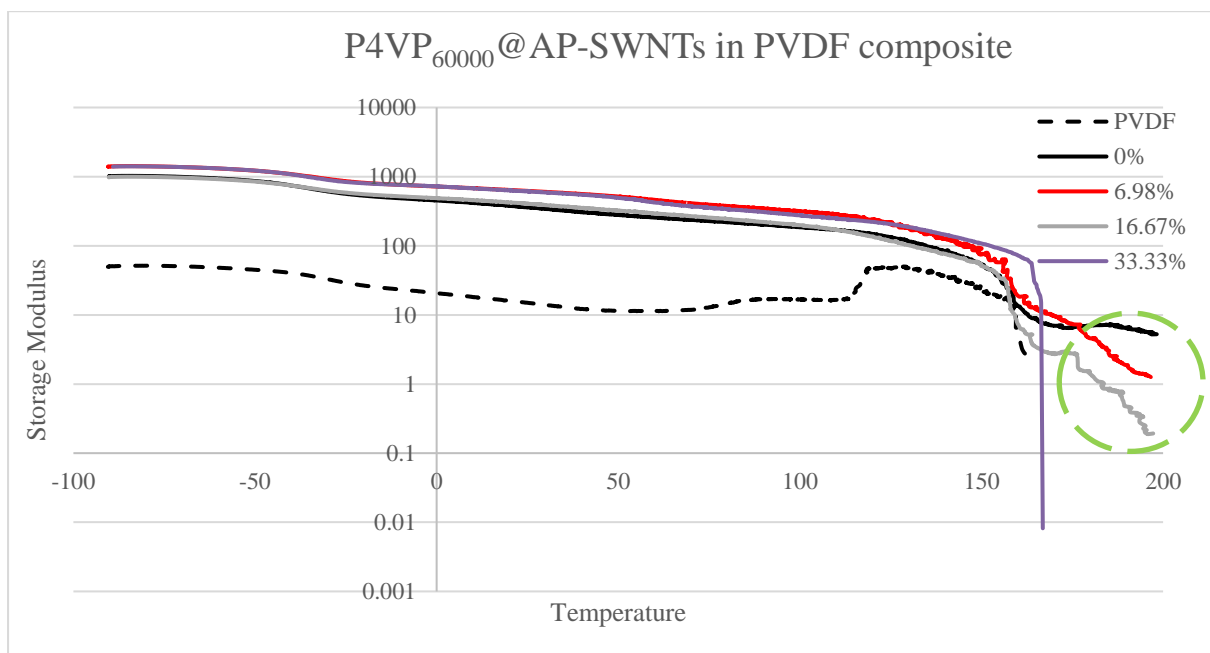


Fig. 6.3.4B: Storage modulus measurement of PVP<sub>60000</sub> functionalized AP-SWNTs in PVDF composites.

The storage modulus of PVP<sub>55000</sub> and P4VP<sub>60000</sub> functionalized nanotube composite prepared at a range of PVP/P4VP concentrations are shown in Fig. 6.3.4A & Fig. 6.3.4B. The result confirms an increase in storage modulus of the PVDF composite with the introduction of AP-SWNTs. A further enhancement in storage modulus can be achieved through a stable

dispersion of nanotubes as a result of improved polymer-nanotube interaction and such an observation is exhibited by both PVP<sub>55000</sub> and P4VP<sub>60000</sub> functionalized nanotube composites.

Unmodified AP-SWNTs in PVDF composites tend to exhibit some kind of a network like formation of nanotubes, owing to their high aspect ratio which helps the composite to maintain a mechanical strength at temperatures as high as 198.26 °C. Functionalization of nanotubes with PVP<sub>55000</sub> tend to improve the polymer nanotube interaction leading to a minor increase in storage modulus but yet they are unable to withstand temperatures as high as the unmodified nanotube composites. Thermal conductivity enhancement is observed in PVP<sub>55000</sub> functionalized composite at a concentration of 6.98 wt. %, but the mechanical strength of this composite is unable to withstand high temperatures and tends to reach a yielding point at 182.70 °C. Composites prepared with P4VP functionalization of nanotubes also exhibit a similar behaviour. Thermal conductivity enhancement is observed at a concentration of 6.98 wt. % and although this composite is able to withstand a temperature as high as 196.37 °C, they exhibit lower mechanical strength compared to unmodified nanotube composites. This confirms that PVP<sub>55000</sub> and P4VP<sub>60000</sub> functionalized nanotube composites could not provide a stable network like formation of nanotubes beyond the melting temperature of PVDF as effective as an unmodified AP-SWNTs in PVDF composite.

### P3 Single-walled nanotubes

#### *6.3.5 Thermal Conductivity*

Comparative thermal conductivity results for composites prepared with PVP/P4VP functionalized P3-SWNTs are shown in Fig. 6.3.5.

The thermal conductivity of a P3-SWNTs in PVDF composite is observed to be 2.93 W·m<sup>-1</sup>·K<sup>-1</sup> (highlighted in a solid black circle) but a further enhancement in thermal conductivity can be achieved through a stable dispersion of nanotubes in the polymer matrix. PVP<sub>55000</sub> functionalized nanotube composite exhibits a stable dispersion of nanotubes at a concentration of 23.08 wt. % leading to a thermal conductivity enhancement up to 4.27 W·m<sup>-1</sup>·K<sup>-1</sup>. However, nanotubes functionalized with P4VP<sub>60000</sub> polymer do not seem initiate any dispersion effect in the PVDF matrix. This is reflected in the very low thermal conductivity result observed in Fig. 6.3.5 for the P4VP<sub>60000</sub> functionalized nanotube composite compared to the unmodified nanotube composite. This hypothesis is supported by the crystallization behaviour observed for the composite prepared with PVP<sub>55000</sub> and P4VP<sub>60000</sub> functionalized nanotubes (See Fig. 6.3.6).

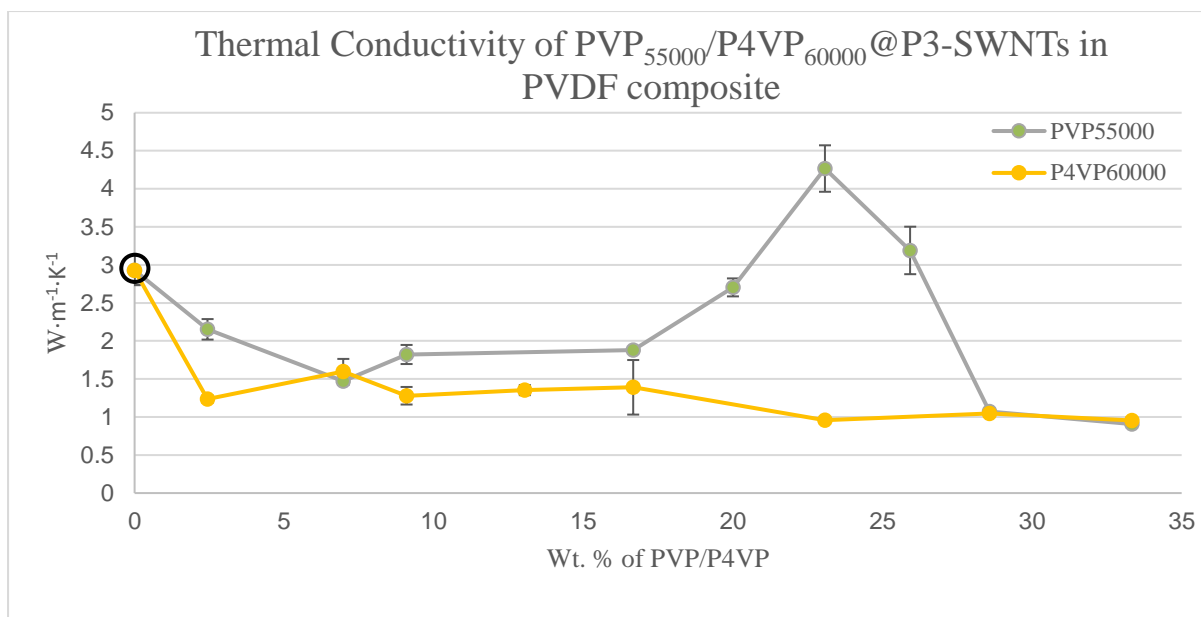


Fig. 6.3.5: Thermal conductivity measurements of PVP/P4VP functionalized P3-SWNTs in PVDF composites (PVP data reproduced from Fig. 4.3.1A in chapter 4).

### 6.3.6 Crystallization behaviour of PVP/P4VP@P3-SWNT in PVDF composites

A crystallization extent of 38.56 % is observed for unmodified nanotube composites and a 40.01 % crystallization is observed in composites prepared with PVP<sub>55000</sub> functionalized nanotubes at a PVP concentration of 23.08 wt. %, which also exhibited the thermal conductivity enhancement shown in Fig. 6.3.6. However, no such enhancement in the degree of crystallization is observed with P4VP<sub>60000</sub> functionalized nanotube composite and similar to the thermal conductivity result, a lower degree of crystallization is exhibited in these composites. The degree of crystallization tends to decrease even further at higher concentration of P4VP. This confirms either the absence of a dispersion effect or the presence of a very low dispersion effect in P4VP<sub>60000</sub> functionalized nanotube composites compared to the unmodified nanotube composite.

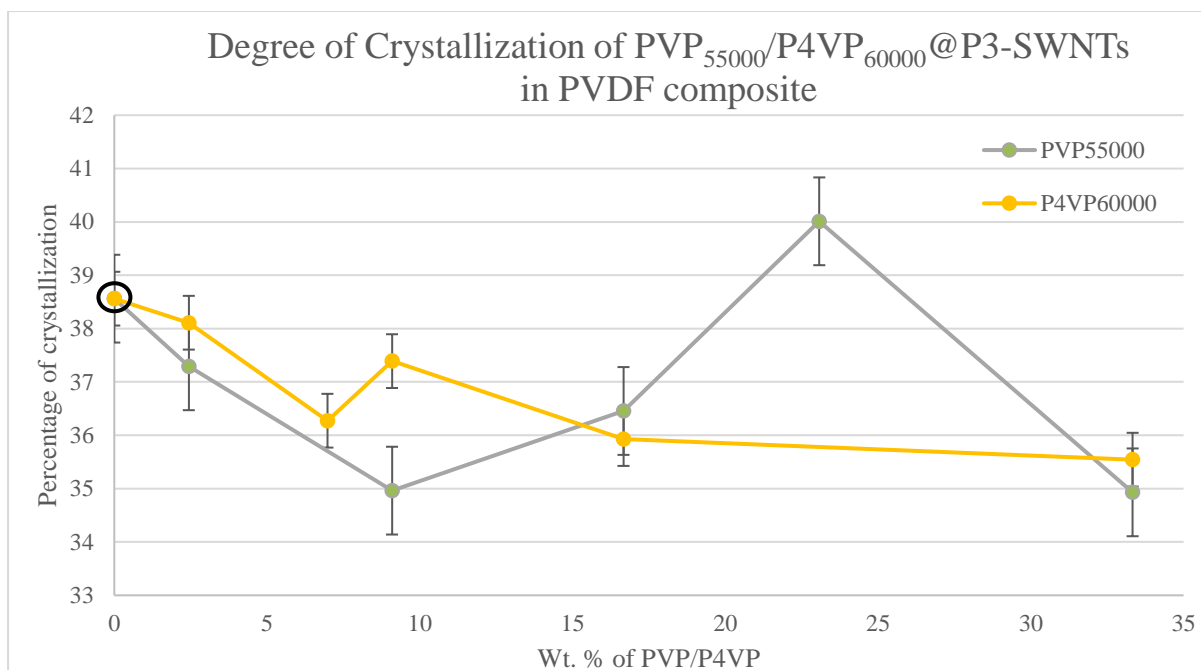


Fig. 6.3.6: Crystallization vs PVP/P4VP wt. % of non-covalently functionalized P3-SWNTs in PVDF composites (PVP data reproduced from Fig. 4.3.2 in chapter 4).

This could be due to the influence of the aspect ratio of SWNT over the conformational morphology of P4VP. Su et al. reported that non-covalent functionalization of SWNTs with P4VP in CO<sub>2</sub> expanded liquids has shown the presence of a stable dispersion of SWNTs in both organic solvents and aqueous medium [2]. However, the aspect ratio of SWNTs used were very high compared to the P3-SWNTs used in this research which possess an average diameter of 1.4 nm (bundle diameter of 4 - 5 nm) and a length of about 1 micron. Likewise, Yoon et al. reported a high stability in the dispersion of low aspect ratio SWNTs with P4VP functionalization [3], whereas the molecular weight of P4VP used was 200000 g·mol<sup>-1</sup>. The molecular weight of polymer plays a key role in the selective dispersion of SWNTs in organic solvents [4]. There is a chance that the low aspect ratio of the SWNTs used here would not have favoured a helical or kebab like conformation of P4VP leading to the low thermal conductivity result and poor crystallization behaviour of P4VP functionalized nanotube composite observed in Fig. 6.3.5 & 6.3.6. This could be due to the incompatibility between the aspect ratio of the SWNTs and the molecular weight of P4VP in order to achieve an effective dispersion.



### 6.3.7 Electrical Conductivity

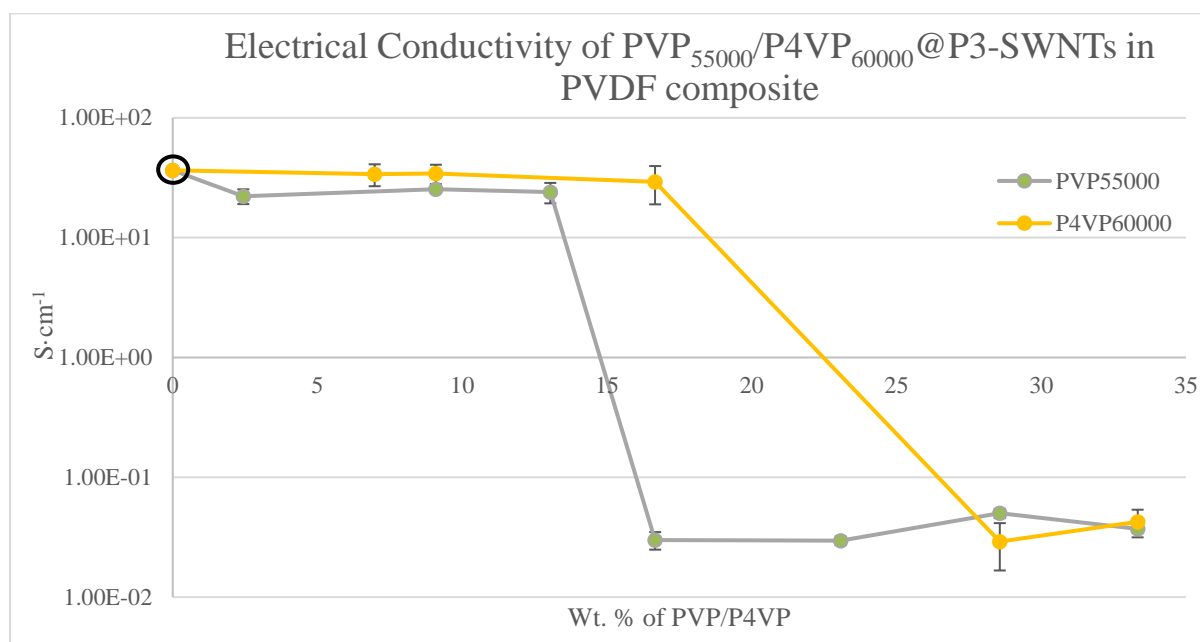


Fig. 6.3.7: Electrical conductivity measurements of PVP/P4VP functionalized P3-SWNTs in PVDF composites (PVP data reproduced from Fig. 4.3.3 in chapter 4).

Unmodified nanotube composites exhibit an electrical conductivity of about  $36.5 \text{ S}\cdot\text{cm}^{-1}$  and P4VP<sub>60000</sub> functionalization of nanotubes do not tend to exhibit any significant dispersion effect in the composite as observed from the crystallization behaviour shown in Fig. 6.3.6. As a result, the presence of P4VP do not happen to have much influence over the electrical conductivity of the composite at low concentration. An electrical conductivity of  $33.9 \text{ S}\cdot\text{cm}^{-1}$  and  $34.3 \text{ S}\cdot\text{cm}^{-1}$  observed at a P4VP concentration of 6.98 wt. % and 9.09 wt. % could still have been achieved due to the influence of the unmodified nanotubes that are present in the composite. A small decrease in electrical conductivity exhibiting a value of  $29.3 \text{ S}\cdot\text{cm}^{-1}$  is observed at a P4VP concentration of 16.67 wt. % and a larger decrease in electrical conductivity is observed with further increase in concentrations of P4VP and a threshold point is reached at 28.57 wt. %. This could have been due to the change in solution viscosity achieved at higher concentrations of P4VP polymer. Molecular weight of the polymer has a large impact on the overall solution viscosity [5] and Cheng et al. reported that solvent viscosity have some influence on the individualization and stabilization of SWNT dispersions in pure solvent [6]. However, composites prepared with PVP<sub>55000</sub> functionalized nanotubes exhibits a lower electrical conductivity of  $22.2 \text{ S}\cdot\text{cm}^{-1}$  compared to unmodified nanotube composite at a PVP concentration of 2.44 wt. %. The decrease in electrical conductivity could be the result of PVP functionalization of nanotubes and a larger decrease is observed at a concentration of 16.67 wt.

% thus reaching a threshold point beyond which no significant change in electrical conductivity is observed. This is due to the fact that a higher amount of polymer present in the composite restricts the movement of electrons from a nanotube to neighbouring nanotubes and lowers the conductivity of the composite.

### 6.3.8 Mechanical Characterization

The storage modulus of PVP<sub>55000</sub> and P4VP<sub>60000</sub> functionalized nanotube composite prepared at a range of PVP/P4VP concentration are shown in Fig. 6.3.8A & Fig. 6.3.8B. The storage modulus of the PVDF composite is significantly improved with the introduction of P3-SWNTs (solid black line) and they tend to exhibit mechanical strength at temperatures as high as 169.02 °C.

Whereas, composites prepared with PVP<sub>55000</sub> functionalized nanotubes provides similar storage modulus but are observed to maintain mechanical strength at temperatures higher than the yielding point of unmodified nanotube composite as shown in Fig. 6.3.8A. This confirms that the PVP functionalization of nanotubes leads to an increased interaction between the PVDF polymer and nanotubes. Among the PVP<sub>55000</sub> functionalized nanotube composites, the sample prepared at a concentration of 23.08 wt. % achieves a stable dispersion of nanotubes as shown in Fig. 6.3.6 and also records a high thermal conductivity. This composite tends to exhibit a higher storage modulus at a high temperature range compared to composites prepared at other concentrations of PVP<sub>55000</sub> and it can also withstand temperatures as high as 197.24 °C. This could be due to the presence of a network like formation of nanotubes.

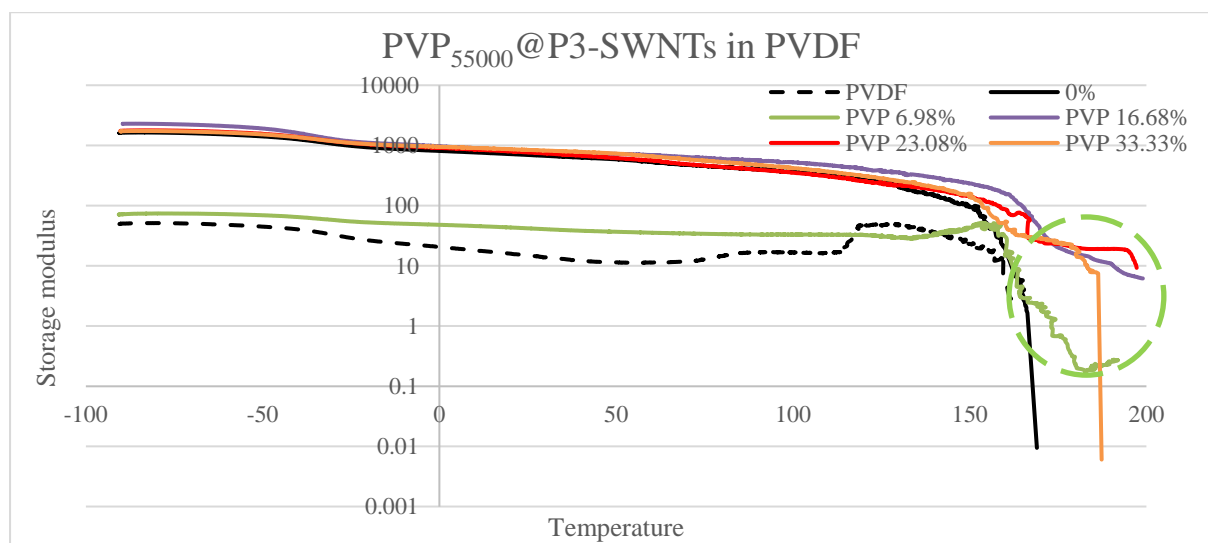


Fig. 6.3.8A: Storage modulus measurement of PVP<sub>55000</sub> functionalized P3-SWNTs in PVDF composites (data reproduced from Fig. 4.3.4B in chapter 4).

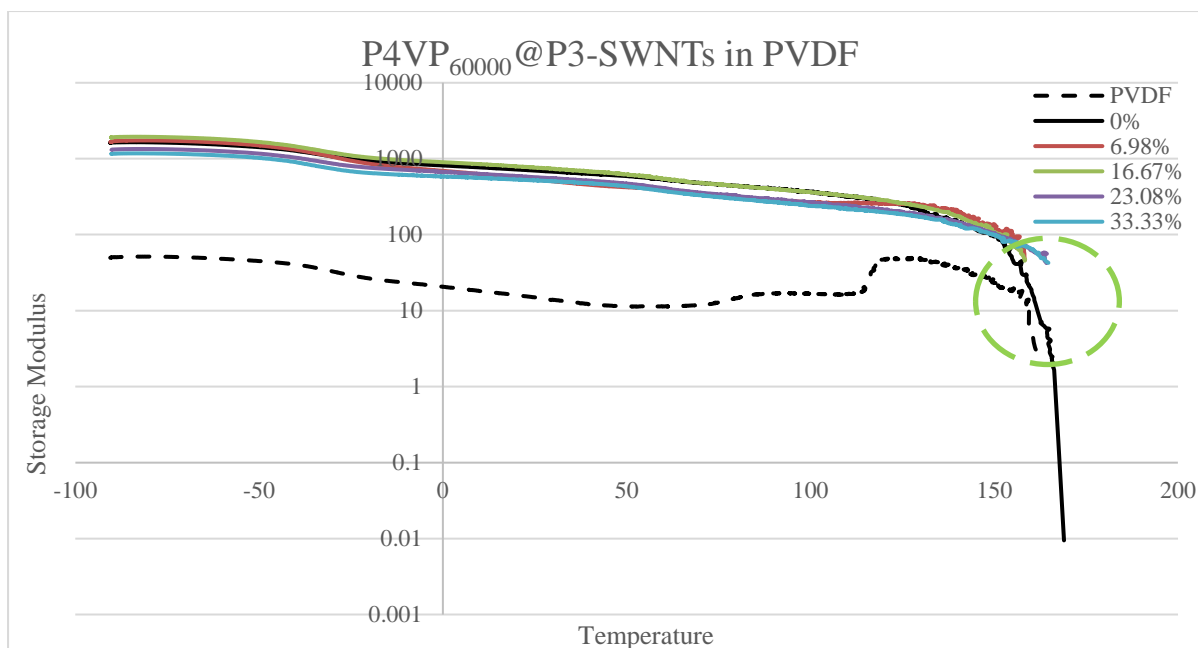


Fig. 6.3.8B: Storage modulus measurement of PVP<sub>60000</sub> functionalized P3-SWNTs in PVDF composites.

The storage modulus of the P4VP<sub>60000</sub> functionalized nanotube composites shown in Fig. 6.3.8B exhibit some resemblance to their respective thermal conductivity result and crystallization behaviour. The composites exhibit a storage modulus similar to an unmodified nanotube composite, but they could not withstand temperatures as high as an unmodified nanotube composite. The composites tend to yield at a temperature range slightly lower than the yielding point of unmodified nanotube composite. This confirms the absence of a dispersion effect in the P4VP<sub>60000</sub> functionalized composites.

### Multi-walled nanotubes

#### 6.3.9 Thermal Conductivity

Comparative thermal conductivity results for composites prepared with PVP/P4VP functionalized MWNTs are shown in Fig. 6.3.9.

The thermal conductivity of unmodified MWNTs in PVDF composite is observed to be  $1.48 \text{ W}\cdot\text{m}^{-1}\cdot\text{K}^{-1}$  and an improvement in the dispersion of nanotubes enhances the interaction between the PVDF polymer and nanotubes leading to a further enhancement in thermal conductivity. A stable dispersion of nanotubes is achieved in both PVP<sub>55000</sub> and P4VP<sub>60000</sub> functionalized composites but in different concentration ranges. PVP<sub>55000</sub> functionalized nanotube composites exhibit a stable dispersion of nanotubes at a PVP concentration of 23.08 wt. %, which leads to an increased thermal conductivity value of  $2.36 \text{ W}\cdot\text{m}^{-1}\cdot\text{K}^{-1}$ . Whereas, a

stable dispersion of nanotubes is achieved in the P4VP<sub>60000</sub> functionalized composite at comparatively higher concentration of 37.5 wt. %, exhibiting a thermal conductivity value of 2.79 W·m<sup>-1</sup>·K<sup>-1</sup> followed by a minor decrease in thermal conductivity to a value of about 2.64 W·m<sup>-1</sup>·K<sup>-1</sup> but still higher than the thermal conductivity of an unmodified nanotube composite.

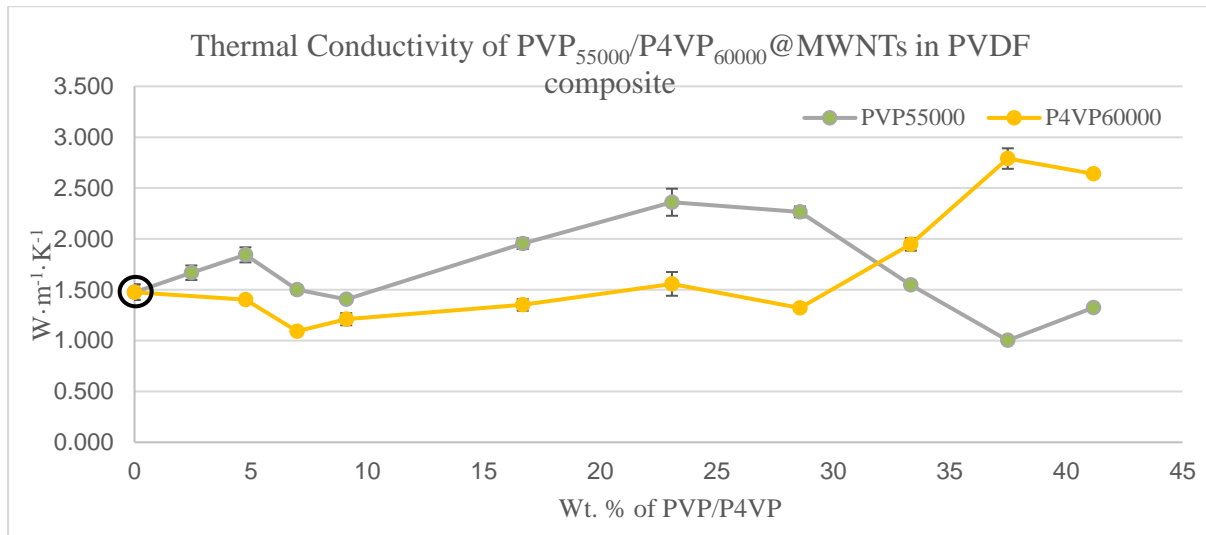


Fig. 6.3.9: Thermal conductivity measurements of PVP/P4VP functionalized MWNTs in PVDF composites (PVP data reproduced from Fig. 5.3.1 in chapter 5). Reproduced with permission.

### 6.3.10 Crystallization behaviour of PVP/P4VP@MWNT in PVDF composites

The crystallization behaviour of unmodified MWNTs in PVDF composites shown in Fig. 6.3.10 exhibits a 40.74 % crystallization. Functionalization improves nanotube dispersion in the composite which then initiates increased nucleation effect leading to an increase in the degree of crystallization. This type of behaviour is observed in PVP<sub>55000</sub> and P4VP<sub>60000</sub> functionalized nanotube composite at the same concentration range that also records high thermal conductivity. PVP<sub>55000</sub> and P4VP<sub>60000</sub> functionalized nanotube composite exhibited a 41.46 % and 41.28 % crystallization at a concentration of 23.08 wt. % and 37.5 wt. %. This small enhancement in the crystallization extent could be attributed to the enhanced nucleation effect due to higher degree of nanotube dispersion.

Liu et al. studied the functionalization of MWNTs with crystalline P4VP in CO<sub>2</sub>-expanded liquids (CXLs) and reported that unlike SWNTs, P4VP crystallization on MWNTs undergo a multi-helical wrapping pattern similar to the helical wrapping pattern of PVP on MWNTs [7]. According to O'Connell multi-helical wrapping might also takes place with PVP functionalization of MWNTs allowing a higher surface area coverage with a low backbone strain of PVP [1]. Although, the wrapping pattern and molecular weight are similar for PVP<sub>55000</sub>

and P4VP<sub>60000</sub> polymers, a stable dispersion is achieved at different concentrations of PVP or P4VP due to the fact that the structure of PVP and P4VP are completely different. A dispersion is achieved in PVP functionalization through  $\pi$ - $\pi$  interaction between the  $\pi$  system in the carbonyl group of PVP and the  $\pi$  electron in the carbon nanotube. Whereas, a dispersion is achieved in P4VP functionalization through  $\pi$ - $\pi$  stacking between the aromatic side chains of P4VP and the sidewalls of multi-walled carbon nanotubes [8]. This could have led to a difference in surface coverage of MWNTs achieved through PVP or P4VP functionalization, thus requiring different concentrations of functionalization polymer in order to achieve a stable dispersion. Also, functionalization of MWNT by P4VP achieved at a concentration higher than 41.18 wt. % leads to very uneven distribution of nanotubes in the PVDF matrix exhibiting not just a low degree of polymer-nanotube interaction but also makes it very hard to deposit over a solid substrate, thus not allowing for a composite preparation beyond a concentration of 41.18 wt. %. However, no such behaviour is observed with PVP functionalization along the same concentration range, which confirms the different degree of surface coverage of MWNT achieved by PVP and P4VP leading to a different degree of dispersion.

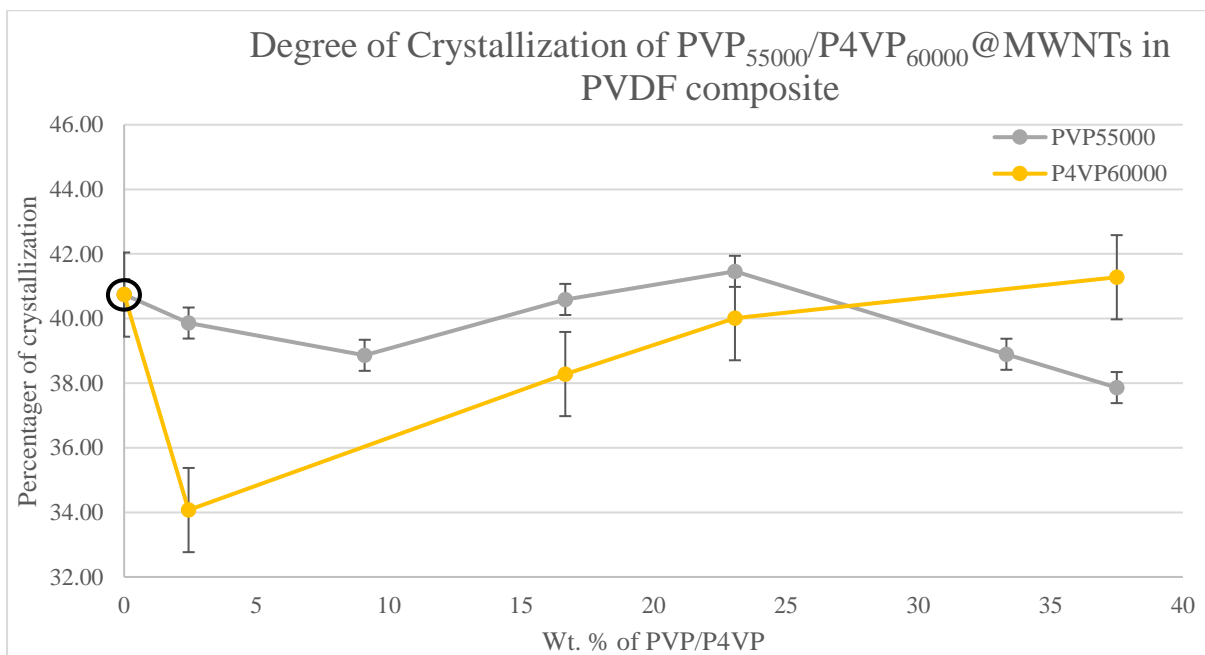


Fig. 6.3.10: Crystallization vs PVP/P4VP wt. % of non-covalently functionalized MWNTs in PVDF composites (PVP data reproduced from Fig. 5.3.2 in chapter 5).

### 6.3.11 Electrical Conductivity

The electrical conductivity of an unmodified MWNTs in PVDF composite shown in Fig. 6.3.11 is about  $26.1 \text{ S}\cdot\text{cm}^{-1}$  and a decrease in electrical conductivity is observed with both PVP and P4VP functionalization. PVP<sub>55000</sub> functionalized nanotube composite exhibit an electrical conductivity of  $1.09 \text{ S}\cdot\text{cm}^{-1}$  at a PVP concentration of 2.44 wt. % and decreases further with increasing PVP concentration leading to a threshold point at 23.08 wt. %. P4VP<sub>60000</sub> functionalized nanotube composite exhibits a similar result with an electrical conductivity of  $2.22 \text{ S}\cdot\text{cm}^{-1}$  at a P4VP concentration of 2.44 wt. % and also reaches the threshold point at a comparatively lower concentration of 9.09 wt. %. The low electrical conductivity observed could be attributed to the formation of a poor electrically conductive network, owing to the fact that longer polymer chain of PVP<sub>55000</sub> and P4VP<sub>60000</sub> could lead to higher surface coverage of nanotubes thus compromising the contacts between nanotubes in the composite. This could have forced the electrons to transport from a nanotube through a layer of functionalization polymer (PVP/P4VP) to reach the neighbouring nanotube in the network, which is possible with phonon transport to a certain extent but hinders the transport of electrons in the overall composite, yielding a comparatively low electrical conductivity.

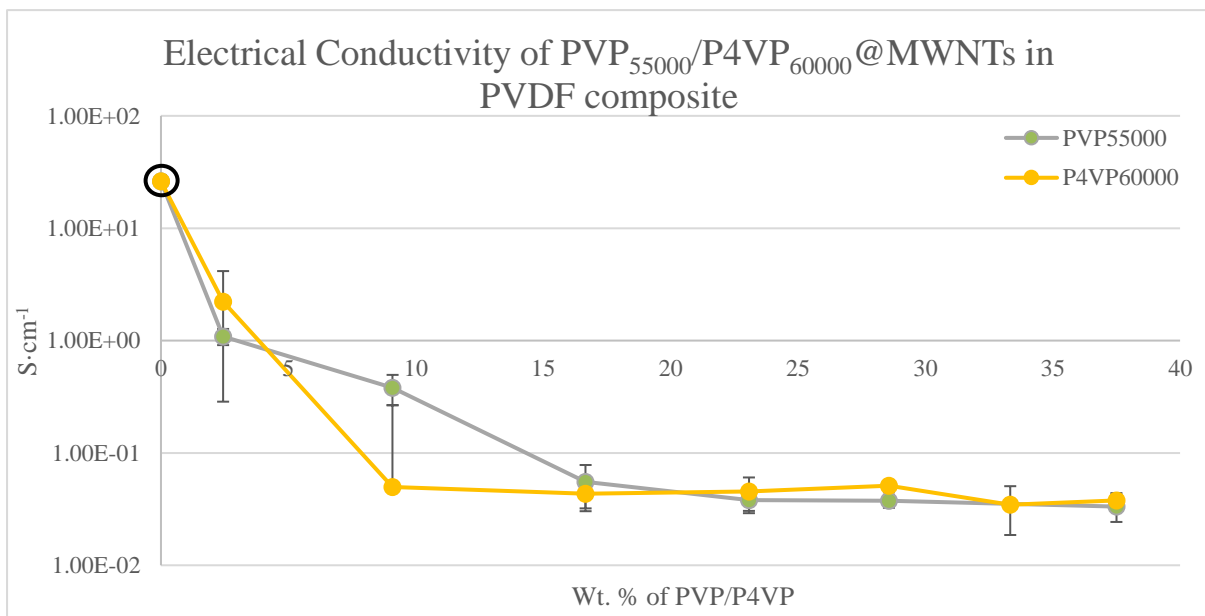


Fig. 6.3.11: Electrical conductivity measurements of PVP/P4VP functionalized MWNTs in PVDF composites (PVP data reproduced from Fig. 5.3.3 in chapter 5).

### 6.3.12 Mechanical Characterization

The storage modulus of PVP<sub>55000</sub> and P4VP<sub>60000</sub> functionalized nanotube composites prepared at a range of PVP/P4VP concentrations are shown in Fig. 6.3.12A & Fig. 6.3.12B. A significant increase in storage modulus of the PVDF composite is observed with the introduction of MWNTs (solid black line) and the composites tend to maintain the mechanical strength at temperatures as high as 184.78 °C above the melting temperature of the PVDF polymer which is 162.69 °C.

Composites prepared with PVP<sub>55000</sub> functionalized nanotubes exhibit a storage modulus similar to an unmodified nanotube composite and are able to maintain some mechanical strength at temperatures higher than the yielding point of an unmodified nanotube composite as shown in Fig. 6.3.12A, highlighted in green dashed circle. High thermal conductivity and a higher degree of dispersion is observed in the MWNTs in PVDF composite functionalized at a PVP<sub>55000</sub> concentration of 23.08 wt. % and this composite exhibited a higher storage modulus compared to unmodified nanotube composite at high temperature range and can withstand temperatures as high as 197.53 °C.

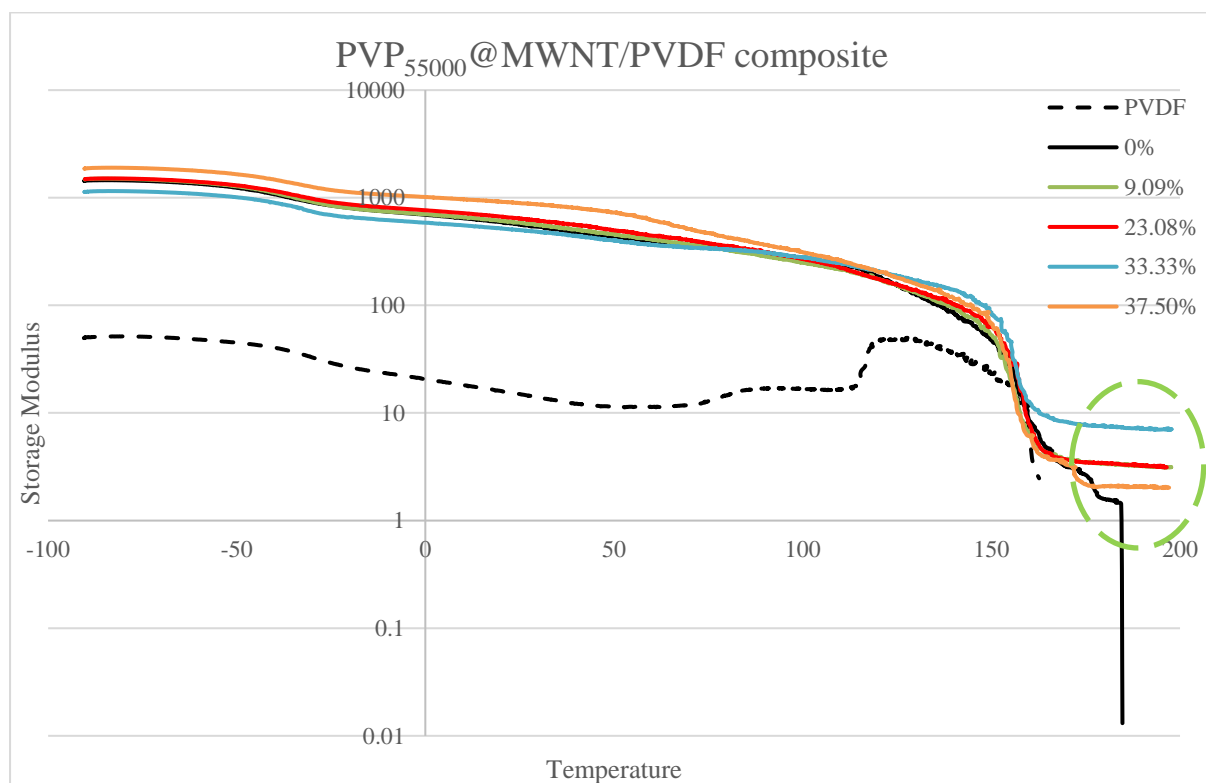


Fig. 6.3.12A: Storage modulus measurement of PVP<sub>55000</sub> functionalized MWNTs in PVDF composites (data reproduced from Fig. 5.3.4D in chapter 5).

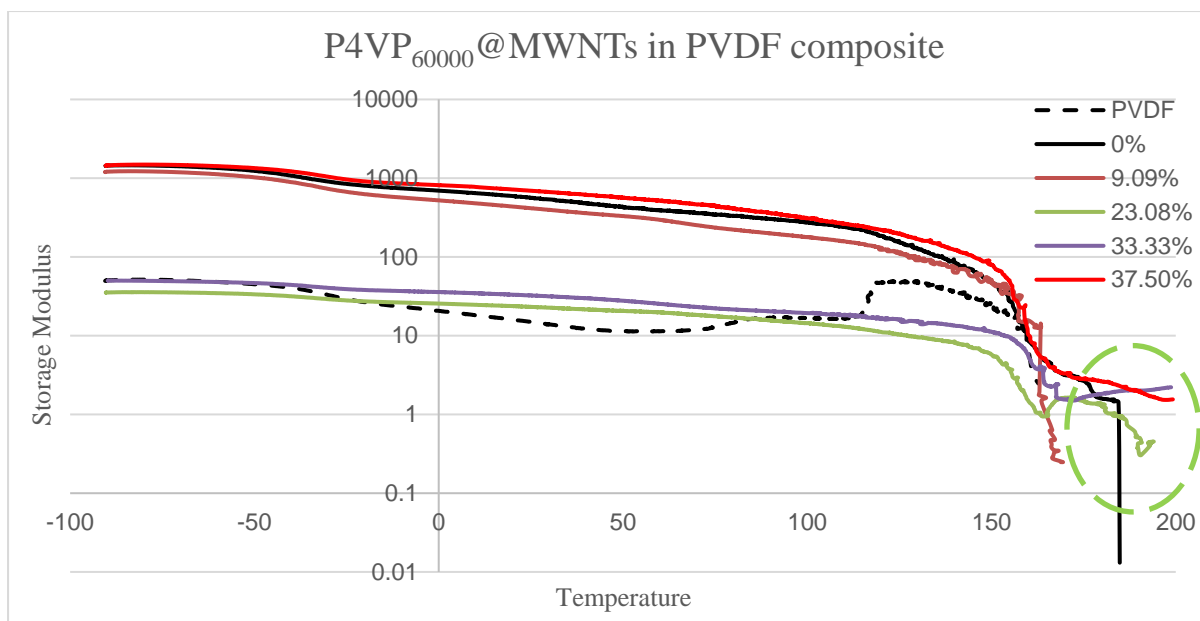


Fig. 6.3.12B: Storage modulus measurement of PVP<sub>60000</sub> functionalized MWNTs in PVDF composites.

A similar observation is seen in the composites prepared with P4VP functionalization of nanotubes as shown in Fig. 6.3.12B. High thermal conductivity and higher degree of crystallization is observed at a concentration of 37.5 wt. %. The mechanical strength of this composite is higher than unmodified nanotube composite at high temperatures and is able to withstand a temperature of 199.18 °C. This confirms the presence of a network like formation of nanotubes that exhibits an increased interaction between the PVDF polymer and MWNTs as a result of stable dispersion of nanotubes in the composite, which allows the composite to hold together even beyond the melting temperature of PVDF polymer.

#### 6.4 CONCLUSION

A comparative study on the physical properties of PVP or P4VP functionalized CNT/PVDF composites with the functionalization polymer of similar molecular weight (PVP<sub>55000</sub> and P4VP<sub>60000</sub>) and two different structures were undertaken. Polyvinylpyrrolidone (PVP) contains a pyrrolidone moiety and an alkyl group but Poly(4-vinylpyridine) (P4VP) is a derivative of pyridine ring with a vinyl group. The experiment was performed on three different nanotubes and an analysis based on the polymer wrapping pattern were discussed.

Unmodified AP-SWNTs in PVDF composites exhibit an improvement in the dispersion of nanotubes with both PVP<sub>55000</sub> and P4VP<sub>60000</sub> functionalization leading to an enhancement in the degree of crystallization yet it is unable to construct a conductive nanotube network leading to low thermal conductivity. This is also reflected in the low mechanical characterization of



the composites compared to unmodified nanotubes composite. Whereas, the unmodified P3-SWNTs in PVDF composites exhibit higher degree of nanotube dispersion with PVP<sub>55000</sub> functionalization but not with P4VP<sub>60000</sub> functionalization. This leads to an enhancement in the degree of crystallization, thermal conductivity and a composite that can exhibit mechanical strength at temperatures higher than unmodified nanotube composite, but no such improvement is observed in P4VP functionalization of P3-SWNTs in PVDF composite. This difference in the dispersion effect observed with AP-SWNT and P3-SWNT could be due to the different polymer wrapping pattern of PVP and P4VP. As explained in section 6.3.2, the kebab like conformation of P4VP tend to be highly influenced by the diameter and the length of the nanotubes. This leads to the poor formation of network in composites with AP-SWNTs due to their small diameter and a failure to exhibit a successful dispersion of nanotubes in composites with P3-SWNTs due to their small diameter and smaller length compared to AP-SWNTs.

However, the wrapping pattern of PVP and P4VP polymer is similar in multi walled nanotubes and as a result a stable dispersion of nanotubes is achieved in both PVP and P4VP functionalized composites. This leads to an enhancement in thermal conductivity, crystallization behaviour and improved mechanical strength observed in both polymers but at different concentrations. This could be because different the polymer structure leads to different surface coverage on the nanotubes and as a result a stable dispersion is achieved at different concentrations.

## 6.5 REFERENCES

1. O'Connell, M.J., et al., *Reversible water-solubilization of single-walled carbon nanotubes by polymer wrapping*. Chemical Physics Letters, 2001. **342**(3): p. 265-271.
2. Su, M., *Remarkable crystallization morphologies of poly(4-vinylpyridine) on single-walled carbon nanotubes in CO<sub>2</sub>-expanded liquids*. Express Polymer Letters, 2011. **5**: p. 1102-1112.
3. Yoon, B., S.F. Liu, and T.M. Swager, *Surface-Anchored Poly(4-vinylpyridine)-Single-Walled Carbon Nanotube-Metal Composites for Gas Detection*. Chemistry of Materials, 2016. **28**(16): p. 5916-5924.
4. Jakubka, F., et al., *Effect of Polymer Molecular Weight and Solution Parameters on Selective Dispersion of Single-Walled Carbon Nanotubes*. ACS Macro Letters, 2012. **1**(7): p. 815-819.
5. Rimmer, S., *Principles of polymer chemistry*, edited by A. Ravve. Plenum Press, New York, 1995. pp. xiv + 496, price US\$71.40. ISBN 0-306-44873-4. 1996. **39**(2): p. 164-164.
6. Cheng, Q., et al., *Ultrasound-Assisted SWNTs Dispersion: Effects of Sonication Parameters and Solvent Properties*. The Journal of Physical Chemistry C, 2010. **114**(19): p. 8821-8827.

7. Liu, Y., *Crystalline polymer decoration on multiwalled carbon nanotubes: MWCNT-induced P4VP periodic crystallization in CO<sub>2</sub>-expanded liquids*. eXPRESS Polymer Letters, 2010. **5**: p. 60-72.
8. Jannuzzi, S., et al., *Supramolecular Approach to Decorate Multi-Walled Carbon Nanotubes with Negatively Charged Iron(II) Complexes*. Journal of the Brazilian Chemical Society, 2016. **28**: p. 2-10.

## CHAPTER 7

# PEI FUNCTIONALIZED CARBON NANOTUBES IN PVDF COMPOSITES

## 7.1 CHAPTER INTRODUCTION

In this chapter, the non-covalent functionalization of carbon nanotubes by polyethylenimine (PEI) with molecular weights  $800 \text{ g}\cdot\text{mol}^{-1}$  or  $25000 \text{ g}\cdot\text{mol}^{-1}$  were compared and the physical properties of the composites prepared with the addition of PEI<sub>800</sub>/PEI<sub>25000</sub> functionalized CNTs to PVDF polymer are analysed extensively. Carbon nanotubes of three different structures were used in this study.

## 7.2 SAMPLE DETAILS

The composites used in the study were prepared with 1mg of unmodified CNTs functionalized with polyethylenimine (PEI) of various concentrations from 0 to 23.08 weight percent (and up to 28.57 weight percent in the electrical conductivity measurement of PEI functionalized MWNTs in PVDF composite), dispersed in 20 mg of PVDF polymer. The amount of CNTs and PVDF polymer were maintained constant throughout the study. A minimum of three composites for every concentration range were prepared and an average result is determined.

## 7.3 RESULTS & DISCUSSION

### AP Single-walled nanotubes

#### *7.3.1 Thermal Conductivity*

Comparative thermal conductivity results for composites prepared with PEI functionalized AP-SWNTs are shown in Fig. 7.3.1.

The thermal conductivity value of pristine AP-SWNTs in PVDF composites is observed to be  $4.37 \text{ W}\cdot\text{m}^{-1}\cdot\text{K}^{-1}$  which is highlighted with a solid black circle in Fig. 7.3.1. An improvement in the thermal conductivity value up to  $13.95 \text{ W}\cdot\text{m}^{-1}\cdot\text{K}^{-1}$  is observed in composites functionalized with PEI<sub>25000</sub> at a concentration of 4.76 wt. %. This shows that a stable dispersion of nanotubes exists in the PVDF matrix leading to a conductive network like formation of nanotubes is observed with the PEI<sub>25000</sub> functionalized AP-SWNT composite. This could be attributed to the fact that PEI and in general amines, are known to effectively interact with carbon nanotubes on the sidewalls via physisorption and initiate higher degree of dispersion in the solvents [1, 2]. J. Sun and L. Gao studied the development of a dispersion process for carbon nanotubes and confirmed that the dispersion state of CNTs could be much improved by the adsorption of a cationic dispersant of polyethylenimine [3]. L. Ma et al. also reported that PEI acts as a good candidate to functionalize and improve interfacial properties in the carbon fibre (CF)/epoxy

composite through the formation of “cross-bridges” to connect CF and epoxy matrix [4]. PEI<sub>800</sub> functionalized nanotube composites also exhibit a small enhancement in thermal conductivity at a similar PEI concentration range of 4.76 wt. % but the thermal conductivity was lower than the thermal conductivity of the unmodified nanotube composite at all PEI<sub>800</sub> concentrations. This small increase could be the presence of an increment in the degree of nanotube dispersion and the formation of a poor conduction path leads to low thermal conductivity.

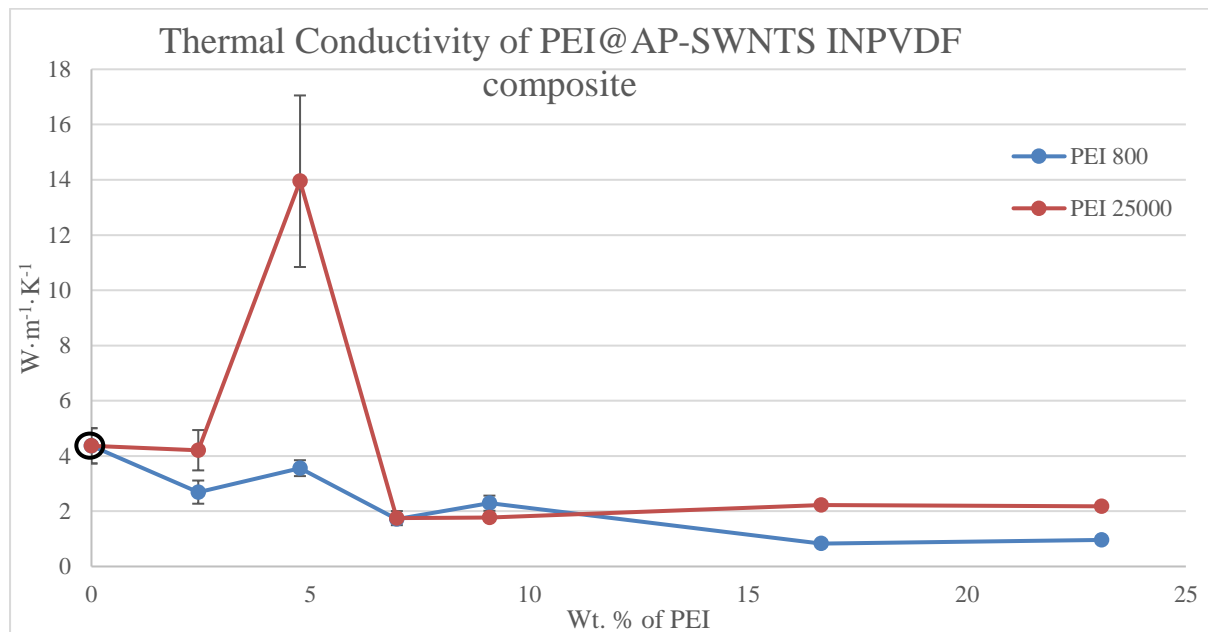


Fig. 7.3.1: Thermal conductivity measurements of PEI functionalized AP-SWNTs in PVDF composites.

### 7.3.2 Electrical Conductivity

Unmodified nanotube composites exhibit an electrical conductivity of about  $25.1 S \cdot cm^{-1}$  in Fig. 7.3.2 and an increase in the electrical conductivity is observed with PEI<sub>25000</sub> functionalized nanotube composite with a highest value of  $37.9 S \cdot cm^{-1}$  observed at a concentration of 4.76 wt. %. This could be attributed to the higher degree of nanotube dispersion and the subsequent formation of a conductive nanotube network. However, a decrease in electrical conductivity is observed at a concentration of 9.09 wt. % and further decrease is observed with increasing concentration of PEI, owing to the fact that the individualization and stabilization of the SWNT dispersion in organic solvent is highly influenced by the change in solution viscosity [5] observed at higher concentrations of the PEI polymer. This change in solution viscosity due to the higher amount of polymer could affect the thickness of polymer wrapping in the composite restricting the movement of electrons from a nanotube to neighbouring nanotubes thus lowering the conductivity of the composite. Similarly, the composites prepared with PEI<sub>800</sub>

functionalized nanotube composite exhibit a small increase in electrical conductivity value to about  $27.4 \text{ S}\cdot\text{cm}^{-1}$  at a concentration of 4.76 wt. %.

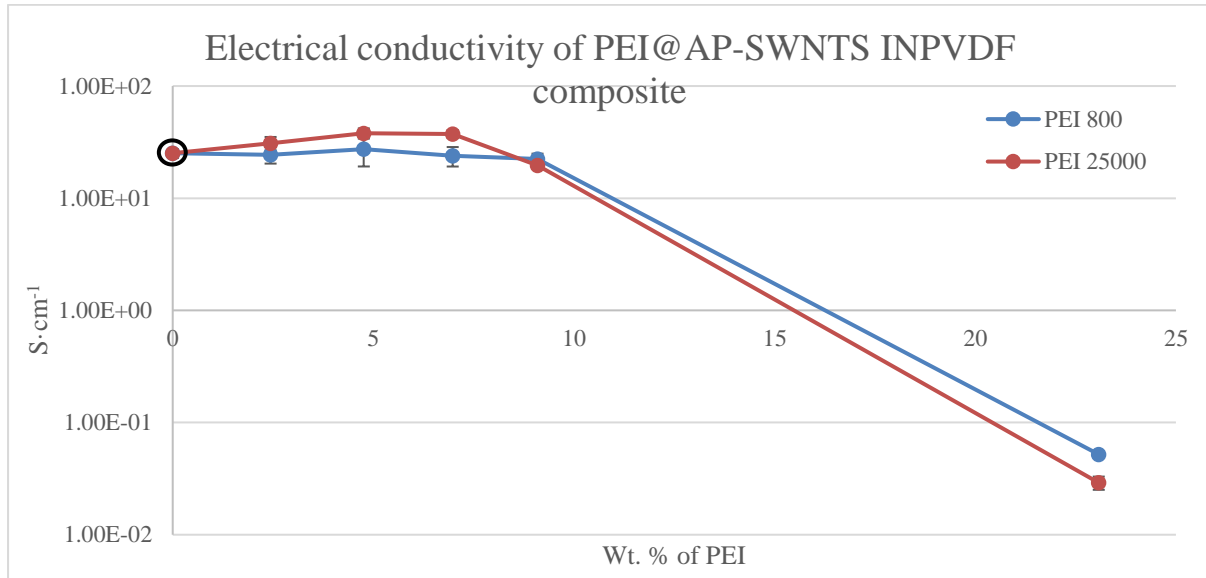


Fig. 7.3.2: Electrical conductivity measurements of PEI functionalized AP-SWNTs in PVDF composites.

### 7.3.3 Mechanical Characterization

The storage modulus of PEI<sub>800</sub> and PEI<sub>25000</sub> functionalized nanotube composite prepared at a range of PEI concentrations are shown in Fig. 7.3.3A & Fig. 7.3.3B.

The high aspect ratio and high mechanical strength of AP-SWNTs fillers have significantly increased the storage modulus of the PVDF composite as shown in Fig. 7.3.3A. Moreover, the storage modulus measurement of AP-SWNTs in PVDF composite (solid black line) exhibits mechanical strength at a temperature range above the melting temperature of a pure PVDF polymer, which is at  $162.69 \text{ }^\circ\text{C}$ , and can withstand temperatures as high as  $198.26 \text{ }^\circ\text{C}$ .

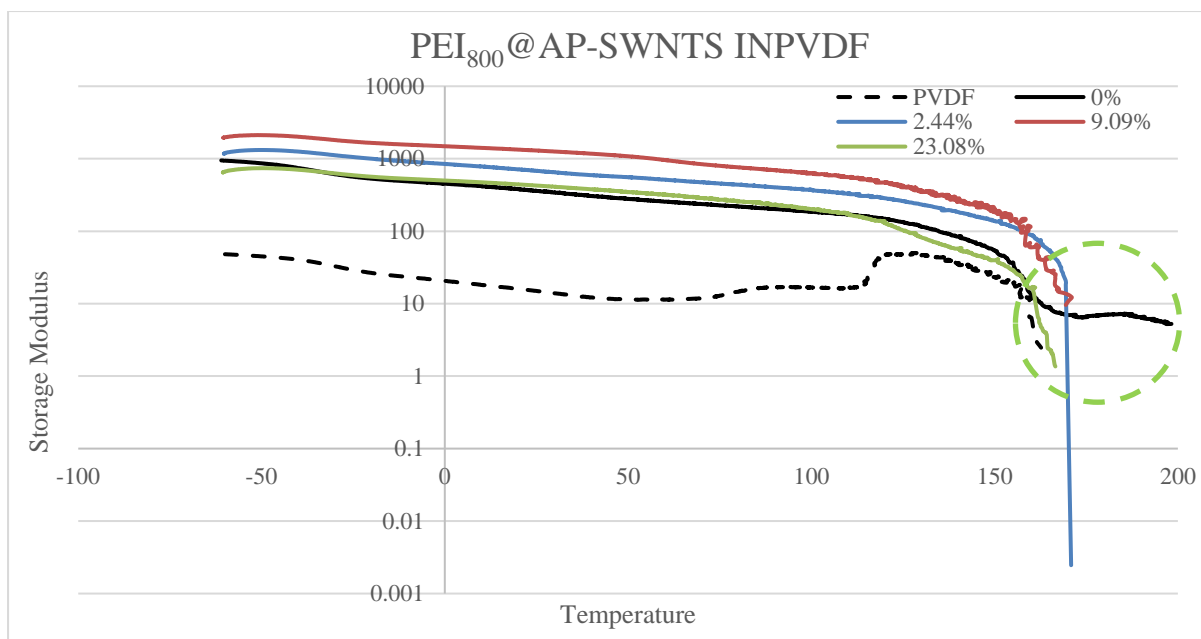


Fig. 7.3.3A: Storage modulus measurement of PEI<sub>800</sub> functionalized AP-SWNTs in PVDF composites.

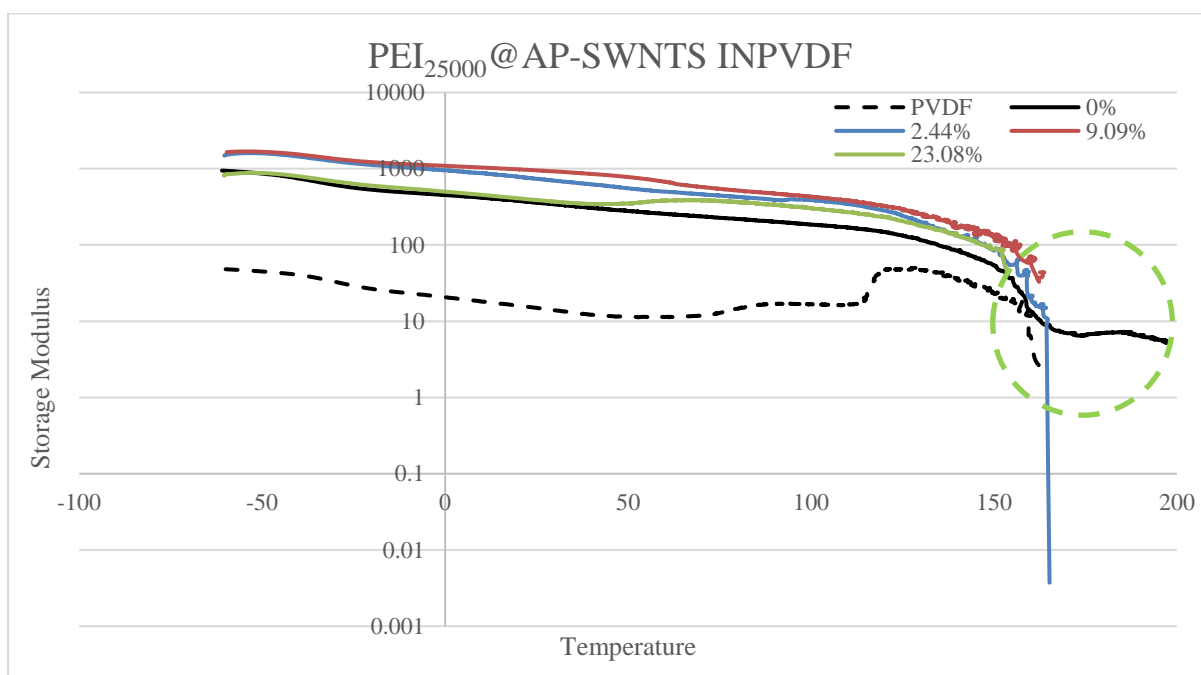


Fig. 7.3.3B: Storage modulus measurement of PEI<sub>25000</sub> functionalized AP-SWNTs in PVDF composites.

PEI<sub>800</sub>/PEI<sub>25000</sub> functionalized nanotube composites prepared at low concentrations of PEI tend to exhibit an increase in storage modulus compared to the storage modulus of unmodified nanotube composite due to the increased interaction between the PVDF polymer and nanotubes as a result of higher degree of nanotube dispersion. PEI functionalized nanotube composites prepared at high concentrations of PEI exhibit a similar storage modulus as unmodified nanotube composites. This could be attributed to the change in solution viscosity with increased

concentration of PEI leading to a decreased interaction between the nanotubes and polymer. However, PEI<sub>800</sub>/PEI<sub>25000</sub> functionalized nanotube composites are not capable of maintaining the mechanical strength of the composite at high temperatures leading to a yielding point at a temperature just above the melting temperature of PVDF polymer and far below the yielding point of an unmodified nanotube composite, as highlighted in a green dashed circle. This could be due to the low melting temperature of polyethylenimine, which is about 73 - 75 °C.

### P3 Single-walled nanotubes

#### *7.3.4 Thermal conductivity*

Comparative thermal conductivity results for composites prepared with PEI functionalized P3-SWNTs are shown in Fig. 7.3.4.

The thermal conductivity value of unmodified P3-SWNTs in PVDF composite is observed to be  $2.93 \text{ W}\cdot\text{m}^{-1}\cdot\text{K}^{-1}$  which is highlighted with a solid black circle. PEI functionalization of P3-SWNTs do not tend to exhibit an increase in the thermal conductivity of the composite. This could be attributed to the small aspect ratio of P3-SWNTs, that either could not have achieved a successful polymer wrapping with both the molecular weights of PEI polymer used in this study or could have initiated the formation of a weak nanotube network. PEI<sub>800</sub> functionalized nanotube composite exhibited a decrease in thermal conductivity with increasing concentration of PEI. Whereas, PEI<sub>25000</sub> functionalized nanotube composite showed an increase in thermal conductivity at a PEI concentration of 4.76 wt. % exhibiting a value of  $2.80 \text{ W}\cdot\text{m}^{-1}\cdot\text{K}^{-1}$  which is still lower than the thermal conductivity observed for unmodified nanotube composite and a further decrease in thermal conductivity is observed with increasing concentration of PEI. This confirms that the presence of PEI<sub>800</sub>/PEI<sub>25000</sub> polymer in the composite do not tend to influence or initiate the dispersion of nanotubes leading to decreasing a thermal conductivity with increasing PEI concentration.



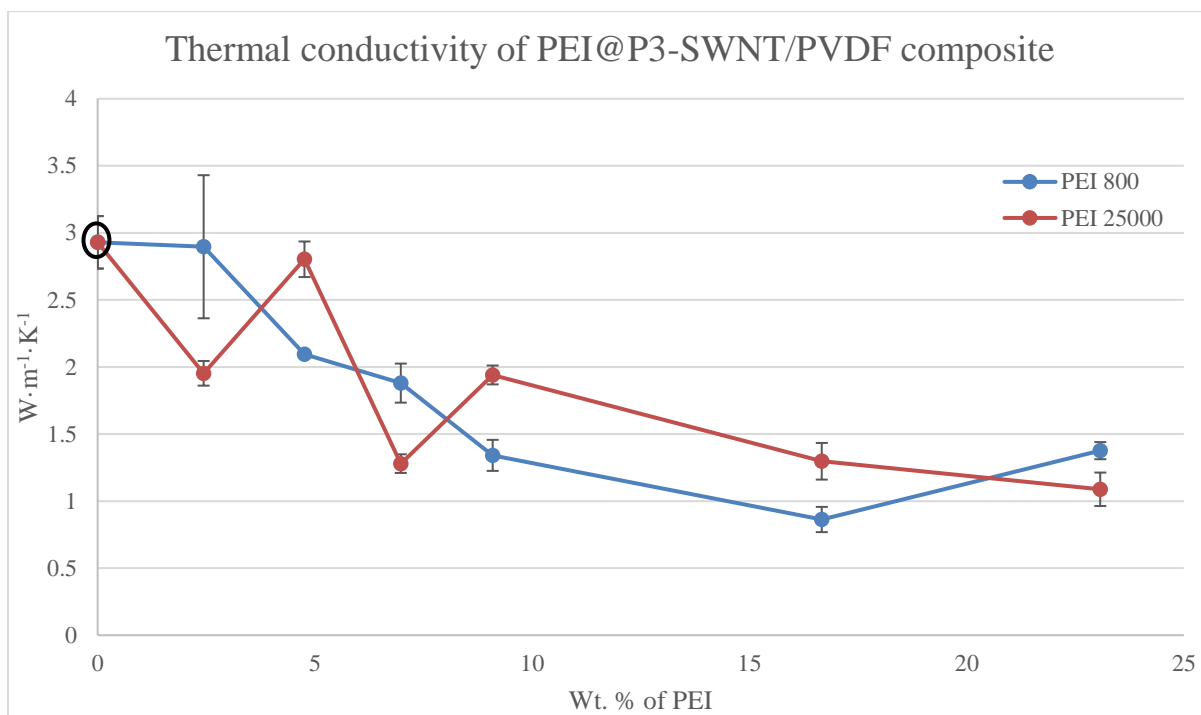


Fig. 7.3.4: Thermal conductivity measurements of PEI functionalized P3-SWNTs in PVDF composites.

### 7.3.5 Electrical Conductivity

Unmodified nanotube composite exhibits an electrical conductivity value of  $36.5 \text{ S}\cdot\text{cm}^{-1}$ . Composites prepared with PEI<sub>800</sub> functionalized nanotubes exhibits good conductivity but comparatively lower than unmodified nanotube composites with a highest value of  $30.5 \text{ S}\cdot\text{cm}^{-1}$  observed at a PEI concentration of 6.98 wt. % followed by a decrease in conductivity at a concentration of 9.09 wt. % and tend to decrease even further with increasing concentration of PEI. Whereas, PEI<sub>25000</sub> functionalized nanotube composite exhibits an increase in electrical conductivity measurement to a value of about  $35.3 \text{ S}\cdot\text{cm}^{-1}$  at a concentration of 4.76 wt. % mirroring the trends observed in the thermal conductivity measurements. There is a gradual decrease in conductivity observed at a concentration of 9.09 wt. % and an abrupt decrease with further increase in PEI concentration.

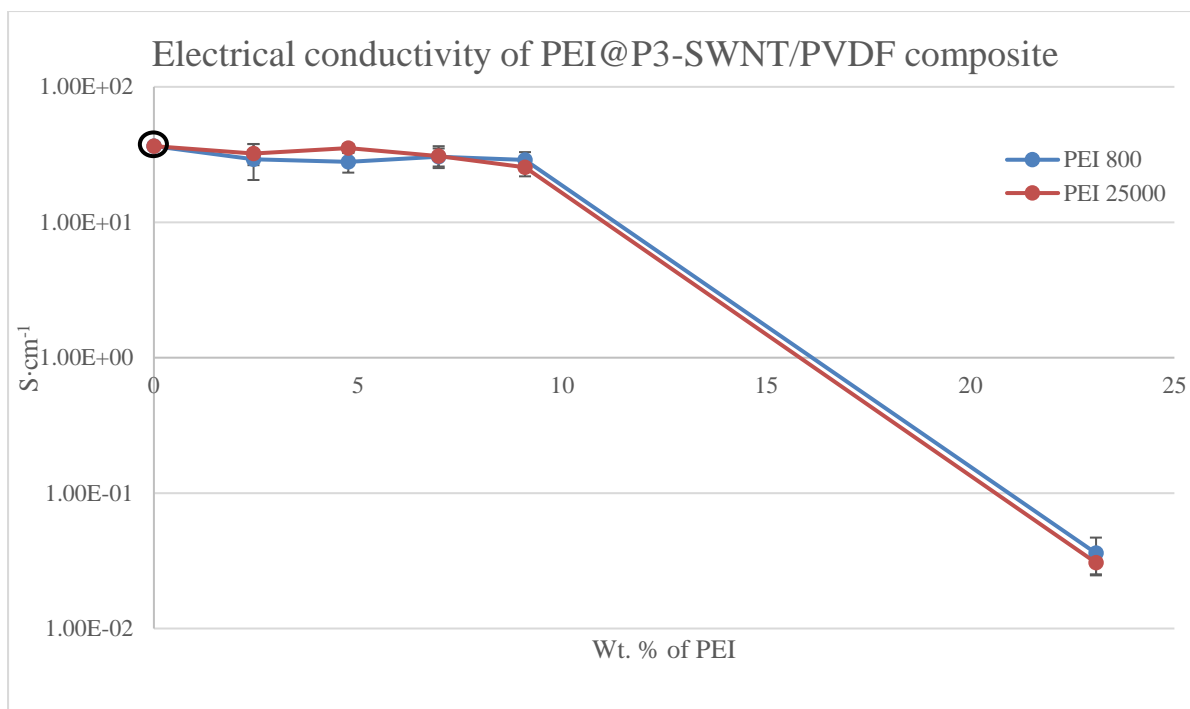


Fig. 7.3.5: Electrical conductivity measurements of PEI functionalized P3-SWNTs in PVDF composites.

### 7.3.6 Mechanical Characterization

The storage modulus of PEI<sub>800</sub> and PEI<sub>25000</sub> functionalized P3-SWNTs in PVDF composites prepared at a range of PEI concentrations are shown in Fig. 7.3.6A & Fig. 7.3.6B.

Unmodified P3-SWNTs in PVDF composites (solid black line) are observed to exhibit higher storage modulus compared to pure PVDF (dashed black line) and is able to maintain mechanical strength at temperatures as high as 169.02 °C.

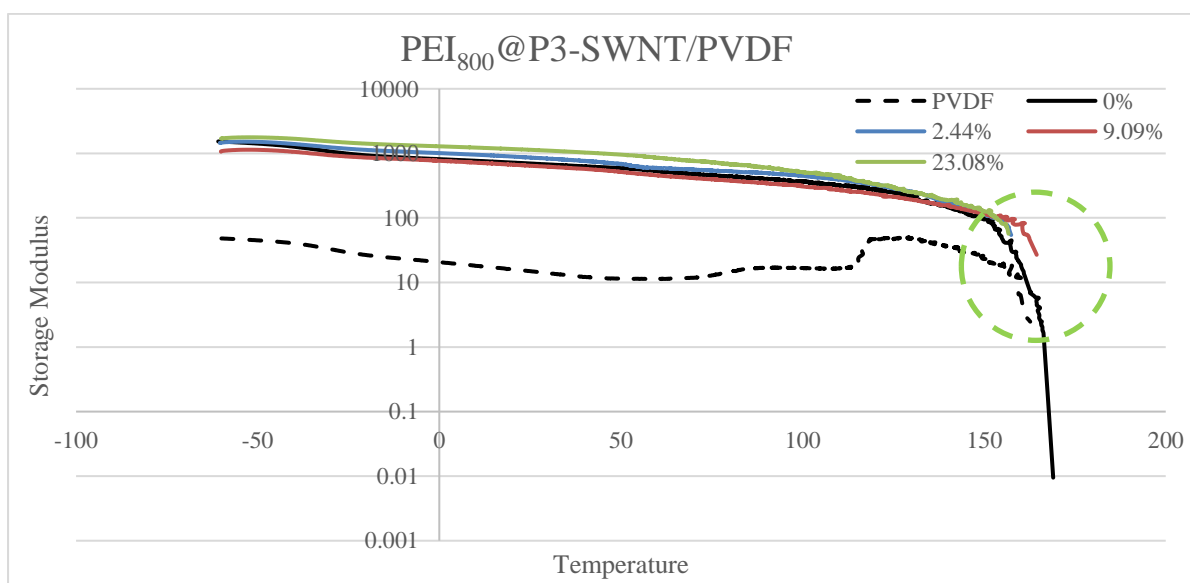


Fig. 7.3.6A: Storage modulus measurement of PEI<sub>800</sub> functionalized P3-SWNTs in PVDF composites.

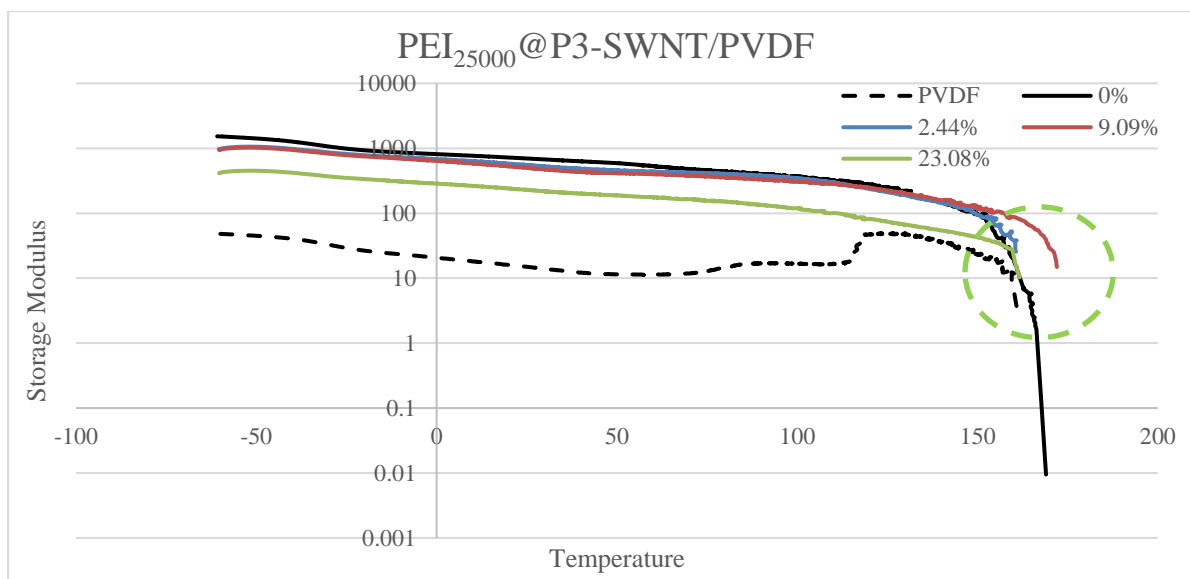


Fig. 7.3.6B: Storage modulus measurement of PEI<sub>25000</sub> functionalized P3-SWNTs in PVDF composites.

PEI<sub>800</sub> functionalized nanotube composites exhibit a similar storage modulus as observed in unmodified nanotube composite but the functionalized composites are unable to withstand temperatures higher than the yielding point of an unmodified nanotube composite. This could mean that PEI<sub>800</sub> functionalization of nanotubes has not changed the dispersion of nanotubes in polymer matrix, leading to the fact that the interaction between the nanotube and the PVDF polymer has not shown much increase with the presence of PEI polymer. PEI<sub>25000</sub> functionalized nanotube composite also exhibit a similar storage modulus as observed in an unmodified nanotube composite. However, the composites prepared at a concentration of 9.09 wt. % exhibit mechanical strength at a temperature of about 172.12 °C, which is slightly higher than the yielding point of an unmodified nanotube composite. This could mean that a mild improvement in the degree of nanotube dispersion is observed with PEI<sub>25000</sub> functionalization of nanotubes along the concentration range of 9.09 wt. % which allows for an increased interaction between the nanotubes and the PVDF polymer compared to an unmodified nanotube composite.

### Multi-walled nanotubes

#### 7.3.7 Thermal Conductivity

Comparative thermal conductivity results for composites prepared with PEI functionalized MWNTs are shown in Fig. 7.3.7.

The thermal conductivity value of unmodified MWNTs in PVDF composite is observed to be 1.48 W·m<sup>-1</sup>·K<sup>-1</sup> which is highlighted with a solid black circle. An improvement in thermal

conductivity is observed with PEI functionalization of MWNTs. PEI<sub>800</sub> functionalized nanotube composites exhibit an enhanced thermal conductivity value to about  $1.99 \text{ W}\cdot\text{m}^{-1}\cdot\text{K}^{-1}$  at a concentration of 2.44 wt. % followed by a decrease in thermal conductivity at higher concentrations of PEI. Similarly, an increase in thermal conductivity value to about  $1.67 \text{ W}\cdot\text{m}^{-1}\cdot\text{K}^{-1}$  is observed with PEI<sub>25000</sub> functionalized nanotube composites at a concentration of 6.98 wt. %. This confirms that PEI functionalization achieves stable dispersion of MWNTs, allowing a higher level of interaction between the nanotubes and PVDF polymer compared to unmodified nanotube composites leading to a formation of conductive nanotube network. A. Azadbakht and M. B. Gholivand studied polyethyleneimine wrapped MWNT in situ gold nanoparticle composite and confirmed that cationic PEI was coated onto CNTs-COOH by electrostatic forces and initiates a higher degree of nanotube dispersion, thus giving the composite higher stability [6]. Moreover, amines on PEI possesses high affinity for physisorption along the CNTs-COOH surface which was similar to the polymer wrapping process [1, 7].

Additionally, the thermal conductivity result of PEI functionalized MWNTs in PVDF composite observed in Fig. 7.3.7 exhibit some resemblance to the thermal conductivity result of PVP functionalized MWNTs in PVDF composite shown in Chapter 5 Section 5.3.1 such that the functionalization polymer of low molecular weight (PEI<sub>800</sub>) tend to achieve stable dispersion of nanotubes at low concentration leading to an increase in thermal conductivity. Whereas, PEI<sub>25000</sub> functionalization achieve stable dispersion at moderately high concentration range giving a peak in the thermal conductivity which is higher than unmodified nanotube composite. This is be attributed to the fact that the longer molecular chain polymer could have wrapped higher surface area of the nanotubes compared to the short molecular chain polymer, thus allowing the transport of phonons to happen from a nanotube though a layer of PEI polymer in order to reach the neighbouring nanotube, leading to a reduction in thermal conductivity of the overall composite.

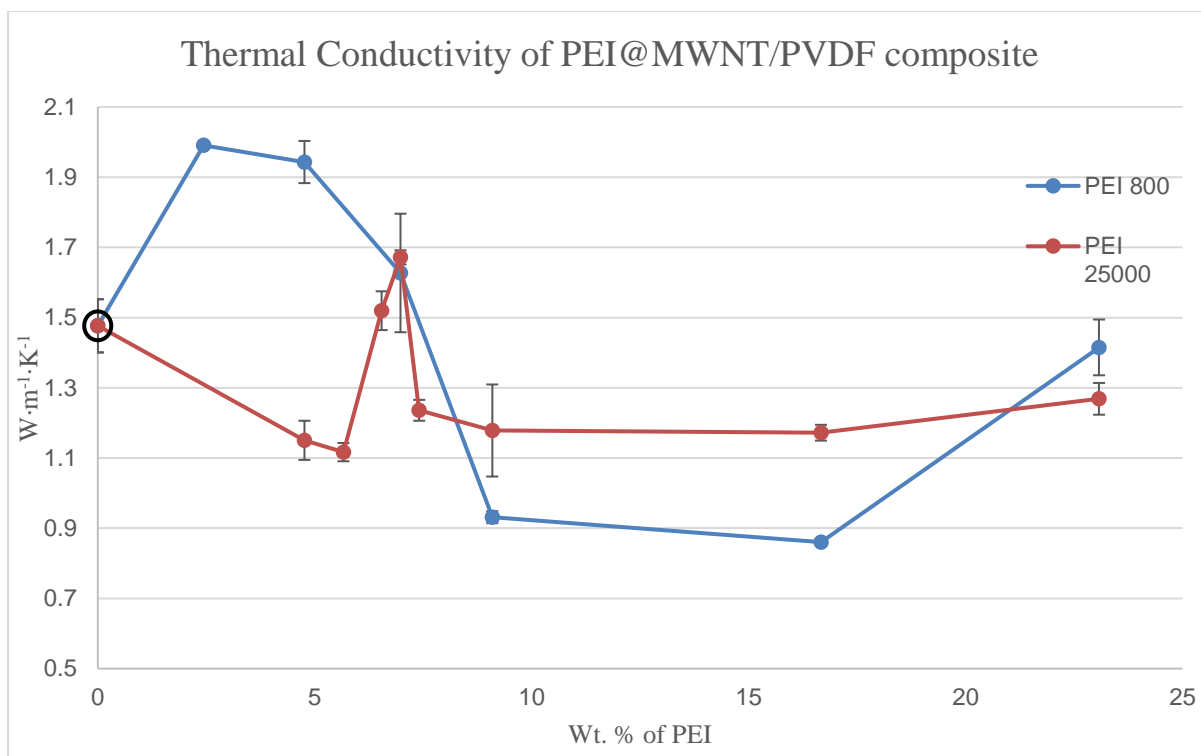


Fig. 7.3.7: Thermal conductivity measurements of PEI functionalized MWNTs in PVDF composites.

### 7.3.8 Electrical Conductivity

As shown in Fig. 7.3.8, the electrical conductivity of an unmodified MWNTs in PVDF composite is observed to be  $26.1 \text{ S}\cdot\text{cm}^{-1}$  and PEI functionalization of nanotubes has increased the nanotube polymer interaction leading to an increase in electrical conductivity. However, the difference in surface coverage of nanotubes achieved by PEI polymer of different molecular weights leads to an electrical conductivity enhancement in different concentration ranges. PEI<sub>800</sub> functionalized nanotube composites exhibit a gradual increase in electrical conductivity with increasing concentration of PEI with the highest conductivity value of  $44.1 \text{ S}\cdot\text{cm}^{-1}$  observed at a concentration of 23.08 wt. % followed by a decrease in electrical conductivity observed at a concentration of 28.57 wt. %. Whereas, PEI<sub>25000</sub> functionalized nanotube composite exhibits a high conductivity value of  $28.1 \text{ S}\cdot\text{cm}^{-1}$  at a concentration of 9.09 wt. % followed by a gradual decrease in conductivity value.

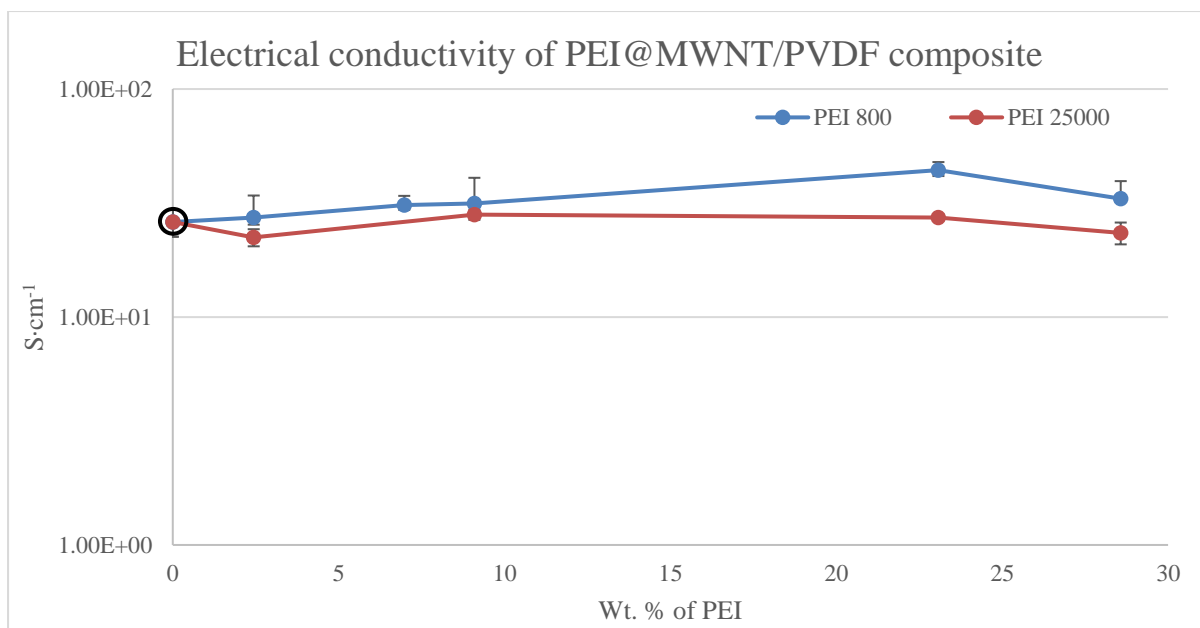


Fig. 7.3.8: Electrical conductivity measurements of PEI functionalized MWNTs in PVDF composites.

### 7.3.9 Mechanical Characterization

The storage modulus of PEI<sub>800</sub> and PEI<sub>25000</sub> functionalized MWNTs in PVDF composite prepared at a range of PEI concentration are shown in Fig. 7.3.9A & Fig. 7.3.9B.

The storage modulus of the PVDF composites is improved significantly with the presence of MWNT fillers (solid black line) and is observed to maintain mechanical strength at temperatures as high as 184.78 °C above the melting temperature of the PVDF polymer which is at 162.69 °C.

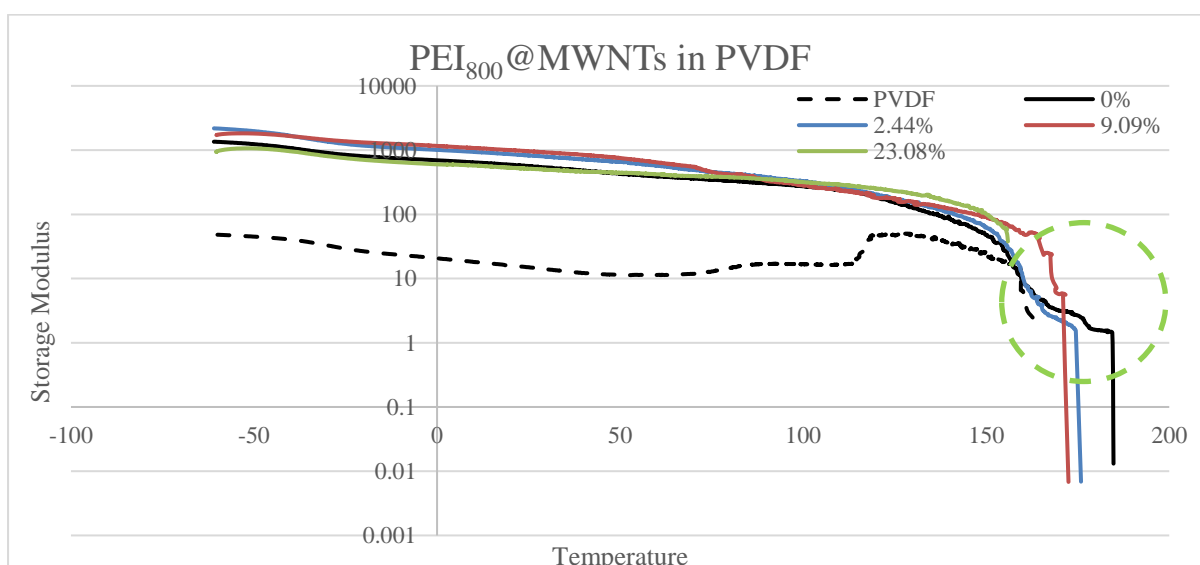


Fig. 7.3.9A: Storage modulus measurement of PEI<sub>800</sub> functionalized MWNTs in PVDF composites.

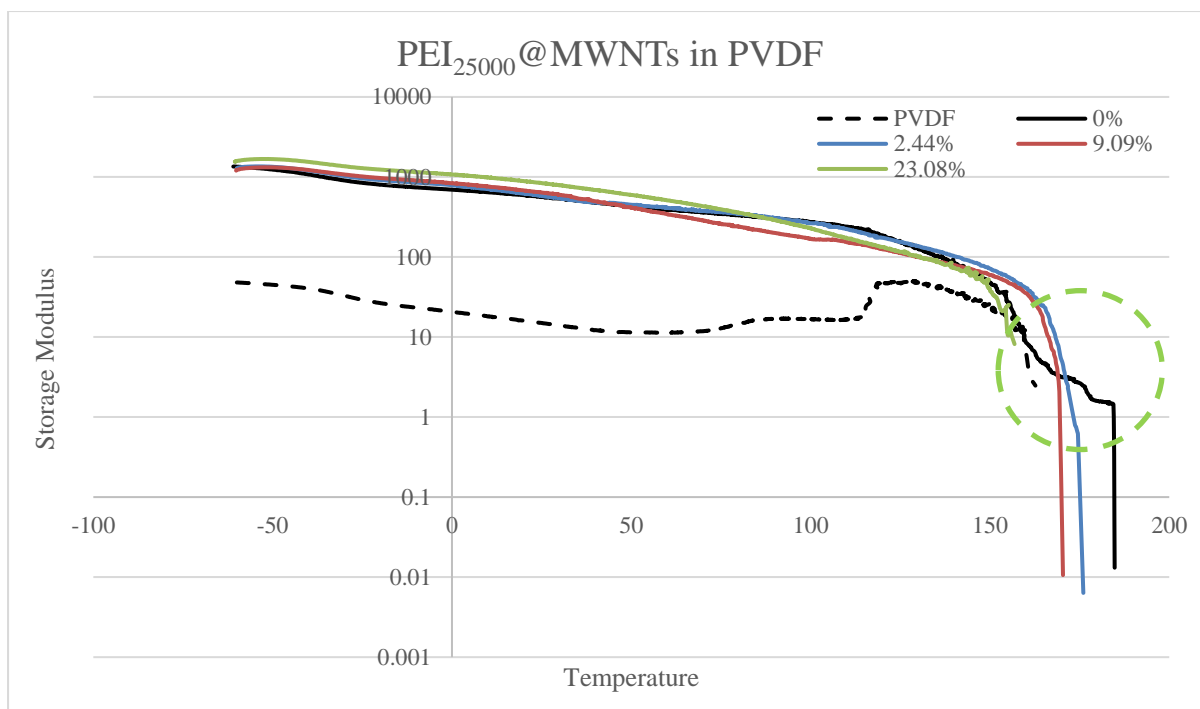


Fig. 7.3.9B: Storage modulus measurement of PEI<sub>25000</sub> functionalized MWNTs in PVDF composites.

PEI functionalized MWNTs in PVDF composites exhibit either a similar or slightly higher storage modulus compared to an unmodified nanotube composite. This could be attributed to the higher degree of nanotube dispersion that allows increased interaction between the nanotubes and PVDF matrix. However, the mechanical strength of PEI functionalized nanotube composite is weak compared to unmodified nanotube composite at high temperature range. The composites prepared at a PEI<sub>800</sub>/PEI<sub>25000</sub> concentration of 2.44 wt. % yields at a temperature slightly lower than the yielding point of an unmodified nanotube composite and the composite prepared at a higher PEI concentration tend to yield at a comparatively lower temperature. Both PEI<sub>800</sub> and PEI<sub>25000</sub> functionalized composite exhibits a similar observation at high temperatures. Although, a stable dispersion and a conductive formation of nanotube network is achieved with PEI functionalization, their instability at high temperatures could be attributed to the low melting temperature of PEI polymer.

#### 7.4 CONCLUSION

A comparative study on the physical properties of PVDF polymer composites prepared with PEI functionalized CNTs using PEI of two different molecular weights were undertaken.

A higher degree of dispersion is achieved in AP-SWNTs in PVDF composite with PEI<sub>25000</sub> functionalization leading to an enhanced thermal and electrical conductivity but the composites prepared with PEI<sub>800</sub> functionalization are unable to achieve a higher degree of nanotube

dispersion compared to unmodified nanotube composite leading to the formation of a weak nanotube network and eventually low thermal and electrical conductivity in PVDF composites with PEI<sub>800</sub> functionalized nanotube. This could be attributed to the difference in surface coverage of nanotubes achieved by PEI<sub>800</sub> and PEI<sub>25000</sub> functionalization of nanotubes in order to achieve uniform dispersion in the polymer composite and higher concentrations of PEI<sub>800</sub> could lead to higher degree of dispersion as observed in PEI<sub>25000</sub> but an increase in solution viscosity still might affect the morphology of polymer wrapping in the composite thus lowering conductivity. The mechanical characteristic of the composites prepared with PEI<sub>800</sub>/PEI<sub>25000</sub> functionalized P3-SWNTs tend to exhibit a fairly similar storage modulus as an unmodified nanotube composite.

However, PVDF composites prepared with PEI functionalized P3-SWNTs do not tend to exhibit an effective stable dispersion of nanotubes in the PVDF matrix. This leads to a low thermal and electrical conductivity compared to unmodified nanotube composite and the mechanical characterization of the composite were also not improved with PEI functionalization. This could be due to the incompatibility between the molecular weight of PEI and the structure of P3-SWNTs used in this research in order to achieve a stable dispersion in the PVDF matrix. Whereas, PEI<sub>800</sub>/PEI<sub>25000</sub> functionalized MWNTs in PVDF composites exhibit higher degree of nanotube dispersion compared to unmodified nanotube composite, with PEI<sub>800</sub> functionalized nanotube composite exhibiting a higher degree of dispersion at low concentration range and PEI<sub>25000</sub> functionalized nanotube composites exhibits a lower degree of dispersion at a comparatively higher concentration range. This is reflected in the thermal and electrical conductivity result of the composite, but the mechanical characterisation of the composites exhibits a storage modulus similar to an unmodified nanotube composite.

A higher degree of dispersion is observed with PEI<sub>800</sub>/PEI<sub>25000</sub> functionalized MWNTs in PVDF composites and PEI<sub>25000</sub> functionalized AP-SWNTS INPVDF composites that leads to increased thermal and electrical conductivity compared to an unmodified nanotube composite. An improvement in the mechanical strength of the PEI functionalized composite at high temperature range is not observed due to the low melting temperature of PEI polymer of about 73-75 °C. This leads to the instability of nanotube network at higher temperatures especially at temperatures above the melting point of PVDF polymer.



## 7.5 REFERENCES

1. Muñoz, E., et al., *Highly Conducting Carbon Nanotube/Polyethyleneimine Composite Fibers*. *ADVANCED MATERIALS*, 2005. **17**: p. 1064+.
2. Basiuk, E.V., et al., *Interaction of Oxidized Single-Walled Carbon Nanotubes with Vaporous Aliphatic Amines*. *The Journal of Physical Chemistry B*, 2002. **106**(7): p. 1588-1597.
3. Sun, J. and L. Gao, *Development of a dispersion process for carbon nanotubes in ceramic matrix by heterocoagulation*. *Carbon*, 2003. **41**(5): p. 1063-1068.
4. Ma, L., et al., *Improving the interfacial properties of carbon fiber-reinforced epoxy composites by grafting of branched polyethyleneimine on carbon fiber surface in supercritical methanol*. *Composites Science and Technology*, 2015. **114**: p. 64-71.
5. Cheng, Q., et al., *Ultrasound-Assisted SWNTs Dispersion: Effects of Sonication Parameters and Solvent Properties*. *The Journal of Physical Chemistry C*, 2010. **114**(19): p. 8821-8827.
6. Azadbakht, A. and M.B. Gholivand, *polyethyleneimine wrapped carbon nanotubes in situ formed gold nanoparticles decorated with DNA and NAD(+) as a novel bioelectrochemical sensing platform*. *Electrochimica Acta*, 2014. **133**: p. 82-92.
7. Correa-Duarte, M.A., et al., *Linear Assemblies of Silica-Coated Gold Nanoparticles Using Carbon Nanotubes as Templates*. 2004. **16**(23-24): p. 2179-2184.

CHAPTER 8  
CONCLUSIONS

In summary, two kinds of nanocomposites, i.e. PVDF composites prepared with pristine CNTs and PVDF composites prepared with non-covalently functionalized CNTs were prepared. Carbon nanotubes of different aspect ratio, carboxyl content and structure were non-covalently functionalized with polymers such as Polyvinylpyrrolidone, Poly(4-vinylpyridine) and Polyethylenimine in this work. It is clear that a uniform dispersion of nanotubes in a polymer matrix achieved through non-covalent functionalization of nanotubes by a functionalization polymer of low concentration irrespective of the polymer chain length can exhibit excellent thermal, electrical and mechanical properties.

Polyvinylpyrrolidone (PVP) acts as excellent surface modifier that enhances nanotube dispersion in the polymer matrix with all the three types of nanotubes. Compared with the PVDF composites prepared with unmodified nanotubes, PVP functionalization of nanotubes have induced a more ordered nanotube network in the PVDF composites leading to an enhancement in the physical properties of the composites. However, PVP of only a certain molecular weight is compatible to CNTs based on their aspect ratio and structure. PVP of low molecular weight exhibits a promising outcome with both AP-SWNTs and MWNTs polymer composites in their physical properties at low PVP concentration but higher molecular weights are not suitable with AP-SWNTs unless there is a change in the nanotube diameter. However, higher molecular weights of PVP exhibit a similar result with MWNTs as observed with low molecular weights but only at high concentrations of PVP. This clearly confirms the influence of nanotube diameter towards polymer wrapping and uniform dispersion of nanotubes in the PVDF composite. Whereas, P3-SWNTs exhibit a similar result with PVP of low molecular weight at low PVP concentration only at lower weight percent of P3-SWNTs compared to other two nanotube types and increasing amount of nanotube content requires longer polymer chains to achieve a similar outcome again confirming the influence of the amount of nanotubes in order to achieve uniform dispersion of nanotubes in the PVDF composite.

On the contrary, Poly(4-vinylpyridine) (P4VP) functionalization of SWNTs failed to achieve a conductive network formation of nanotubes as observed with PVP of similar molecular weight (polymer chain length) due to the difference in wrapping patterns. Unlike SWNTs, the wrapping pattern of P4VP in MWNTs are helical as observed in PVP functionalization of MWNTs, but happens only at a higher concentration of P4VP compared to PVP due to the difference in polymer structure leading to different surface coverage of nanotubes in order to achieve higher degree of nanotube dispersion compared to composites with PVP modified MWNTs. This confirms the influence of the structure of functionalization polymer towards

polymer wrapping. The carboxyl content in the nanotubes do not have much influence towards PVP and P4VP functionalization as they happen through strong  $\pi$ - $\pi$  interaction between the polymer and sidewalls of nanotubes. The influence of carboxyl content on the physical properties of CNTs are significant and thus on the overall composite containing PVP/P4VP functionalized nanotubes.

As explained in chapter 7 section 7.3 in the MWNT subsection, the amines on PEI possess high affinity for physisorption along the CNTs-COOH surface leading to a wrapping like behaviour. This means that the presence of carboxyl content could have influenced PEI functionalization of CNTs. However, the presence of PEI<sub>25000</sub>/PEI<sub>800</sub> do not tend to initiate any impact towards the dispersion of P3-SWNTs in the PVDF composites but achieve a uniform dispersion of MWNTs in the PVDF composite as observed with PVP in chapter 5. This confirms the influence of nanotube diameter in PEI functionalization. The length of the nanotubes plays a key role as well. This is observed with PEI functionalization of AP-SWNTs, as only PEI of higher molecular weight exhibited enhanced thermal and electrical properties with AP-SWNTs in the PEI concentration range analyzed. The result observed with nanotubes of different dimensions could be attributed to a failure of balance between the concentrations of PEI and the surface area of nanotubes functionalized, meaning a higher concentration of PEI for a specific amount of nanotube of certain dimensions may not just functionalize the nanotubes but may also lead to aggregation through a higher amount of ionic interactions between the amines on PEI and the carboxyl content of nanotubes. This could be the reason for PEI functionalization being not effective with the dispersion of P3-SWNTs in PVDF matrix in the same concentration range of PEI that exhibits an effective dispersion of MWNTs. The high aspect ratio of MWNTs compared to P3-SWNTs could have played a vital role.

It is clear that PVP functionalization of nanotubes exhibits a higher degree of dispersion of all the different types of nanotubes compared to unmodified nanotube composite leading to enhanced thermal and mechanical properties. The enhancement in electrical properties is generally observed when a uniform dispersion of nanotubes in the polymer matrix is achieved at low concentrations of PVP irrespective of PVP molecular weight. This is attributed to the fact higher surface coverage of nanotubes or excess amount of polymer may mean that the thick insulating polymer layers around the nanotubes prevent electron conduction. The high polymer concentration can also alter the viscosity of the composite meaning a lack of effective dispersion in the matrix leading to an improper formation of nanotube network restricting electron movement. This is observed with P4VP and PEI polymers as well. Although, the

melting temperature of PEI meant that the mechanical stability of the polymer composites at high temperatures was not maintained as observed with PVP and P4VP.

## CHAPTER 9

# FUTURE DIRECTIONS AND RECOMMENDATIONS

Although, significant achievements have been made in this research study, several challenges are yet to be addressed in order to construct a polymer-based nanocomposite with enhanced physical properties.

### *9.1 Polymer wrapping*

The research study confirms that polyvinylpyrrolidone (PVP) has been proven to be a suitable surface modifier to disperse and stabilize CNTs dispersion in PVDF matrix while preserving the structure and properties of CNTs. Similarly, in other work, addition of PVP was proven to facilitate uniform distribution and stabilization of MWNTs in a Poly(vinylalcohol) matrix [1] and SWNTs in N-methyl-2-pyrrolidone matrix [2]. However, the concentration of PVP that could facilitate uniform dispersion of a specific amount of nanotube differs with respect to the organic solvent. Therefore, conducting extensive research by replacing different polymer matrices without altering the parameters of both nanotubes and PVP is essential in order to understand the variation in polymer wrapping and nanotube dispersion with respect to a different polymer matrix.

It was found that AP-SWNTs exhibits an enhanced physical property with PVP of low molecular weight. Our hypothesis was that the diameter of the nanotubes plays a key role in polymer wrapping. If so, an experiment with AP-SWNTs of same length and different diameter would provide a clear understanding on the relation between polymer wrapping and diameter of the nanotubes. It would be crucial in constructing a polymer nanocomposite of lower density and to further understand the role of aspect ratio in the dispersion of nanotubes in polymer matrix.

In addition to the thermal conductivity analysis of PVP functionalized P3-SWNTs in PVDF composites of different weight percent of nanotubes, conducting an electrical and mechanical analysis would further explain the correlation between the amount of nanotubes and polymer molecular weight. Achieving a more effective formation of nanotube network with lower weight percent of nanotubes would open a lot of possibilities in the field of transparent electronics[3].

Non-covalent functionalization using poly(4-vinylpyridine) (P4VP) and Polyethylenimine (PEI) tend to exhibit a higher degree of dispersion in MWNTs but not in SWNTs. Conducting a similar experiment with different diameters of SWNTs would be important research to analyze the interaction between P4VP/PEI and SWNTs and to understand their stability in the

polymer matrix. Finally, compatibility between surfactants and polymer matrices is an important parameter to explore in terms of cost-effectiveness.

### 9.2 Mechanical Characterization

Although, storage modulus and glass transition temperatures of the composite provide an understanding on the interaction of CNTs and polymer matrix, analyzing the composite for properties such as elongation at break and flexibility are important in the application of flexible sensors and flexible electronics. Standard mechanical testing such as tensile testing could also provide additional information. Moreover, the dispersion of nanotubes in the composite have a direct connection to flexibility and stretchability of the composite. Strong EMI shielding, superior flexibility and shielding stability can be attributed to the percolated and flexible network structure of nanotubes with polymer matrix [4]. It has also been found that uniformly dispersed nanofiller in polymer composite exhibit high stretchability and it might be related to the high flexibility of the matrix and the conductive network structure formed by the nanofillers [5].

### 9.3 Surface Analysis

Although, SEM imaging confirms the presence of PVP in the composites and distribution of nanotubes without agglomeration. A clearer characterization on the morphology of polymer wrapping could be achieved through an in-situ TEM and FIB analysis.

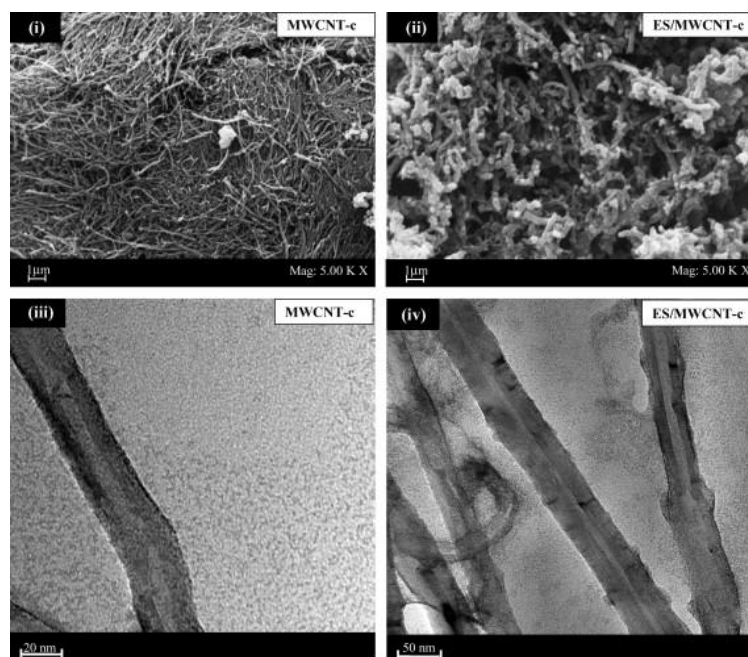


Fig. 9.3A: SEM (i and ii) and TEM (iii and iv) micrograph of MWNT in the composite film and Emeraldine Salt (ES) wrapped MWNT in the composite film. Reproduced with permission from Ref. [6]



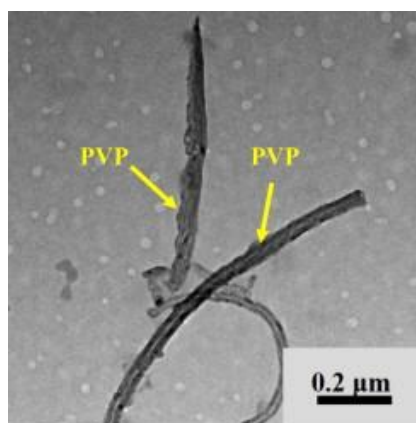


Fig. 9.3B: TEM image showing the typical morphology of PVP treated MWNTs. Reproduced with permission from Ref. [7]

This would be a valuable addition to understand the difference in the morphology of polymer wrapping of nanotubes resulting from the change in polymer chain length and diameter of the nanotubes. Moreover, the helical conformation of PVP and the kebab like conformation of P4VP could be probed.

#### 9.4 Reference

1. Huang, Y., et al., *Poly(vinyl pyrrolidone) wrapped multi-walled carbon nanotube/poly(vinyl alcohol) composite hydrogels*. *Composites Part A: Applied Science and Manufacturing*, 2011. **42**(10): p. 1398-1405.
2. Hasan, T., et al., *Stabilization and "Debundling" of Single-Wall Carbon Nanotube Dispersions in N-Methyl-2-pyrrolidone (NMP) by Polyvinylpyrrolidone (PVP)*. *The Journal of Physical Chemistry C*, 2007. **111**(34): p. 12594-12602.
3. Hellstrom, S.L., H.W. Lee, and Z. Bao, *Polymer-Assisted Direct Deposition of Uniform Carbon Nanotube Bundle Networks for High Performance Transparent Electrodes*. *ACS Nano*, 2009. **3**(6): p. 1423-1430.
4. Jia, L.-C., et al., *High Strain Tolerant EMI Shielding Using Carbon Nanotube Network Stabilized Rubber Composite*. *Advanced Materials Technologies*, 2017. **2**(7): p. 1700078.
5. Zheng, Y., et al., *A highly stretchable and stable strain sensor based on hybrid carbon nanofillers/polydimethylsiloxane conductive composites for large human motions monitoring*. *Composites Science and Technology*, 2018. **156**: p. 276-286.
6. Dhand, C., et al., *Preparation of polyaniline/multiwalled carbon nanotube composite by novel electrophoretic route*. *Carbon*, 2008. **46**(13): p. 1727-1735.
7. Zhang, W.-b., et al., *High thermal conductivity of poly(vinylidene fluoride)/carbon nanotubes nanocomposites achieved by adding polyvinylpyrrolidone*. *Composites Science and Technology*, 2015. **106**: p. 1-8.